FLOW SYNTHESIS OF NATURAL PRODUCTS: ASCORBIC ACID AND N5-OH-*L*-ORNITHINE SYNTHESIS

by

Maduabuchi Angus Modum

B.Sc., Federal University of Technology Owerri, 2021

THESIS SUBMITTED IN PARTIAL FULFILLMENT OF
THE REQUIREMENTS FOR THE DEGREE OF
MASTER OF SCIENCE
IN
CHEMISTRY

UNIVERSITY OF NORTHERN BRITISH COLUMBIA

April 2025

Abstract

Flow synthesis has emerged as a transformative approach in pharmaceutical manufacturing, offering unique control over reaction parameters, enhanced safety, and improved efficiency. This transformation from traditional batch processes to flow systems has the potential to revolutionize the production of vital compounds, addressing the growing demand for sustainable and cost-effective manufacturing methods in the pharmaceutical industry.

This study explored the application of flow chemistry to two distinct yet equally important synthetic targets: *L*-ascorbic acid (vitamin C) and N5-OH-Ornithine, a key intermediate in piperazic acid synthesis. The goal was to develop more efficient and scalable routes to these compounds, which play crucial roles in nutrition and drug development.

For *L*-ascorbic acid synthesis, the study adapted a modified Reichstein process from batch to flow conditions. Starting with *D*-glucose, four of the five steps, reduction, protection, oxidation, and lactonization, were successfully implemented in flow systems. These steps showed improved yields and shorter reaction times compared to batch methods. The second step, enzymatic oxidation, remains under investigation. The secondary objective, protecting *L*-Ornithine in the flow, faced challenges due to foaming and CO_2 evolution, which caused clogging in the flow system. Strategies to address these challenges include larger tubing, continuous stirred tank reactors, and liquid-gas separators.

Success with *L*-ascorbic acid synthesis highlights the power of flow synthesis in improving reaction efficiency and product yield. In contrast, the challenges encountered in *L*-Ornithine protection highlights the complexities of gas-evolving reactions in flow systems. This work contributes to the growing knowledge of applying flow chemistry in natural product synthesis.

Table of Contents

List of Tables

List of Figures

List of Schemes

List of Abbreviations and Symbols

^{13}C	Carbon 13 NMR
^{1}H	Proton NMR
°C	degrees Celsius
δ	chemical shift in parts per million
ID	One dimensional
2D	Two dimensional
2-KGA	2-keto-*L*-gulonic acid
$(Boc)_2O$	Di-tert-butyl dicarbonate
Boc	tert-butyloxycarbonyl
BPR	Back Pressure Regulator
CAGR	Compound annual growth rate
Cbz-cl	Benzyl Chloroformate
Cbz-Osu	Benzyl N-succinimidyl carbonate
$CDCl_3$	Deuterated chloroform
COSY	Correlated Spectroscopy
CO_2	Carbon dioxide
CSTR	Continuous Stirred Tank Reactor
Cu (II)	Copper (II)
$CuSO_4$	Copper (II) sulfate
DAB	Deacetylbaccatin
DAS	Diacetone-*L*-Sorbose
DHA	Dehydro-*L*-ascorbic acid
DMSO-d_6	Deuterated dimethyl sulfoxide
EDTA	Ethylenediaminetetraacetic acid

Eq.	Equivalents
FDA	Food and Drug Administration
FT-IR	Fourier Transform Infrared Spectroscopy
H_2SO_4	Sulfuric acid
HCl	Hydrochloric acid
HSQC	Heteronuclear Single Quantum Coherence
HMBC	Heteronuclear Multiple Bond Correlation
$KMnO_4$	Potassium permanganate
KOH	Potassium hydroxide
mCPBA	meta-Chloroperoxybenzoic acid
MCM-41	Mobil Composition of Matter-41
MeOH	Methanol
$NaBH_4$	Sodium borohydride
NaOH	Sodium hydroxide
$NaHCO_3$	Sodium bicarbonate
Na_2SO_4	Sodium sulfate
NMR	Nuclear Magnetic Resonance
N-N	Nitrogen to nitrogen
NRPS	Nonribosomal peptite synthetase
PCF	Plant cell fermentation
Piz	Piperazic acid
Ppm	Parts per million
Psi	Pounds per square inch
PTFE	Polytetrafluoroethylene
RDA	Recommended dietary allowance

RT	Room temperature
Ru	Ruthenium
ZSM-5	Zeolite Socony Mobil-5

Acknowledgement

I am deeply grateful to Almighty God for his unwavering guidance, strength and perseverance throughout my journey. My heartfelt appreciation goes to my supervisor, Dr. Kalindi Morgan, for her constant support since the beginning of this journey. Her mentorship and guidance have been instrumental in shaping my research and academic growth, and I feel lucky to have such an energetic and amazing supervisor.

I would also like to sincerely thank my supervisory committee members, Dr. Todd Whitcombe, Dr. Andrea Gorrell and Dr. Oliver Iorhemen, for their kind assistance, encouragement, and insightful feedback whenever needed. Their contributions and feedback have greatly enriched my work. I gratefully acknowledge MITACS for its financial support, which enabled the beginning of this research.

To my colleagues in the Morgan lab, schoolmates, and friends, thank you for making this journey enjoyable and memorable. Your camaraderie and support have been invaluable.

I am grateful to my mother, Mrs. Uche Modum, for her endless prayers and support. Her love and encouragement have been a guiding light in my life.

Dedication

In loving memory of my beloved late father, Engr. Patrick Modum, whose unwavering guidance and profound belief in my potential, charted the course of my life's journey. This thesis stands as a testament to his enduring influence.

1. Introduction

1.1 Flow Synthesis

The past 100 years have witnessed a remarkable leap forward in our comprehension and creation of organic compounds. However, there is a striking contrast in research laboratory practices compared to commercial or industrial production. Despite the advancements in organic chemistry knowledge, laboratory methods and equipment have remained largely unchanged. Researchers continue to rely on traditional tools such as round bottom flasks, magnetic stir bars, and reflux condensers, with many processes still requiring significant hands-on effort. This highlights a gap between theoretical progress and practical implementation in organic chemistry. While batch chemistry, the traditional approach, can achieve the desired chemical changes (transformations) in most cases without requiring alternative methods like flow chemistry, a growing body of research highlights the numerous advantages of flow synthesis.[1–10]

Flow synthesis, also known as flow chemistry, as shown in Figure 1, is a chemical production method where reactants are pumped through a reactor,[11,12] generating a stream of products. In contrast to traditional batch processes, where reactions occur in a fixed volume, flow chemistry enables a dynamic and continuous reaction environment. Reactants are precisely mixed in specialized reactors, often microreactors or tubular systems, which provide excellent control over reaction parameters[5,6] such as temperature, pressure, and residence time. As the reaction mixture flows through the system, it undergoes controlled transformations, resulting in a constant and steady product output. Furthermore, flow synthesis facilitates real-time monitoring and adjustment of reaction conditions[10–12], improving the final product's consistency and quality. These features make flow chemistry an

increasingly attractive option for both research and industrial applications, offering potential improvements in efficiency, sustainability, and process control compared to traditional batch methods.

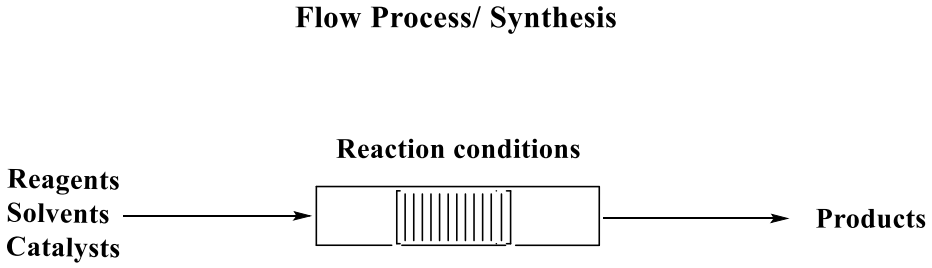

Figure 1: Flow Process or Flow Synthesis simple diagram.

1.1.1 Differences between Flow Synthesis and Batch Process

Flow synthesis and batch processing exhibit fundamental differences that significantly impact their application in various industries. In flow synthesis, each portion of the reaction mixture is processed individually in a controlled manner, allowing for easier detection and correction of defects. In batch processing, all reactants are mixed in a single vessel, and the reaction is completed before the final product is analyzed.[13–16] This characteristic of flow synthesis enhances quality control and enables immediate adjustments to the process, ensuring consistent quality throughout production. Furthermore, flow synthesis can lead to cost savings by reducing waste, inventory, and transportation costs due to its scalability and compact setup, as well as increasing productivity[13,16] and stability, offering better adaptability to customer needs compared to batch processing. Additionally, flow systems require less space, make better use of raw materials, and produce a higher volume of consistent products,[14,16] making them more

cost-effective and increasingly popular in manufacturing.[16,17] Flow processes are inherently safer in many cases due to the smaller quantities of materials at any given time.[17] This is particularly advantageous when dealing with hazardous or highly reactive compounds. Figure 2 below is a simple diagram that shows the difference between the batch and flow processes.

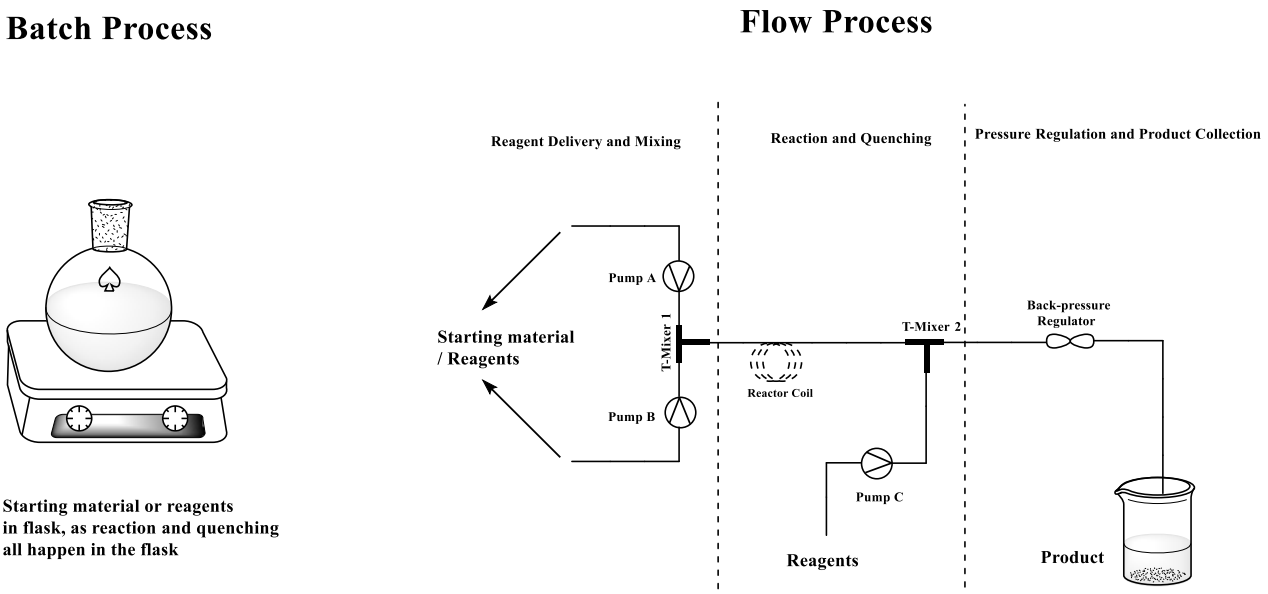

Figure 2: Difference between Batch process and Flow Process

1.1.2 Benefits of Flow Synthesis

Flow synthesis offers many benefits over traditional batch processing.[18,19] One primary advantage of flow synthesis is enhanced safety,[10,19] which allows for better control of process parameters and improved product quality control.[6,19] This heightened safety is attributed to the precise management of key reaction parameters such as mixing, heating, and residence time, which are more attainable in flow systems than conventional batch reactions. As a result, the potential for unwanted side reactions and hazardous conditions is

minimized, making flow synthesis an attractive option for industries where safety is paramount.[18–20] An additional benefit is that flow synthesis contributes to greater sustainability in chemical and pharmaceutical manufacturing. Reducing waste and energy consumption associated with flow processes aligns with the increasing emphasis on sustainable practices within the industry. It is an appealing choice for companies seeking to enhance their sustainability profile.[18,20] Another key advantage of flow synthesis is its ability to deliver faster reactions, increased flexibility, and automation, rendering it suitable for a wide range of industries, particularly pharmaceuticals.[18]

In conclusion, the benefits of flow synthesis have led to its growing popularity in various industries, including pharmaceuticals and manufacturing. As such, this thesis utilized this strategy for vitamin C production in collaboration with an industrial partner. The nature of the flow process can lead to improved productivity and quality control, addressing some of the limitations of the Reichstein process in batch production.[14] The flow production method may offer potential advantages in addressing some of these limitations, although further research and development are needed to fully assess the viability of Vitamin C production.[2, 14]

1.1.3 Continuous Flow Synthesis

Continuous flow synthesis is a method of chemical production where reactants and their resulting products are continuously fed through a series of reactors,[3,4,21] generating a collection of products at the outlet without interruption rather than mixing them in a single batch. The reaction occurs in an unbroken stream, with no clear separation between individual reaction volumes, and they mix and react under tightly controlled conditions such as temperature, pressure, and flow rate. Continuous flow synthesis represents a pivotal advancement in the field of chemical synthesis,[21–23] revolutionizing the production of pharmaceuticals and fine chemicals. It is often preferred for large-scale production and processes that benefit from steady-state conditions,[22,23] while segmented flow, a flow chemistry technique in which a continuous stream of liquid or gas is divided into discrete segments, can be advantageous for high-throughput experimentation[24] and reactions that require precise control over individual reaction volumes. The choice between continuous and segmented flow often depends on the reaction's specific requirements, the production scale, and the desired level of control over individual reaction volumes.[25,26] Traditional batch processes are time-consuming and energy-intensive, and the transition from traditional batch mode to modern continuous flow chemistry signifies a significant shift in the approach to chemical synthesis.[17,21,23,27,28]

Historically, continuous flow reactors have been used industrially for over 100 years[8,11,15] to synthesize bulk chemicals and are now increasingly applied to synthesizing pharmaceuticals from multiple sources such as marine, plant and bacterial natural products.[17] The application or research on continuous flow chemistry continues to thrive in

academic and industrial laboratories, driven by developing efficient and innovative syntheses. This discipline has diversified and expanded to provide novel and practical solutions to various fields, including synthetic organic chemistry, biochemistry, renewable fuels, and materials synthesis.[18,19,21,22,28]

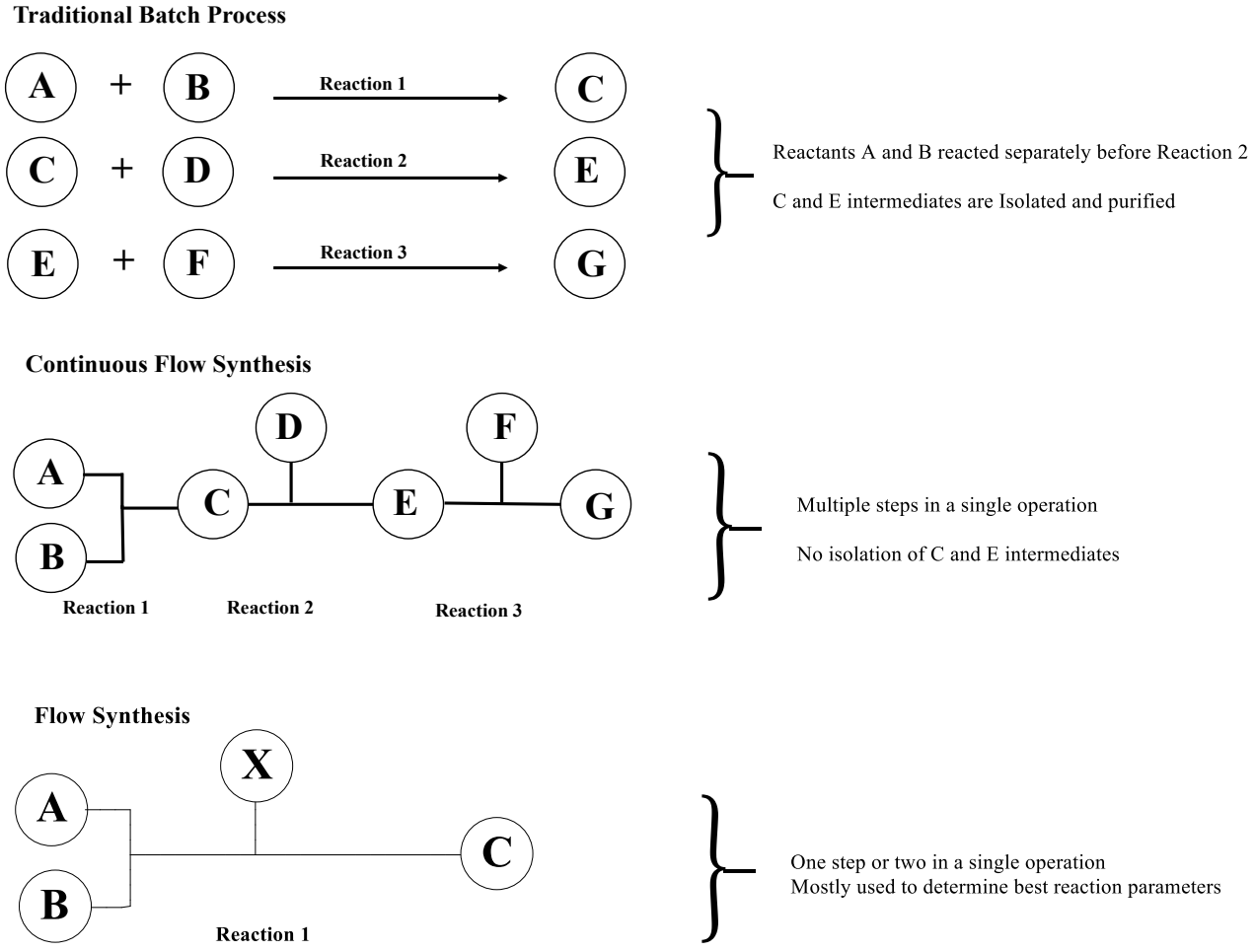

Figure 3: Comparison /Differences between traditional batch process, flow process and Continuous flow process

1.2 Flow Synthesis Components

Flow synthesis offers a modern and efficient approach to chemical reactions. The

components of flow synthesis systems typically include pumps, flow meters, cooling/heating units, valves, separators, and regulators. These components are essential for maintaining the continuous flow of reagents, controlling the reaction temperature, and ensuring the safe and efficient operation of the system.[27]

1.2.1 Pumps

Continuous flow systems rely on pumps to maintain a consistent flow of reagents. These pumps are essential components that ensure the precise and continuous delivery of reactants, solvents, and other fluids, thereby enabling the efficient operation of the flow synthesis process.[26,27] Various types of pumps are used in continuous flow systems, including syringe, peristaltic, and diaphragm pumps. The selection and use of pumps in continuous flow systems is critical for achieving precise fluid control and ensuring the reliability and long-term operation of the continuous flow process.[26,27,29,30] Syringe pumps (see Figure 4) offer high-precision fluid delivery and are often used in laboratory-scale continuous flow setups.[27] In this project, syringe pumps were utilized as proof of concept.

Figure 4: The syringe pump used in the laboratory (New Era Pump Systems Inc.).

1.2.2 Lines and Mixers

Lines and mixers are required in continuous flow systems to ensure the efficient and homogeneous mixing of solid and liquid feed components.[31] In this context, lines refer to the piping and tubing that transport the various components to the mixer. In contrast, mixers are the devices responsible for combining these components into a uniform mixture. In-line mixers are widely used in various industries and designed to be integrated into the processing system, allowing ingredients to be mixed as they flow through the mixer.[27,31] This continuous flow of ingredients ensures a seamless and uninterrupted mixing process, making in-line mixers ideal for applications that demand high precision, such as pharmaceuticals, cosmetics, and personal care products. The Y-mixer and T-mixer (Figure 5) are inline mixers[26,27] used for producing homogenous mixtures. The Y-mixer is widely used to produce homogeneous mixtures from bulk components, offering an efficient solution for mixing solid and liquid feed components.[27,32] Conversely, T-mixers, micro-T mixers, and oriented Y-mixers are primarily discussed in the context of microfluidics and their mixing performances with single fluids, focusing on pressure drop and energy considerations.[33,34]

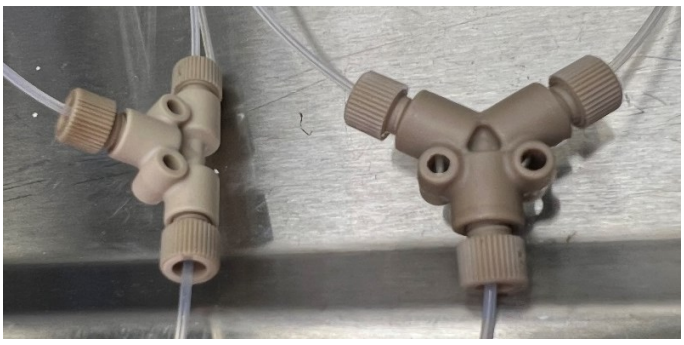

Figure 5: T-mixer and Y-mixer (from IDEX Health and Science LLC.).

1.2.3 Back Pressure Regulators

A back pressure regulator (BPR), as shown in Figure 6, is a device used to control and maintain pressure in a system[27] by regulating the flow of a gas, liquid, or multiphase fluid. BPRs are commonly employed in various industrial processes, including continuous flow systems, to ensure stable and controlled pressure conditions. The BPR works by limiting the upstream pressure, thereby maintaining the desired pressure at the outlet, and it does so by adjusting the orifice area to control the flow.[35,36] Back pressure regulators offer several advantages over traditional pressure control methods, making them an asset in various industrial applications. One key benefit is their ability to enable remote pressure control[37,38] at a safe distance, enhancing operational safety and flexibility. This feature allows operators to adjust and maintain pressure levels from a distance, reducing the risk of exposure to potentially hazardous environments. Additionally, BPRs have a low-pressure drop under dynamic conditions,[38] ensuring efficient pressure control without significantly affecting the flow rate. This characteristic is particularly advantageous in processes where maintaining a consistent flow rate is critical. Furthermore, BPRs can be used with low-pressure inert gases, making them suitable for various applications, including those requiring inert gases for specific process requirements.[35,39]

Figure 6: Back Pressure Regulator (IDEX Health and Science) Used in the Laboratory Setup (75 psi).

1.2.4 Inline Separators

Inline separators are crucial components in various industrial processes,[40] playing a significant role in the continuous flow separation of solvents and other substances. These devices are designed to be integrated directly into pipelines, allowing for seamless and efficient separation without interrupting the flow of materials. The primary mechanism of the inline separators involves creating a centrifugal spinning action within the flow stream. The spinning motion effectively separates liquid entrainment droplets in gases,[40] making these separators essential for steam, air, and gas processing applications. The centrifugal force generated within the separator causes heavier liquid droplets to be thrown outwards toward the walls of the separator. At the same time, the lighter gas continues to flow through the center. Using inline separators in continuous flow processes offers several advantages, including efficient separation, which reduces waste by effectively separating substances during the flow process and improves process performance by maintaining the purity of products.[40,41] Inline separators are instrumental in supporting the transition towards more sustainable and efficient manufacturing practices, particularly in industries such as pharmaceuticals and specialty chemicals, where the responsible use of solvents and other substances is a key consideration.[19,40,42,43] By enabling continuous separation and recycling of solvents, inline separation contributes to reduced solvent consumption, improved product quality, enhanced safety and lower environmental impact, aligning with green chemistry principles.

1.2.5 Drying in Flow

Flow drying involves uninterrupted movement of the material through the drying system,

allowing for a homogeneous and efficient drying process. In the context of drying, molecular sieves, silica gel, and other drying agents are used to remove moisture from solvents and other materials.[44] Molecular sieves are crystalline metal aluminosilicates with uniform pores that selectively absorb water and other polar molecules.[44] They are commonly used in drying processes to achieve very low moisture levels in solvents and gases.[44,45] Molecular sieves are available in different types, such as type 3A, 4A, and 5A, each with a specific pore size and adsorption capacity.[44,45] Type 3A molecular sieves are commonly used for drying polar liquids and gases, while type 4A molecular sieves are suitable for drying non-polar liquids and gases. Type 5A molecular sieves are used for drying and purifying gases and fluids in the presence of water. The choice of molecular sieve depends on the specific application and the level of moisture removal required.[44]

Figure 7: Molecular sieve columns (4A and 3A - top to bottom) used in the laboratory setup.

Silica gel is another popular drying agent with a high affinity[44] for water molecules. It is often used in desiccators and as a drying agent in various industrial processes. The difference between molecular sieves and silica in continuous-flow drying is their specific properties and performance characteristics. Silica gel, which has an affinity for water molecules, removes moisture from solvents and gases and is available in different pore sizes, and it can be regenerated for reuse. However, it is generally less effective than molecular sieves in removing water and may not maintain water uptake at elevated

temperatures as effectively as molecular sieves, as its ability to continue absorbing water diminishes. Therefore, while both molecular sieves and silica are used as drying agents, molecular sieves are often preferred for applications requiring high water absorption capacity, selective adsorption, and the ability to maintain water uptake at elevated temperatures, such as in compressed air drying and gas dehydration processes.[45–47]

1.2.6 Legends for Flow Components in Diagrams

Throughout this thesis, diagrams are used to indicate flow components. As shown in Figure 8, the individual components are represented using the following standardized symbols or legends.

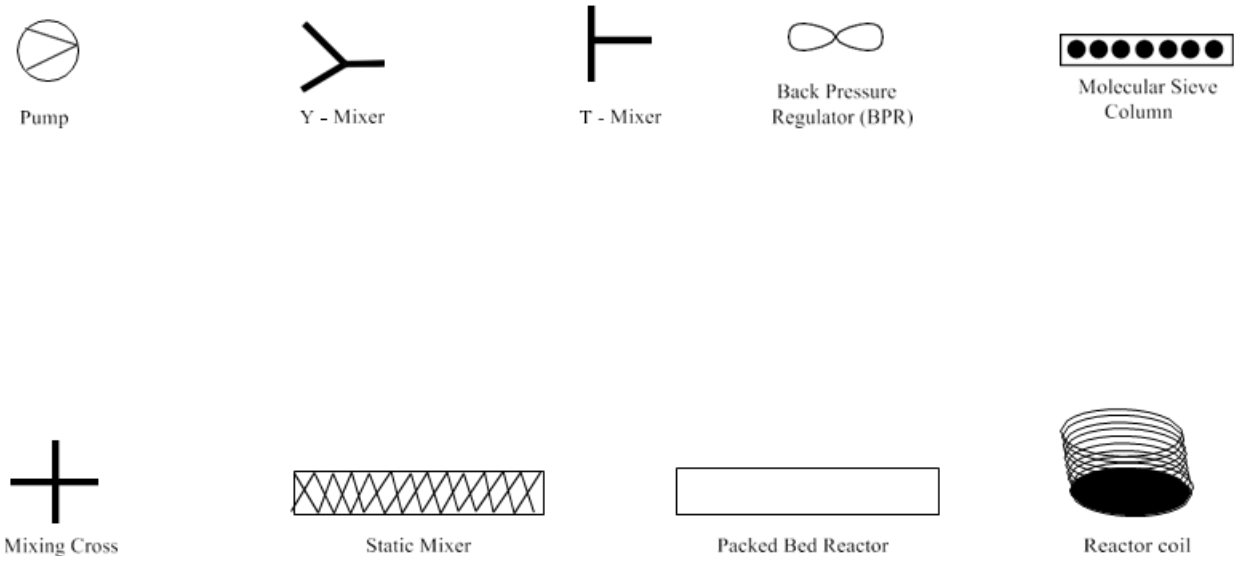

Figure 8: Standard Flow Reactor Component/ Equipment

1.3 Challenges and Potential Solutions in Flow Synthesis

While having numerous advantages, flow synthesis also presents several challenges. One of the key challenges is the precise control of reaction parameters,[18,48] such as temperature, pressure, and flow rates. The precise control of reaction parameters is a fundamental challenge in continuous flow synthesis,[48] as it directly impacts the quality and efficiency of the production process. Achieving and maintaining the necessary control over these reaction parameters requires advanced instrumentation and monitoring systems to meet the desired conditions consistently. Another challenge is the scale-up and integration of processes from the laboratory to industrial scale,[18,23] which can be difficult due to the need for specialized equipment and engineering considerations.

Safety and hazard mitigation are also significant concerns in continuous flow systems, especially when handling reactive or hazardous chemicals and in the event of a system failure or blockage. Ensuring the compatibility of catalysts and reactors in continuous flow systems,[21,23] particularly when using heterogeneous catalysts, is also a challenge that can affect the efficiency and productivity of the process. Addressing these challenges is crucial for the widespread adoption and successful implementation of flow synthesis in various industries, including pharmaceuticals and specialty chemicals.[18,21,23] It requires a multidisciplinary approach, incorporating advanced process control, engineering solutions, safety protocols, a comprehensive understanding of the specific requirements and operating conditions of flow systems, research and development efforts to advance the capabilities of flow synthesis in industrial, as well as the development and implementation of advanced solutions to overcome these limitations.[18,21,23,48,49]

1.4 Natural Products in Health and the Economy

To organic and medicinal chemists, natural products are the small organic molecules (less than 2000 g/mol) known as secondary metabolites produced by living organisms for ecological adaptations. Their role in helping their producing organism adapt to their environment has driven their chemical complexity. Their chemical complexity, rich with heteroatoms and stereocenters, is involved in their biological activities, which is important in their historical and current role as medicines. Natural products have been pivotal in human history, serving as medicinal, nutritional, and culturally significant sources for thousands of years. Natural products (secondary metabolites) are the most successful source of potential drug candidates.[50–54] Despite a recent decline in their utilization within drug discovery and development processes,[50] natural products remain an unparalleled source of structural diversity. This unique characteristic offers significant advantages over conventional combinatorial chemistry approaches, particularly in identifying novel, low molecular weight lead compounds. It is worth noting that less than 10% of the world's biodiversity has been assessed for potential biological activity, suggesting that a vast reservoir of useful natural lead compounds remains unexplored.[53]

Using natural products for medicinal purposes has a rich history spanning thousands of years. Ancient civilizations, including Mesopotamia, Egypt, and China, documented the medicinal uses of plants and other natural sources in texts like cuneiform tablets (2600 BC), the Ebers Papyrus (2900 BC), and Chinese Materia Medica.[53] These early records detailed hundreds of plant-based drugs and their applications, covering various medical conditions and treatments.[53] The establishment of privately owned pharmacies by Arabs in

the 8th century marked a significant development in pharmacy history.[53] Persian scholars, notably Avicenna, made substantial contributions to the field, with his Canon Medicinae influencing pharmacy and medicine for centuries in Europe and the Islamic world.[53] This rich history underscores the enduring importance of natural products in human medicine. It highlights the cross-cultural exchange of knowledge that has shaped our understanding of medicinal plants over the millennia.

The systematic study of natural products began in the 19th century with Friedrich Sertürner's isolation of morphine in 1805, marking the start of modern natural product chemistry and pharmacology. Throughout the 19th and early 20th centuries, numerous important drugs were isolated from natural sources, including quinine, salicin (aspirin's precursor), and penicillin, revolutionizing healthcare[55–66] The modern development of aspirin began in 1853 when Charles Frédéric Gerhardt first synthesized acetylsalicylic acid by treating sodium salicylate with acetyl chloride.[56,67] However, it wasn't until 1897 that Felix Hoffmann at Bayer Company refined the synthesis process, motivated by his father's intolerance to salicylic acid.[67] Hoffmann's method involved replacing the hydrogen from the hydroxy group on salicylic acid's benzene ring with an acetyl group, creating a more stomach-friendly compound.[67] The synthesis of aspirin is an esterification reaction where salicylic acid reacts with acetic anhydride, typically catalyzed by small amounts of sulfuric or phosphoric acid. This process yields aspirin and acetic acid as a byproduct.[56,67] Bayer began marketing aspirin globally by 1899.[56,67] Penicillin, another revolutionary drug, was discovered by Alexander Fleming in 1928 when he noticed a mold contaminating his Staphylococcus culture plates, which had antibacterial properties.[57]

Vitamins are typically part of a broader, cultural definition of natural products encompassing anything derived from a living organism and having health benefits. Most vitamins are still small organic molecules but are essential to the growth and repair of the producing organisms. Vitamins, particularly vitamin C, play vital roles in numerous physiological processes. Vitamin C, for instance, functions as a cofactor for enzymes involved in collagen synthesis, neurotransmitter production, and carnitine biosynthesis.[68,69] It is also a powerful antioxidant, protecting cells from oxidative stress.[68] The biosynthesis of vitamin C is essential for most organisms. Still, humans and some other primates have lost this ability due to mutations in the gene encoding the enzyme *L*-gulono-γ-lactone oxidase.[68] This evolutionary loss has made humans dependent on dietary sources of vitamin C, highlighting the importance of understanding its biosynthesis and regulation in plants and other organisms. The ability to synthesize or obtain adequate amounts of vitamins, including vitamin C, is crucial for maintaining health, supporting growth, and enabling proper cellular function across various species.

The pharmaceutical industry has been one of the primary beneficiaries of natural product research.[65,66] Between 1981 and 2014, 33% of all Food and Drug Administration (FDA)-approved small-molecule drugs were either natural products or their derivatives.[66] In certain therapeutic areas, the impact of natural products is even more pronounced. For instance, in anti-cancer drugs, over 60% of approved drugs between 1981 and 2014 were derived from natural products.[66] Some of the most economically significant drugs derived from natural products include Paclitaxel (Taxol), a potent anti-cancer drug, with annual sales exceeding $1 billion at its peak. Paclitaxel (Taxol) was originally isolated from the bark of the Pacific yew tree (Taxus brevifolia). However, the low yield and ecological

concerns associated with harvesting yew bark led to the development of alternative production methods. Bristol-Myers Squibb (BMS) pioneered a semisynthetic approach using 10-deacetylbaccatin III (10-DAB), extracted from the renewable leaves and twigs of the European yew (Taxus baccata).[70] This process involves 11 chemical transformations and 7 isolations to convert 10-DAB into paclitaxel.[71] BMS developed a plant cell fermentation (PCF) technology to improve further sustainability, which cultivates specific Taxus cell lines in aqueous media under controlled conditions.[71] The PCF process eliminates the need for chemical transformations as it does not rely on traditional chemical synthesis methods, instead leverages biological processes within plant cell cultures to directly produce the target compound (paclitaxel), reducing the use of hazardous chemicals and solvents while allowing year-round production.[71] This innovative approach has significantly enhanced paclitaxel production's efficiency and environmental sustainability, ensuring a stable supply for cancer treatment.

Artemisinin is an anti-malarial drug derived from sweet wormwood (Artemisia annua) that has saved millions of lives worldwide.[72] It is now produced through semisynthesis to meet global demand. The process involves extracting artemisinic acid from genetically engineered yeast, which is then converted to artemisinin through photochemical oxidation.[72,73] This method, developed by Sanofi, has significantly increased artemisinin production capacity.[72,73]

Statins, a cholesterol-lowering drug inspired by compounds found in red yeast rice, has global sales of billions of dollars annually.[66] Statins are primarily produced through chemical synthesis. The most common statin, atorvastatin (Lipitor), is synthesized in a

multi-step process starting from (R)-4-cyano-3-hydroxybutyric acid, with a key step involving an asymmetric aldol reaction to form the statin core structure.[74] Other statins, like simvastatin, are produced by semisynthesis from lovastatin, obtained through fermentation of Aspergillus terreus.[75,76]

Red yeast rice, the natural source of statins, contains monacolins produced by fermenting rice with Monascus purpureus. Monacolin K, structurally identical to lovastatin, is the primary active compound.[77] However, due to variability in monacolin content and potential contamination, the FDA has issued warnings against using red yeast rice products as statin substitutes.[76,78] The pharmaceutical industry has developed more controlled and standardized methods for statin production to ensure consistent quality and efficacy. The economic impact of these and other natural product-derived drugs produced through a combination of methods, with a trend towards increased use of semisynthesis and total synthesis, is substantial, not only in direct sales but also in their contribution to public health and reduced healthcare costs.

The food and beverage industry relies heavily on natural products for flavours, colours, and preservatives. Essential oils, extracts, and other natural compounds enhance the taste and aroma of foods and drinks, for example, vanillin, which is the primary component of vanilla flavour. Although synthetically produced, it is still a natural product that has become a major global commodity.[79] Natural products are also increasingly important in cosmetics and personal care. The production of natural products involves complex biosynthetic pathways in living organisms, primarily utilizing building blocks derived from acetyl coenzyme A, shikimic acid, mevalonic acid, and 1-deoxyxylulose-5-phosphate.[60]

These pathways create various secondary metabolites with diverse biological activities. However, pharmaceutical companies often employ alternative methods for large-scale production due to the challenges of extracting and isolating compounds from natural sources.[80]

Pharmaceuticals and vitamins are primarily produced through three major approaches: Chemical synthesis involves creating compounds through controlled chemical reactions, often used for less complex molecules or those needed in large quantities.[60,80] Semisynthesis, which combines natural product extraction with chemical modification. For example, paclitaxel is produced by extracting 10-deacetylbaccatin from yew needles and performing a four-stage synthesis.[80] The third approach to the production is fermentation and biotechnology. Increasingly, genetically engineered microorganisms are used to produce pharmaceuticals and vitamins. For instance, artemisinic acid, a precursor to the antimalarial drug, is now produced using engineered yeast.[81] This method is particularly favoured for its sustainability and scalability.[81] These production methods aim to overcome the limitations of traditional natural product extraction, such as low yields, environmental variability, and sustainability concerns, while still harnessing the unique structural complexity and bioactivity of natural products.[80]

1.4.1 Value and Techniques for Localized Production of Natural Products

In recent years, there has been a growing interest in the localized production of natural products, driven by sustainability concerns, supply chain security, and the desire for higher-quality and more diverse compounds. Localized production of natural products offers significant value[82] utilizing local biomass resources can enhance sustainability and reduce

transportation costs. Key techniques include biorefinery processes, which integrate various biomass conversion methods to efficiently produce biofuels, chemicals, and pharmaceuticals. Microbial fermentation is another versatile technique, allowing for producing high-value products like antibiotics and vitamins from local resources, adaptable to meet local demand.[83] Localized production can enable the creation of a wider variety of natural products, including rare or endangered species that may not be viable for large-scale cultivation. This diversity is particularly valuable in drug discovery, where novel compounds can lead to breakthrough treatments.[84] Additionally, phytochemical extraction enables the harvesting of bioactive compounds from native plants,[85] contributing to the production of cosmetics and pharmaceuticals. Finally, incorporating green chemistry principles ensures these production techniques minimize environmental impact, promoting a more sustainable approach to natural product synthesis. Together, these techniques or methodologies cultivate a resilient framework for localized production, driving economic and environmental benefits.

1.5 Research Objective

The objectives of this thesis were:

- To develop a flow synthesis method to synthesize *L*-ascorbic acid from *D*-glucose.
- To achieve the protection of *L*-ornithine for synthesizing N5-Hydroxy-*L*-Ornithine towards the chemoenzymatic synthesis of Piperazic acid.

Moreover, this thesis will compare the flow synthesis and batch process methods for synthesizing *L*-ascorbic acid.

2. Flow Synthesis Method of Ascorbic Acid

2.1 Chapter Overview

The flow synthesis of *L*-ascorbic acid (vitamin C) explored in this study presents an alternative approach to traditional batch processes. It provides insights into alternative reaction conditions compared to traditional batch processes, demonstrating potential reaction time and yield improvements. This chapter examines the initial efforts in applying flow chemistry techniques to specific steps in synthesizing *L*-ascorbic acid from *D*-glucose, comparing these flow processes with their batch counterparts. The conversion of selected batch reaction steps to continuous flow processes is investigated, focusing on synthesizing key intermediates in the *L*-ascorbic acid production pathway. Reaction parameters and yields will be compared between batch and flow methods for specific synthetic steps. The results of these flow chemistry experiments on selected steps in the ascorbic acid synthesis will be presented, as well as reaction times and yields for these specific transformations between batch and flow methods.

2.1.1 Value and Production of Ascorbic Acid

Vitamins are organic substances crucial for normal physiological functions in living organisms, particularly in higher forms of animal life.[86] These micronutrients are required in small quantities for various critical processes within the body, including growth, development, and overall health maintenance.[86] Unlike macronutrients such as proteins, carbohydrates, and lipids, vitamins generally cannot be synthesized by the body in sufficient amounts to meet its needs. They must be obtained through diet or supplementation.[86] There are 13 essential vitamins, each serving distinct yet often

overlapping bodily functions.[87] These vitamins are categorized according to their solubility: fat-soluble vitamins (A, D, E, and K) and water-soluble vitamins (C and the B-complex vitamins).[87]

L-ascorbic acid (Figure 9), also known as vitamin C, is one of these essential vitamins. As a water-soluble vitamin, it is not stored in the body and must be regularly consumed through diet or supplementation.[87,88,89,90] Ascorbic acid is primarily used to treat and prevent scurvy, an illness resulting from a severe lack of this essential nutrient.[90,91] Scurvy manifests symptoms such as fatigue, joint pain, gum disease, and poor wound healing.[90–92] Beyond its crucial role in combating scurvy, ascorbic acid offers a range of health benefits. It supports the immune system,[92,93] helps the body fight infections and illnesses, forms and maintains bones, cartilage, skin, and blood vessels, and acts as an antioxidant.[92] It is also essential for the formation of collagen,[94] a protein that is vital for the health of the skin, bones, and blood vessels. Vitamin C is an antioxidant, protecting the body from damage caused by free radicals, which may contribute to aging and developing certain diseases.[95] Among all vitamins, it stands out as the simplest in structure and was one of the pioneering vitamins to be isolated, characterized, purified, and have its molecular structure elucidated.[96] *L*-ascorbic acid is the biologically active form of Vitamin C. The recommended dietary allowances (RDAs) for vitamin C vary by age and gender, with fruits and vegetables[89] being the best sources of this vitamin.

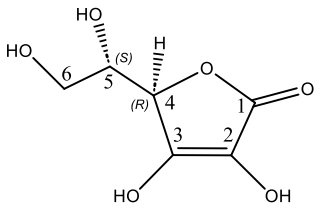

Figure 9: Chemical structure of L-ascorbic acid (vitamin C)

Vitamin C exists primarily as *L*-ascorbic acid in nature, with its primary interconversion occurring between *L*-ascorbic acid and its oxidized form, dehydro-*L*-ascorbic acid (DHA), through a reversible redox reaction (Figure 10).[97,98] This oxidation process involves losing electrons and protons sequentially, transforming *L*-ascorbic acid to a semi-dehydroascorbate radical and then to DHA. The oxidation of *L*-ascorbic acid to DHA occurs in two steps: *L*-ascorbic acid loses one electron and one proton to form an intermediate called semidehydroascorbate (also known as ascorbyl radical), then semidehydroascorbate loses another electron and proton to form DHA.[97,98] This oxidation process can occur spontaneously in the presence of oxygen. Still, it is accelerated by various factors such as heat, light, and metal ions like iron or copper.[99] The reaction is pH-dependent, with oxidation occurring more rapidly in alkaline conditions.[100] *L*-ascorbic acid demonstrates biological activity, making it the sole form valuable for medical applications.[97]

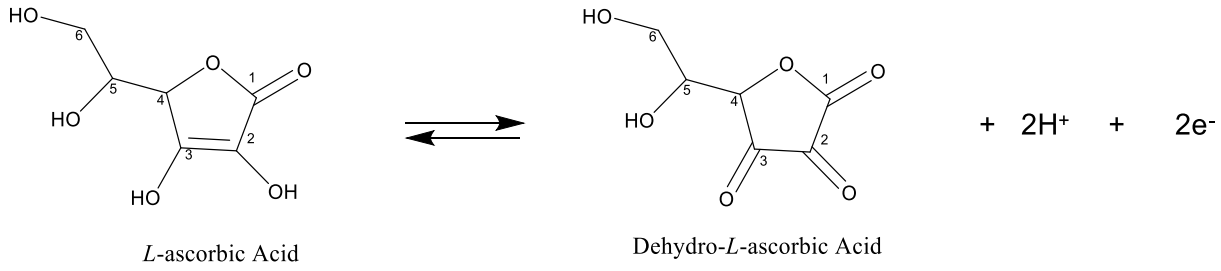

Figure 10: The oxidation process of L-ascorbic acid to DHA losing protons and electrons

Historically, vitamin C deficiency, known as scurvy,[91,96] was a significant health concern, particularly among sailors and explorers who lacked access to fresh fruits and vegetables during long voyages, which led to the need for vitamin C production.[96] Its symptoms include hemorrhaging from mucous membranes, a significant decrease in red blood cell

count leading to anemia, and, if left untreated, is ultimately fatal.[89,91,96] In 1937, Dr. Albert Szent-Györgyi was awarded the Nobel Prize in Physiology or Medicine for his groundbreaking work isolating the vitamin C molecule from red peppers and elucidating its crucial role in preventing scurvy.[94,97] Ascorbate, the less acidic or salt form of vitamin C,[101] is synthesized by many vertebrates. In fish, amphibians, and reptiles, ascorbate is synthesized in the kidneys, whereas in mammals, the liver is responsible for its production.[101]

2.1.2 Global Market and Applications

The global market for ascorbic acid has been experiencing steady growth, driven by increasing awareness of its health benefits and expanding applications across multiple sectors. The global ascorbic acid market was valued at USD 1.7 billion in 2023 and is projected to reach USD 2.9 billion by 2033, growing at a compound annual growth rate (CAGR) of 5.60%.[102] This growth is attributed to several factors, including rising consumer health consciousness, increasing demand for fortified food and beverages, and expanding applications in pharmaceuticals and personal care products.[102]

Roughly 110 kilotons of vitamin C are produced annually[89,95] which is used primarily by the pharmaceutical industry (50 %), followed by the use of antioxidants in food (25 %) and beverages sector (15 %). Only about 10 % of the vitamins are used for animal feed applications.[95] This contrasts with all other vitamins, where the feed sector is the major application area of vitamins. More than 80 % of today's world demand for vitamin C is satisfied by Chinese producers, with the remaining production distributed across the European Union (particularly Germany and the Netherlands), India, the United States,

Mexico, and a few other countries.[103] However, these collectively represent a small fraction of global vitamin C manufacturing. In the late 1950s, Chinese production capacity was only 30 tons annually.[95] Supply was controlled by big European and Japanese manufacturers such as Roche, BASF, Merck, and Takeda Pharmaceutical.[89,95] By the early 1990s, 26 Chinese manufacturers had already gained one-third of the world's vitamin C market.[89,95] Recognizing the threat, the established producers tried to prevent Chinese companies from entering the market through several severe price cuts. By 2002, only four Chinese manufacturers had survived, and the price had hit record lows.[89,95] Since 2002, the production and export activities of Chinese vitamin C manufacturers have been under the supervision of the trade association CCCMHPIE (China Chamber of Commerce for Import and Export of Medicines and Health Products),[89,95] which is close to the Ministry of Commerce of the central Chinese Government. Today's leading Chinese producers are Northeast Pharmaceutical Group Co., Ltd (NEPG) of Shenyang Liaoning Province, Weisheng Pharmaceutical Company (CSPC) of Shijiazhuang, Hebei Province, Welcome Pharmaceutical Company (NCPC), Shijiazhuang, Hubei Province, and Jiangsu Jiangshan Pharmaceutical (new name is Aland Nutraceutical Co., Ltd.) of Jingjiang, Jiangsu Province.[89,95] The global market for ascorbic acid is robust and diverse, with applications spanning multiple industries. Its role in promoting health and wellness and its functional properties in food preservation and personal care ensure a steady demand. As consumer awareness grows and new applications emerge, the ascorbic acid market is set to experience further expansion. However, industry players must navigate challenges such as sustainability concerns and regulatory requirements to capitalize on these opportunities fully.

2.1.3 Industrial Production Methods

Traditionally, the industrial production of ascorbic acid has relied on the Reichstein-Grussner process.[89,96] Since its first chemical synthesis in 1933,[89,96] the industrial production of ascorbic acid has evolved considerably, driven by increasing demand across various sectors, including pharmaceuticals, food and beverages, and cosmetics.

2.1.3.1 Reichstein Process

The Reichstein process is a chemical and microbial method for the industrial production of *L*-ascorbic acid (vitamin C) from D-glucose. It was designed in 1933[95] with optimizations over time[95] and has been a mainstay in vitamin C production for over 60 years.[95,104] The process as shown in Scheme 1 involves several steps, including the hydrogenation of *D*-glucose to *D*-sorbitol, followed by microbial oxidation or fermentation of sorbitol to *L*-sorbose,[89,95] the conversion of *L*-sorbose into 2-keto-L-gulonic acid, which is a key intermediate[89] in the production of vitamin C and, finally, the lactonization of 2-keto-*L*-gulonic acid to give ascorbic acid.

Various reduction strategies are used to reduce *D*-glucose to *D*-sorbitol.[105–107,107,108] One of these strategies is catalytic transfer hydrogenation[105,106] which involves using a catalyst to facilitate hydrogen transfer, leading to the efficient reduction of *D*-glucose to *D*-sorbitol. *D*-glucose is hydrogenated to *D*-sorbitol using a catalyst such as nickel.[105,106] Under high temperature and pressure, this reduction has been achieved most recently in industrial settings. This process has been optimized to achieve a high yield of *D*-sorbitol.[89,106] Another strategy is utilizing supported metal catalysts such as ruthenium (Ru) supported on MCM-41[107,108] or ZSM-5,[108] is an effective strategy for the conversion of *D*-glucose into *D*-

sorbitol. Another strategy is the use of carbonized cassava dregs- supported ruthenium nanoparticles as a catalyst[107] which has been studied for the efficient conversion of *D*-glucose into *D*-sorbitol, demonstrating the influence of carbonization temperature on the *D*-glucose conversion and *D*-sorbitol yield. These strategies demonstrate the diverse approaches employed in reducing *D*-glucose to *D*-sorbitol, each with its own advantages and considerations.

The next step is the microbial oxidation or fermentation of sorbitol to *L*-sorbose. The most prominent industrial method of producing *L*-sorbose is the biotransformation of *D*-sorbitol to *L*-sorbose in Gluconobacter or Acetobacter species.[109,110] During the process, two hydrogen atoms were removed from one *D*-sorbitol molecule to form one *L*-sorbose molecule. This two-step fermentation method used in the industrial production of vitamin C includes both chemical reaction and biological fermentation steps, making it difficult to replicate synthetically.[111] The microbial oxidation or fermentation of *D*-sorbitol to *L*-sorbose is important to oxidize the correct secondary alcohol due to the regiospecificity of the enzymatic reaction. This process involves converting the alcohol group at the C-5 position of *D*-sorbitol to a ketone group at the C-5 position of *L*-sorbose, as shown in Figure 11. This regiospecificity is essential for producing *L*-sorbose,[109] which is a crucial intermediate in the industrial synthesis of vitamin C (ascorbic acid). Achieving this regiospecific oxidation synthetically would be challenging due to the need for highly selective and controlled chemical reactions[109] to specifically target the C-5 position of *D*-sorbitol without affecting other functional groups or carbon positions. Microbial fermentation offers a more efficient and selective approach to achieve this regiospecific oxidation, as the enzymes involved in the process exhibit high selectivity for the targeted alcohol group,[109] leading to near-

quantitative yields of *L*-sorbose.

Doing this process synthetically is challenging due to the complexity of the biochemical reactions involved and the need for specific enzymes and microorganisms to catalyze the conversion.[111] Furthermore, the use of protective groups and the specific conditions required for microbial oxidation or fermentation add to the complexity of synthetic production.

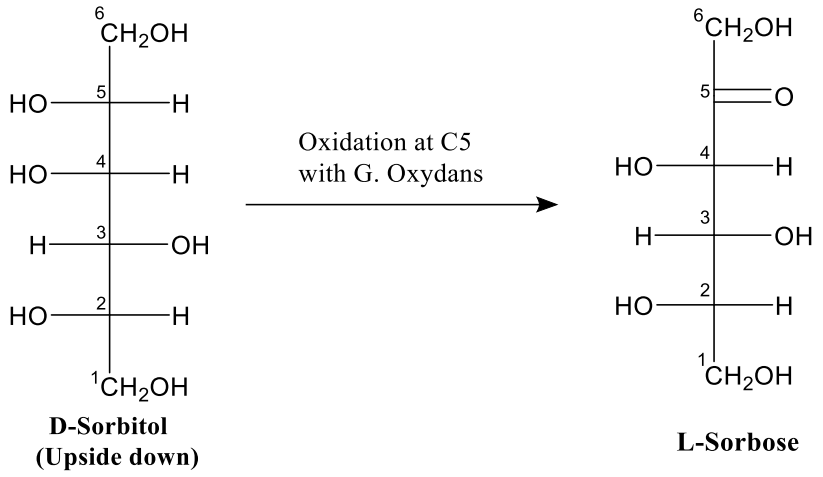

Figure 11: Regioselective oxidation of D-Sorbitol at C5 using Gluconobacter Oxydans to L-Sorbose

D-sorbitol, which is a sugar alcohol, is oxidized to *L*-sorbose by G. Oxydans.[89] This microbial oxidation process is preferred over chemical oxidation due to the microbial enzymes' specificity. Microorganisms possess highly specific enzymes that can selectively oxidize the C-5 alcohol group of *D*-sorbitol to form *L*-sorbose,[109] while chemical oxidation may lead to overoxidation/ the formation of undesired by-products.[89,112] Therefore, the use of microbial fermentation in the Reichstein process ensures the production of *L*-sorbose,[112] which is a key intermediate in the synthesis of vitamin C.[113] Subsequently, the 4 hydroxyl groups in *L*-sorbose are protected by forming an acetal[95] with acetone and an acid, leading to the production of diacetone-*L*-sorbose.[95] The next step involves organic oxidation with

potassium permanganate to produce diprogulic acid, which is then heated with water to yield 2-keto-*L*-gulonic acid. The process is then completed with a ring-closing step or gamma lactonization with water removal.[89,95]

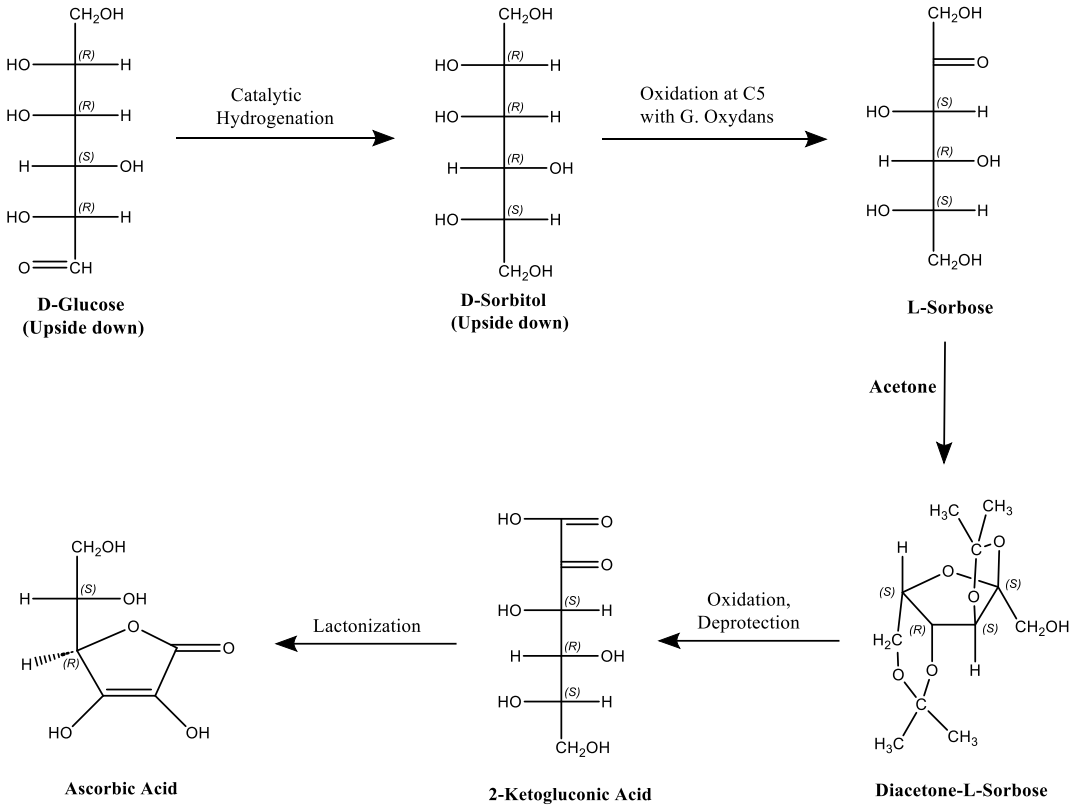

Scheme 1: The Reichstein process for vitamin C synthesis. The L-configuration of ascorbic acid is derived from D-glucose by inversion of the carbon skeleton.

2.1.3.2 Advantages and Limitations of Reichstein Process

The Reichstein process is known for its high conversion efficiency and chemically stable intermediate production. As discussed earlier, it is a well-established and widely used method that has been used for over six decades, providing a reliable approach to vitamin C production.[89,114] Secondly, the process has demonstrated commercial viability and has been used to meet the global demand for *L*-ascorbic acid.[95]

However, despite its advantages, the process presents several challenges and limitations. First, it is characterized by a long production time, which can impact overall productivity and efficiency.[114] The process involves complex chemical and microbial steps, leading to

operational challenges and specialized expertise requirements.[89,114] For example, the hydrogenation step in the process necessitates high temperature and pressure, resulting in increased energy consumption and operational costs.[89,114] Furthermore, the process uses toxic chemicals, raising environmental and safety concerns.[14] The continuous operation of the process can also be challenging, further impacting its efficiency and cost-effectiveness.[114]

Despite these drawbacks, the Reichstein process remains a significant industrial route for Vitamin C production due to its high overall yield and other economic factors. Efforts are being made to find alternatives to this process, such as two-step fermentation, which has been shown to have lower capital and operating costs. Therefore, while the Reichstein process has been instrumental in vitamin C production, it is important to address these challenges and limitations to improve the overall efficiency and sustainability of the production process. Nevertheless, the Reichstein process is only efficient if produced in massive industrial processes.[89,111,115,116] Canada has no local production process and is vulnerable to worldwide shortages.[117] This calls for a more efficient method of vitamin C production that is not dependent on fermentation. Given the benefits of flow synthesis, this thesis explores this method for vitamin C production.

2.1.4 Challenges in Traditional Synthesis

While long-established and versatile, traditional batch synthesis faces several significant challenges in modern chemical manufacturing. One primary issue is the inconsistency in product quality between batches, as replicating exact conditions for each batch is difficult.[16,118] This variability can lead to increased quality control costs and potential product rejections. Batch processes are also time-consuming and resource-intensive, with

considerable downtime between batches for cleaning and preparation.[16,118] The fixed batch sizes often result in underutilized equipment, reducing overall efficiency.[118] From a safety perspective, batch reactions can pose risks due to accumulating reactive intermediates or heat, especially in exothermic processes.[118] Scalability is another major challenge; what works well in a laboratory setting may not translate directly to industrial-scale production, often requiring extensive and costly process development.[16,118] Environmental concerns are also significant, as batch processes typically generate more waste and consume more energy than continuous methods.[118] Additionally, batch synthesis often struggles with reactions requiring precise temperature control or involving highly reactive intermediates.[118] The pharmaceutical industry faces regulatory hurdles when transitioning from batch to continuous processes, as defining a "batch" for regulatory filings becomes complex in continuous manufacturing.[118] These challenges collectively push the industry towards exploring more efficient and sustainable alternatives, such as flow chemistry, which offers potential solutions to many of these issues.

2.2 Developing Flow Synthesis of Ascorbic Acid

The proposed flow synthesis of ascorbic acid would involve a series of interconnected steps, each requiring careful optimization. This research investigates the feasibility of translating key steps in the ascorbic acid synthesis pathway from batch flow processes. This study focuses on specific transformations within the overall synthesis to evaluate potential advantages in reaction efficiency, yield, and process control that flow chemistry might offer compared to traditional batch methods. The proposed flow synthesis relies heavily on the Reichstein process since it is an established methodology, with the key goal of translating the batch synthesis (Scheme 2) into a flow methodology. To do so, each

synthetic reaction must first be developed using batch methodology and then translated to flow synthesis techniques.

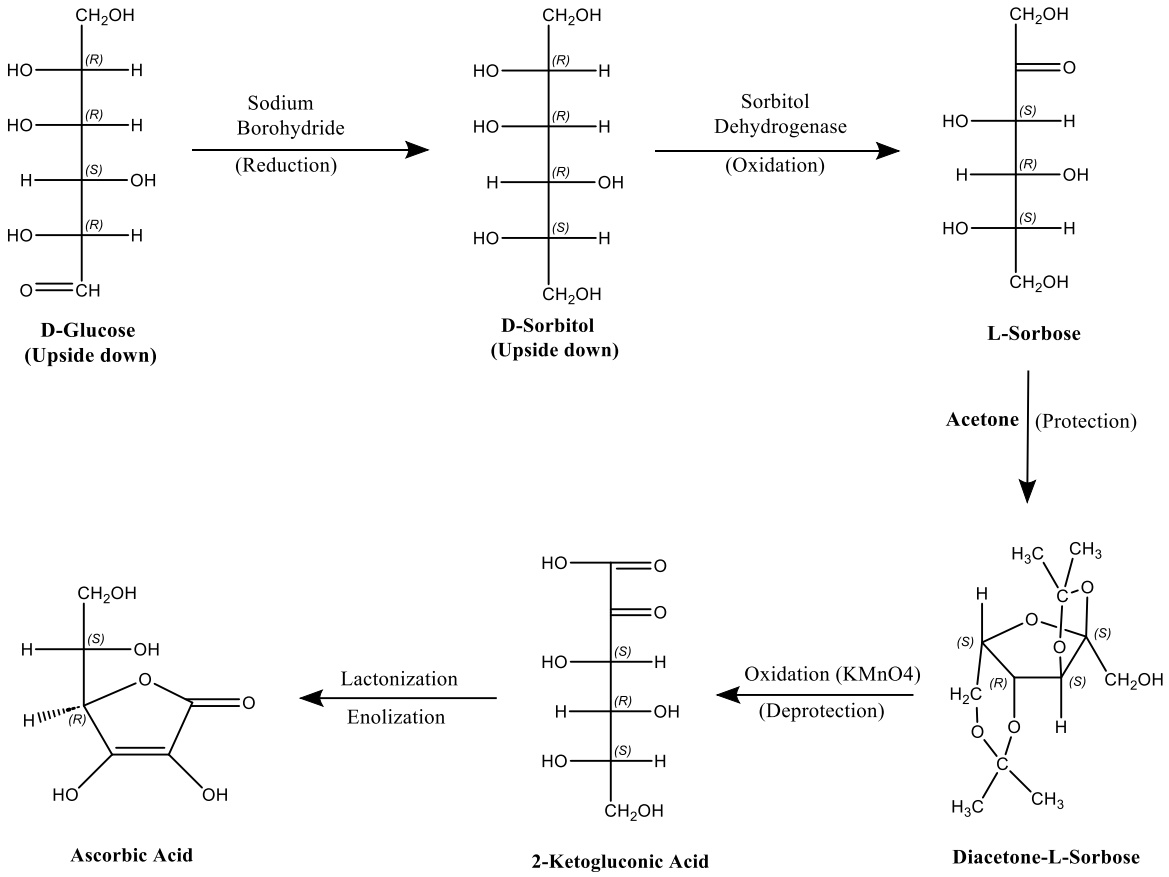

Scheme 2: The proposed methodology for the synthesis of L-ascorbic acid from D-glucose

Scheme 3 shows the proposed method for synthesizing *L*-sorbitol from *D*-glucose in batch and flow. *D*-glucose will be reduced to *D*-sorbitol using the reducing agent sodium borohydride ($NaBH_4$). In Scheme 4, the synthesis is done in the batch, and the reaction is carried out in a round bottom flask, first for the acetonation of *L*-sorbose to diacetone-*L*-sorbose, then the oxidation of diacetone-*L*-sorbose to 2-keto-*L*-gulonic acid using potassium permanganate, and then the lactonization reaction of 2-keto-*L*-gulonic acid to obtain ascorbic acid.

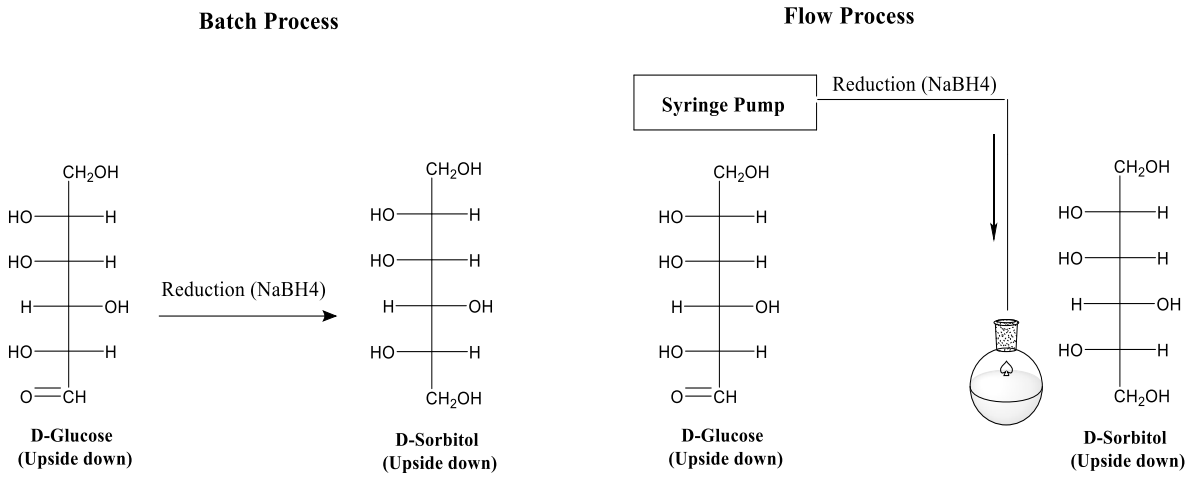

Scheme 3: The proposed methodology (batch and flow process) for the synthesis of D-sorbitol from D-glucose

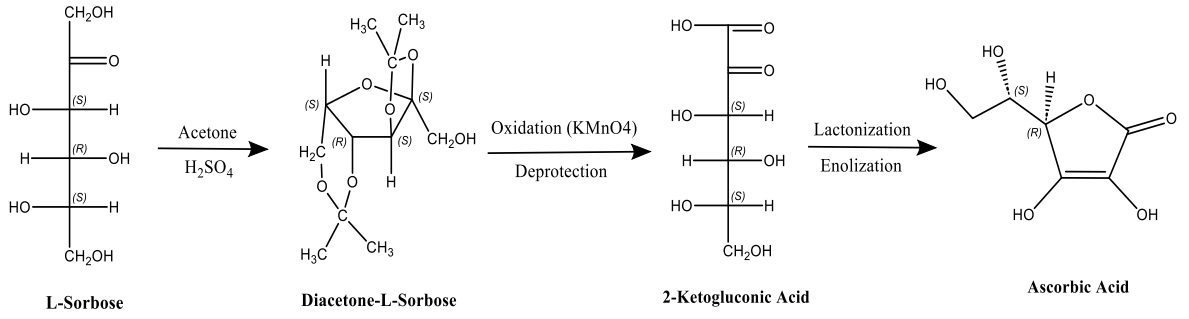

Scheme 4: The proposed methodology/three-batch reaction for vitamin C synthesis from L-sorbose

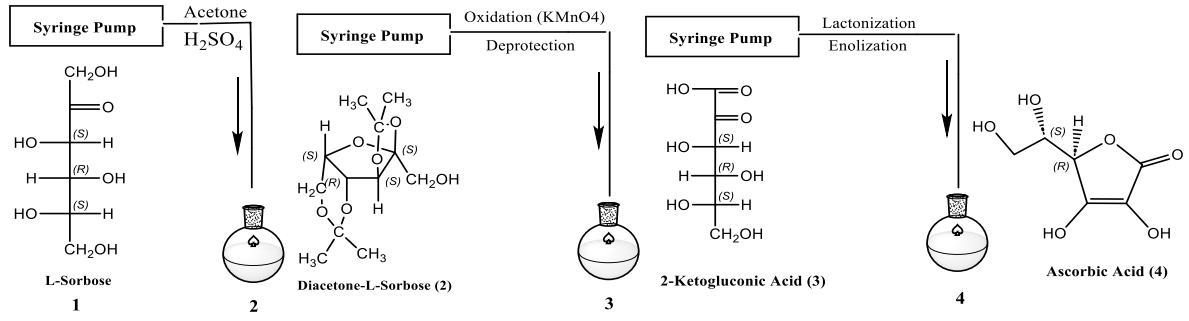

Scheme 5: The proposed methodology/ flow reaction for vitamin C synthesis from L-sorbose

Scheme 5 above shows the method for synthesizing ascorbic acid from *L*-sorbose in flow systems. In Scheme 5, the reactions are done individually, as described in Scheme 4, but in the flow. Ascorbic acid is obtained after the lactonization of 2-keto-*L*-gulonic acid.

The following subsections will discuss the development of the discrete flow synthesis steps utilizing first batch techniques and then transitioning to flow techniques to conduct the reactions of *D*-glucose to *D*-sorbitol and from *L*-sorbose to ascorbic acid, examining the challenges encountered and the strategies employed to overcome them. The goal of the research was to prepare for continuous flow synthesis of Vitamin C. Continuous flow synthesis methodology consists of directly feeding the products of one reaction as the starting material of the next. Although the work described is for discrete flow synthesis steps, minimal purification was undertaken after each step to use the product of the preceding reaction in the subsequent reaction to prepare and plan for transitioning this work to continuous flow synthesis.

2.2.1 *D*-glucose Reduction to Sorbitol in Batch and Flow

2.2.1.1 *D*-glucose Reduction to Sorbitol in Batch – Trial 1

For the batch synthesis, which was done first to obtain parameters for the flow, *D*-glucose (1.01 g, 5.61 mmol) was dissolved in 20 mL of dH_2O. $NaBH_4$ (0.1142 g, 3.02 mmol) dissolved in 10 mL of dH_2O was added to this solution. The solution was allowed to react at room temperature with constant stirring for 20 minutes, as this reaction time was sufficient for conversion based on preliminary optimization studies. After this, to react any excess $NaBH_4$ in the reaction mixture, glacial acetic acid (6 mL) was added dropwise until

universal pH indicator paper indicated the reaction mixture was acidified below 7. Once moderately acidic, the solvent evaporated to dryness under reduced pressure. Excess H_2O was removed, leaving *D*-sorbitol as a white powder (0.821 g, 4.51 mmol, 80%) and analyzed by NMR (300 MHz, DMSO-d_6) and IR. See Figure 12 and Appendices A 1, A 2 and A 3.

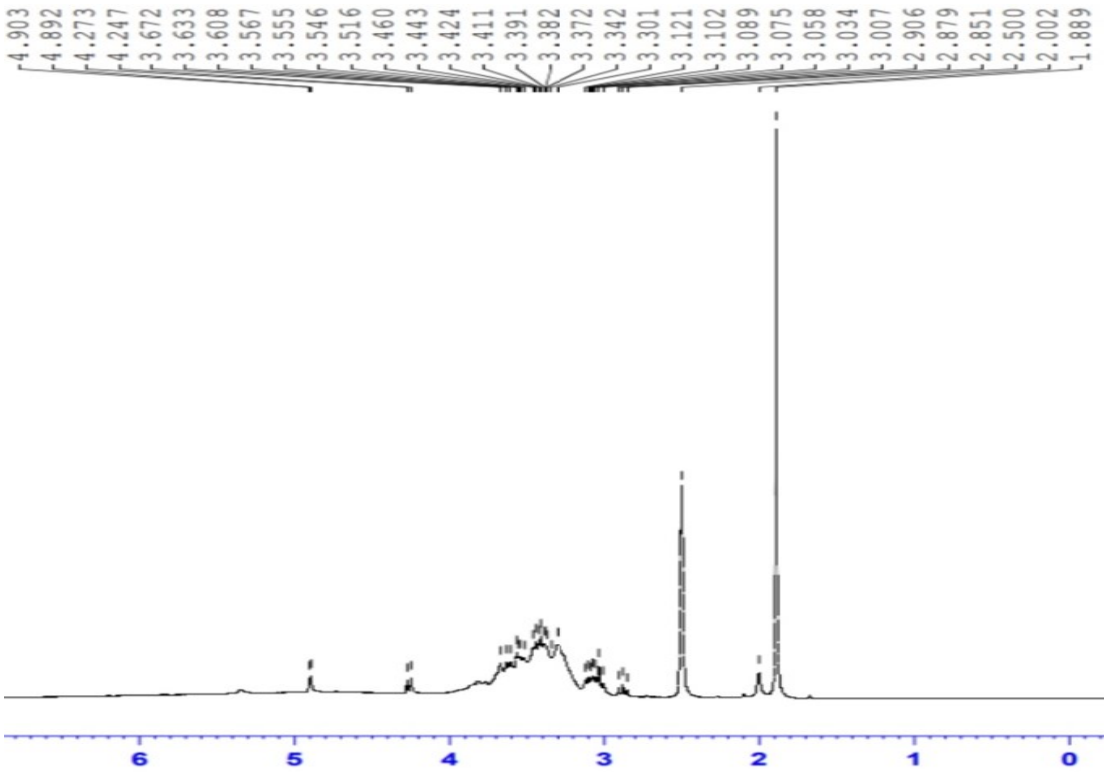

Figure 12: Sorbitol ^{1}H-NMR for Batch 1 recorded in DMSO-d_6 (300 MHz).

2.2.1.2 *D*-glucose Reduction to Sorbitol in Flow – Trial 2

A flow system was set up using PTFE tubing (0.75 mm inner diameter) and syringe pumps, as shown in Scheme 6. *D*-glucose (1.02 g, 5.66 mmol) was dissolved in 20 mL of dH_2O and added to the flow at a 2 ml/min flow rate from a first Pump A. $NaBH_4$ (0.1407 g, 3.72 mmol) dissolved in 10 mL of dH_2O was added to the flow simultaneously at a 1 ml/min flow rate

from a second Pump B. The reaction mixture introduced into the flow system via a T-mixer (T-mixer 1) was passed through a reactor coil maintained at ambient temperature (20 ± 2°C). This temperature was consistently maintained throughout the reaction zone to ensure uniform conditions. Glacial acetic acid (5 mL) was added to the flow at a 0.5 ml/min flow rate from a third Pump C. The product was obtained following a 10-minute residence time in the reactor, and the solvent was evaporated to dryness under reduced pressure. Excess H_2O was removed, leaving *D*-sorbitol as a white powder (1.02 g, 5.59 mmol, 100%) analyzed by NMR (300 MHz, DMSO-d_6). See Figure 13 and Appendices A 4 and A 5.

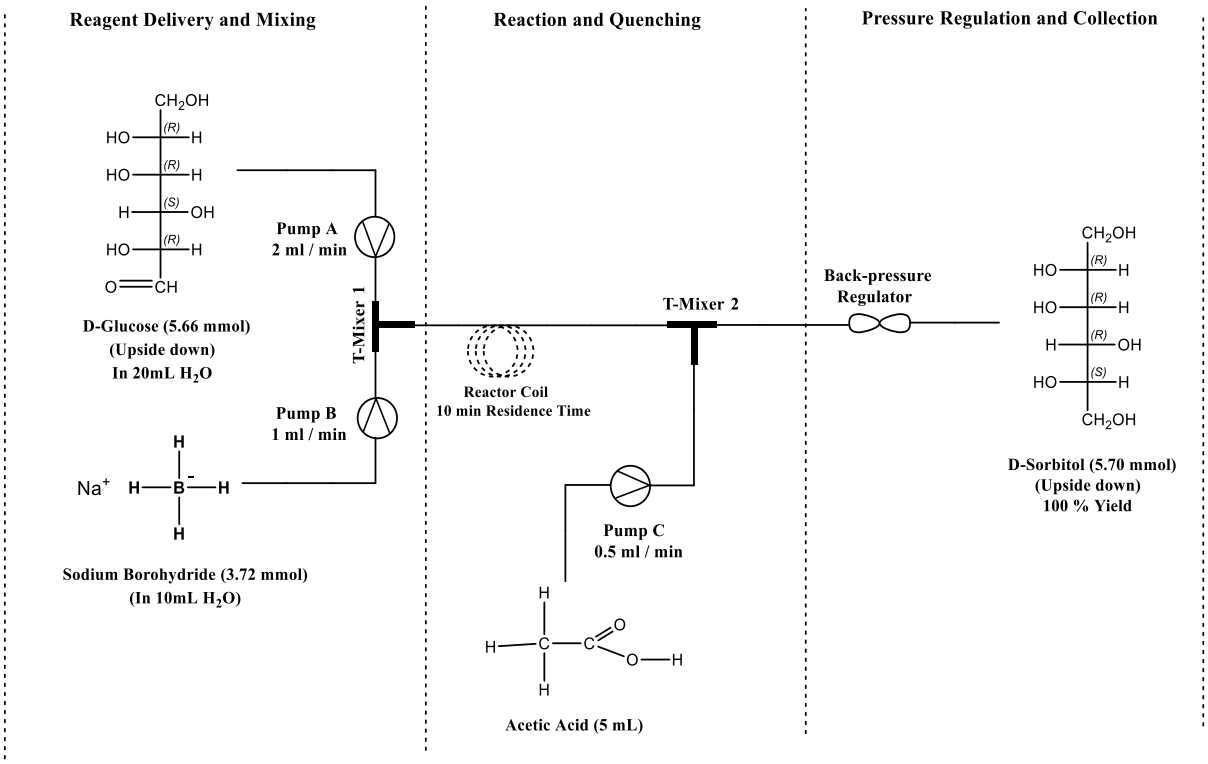

Scheme 6: Reduction of D-glucose to D-sorbitol in the flow – trial 2

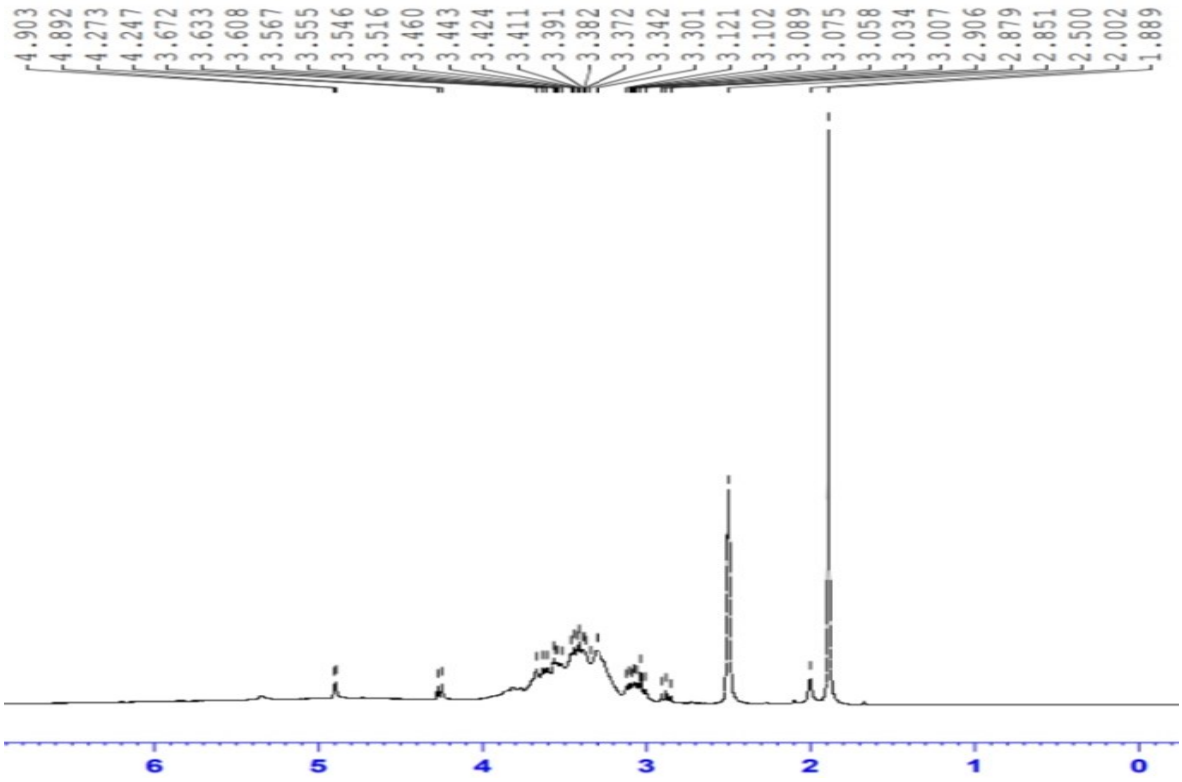

Figure 13: Sorbitol ^{1}H-NMR for Flow 2 recorded in DMSO-d_6 (300 MHz).

2.2.1.3 *D*-glucose Reduction to Sorbitol in Batch – Trial 3

D-glucose (1.01 g, 5.61 mmol) was dissolved in 20 mL of dH_2O. $NaBH_4$ (0.1097 g, 2.90 mmol) dissolved in 10 mL of dH_2O was added to this solution. The solution was allowed to react at room temperature with constant stirring for 30 minutes. After this, Glacial acetic acid (1.5 mL) was added dropwise until the universal pH indicator paper indicated that the reaction mixture was moderately acidic. The product was obtained, and the solvent was evaporated to dryness under reduced pressure. Excess H_2O was removed, leaving *D*-sorbitol as a white powder (1.02 g, 5.59 mmol, 100%) analyzed by NMR (300 MHz, DMSO-d_6) and IR. See Figure 14 and Appendices A 6, A 7, A 8 and A 9.

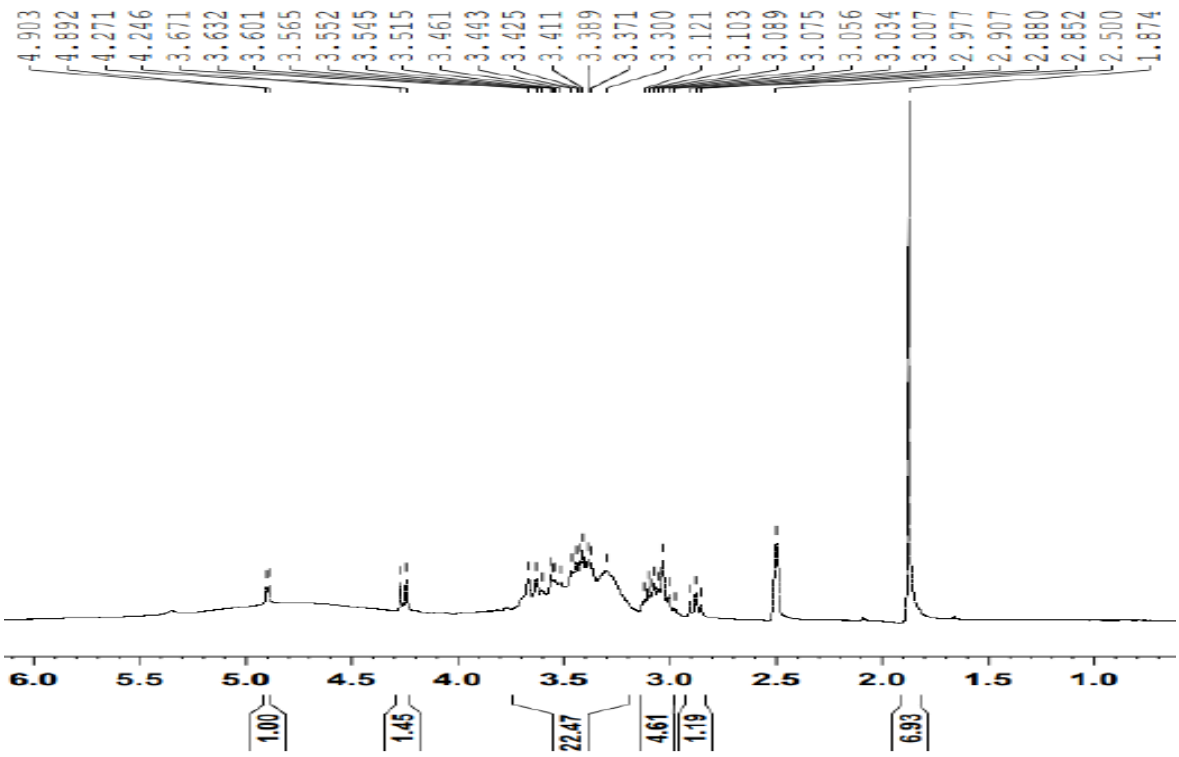

Figure 14: Sorbitol ^{1}H-NMR for Batch 3 recorded in DMSO-d_6 (300 MHz).

2.2.1.4 *D*-glucose Reduction to Sorbitol in Batch – Trial 4

Glacial acetic acid was not used for this trial, and the reaction time was increased to 40 minutes. *D*-glucose (1.02 g, 5.66 mmol) was dissolved in 20 mL of dH_2O. $NaBH_4$ (0.1093 g, 2.89 mmol) dissolved in 10 mL dH_2O was added to this solution. The solution was allowed to react at room temperature with constant stirring for 40 minutes. The product was obtained, and the solvent was evaporated to dryness under reduced pressure. Excess H_2O was removed, leaving *D*-sorbitol as a white powder (1.01 g, 5.54 mmol, 100%) analyzed by NMR (300 MHz, DMSO-d_6) and IR. See Figure 15 and Appendices A 10 to A 13.

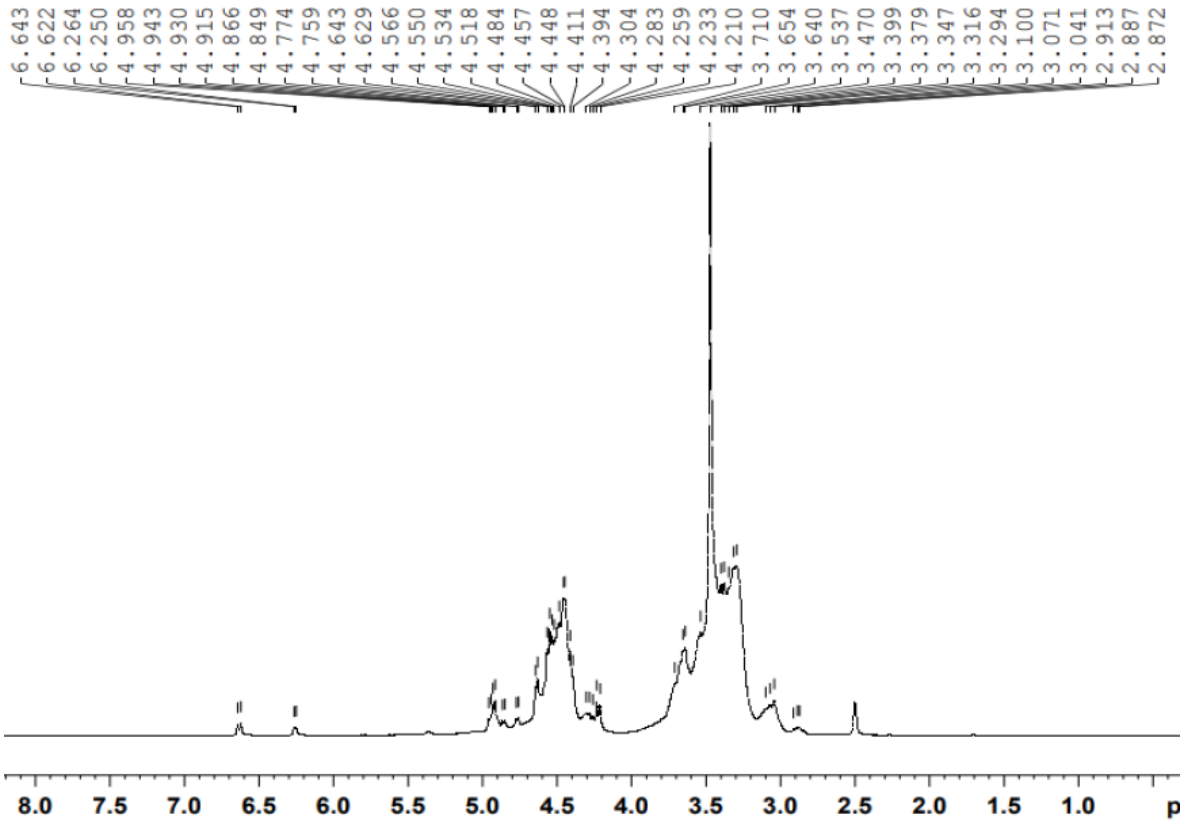

Figure 15: Sorbitol ^{1}H-NMR for Batch 4 recorded in DMSO-d_6 (300 MHz).

2.2.1.5 *D*-glucose Reduction to Sorbitol in Batch – Trial 5

Glacial acetic acid was not used for this trial, and the reaction time was increased to 60 minutes. *D*-glucose (1.10 g, 6.10 mmol) was dissolved in 20 mL of dH_2O. $NaBH_4$ (0.1480 g, 3.91 mmol) dissolved in 10 mL of dH_2O was added to this solution. The solution was allowed to react at room temperature with constant stirring for 60 minutes. The product was obtained, and the solvent was evaporated to dryness under reduced pressure. Excess H_2O was removed, leaving *D*-sorbitol as a white powder (1.04 g, 5.70 mmol, 93%) analyzed by NMR (300 MHz, DMSO-d_6). See Figure 16 and Appendices A 14 and A 15.

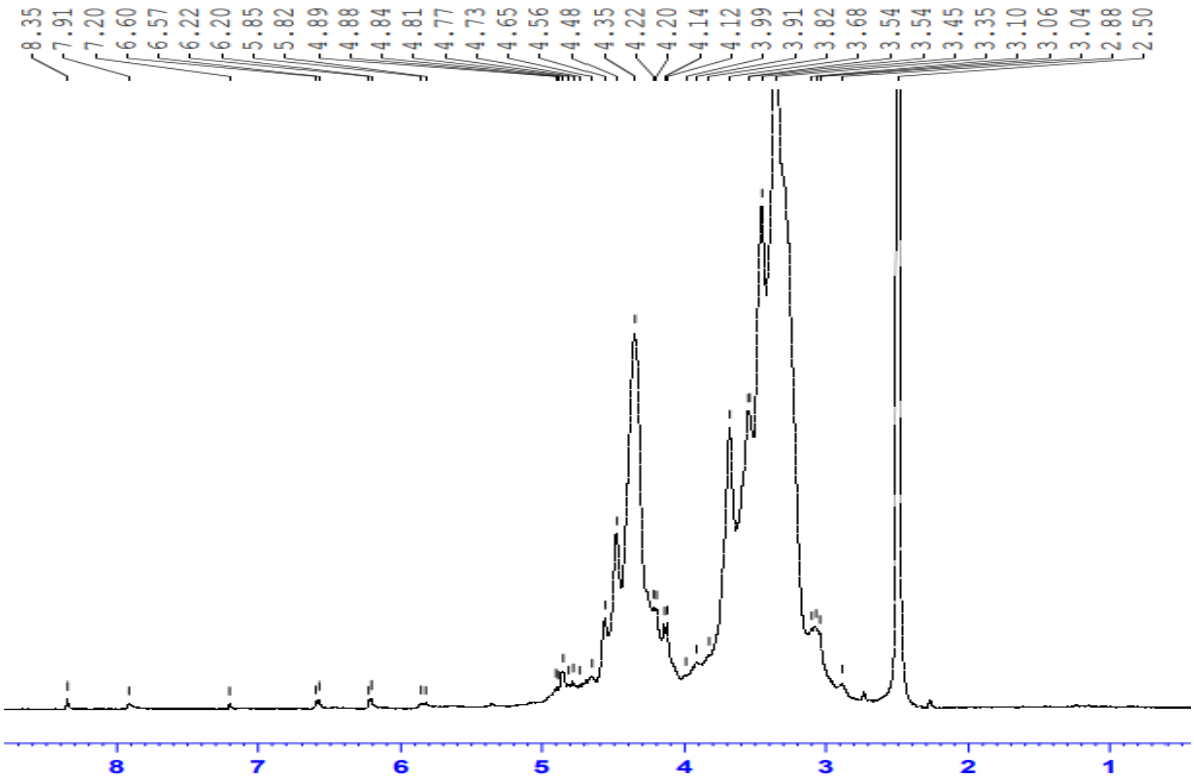

Figure 16: Sorbitol ^{1}H-NMR for Batch 5 recorded in DMSO-d_6 (300 MHz).

2.2.1.6 *D*-glucose Reduction to Sorbitol in Batch – Trial 6

In this trial, the amount of $NaBH_4$ was increased. *D*-glucose (1.05 g, 5.83 mmol) was dissolved in 20 mL of dH_2O. $NaBH_4$ (0.1755 g, 4.64 mmol) dissolved in 10 mL of dH_2O was added to this solution. The solution was allowed to react at room temperature with constant stirring for 60 minutes. The product was obtained, and the solvent was evaporated to dryness under reduced pressure. Excess H_2O was removed, leaving *D*-sorbitol as a white powder (1.03 g, 5.65 mmol, 97%) analyzed by NMR (300 MHz, DMSO-d_6). See Figure 17 and Appendices A 16 and A 17.

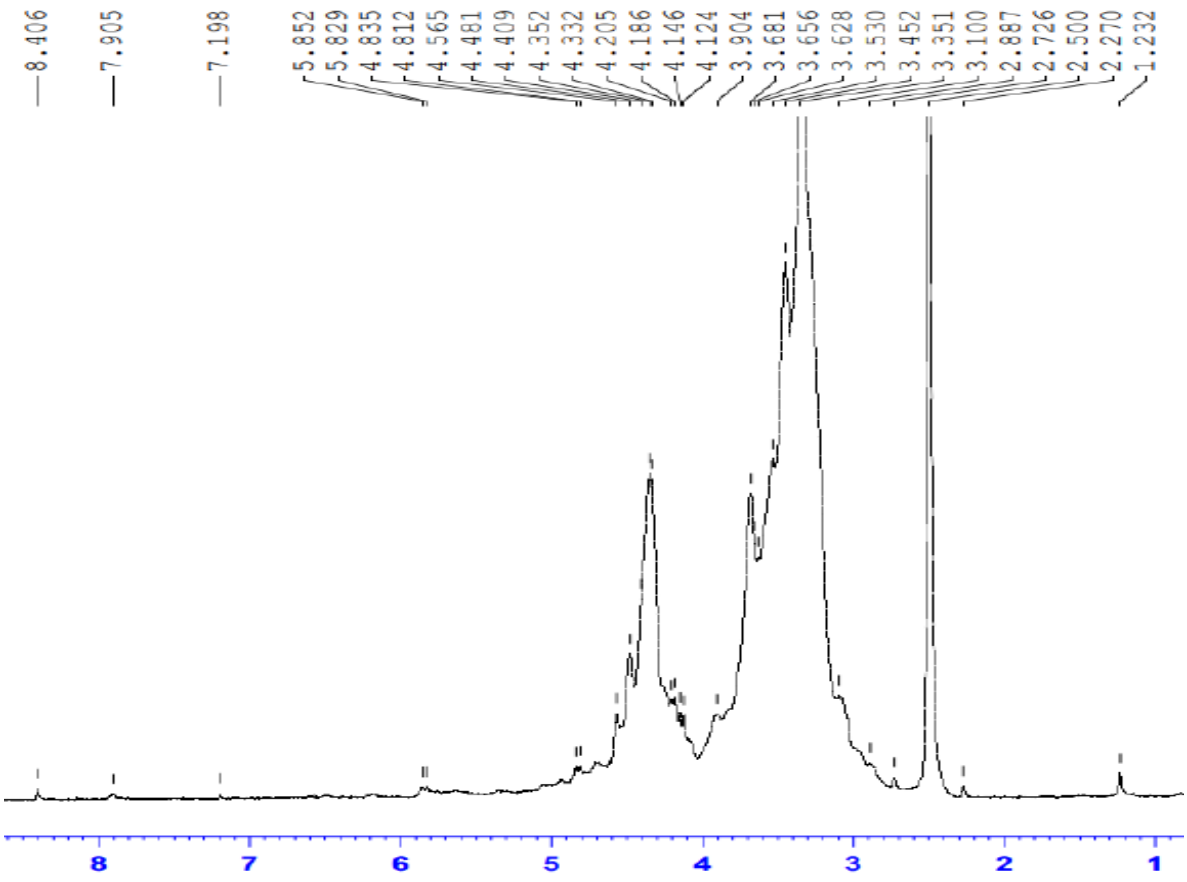

Figure 17: Sorbitol ^{1}H-NMR for Batch 6 recorded in DMSO-d_6 (300 MHz).

2.2.1.7 *D*-glucose Reduction to Sorbitol in Batch – Trial 7

In this trial, the amount of $NaBH_4$ used for the reaction and reaction time was increased. *D*-glucose (1.02 g, 5.66 mmol) was dissolved in 20 mL of dH_2O. $NaBH_4$ (0.2005 g, 5.30 mmol) dissolved in 10 mL of dH_2O was added to this solution. The solution was allowed to react at room temperature with constant stirring for 105 minutes. The product was obtained, and the solvent was evaporated to dryness under reduced pressure. Excess H_2O was removed, leaving *D*-sorbitol as a white powder (1.02 g, 5.59 mmol, 99%) analyzed by NMR (300 MHz, DMSO-d_6). See Figure 18 and Appendix A 18.

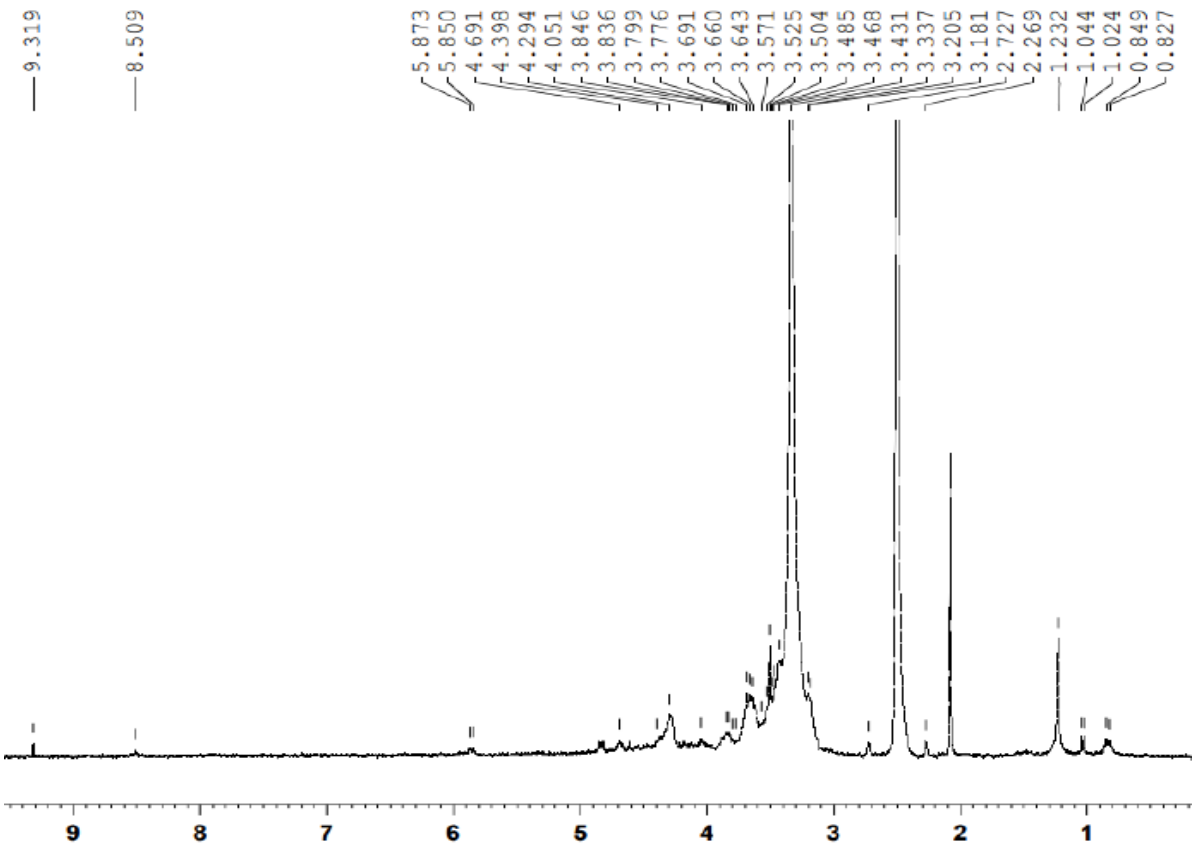

Figure 18: Sorbitol ^{1}H-NMR for Batch 7 recorded in DMSO-d_6 (300 MHz).

2.2.1.8 *D*-glucose Reduction to Sorbitol in Batch – Trial 8

In this trial, the reaction time was increased, $NaBH_4$ was increased at intervals, and aliquots were collected to monitor the sorbitol synthesis. *D*-glucose (1.07 g, 5.94 mmol) was dissolved in 20 mL of dH_2O. $NaBH_4$ (0.1137 g, 3.01 mmol) dissolved in 10 mL of dH_2O was added to this solution. The solution was allowed to react at room temperature with constant stirring for 60 minutes. After 60 minutes, one-third of the reaction (~10 mL) was removed. The product obtained was evaporated to dryness under reduced pressure. Excess H_2O was removed, leaving *D*-sorbitol as a white powder called 8-A (0.35 g, 1.97 mmol, 100%) analyzed by NMR (300 MHz, DMSO-d_6). See Appendices A 19 and A 20. To the remaining mixture, an additional amount of $NaBH_4$ (0.0303 g, 0.801 mmol) was added and stirred for

45 minutes (105 minutes total). Half of the reaction (~10 mL) was removed. The product obtained was evaporated to dryness using a rotary evaporator. Excess H_2O was removed, leaving *D*-sorbitol as a white powder called 8-B (0.35 g, 1.98 mmol, 100%) analyzed by NMR (300 MHz, DMSO-d_6). See Appendices A 21 and A 22. Additional $NaBH_4$ (0.0300 g, 0.793 mmol) was added to the remaining aliquot and allowed to react for an additional 45 minutes (150 minutes total). The product was obtained, and the solvent was evaporated to dryness under reduced pressure. Excess H_2O was removed, leaving *D*-sorbitol as a white powder called 8-C (0.35 g, 1.98 mmol, 100%) analyzed by NMR (300 MHz, DMSO-d_6). See Appendix A 23.

2.2.1.9 *D*-glucose Reduction to Sorbitol in Flow – Trial 9

Using the batch parameters in trial six, which was optimal for the glucose reduction compared to previous trials, a second trial for the flow was done. A flow system was set up using PTFE tubing (0.75 mm inner diameter) and syringe pumps. *D*-glucose (1.04 g, 5.77 mmol) was dissolved in 20 mL of dH_2O and added to the flow at a 2 ml/min flow rate from a first Pump A. $NaBH_4$ (0.1758 g, 4.65 mmol) dissolved in 10 mL of dH_2O was added to the flow simultaneously at a 1 ml/min flow rate from a second Pump B. The reaction mixture introduced into the flow system via a T-mixer (T-mixer 1) was passed through a reactor coil maintained at ambient temperature (20 ± 2°C). This temperature was consistently maintained throughout the reaction zone to ensure uniform conditions. The product was obtained following a 10-minute residence time in the reactor, and the solvent was evaporated to dryness under reduced pressure. Excess H_2O was removed, leaving *D*-sorbitol as a white powder (1.05 g, 5.76 mmol, 100%) analyzed by NMR (300 MHz, DMSO-d_6). See Figure 19 and Appendix A 24.

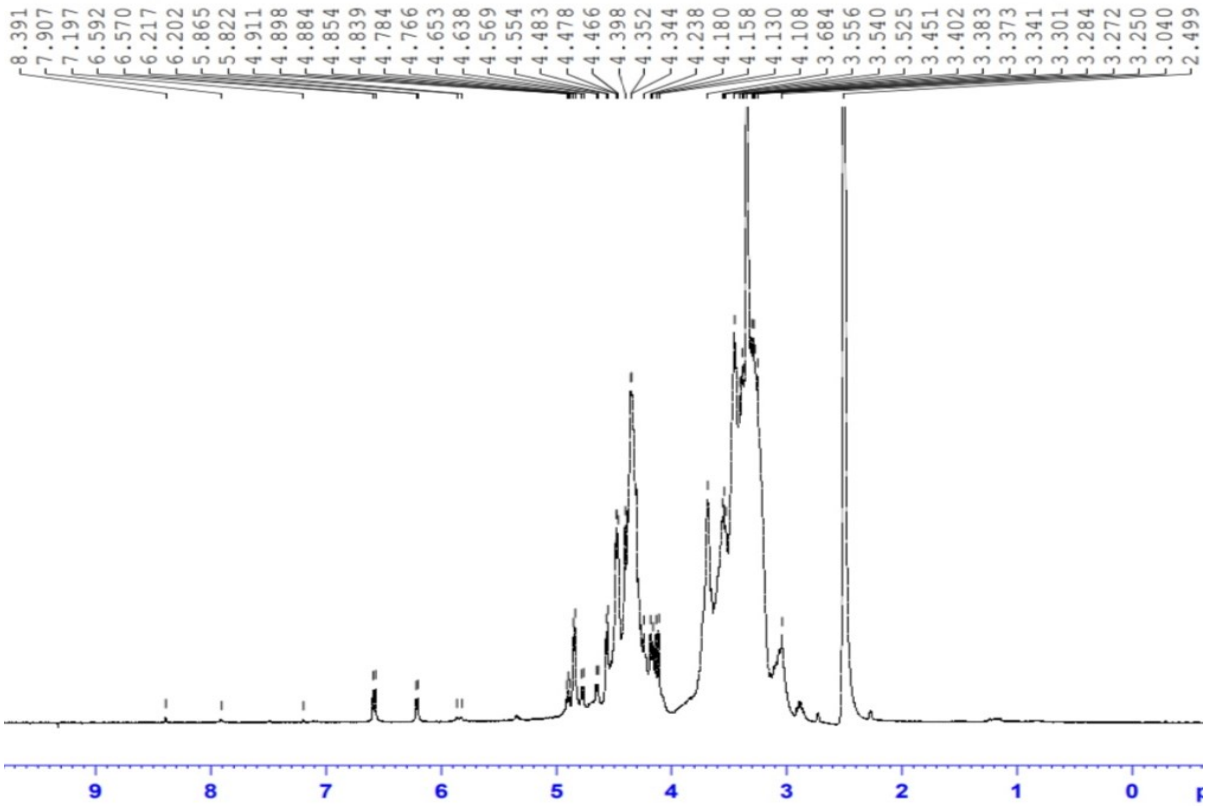

Figure 19: Sorbitol ^{1}H-NMR for Flow 9 recorded in DMSO-d_6 (300 MHz).

2.2.1.10 *D*-glucose Reduction to Sorbitol in Flow – Trial 10

In this trial, the residence time in the flow was increased to let the reaction come to completion. A flow system was set up using PTFE tubing (0.75 mm inner diameter) and syringe pumps, as shown in Scheme 7. *D*-glucose (1.03 g, 5.71 mmol) was dissolved in 10 mL of dH_2O and added to the flow at a 0.5 ml/min flow rate from a first Pump A. $NaBH_4$ (0.1753 g, 4.63 mmol) dissolved in 10 mL of dH_2O was added to the flow simultaneously at a 0.5 ml/min flow rate from a second Pump B. The reaction mixture introduced into the flow system via a T-mixer (T-mixer 1) was passed through a reactor coil maintained at ambient temperature (20 ± 2°C). This temperature was consistently maintained throughout the reaction zone to ensure uniform conditions. The product was obtained following a 20-minute

residence time in the reactor, and the solvent was evaporated to dryness under reduced pressure. Excess H_2O was removed, leaving *D*-sorbitol, a white powder (1.04 g, 5.70 mmol, 99%) analyzed by NMR (300 MHz, DMSO-d_6). See Figure 20 and Appendices A 62 – A 65.

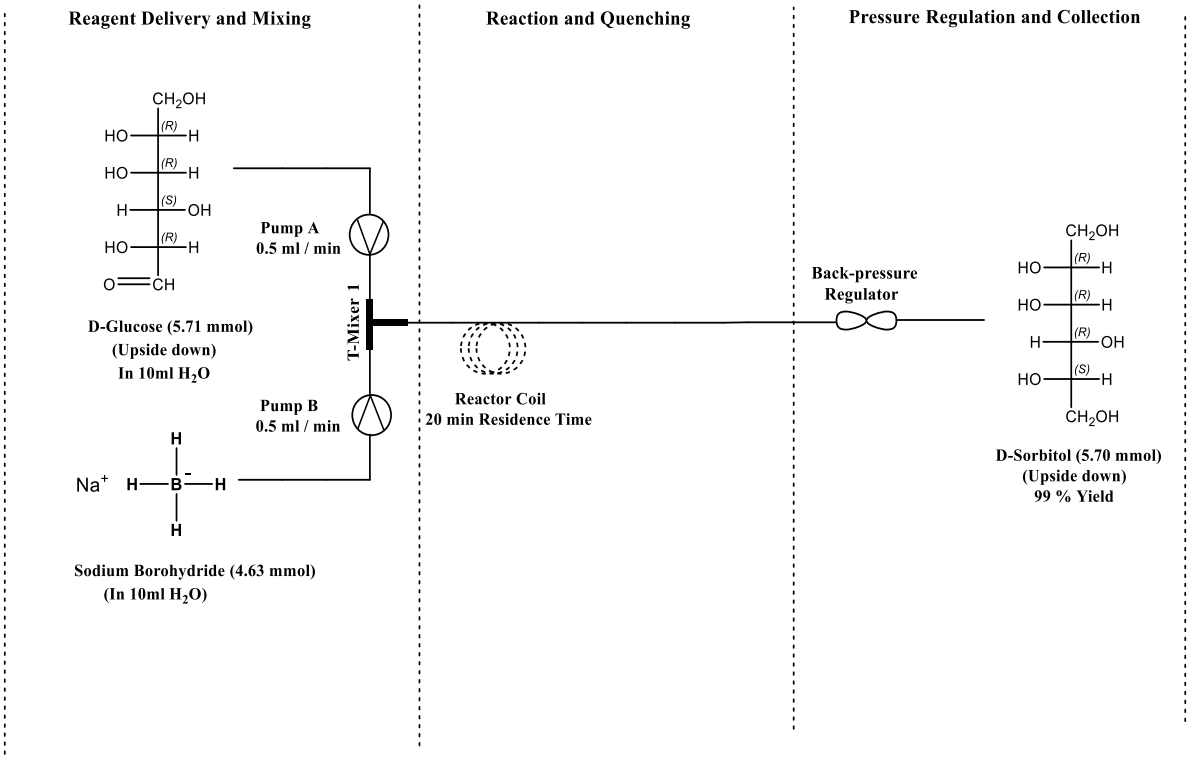

Scheme* 7: *Reduction of D-glucose to D-sorbitol in the flow – trial 10

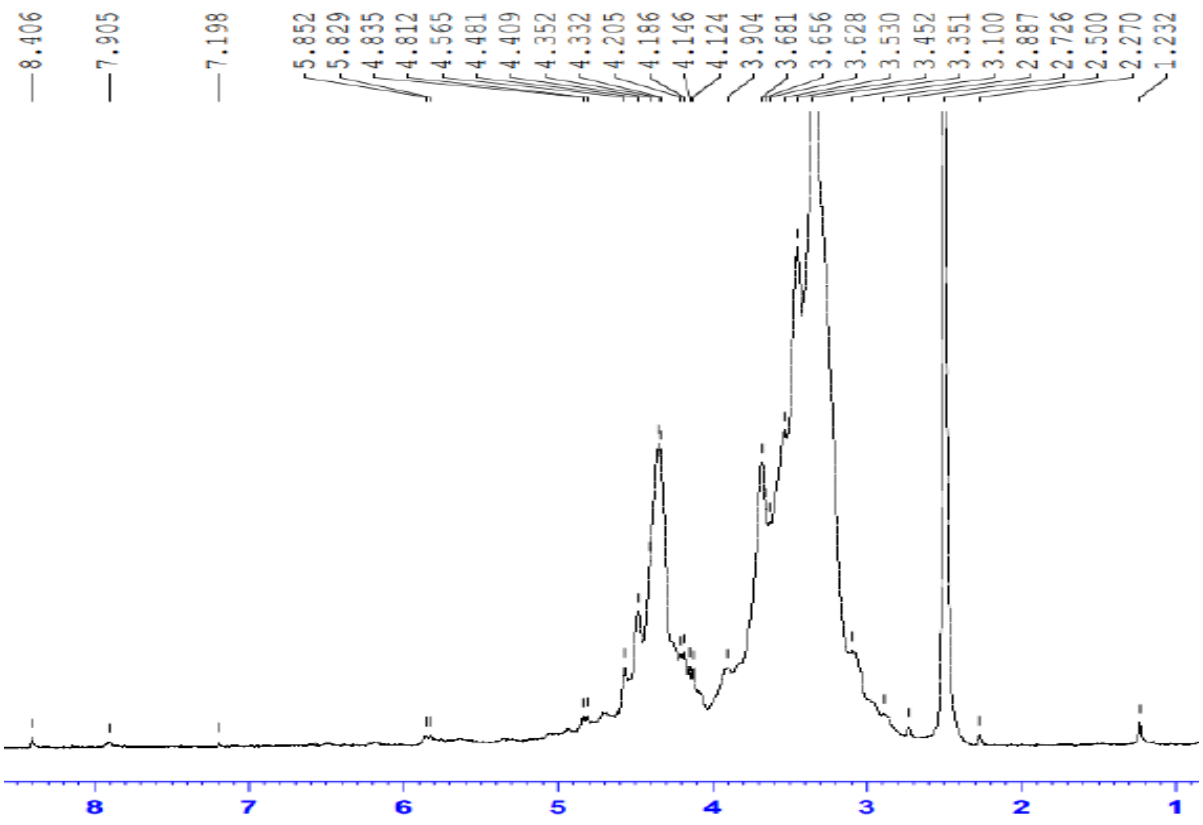

Figure 20: Sorbitol ^{1}H-NMR for Flow 10 recorded in DMSO-d_6 (300 MHz).

2.2.1.11 Sorbitol Product Yields

The reduction of *D*-glucose using $NaBH_4$ successfully yielded *D*-sorbitol, as confirmed by IR and NMR spectroscopic analysis. The reaction trials consistently produced product yields exceeding 100%, except for trial 1 (Table 1). The low yield is attributed to the degradation of the product into a brown mass due to excessive heating.

Table 1: Sorbitol reaction conditions and product yields for various trials in the batch and flow.

Trial	Reaction Process	Acetic acid	Reaction Time (min)	Amount (mmol) *D*-glucose	Amount (mmol) $NaBH_4$	Crude Yield (mmol) *D*-sorbitol	Crude Yield (%)
1	Batch	Yes	40	5.61	3.02	4.51	80
2	Flow	Yes	10	5.66	3.72	5.59	100
3	Batch	Yes	50	5.61	2.90	5.59	100
4	Batch	No	40	5.66	2.89	5.54	100
5	Batch	No	60	6.11	3.91	5.70	93
6	Batch	No	60	5.83	4.64	5.65	97
7	Batch	No	105	5.66	5.30	5.59	99
8-A	Batch	No	60	1.98 (5.94)	3.01	1.97	100
8-B	Batch	No	105	1.98 (5.94)	3.81	1.98	100
8-C	Batch	No	150	1.98 (5.94)	4.60	1.98	100
9	Flow	No	10	5.77	4.65	5.76	100
10	Flow	No	20	5.71	4.63	5.70	99

Yields at or surpassing 100% can be primarily attributed to residual water content.[119] This phenomenon is linked to *D*-sorbitol's nature as a humectant, characterized by its high affinity for water molecules.[119] *D*-sorbitol structure features multiple hydroxyls (-OH) groups, enabling extensive hydrogen bonding with water molecules,[119,120] a process known as sugar hydration. The strong interaction between sorbitol and water likely resulted in incomplete water removal during drying, leading to artificially inflated yields. [119,120] This

persistence of water, despite drying efforts, is a direct consequence of the robust sugar hydration effect. The product may also contain unreacted starting materials, side products, or inorganic salts from the reaction mixture that were not completely removed, as purification has not been done.

2.2.1.12 Optimization and Discussion of Reaction Conditions in Batch

2.2.1.12.1 Sorbitol Synthesis: Acetic acid

Trials 1 and 3, done in the batch, and trial 2 in flow, employed acetic acid to neutralize excess $NaBH_4$ and halt further reactions. The presence of acetic acid is evidenced by distinctive ^{1}H-NMR chemical shifts at 1.89 ppm for trials 1 and 2 and 1.87 ppm for trial 3 (See Figures 12, 13 and 14, respectively). Corroborating ^{13}C-NMR data reveals strongly deshielded signals at 172.25 ppm (1 and 2) and 172.48 ppm (3), further confirming acetic acid's presence (See Appendices A 2, A 5 and A 7). Notably, these acetic acid-containing trials also exhibited signals indicative of unreacted glucose, the anomeric carbons for both α and β isomers, appearing at 4.90 ppm (d, J = 3.3 Hz) and 4.26 ppm (d, J = 7.8 Hz). These chemical shifts are significantly lower than those typical of glycosyl donors (6.0-7.0 ppm), suggesting the formation of glucosides rather than free glucose. The introduction of acetic acid promoted Fischer glycosylation,[119,121] leading to glucose self-condensation. This reaction is known to be catalyzed under acidic conditions, explaining the observed glucoside formation in these trials.

The trials without acetic acid demonstrated a marked decrease in glucoside formation, as evidenced by the reduced intensity of downfield anomeric doublets corresponding to both α and β isomers (See Figures 15 to 20 and Appendices A 10 – A 23). While these acid-free

trials successfully minimized glucoside production, some glucose remained unreacted, varying depending on reaction duration and $NaBH_4$ concentration. Although unreacted glucose was still present, these trials exhibited lower residual reagent levels than trials 1, 2 and 3, as indicated by the diminished intensity of the anomeric signals. The higher proportion of unreacted glucose in trials 1, 2 and 3 can be attributed to competition between Fischer glycosylation and glucose reduction reactions. This competitive effect arose from the acidic conditions introduced by acetic acid, which simultaneously promoted glycosylation while hindering the reduction process.

2.2.1.12.2 Sorbitol Synthesis: Reaction Time

Generally, extending the reaction duration promotes more complete glucose reduction. A comparison between trials 8-A and 8-B revealed that a 45-minute increase in reaction time in the batch resulted in a significant decrease in unreacted glucose, as evidenced by the reduced intensity of ^{1}H-NMR anomeric doublets (See Appendices A 19 and A 21, respectively). However, trial 8-C illustrates that excessive reaction times can increase undesired side reactions (See Appendix A 23). This suggests an optimal reaction window exists, balancing maximal glucose reduction against the onset of secondary product formation.

2.2.1.12.3 Sorbitol Synthesis: Amount of $NaBH_4$

Similar to reaction time, increasing the amount of $NaBH_4$ generally enhances glucose reduction. However, trials with a $NaBH_4$-to-glucose ratio exceeding 0.8 showed an increased presence of unknown impurities, likely resulting from additional side reactions. For instance, trials 7 and 8-C, which used ratios of 0.9 and 0.8, exhibited significant impurity formation (See Appendices A 18 and A 23, respectively). Conversely, insufficient

$NaBH_4$ led to incomplete glucose reduction, as evidenced by the prominent anomeric proton signals observed in the ^{1}H-NMR spectra of trials 1, 2, and 3 (See Appendices A 1, A 4, and A 6, respectively). This highlights the need for an optimal $NaBH_4$ ratio to balance effective glucose reduction with minimal side reactions.

2.2.1.13 Comparison of Sorbitol Yield in Batch and Flow

Based on a comprehensive analysis of various reaction parameters in the batch during this optimization, including the presence or absence of acetic acid, the $NaBH_4$ to *D*-glucose ratio, and reaction duration, trials 5 and 6 yielded the most favourable outcome of sorbitol yields in the batch (See Table 1). These trials employed $NaBH_4$ to *D*-glucose ratios of 0.64 and 0.79, respectively, with a consistent reaction time of 60 minutes for both. Drawing from these results, the optimal conditions for this reaction in the batch were proposed and are;

- $NaBH_4$ to *D*-glucose ratio: 0.7
- Acetic acid: Omitted
- Reaction duration in batch: 60 minutes

These parameters balance efficient glucose reduction and minimal side product formation, offering a refined protocol for synthesizing *D*-sorbitol from *D*-glucose. Implementing a flow setup using the optimized parameters yielded remarkable results, achieving comparable product quality with a significantly reduced reaction or residence time of just 20 minutes, in contrast to the 60-minute duration required for the batch process. This substantial reduction in residence time highlights the superior efficiency of the flow system. The enhanced performance of the flow reaction can be attributed primarily to the more effective mixing dynamics inherent to flow processes. The reagents are continuously

and intimately mixed in flow reactors as they travel through the reactor channels, ensuring uniform concentration throughout the reaction medium. This efficient mixing promoted rapid mass transfer and heat exchange and allowed for faster completion of the glucose reduction. Additionally, the continuous nature of the flow process enabled better control over reaction parameters. It reduced the likelihood of concentration or temperature fluctuations, which could lead to side reactions or incomplete conversion. Consequently, the flow process reduced the reaction time and improved product consistency and yield, as seen in Table 2, demonstrating the advantages of flow chemistry in optimizing this *D*-glucose to *D*-sorbitol reduction process.

Table 2: Comparison of Sorbitol yield and the reaction parameters in Batch versus Flow

D-Glucose to Sorbitol Reduction - Best Results in Batch versus Flow		
	Batch	Flow
Reaction/ Residence time (mins)	60	20
D-sorbitol Yield (mmol)	5.65	5.70
Total Yield (%)	97	99

2.2.2 *L*-Sorbose to Protected Sorbose in Batch and Flow

2.2.2.1 *L*-Sorbose Protection to Diacetone-*L*-Sorbose (DAS) Batch – Trial 1

The *L*-sorbose protection (the hydroxyl groups at C-2, C-3, C-4, and C-6, as shown in Figure 21) was done by reacting with acetone.

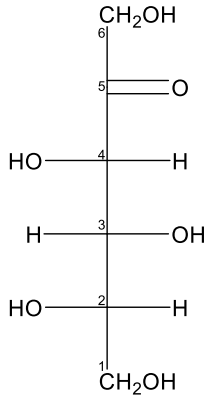

Figure 21: Structure of L-sorbose before the protection of its hydroxyl groups

L-sorbose (0.625 g, 3.46 mmol) was dissolved in 25 mL of acetone (acetone to sorbose ratio of 97: 1). H_2SO_4 (1 mL) was added dropwise to this solution until universal pH indicator paper indicated the reaction mixture was acidified. The solution was allowed to react at room temperature with constant stirring for 180 minutes. After this, sodium bicarbonate (20 mL) was added dropwise until the universal pH indicator paper indicated that the reaction mixture was neutralized. The solvent was evaporated to dryness under reduced pressure. Excess acetone was removed, leaving a white powder (0.41 g, 1.58 mmol, 45 %) analyzed by NMR (300 MHz, DMSO-d_6). See Figure 22/ Appendix A 31.

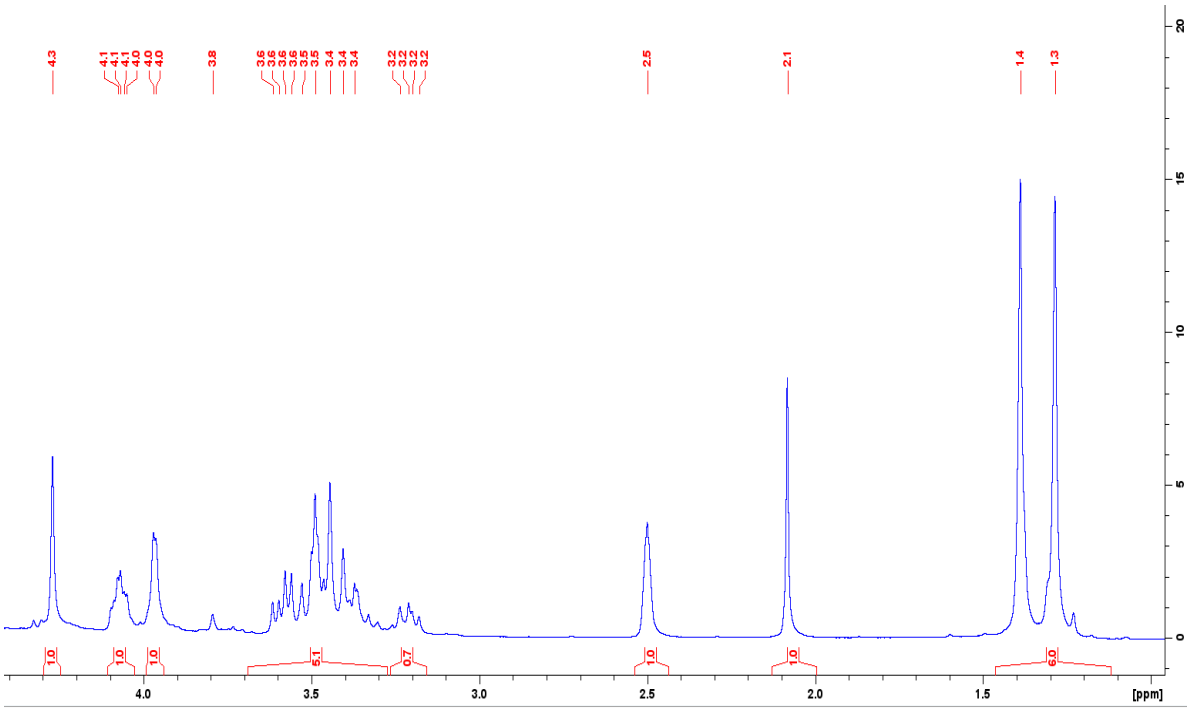

Figure 22: DAS Product ^{1}H-NMR for Batch 1 recorded in DMSO-d_6 (300 MHz).

2.2.2.2 *L*-Sorbose Protection to Diacetone-*L*-Sorbose (DAS) Batch – Trial 2

In this trial, the effect of acetone volume on the reaction completion and yield was investigated by increasing the volume of acetone from 25 mL to 50 mL and the reaction time. *L*-sorbose (0.624 g, 3.46 mmol) was dissolved in 50 mL of acetone (acetone to sorbose ratio of 194: 1). H_2SO_4 (1.2 mL) was added dropwise to this solution until universal pH indicator paper indicated the reaction mixture was acidified. The solution was allowed to react at room temperature with constant stirring for 240 minutes. After this, sodium bicarbonate (20 mL) was added dropwise until the universal pH indicator paper indicated that the reaction mixture was neutralized. The solvent was evaporated to dryness under reduced pressure. Excess acetone was removed, leaving a white powder (0.51 g, 1.95 mmol, 56 %) analyzed by NMR (300 MHz, DMSO-d_6). See Figure 23/ Appendix A 32.

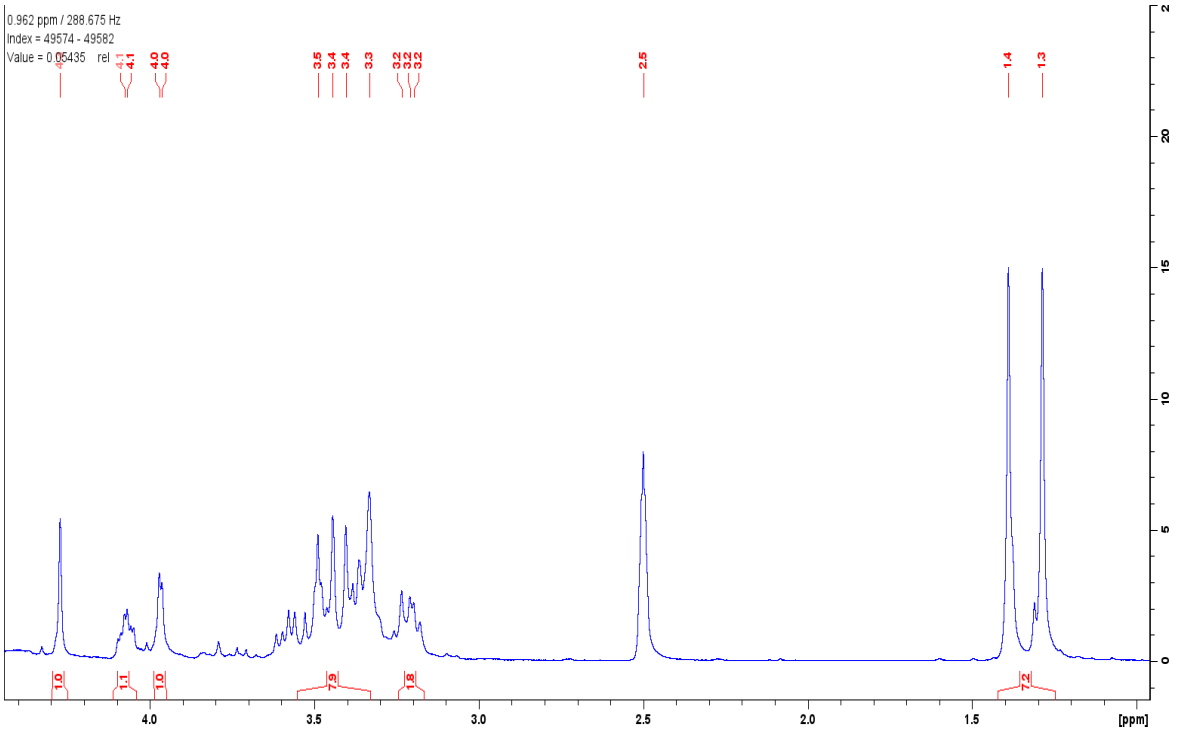

Figure 23: DAS Product ^{1}H-NMR for Batch 2 recorded in DMSO-d_6 (300 MHz).

2.2.2.3 *L*-Sorbose Protection to Diacetone-*L*-Sorbose (DAS) Batch – Trial 3

In this trial, the volume of acetone and reaction time was increased. *L*-sorbose (0.625 g, 3.46 mmol) was dissolved in 60 mL of acetone (acetone to sorbose ratio of 233: 1). H_2SO_4 (1.2 mL) was added dropwise to this solution until universal pH indicator paper indicated the reaction mixture was acidified. The solution was allowed to react in an ice-cold water bath with constant stirring for 300 minutes. After this, sodium bicarbonate (20 mL) was added dropwise until the universal pH indicator paper indicated that the reaction mixture was neutralized. The solvent was evaporated to dryness under reduced pressure. Excess acetone was removed, leaving a white powder (0.54 g, 2.07 mmol, 60 %) analyzed by NMR (400 MHz, DMSO-d_6). See Figure 24, Appendices A 58 to A 61.

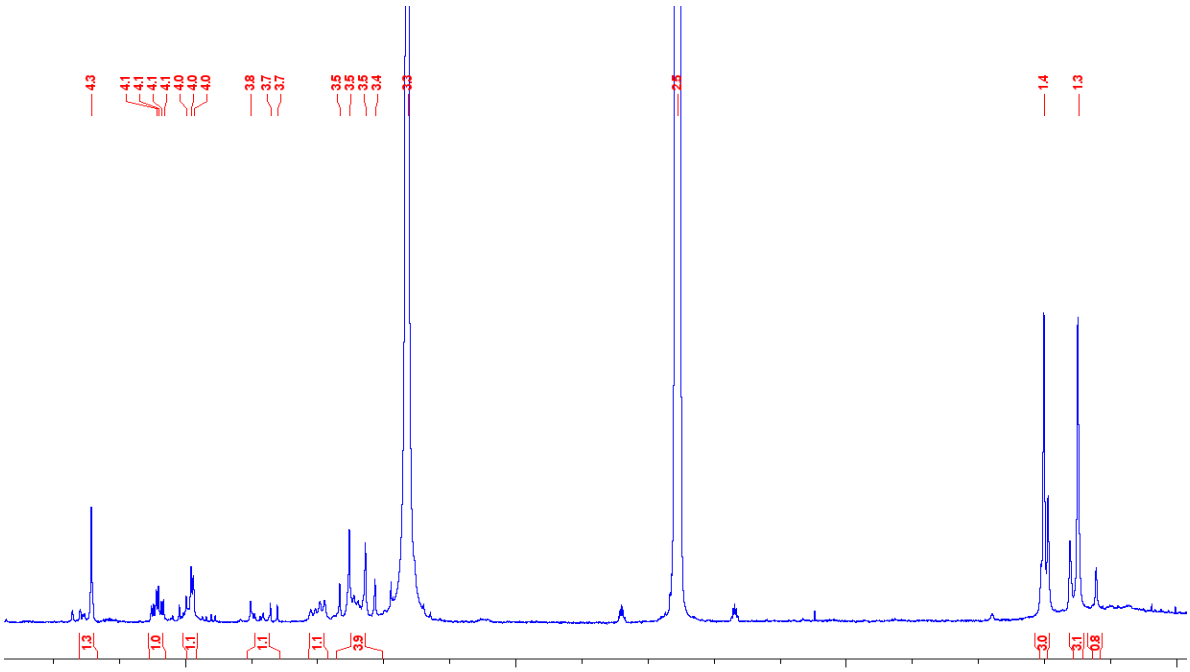

Figure 24: DAS Product ^{1}H-NMR for Batch 3 recorded in DMSO-d_6 (300 MHz).

2.2.2.4 *L*-Sorbose Protection to Diacetone-*L*-Sorbose (DAS) Batch – Trial 4

In this trial, the volume of acetone and reaction time was increased. *L*-sorbose (0.625 g, 3.46 mmol) was dissolved in 80 mL of acetone (acetone to sorbose ratio of 311: 1). H_2SO_4 (1.5 mL) was added dropwise to this solution until universal pH indicator paper indicated the reaction mixture was acidified. The solution was allowed to react in an ice-cold water bath with constant stirring for 300 minutes. After this, sodium bicarbonate (30 mL) was added dropwise until the universal pH indicator paper indicated that the reaction mixture was neutralized. The solvent was evaporated to dryness under reduced pressure. Excess acetone was removed, leaving a white powder (0.70 g, 2.68 mmol, 87 %) analyzed by NMR (300 MHz, DMSO-d_6). See Figure 25/ Appendix A 34.

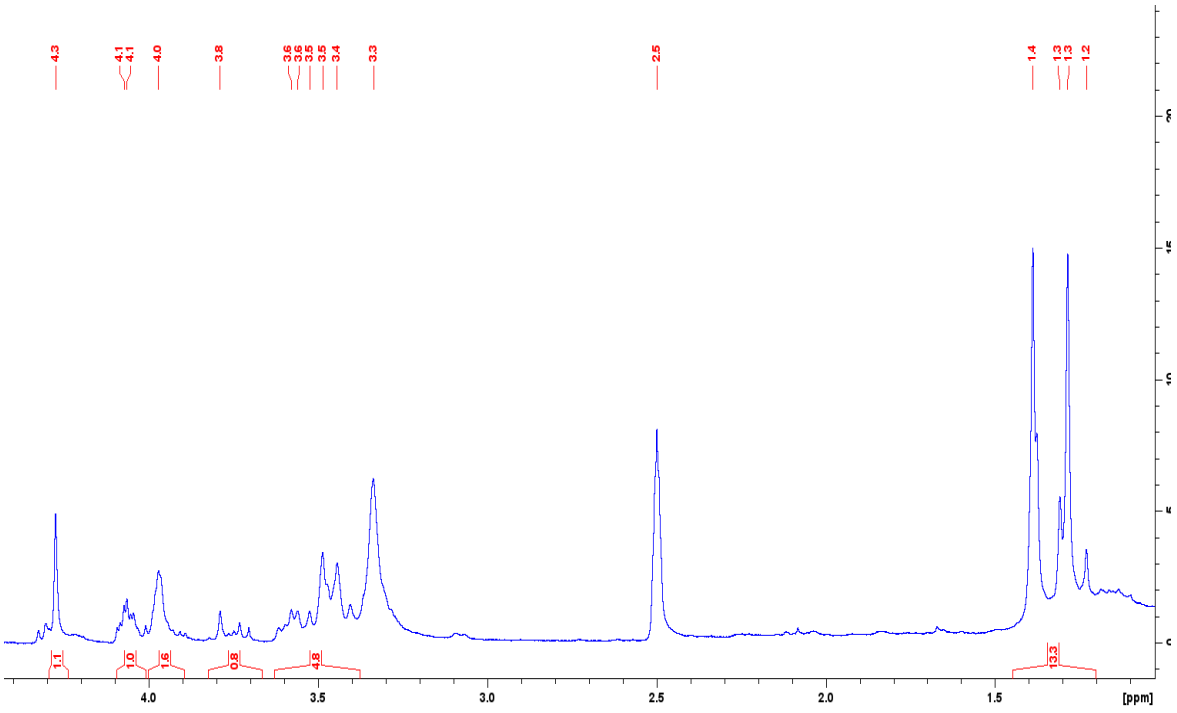

Figure 25: DAS Product ^{1}H-NMR for Batch 4 recorded in DMSO-d_6 (300 MHz).

2.2.2.5 *L*-Sorbose Protection to Diacetone-*L*-Sorbose (DAS) Flow – Trial 5

Flow synthesis was done using the batch parameters in trial 4. A flow system was set up using PTFE tubing (0.75 mm inner diameter) and syringe pumps. *L*-sorbose (0.625 g, 3.46 mmol) was dissolved in 80 mL of acetone and added to the flow at a 4 ml/min flow rate from a first Pump A. H_2SO_4 (1.5 mL) diluted in acetone (20 mL) was added to the flow simultaneously at a 1 ml/min flow rate from a second Pump B. The reaction mixture introduced into the flow system via a T-mixer (T-mixer 1) was passed through a reactor coil in an ice bath (0 - 5 C). This temperature was consistently maintained throughout the reaction zone to ensure uniform conditions. Sodium bicarbonate (20 mL) was added to the flow simultaneously at a 1 ml/min flow rate from a third Pump C. The product was obtained following a 10-minute residence time in the reactor, and the solvent was evaporated to

dryness using a rotary evaporator. Excess acetone was removed under reduced pressure, leaving a white powder (0.69 g, 2.65 mmol, 76 %) analyzed by NMR (300 MHz, DMSO-d_6) and Mass Spectrometry. See Figure 26, Appendices A 35 and A 36, respectively.

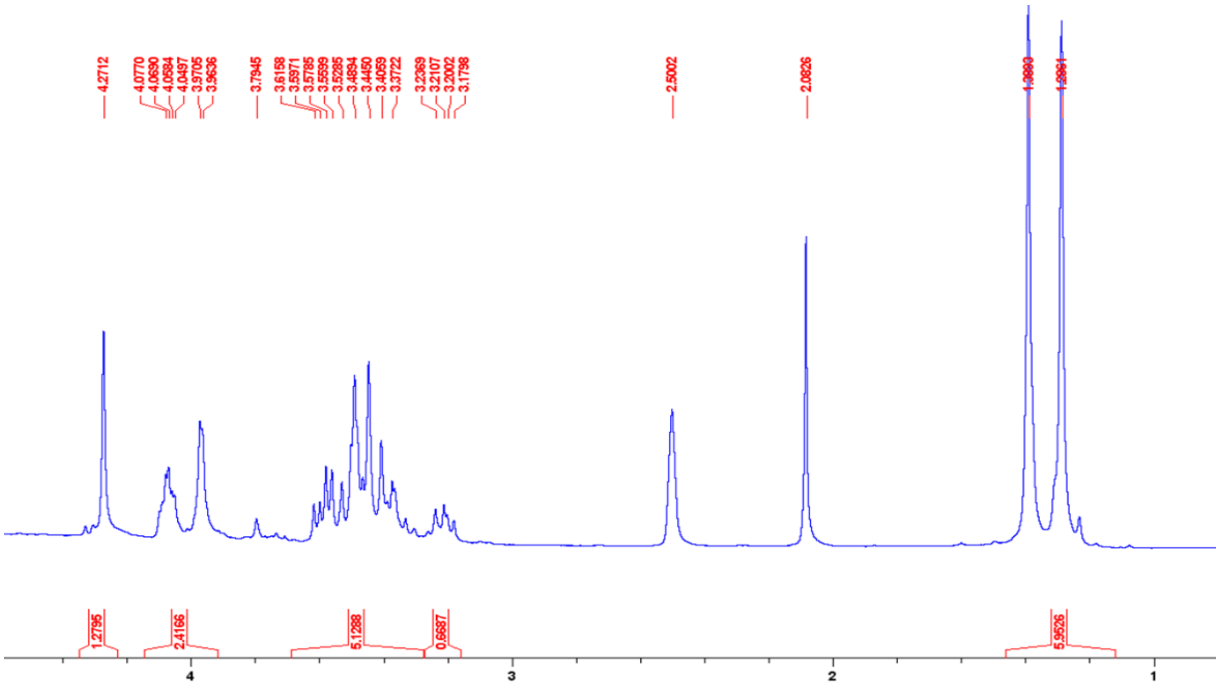

Figure 26: DAS Product 1H-NMR for Flow 5 recorded in DMSO-d_6 (300 MHz).

2.2.2.6 *L*-Sorbose Protection to Diacetone-*L*-Sorbose (DAS) Batch – Trial 6

In this trial, reaction time was increased. *L*-sorbose (0.626 g, 3.47 mmol) was dissolved in 80 mL of acetone (acetone to sorbose ratio of 311: 1). H_2SO_4 (1.5 mL) was added dropwise to this solution until universal pH indicator paper indicated the reaction mixture was acidified. The solution was allowed to react in an ice-cold water bath with constant stirring for 360 minutes. After this, sodium bicarbonate (30 mL) was added dropwise until the universal pH indicator paper indicated that the reaction mixture was neutralized. The solvent was evaporated to dryness under reduced pressure using a rotary evaporator. Excess acetone was

removed, leaving a white powder (0.81 g, 3.11 mmol, 90 %) analyzed by NMR (300 MHz, DMSO-d_6). See Figure 27 / Appendix A 37.

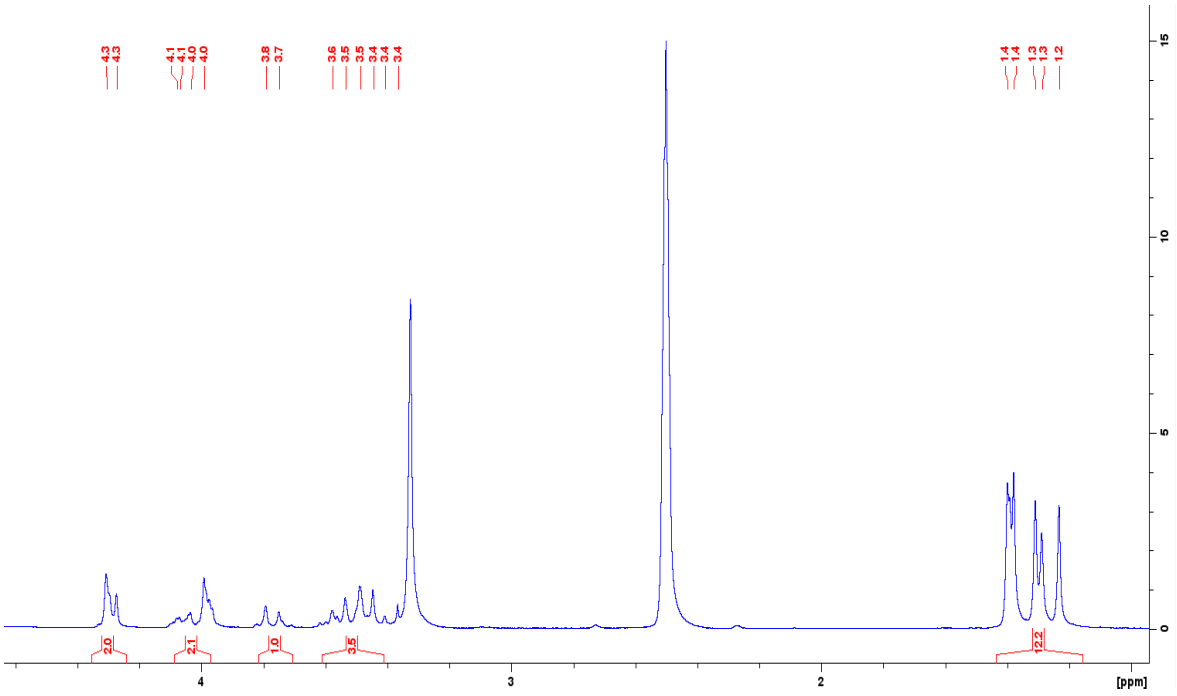

Figure 27: DAS Product ^{1}H-NMR for Batch 6 recorded in DMSO-d$_6$ (300 MHz).

2.2.2.7 *L*-Sorbose Protection to Diacetone-*L*-Sorbose (DAS) Flow – Trial 7

Flow synthesis was done using the batch parameters in trial 6, which was optimal for the L-sorbose protection compared to previous trials, and the residence time was increased. A flow system was set up using PTFE tubing (0.75 mm inner diameter) and syringe pumps. *L*-sorbose (0.625 g, 3.46 mmol) was dissolved in 80 mL of acetone and added to the flow at a 4 ml/min flow rate from a first Pump A. H_2SO_4 (1.5 mL) diluted in acetone (20 mL) was added to the flow simultaneously at a 1 ml/min flow rate from a second Pump B. The reaction mixture introduced into the flow system via a T-mixer (T-mixer 1) was passed through a reactor coil in an ice bath (0 - 5 °C). This temperature was consistently maintained throughout the reaction zone to ensure uniform conditions. Sodium bicarbonate (20 mL) was

added to the flow simultaneously at a 1 ml/min flow rate from a third Pump C. The product was obtained following a 20-minute residence time in the reactor, and the solvent was evaporated to dryness under reduced pressure. Excess acetone was removed, leaving a white powder (0.74 g, 2.84 mmol, 82 %) analyzed by NMR (400 MHz, DMSO-d_6) and Mass Spectrometry. See Figure 28, Appendices A 38 and A 39, respectively.

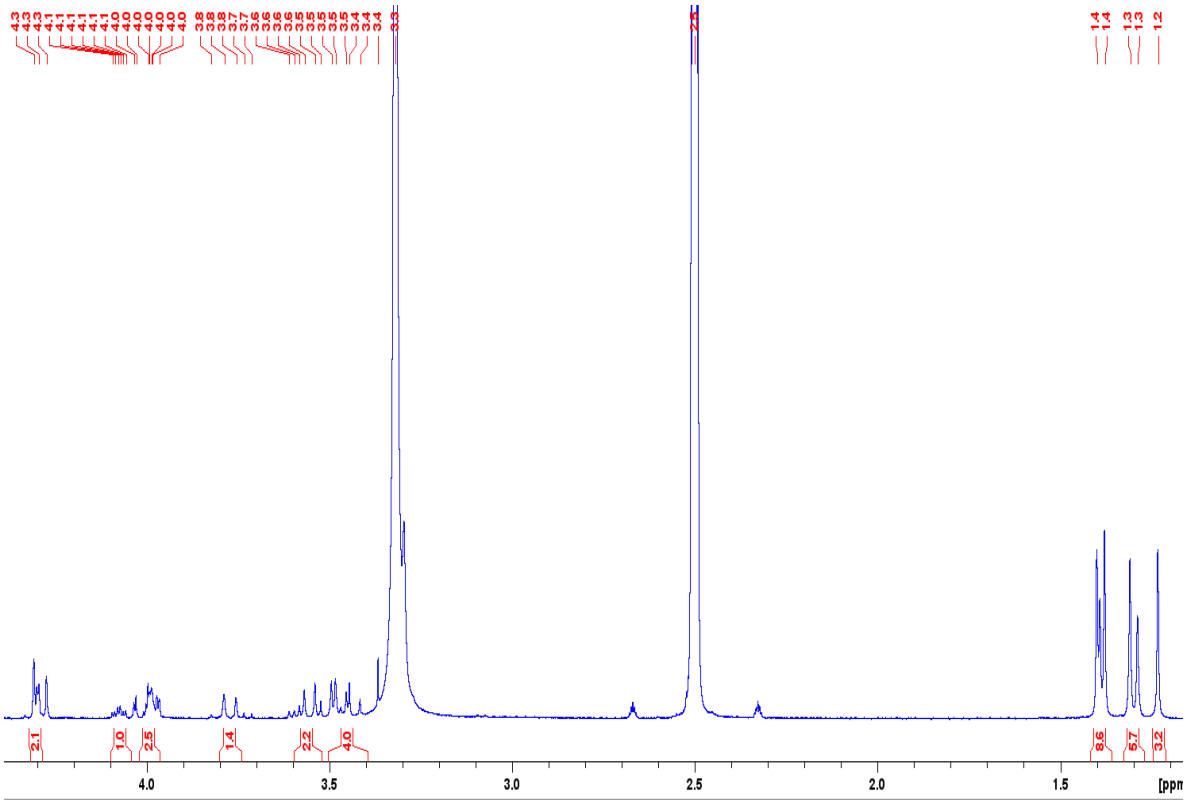

Figure 28: DAS Product ^{1}H-NMR for Flow 7 recorded in DMSO-d_6 (400 MHz).

2.2.2.8 *L*-Sorbose Protection to Diacetone-*L*-Sorbose (DAS) Batch – Trial 8

In this trial, the reaction was done in an ice bath; aliquots were collected at intervals from 30 minutes to monitor the *L*-sorbose protection, using the acetone to sorbose (A/S) ratio of 311:1 to see if reaction time does affect the protection aside from the A/S ratio and reaction temperature. *L*-sorbose (0.64 g, 3.55 mmol) was dissolved in 80 mL of acetone (acetone to

sorbose ratio of 311: 1). H_2SO_4 (1.5 mL) was added dropwise to this solution until universal pH indicator paper indicated the reaction mixture was acidified. The solution reacted in an ice-cold water bath with constant stirring for 30 minutes. At times 30 minutes, 1 hour, 2 hours, 4 hours, 4.5 hours, 5 hours, 5.5 hours, 6 hours, 6.5 hours, 7 hours, 7.5 hours, 8 hours, and 8.5 hours, aliquots were removed, and acetone was removed under reduced pressure to yield fractions 8 A (0.023 g), 8 B (0.023 g), 8 C (0.023 g), 8 D (0.026 g), 8 E (0.026 g), 8 F (0.026 g), 8 G (0.028 g), 8 H (0.031 g), 8 I (0.031 g), 8 J (0.031 g), 8 K (0.031 g), 8 L (0.031 g) and 8 M (0.032 g), respectively. See Appendices A 40 to A 52.

2.2.2.9 *L*-Sorbose Protection to Diacetone-*L*-Sorbose (DAS) Flow – Trial 9

In this trial, the residence time was increased from 20 to 30 minutes. A flow system was set up using PTFE tubing (0.75 mm inner diameter) and syringe pumps. *L*-sorbose (0.625 g, 3.46 mmol) was dissolved in 80 mL of acetone and added to the flow at a 4 ml/min flow rate from a first Pump A. H_2SO_4 (1.5 mL) diluted in acetone (20 mL) was added to the flow simultaneously at a 1 ml/min flow rate from a second Pump B. The reaction mixture introduced into the flow system via a T-mixer (T-mixer 1) was passed through a reactor coil in an ice bath (0 - 5 °C). This temperature was consistently maintained throughout the reaction zone to ensure uniform conditions. Sodium bicarbonate (20 mL) was added to the flow simultaneously at a 1 ml/min flow rate from a third Pump C. The product was obtained following a 30-minute residence time in the reactor, and the solvent was evaporated to dryness under reduced pressure. Excess acetone was removed, leaving a white powder (0.86 g, 3.30 mmol, 95 %) analyzed by NMR (400 MHz, $CDCl_3$). See Figure 29-33, Appendices A 53, A 54, A 55, A 56 and A 57.

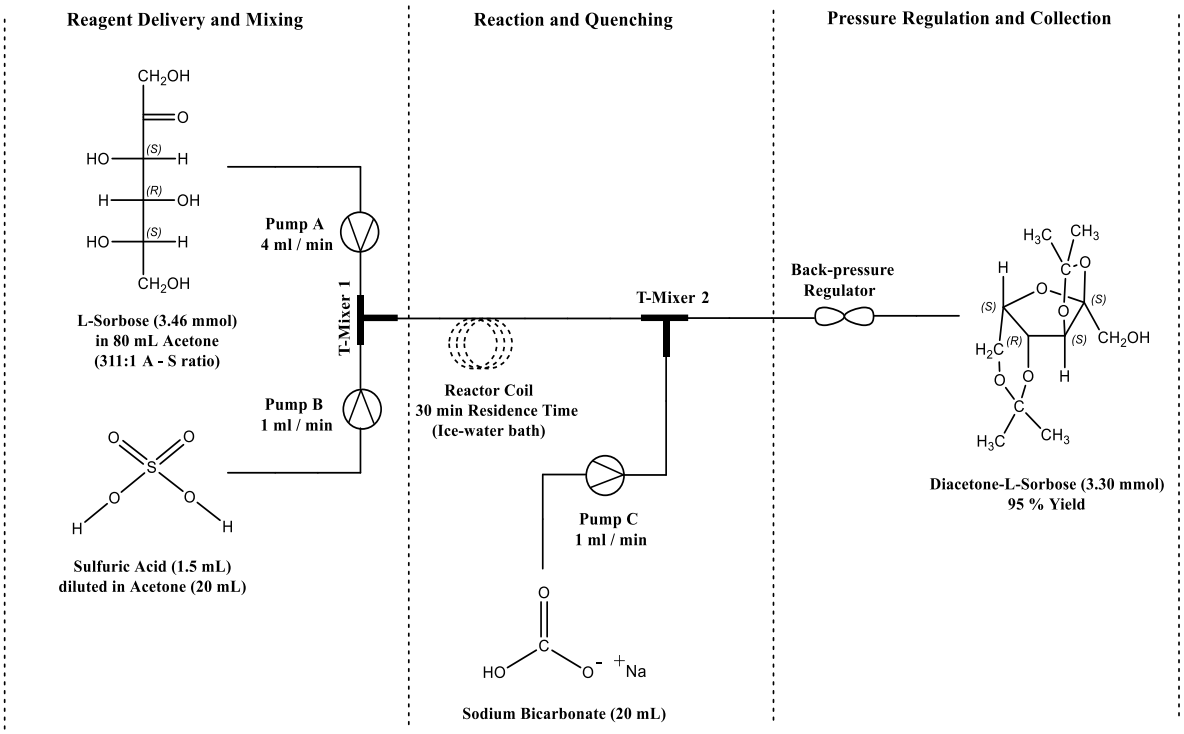

Scheme 8: The protection of L-sorbose to Diacetone-L-Sorbose in the flow

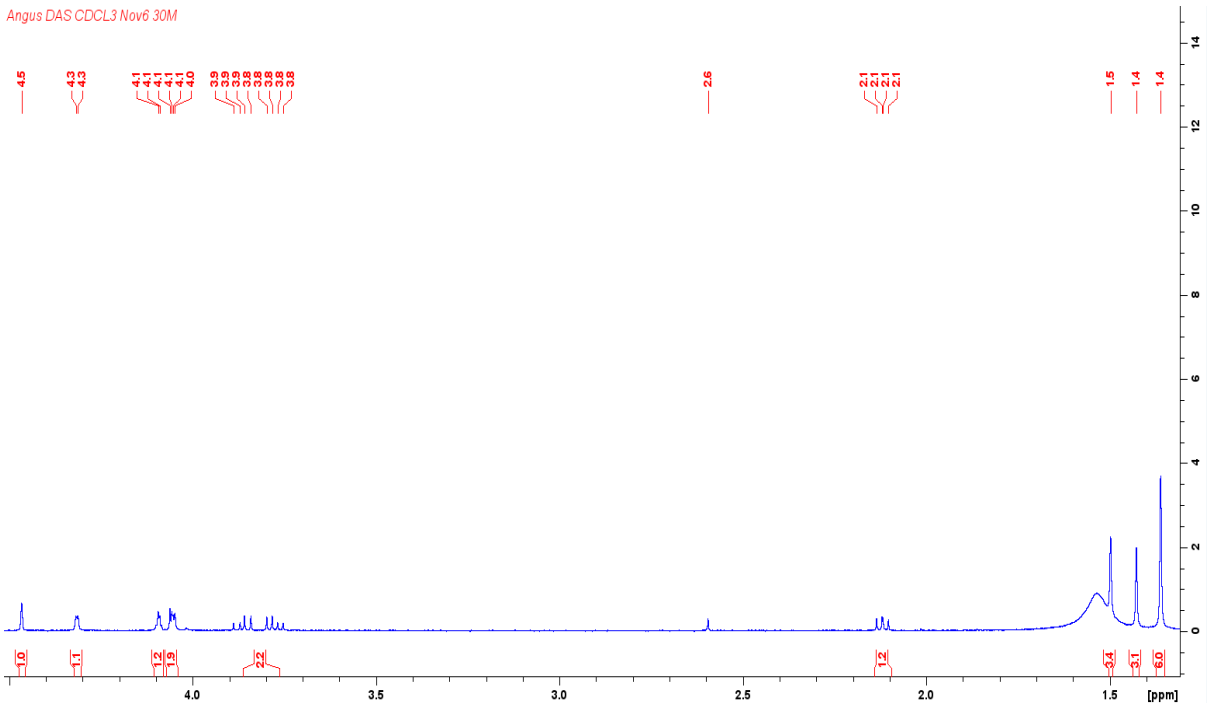

Figure 29: Diacetone-L-sorbose ^{1}H-NMR for Flow 9 recorded in $CDCl_3$ (400 MHz).

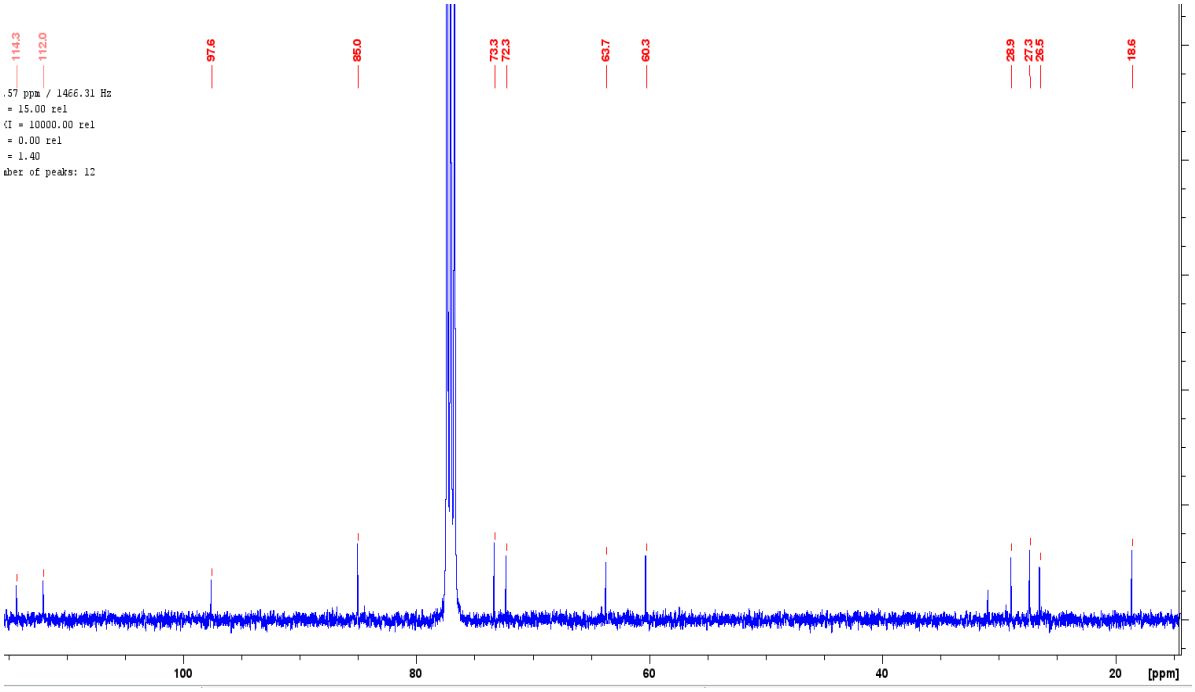

Figure 30: Diacetone-L-sorbose ^{13}C-NMR for Flow 9 recorded in $CDCl_3$ (400 MHz).

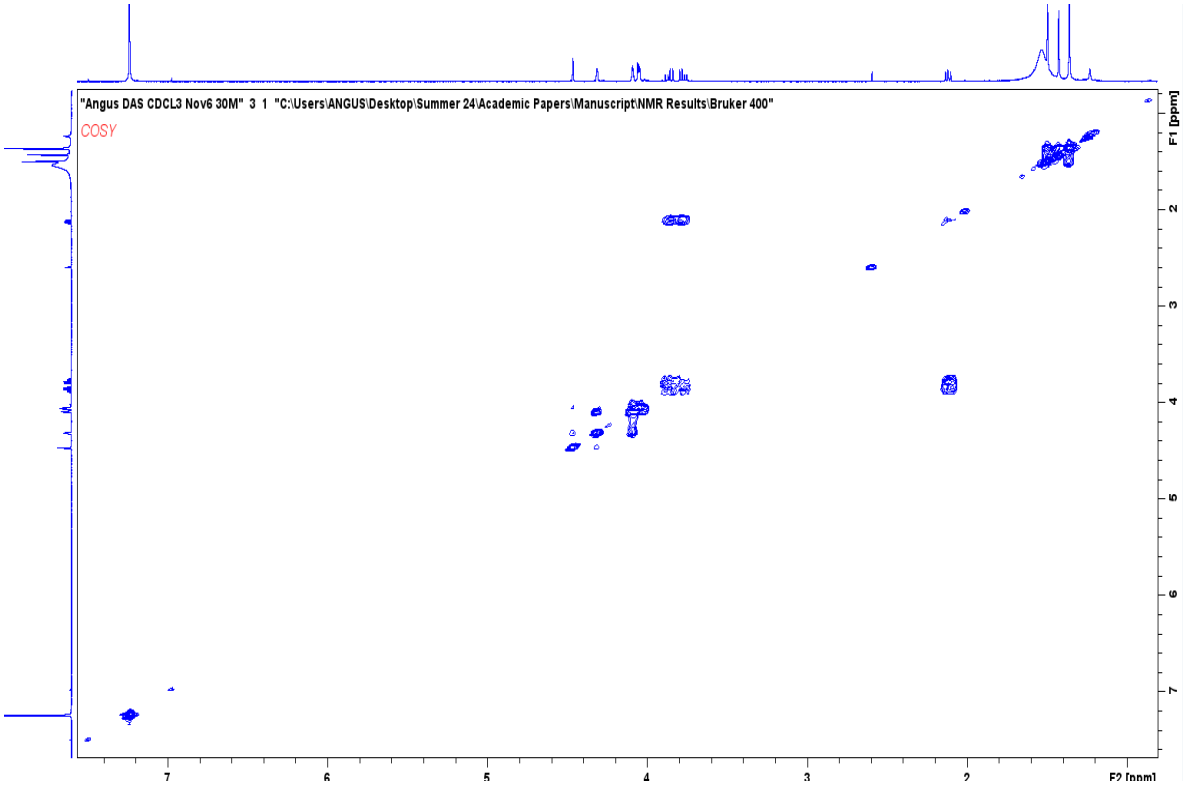

Figure 31: Diacetone-L-sorbose COSY for Flow 9 recorded in $CDCl_3$ (400 MHz).

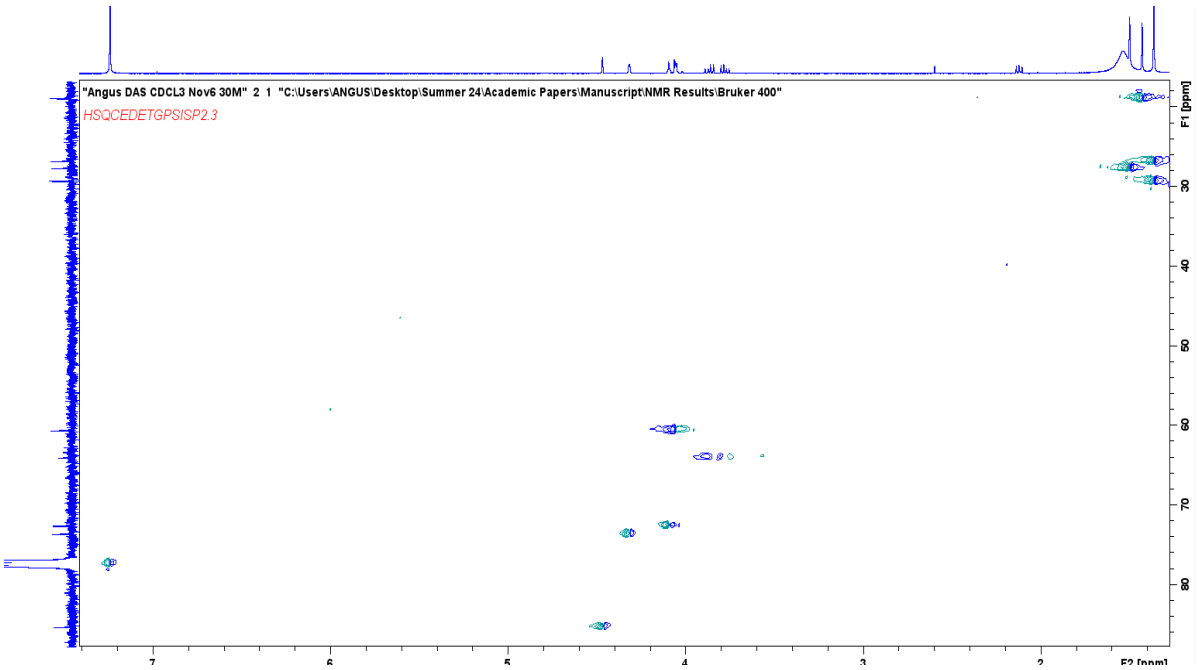

Figure 32: Diacetone-L-sorbose HSQC for Flow 9 recorded in $CDCl_3$ (400 MHz).

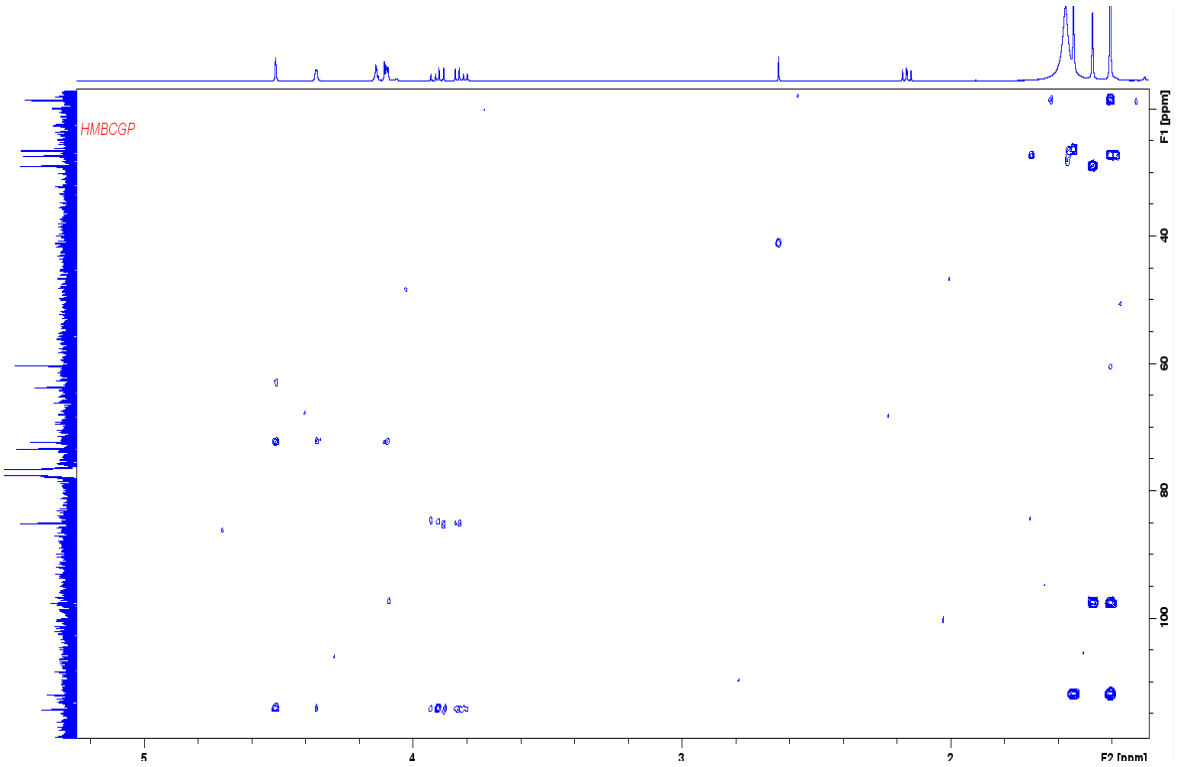

Figure 33: Diacetone-L-sorbose HMBC for Flow 9 recorded in $CDCl_3$ (400 MHz).

2.2.2.10 Diacetone-*L*-Sorbose Product Yields

L-sorbose protection to yield diacetone-*L*-sorbose highly depends on reaction conditions, particularly the acetone-to-sorbose ratio and temperature control. Optimal conversion was achieved with an acetone-to-sorbose molar ratio of 311:1, conducted in a cold-water bath. Experiments with lower acetone-to-sorbose ratios resulted in incomplete protection (See Tables 6 and 7), as evidenced by distinctive ^{1}H-NMR spectral features. Specifically, trials 1, 2, and 5 exhibited characteristic methyl peaks at 1.30 ppm and 1.40 ppm, integrating to 6 H, indicative of partial protection (See Figures 22, 23 and 26, respectively). Complementary ^{13}C-NMR data corroborated these findings, showing additional peaks beyond the 12 carbon signals characteristic of DAS, confirming incompletely protected species and unreacted sorbose (Appendix A 59). In contrast, fully protected diacetone-*L*-sorbose displays an integration of 12 H for its methyl protons, corresponding to the expected 12 methyl protons in the molecule, as shown in Figures 27 and 29.

The synthesis of diacetone-*L*-sorbose (DAS) was optimized through a systematic investigation of reaction time in batch conditions, employing an acetone-to-sorbose ratio of 311:1. Optimal conversion was achieved within a narrow window of 6 to 6.5 hours, yielding fully protected DAS with minimal partially protected intermediates and no detectable side products, as evidenced by spectroscopic analyses. These trials (8 H, 8 I and 9) exhibited characteristic methyl peaks at 1.40 ppm, 1.47 ppm and 1.54 ppm, with integrations of 6 H, 3 H and 3 H, respectively, integrating to 12 H altogether, indicative of DAS methyl protons. (Appendices A 47, A 48 and A 53). The ^{13}C-NMR spectrum displayed 12 carbon peaks (Figure 30 /Appendix 54). At the same time, HMBC experiments revealed the expected correlations between the methyl carbons and the quaternary carbons at 98 ppm and 112 ppm

on both sides of the diacetone-L-sorbose molecule (Figure 33 / Appendix A 57), which was notably absent in the HMBC spectra of the partially protected product (Trials 1, 2, and 3), as only one quaternary carbon at 112 ppm correlated with the methyl carbon, showing that only a part was protected. The other quaternary carbon at 98 ppm, which was to correlate with methyl carbon, was not evident in the HMBC spectra (Appendix A 61). Using the optimal acetone to sorbose ratio of 311:1 at a reaction time of less than 6 hours gave a mixture of partially protected product, and DAS as indicated by the extra peak at 1.60 ppm which is the partially protected product peak, in the ^{1}H-NMR spectra (Appendices A 43 – A 46). Conversely, extending the reaction time beyond 6.5 hours led to the formation of DAS accompanied by side products, as indicated by extra peaks in the ^{1}H-NMR spectra at specific chemical shifts (1.30 ppm, 1.60 ppm, 1.70 ppm and 2.10 ppm). See Appendices A 49 to A 52.

For the flow, the 30-min residence time gave DAS with fewer side products as shown by characteristic methyl peaks at 1.40 ppm, 1.47 ppm and 1.54 ppm, with integrations of 6 H, 3 H and 3 H, respectively, integrating to 12 H altogether, indicative of DAS methyl protons. (Appendix A 53). Residence times below 30 mins gave a mixture of DAS and partially protected product, which was also supported by mass spectra, showing the DAS of molecular weight 260 g/mol and partially protected product (as shown in Figure 34) of 220 g/mol. See Figure 26 / Appendix A 35 and Appendix A 36 for the ^{1}H-NMR and mass spectrum, respectively, for trial 5. For trial 7, See Figure 28 / Appendix A 38 and Appendix A 39 for the ^{1}H-NMR and mass spectrum, respectively.

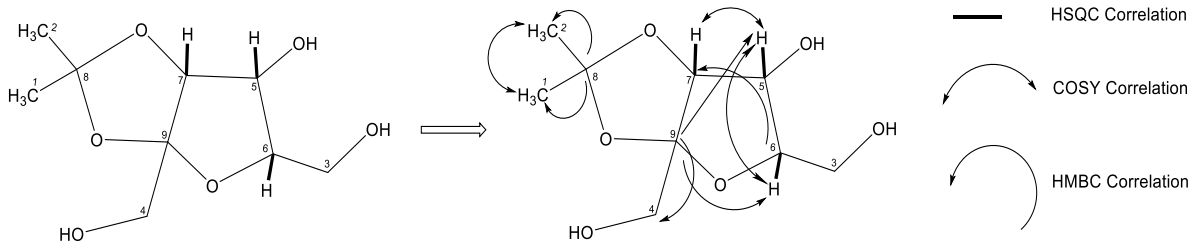

Figure 34: The structure of the partially protected sorbose and the NMR (2-D) correlation.

The NMR Data for the partially protected sorbose is shown in Table 3 below, and Figure 34 above shows the 2 D correlation as seen in Table 3 and Appendices A 58 – A 61. The data showed that only one part of the sorbose was protected.

Table 3: ^{13}C and ^{1}H NMR Data for Partially Protected Sorbose (Batch 3)

Carbon #	^{13}C δ, ppm	^{1}H δ, ppm	COSY	HMBC
1	27.1	1.296	H2	H2
2	28.0	1.399	H1	H1
3	59.4	3.588, 3.4876	H6	-
4	62.5	3.5017, 3.4533	-	-
5	73.9	3.9769	H6, H7	-
6	82.3	4.0831	H3, H5	H7
7	85.1	4.2829	H5	H4’
8	111.2	-	-	H1, H2
9	114.7	-	-	H4, H4’, H5

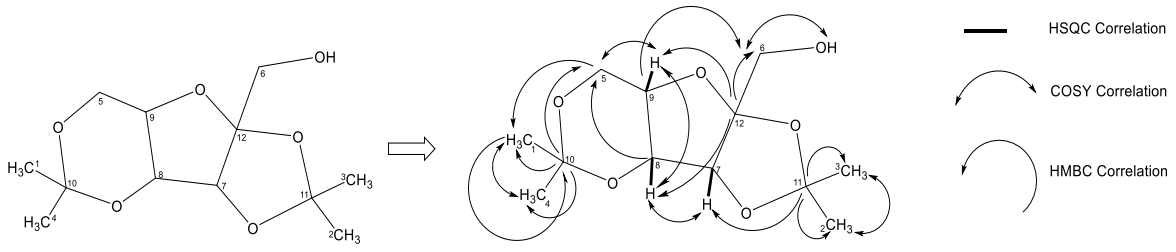

Figure 35: The structure of obtained diacetone-L-sorbose and the NMR (2-D) correlation.

Figure 35 above shows the COSY, HSQC and HMBC Spectra correlation of obtained DAS for Flow 9, and the NMR data is shown in Table 4, while NMR spectra for the product are shown in Figures 29, 30, 31, 32 and 33.

Table 4: ^{13}C and ^{1}H NMR Data for Diacetone-L-sorbose (Flow 9)

Carbon #	^{13}C δ, ppm	^{1}H δ, ppm	COSY	HMBC
1	18.6	1.4272	H4	H4
2	26.5	1.3609	H3	H3
3	27.3	1.4976	H2	H2
4	29.0	1.3609	H1	H1
5	60.3	4.0546	H9	H1
6	63.7	3.8185	OH	H9
7	72.3	4.0903	H8	H8, H9
8	73.3	4.3171	H7, H9	H5, H7, H9
9	85	4.4671	H5, H8	H6
10	97.5	-	-	H2, H4, H5
11	112.0	-	-	H2, H3, H7
12	114.5	-	-	H6, H7, H8, H9

A set of flow chemistry conditions, shown in Table 5 and Table 6, were screened for this protection step throughout the process, and the best conditions obtained were T = -15 to 0° C, Acetone to Sorbose ratio of 311:1, and a residence time of 30 mins. Before optimizing the best conditions, the effect of temperature and the process duration on the sorbose acetonation reaction was studied.

2.2.2.11. Optimization and Discussion of Reaction Conditions

2.2.2.11.1 Diacetone-*L*-Sorbose Synthesis: Temperature and Reaction Time

Incomplete protection occurred when the reaction was done at room temperature and less than 5 hours reaction time for batch, but DAS was synthesized fully when the reaction was carried out in an ice bath.

Table 5: Effect of Temperature and Residence Time on the L-Sorbose Acetonation Process in the Batch

Temperature regime, °C	Process duration, min	DAS yield, %
20 (rt)	60	Incomplete protection
20 (rt)	180	Incomplete protection
20 (rt)	240	Incomplete protection
20 (rt)	300	Incomplete protection
-15, 0 (ice bath)	300	87
-15, 0 (ice bath)	360	90

Table 6: Effect of Temperature and Residence Time on the L-Sorbose Acetonation Process in the Flow

Temperature regime, °C	Residence time, min	DAS yield, %
20 (rt)	10	Incomplete protection
20 (rt)	15	Incomplete protection
-15, 0 (ice bath)	10	76
-15, 0 (ice bath)	20	82
-15, 0 (ice bath)	30	95

Protecting *L*-sorbose with acetone to form diacetone-*L*-sorbose presented a significant challenge due to the potential formation of undesired or isomeric products. A critical issue in this step is the possible formation of 1,2:4,6-di-O-isopropylidene derivative instead of the desired diacetone-*L*-sorbose under certain reaction conditions, as structures are shown in Figure 36. This phenomenon has been observed and reported in the literature,[122] highlighting

researchers' common struggles when dealing with complex protection strategies.[122] Extensive optimization efforts addressed this challenge, carefully controlling reaction parameters such as temperature, catalyst concentration, and reaction time. These optimizations were crucial to ensure the selective formation of diacetone-*L*-sorbose while minimizing the production of its isomeric counterpart. Throughout the process, rigorous NMR analysis was employed to verify the structure of the obtained product, allowing for the differentiation between the desired diacetone-*L*-sorbose and the potentially formed 1,2:4,6-di-O-isopropylidene derivative. This meticulous approach was necessary given these compounds' structural similarity and potential impact on subsequent synthetic steps. After numerous iterations and refinements of the reaction conditions, the successful synthesis of the correct diacetone-*L*-sorbose isomer was achieved and confirmed through comprehensive NMR characterization, as shown in Table 4 and Figure 35.

The structures of potential products and by-products from the reaction, diacetone-*L*-sorbose, partially protected *L*-sorbose and 1,2:4,6-di-O-isopropylidene derivative, which we were trying to avoid, are given below.

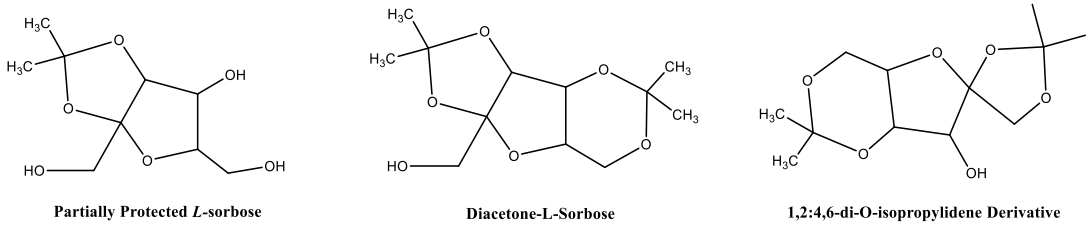

Figure 36: The structures of the potential products: partially protected L-sorbose, diacetone-L-sorbose, and 1,2:4,6-di-O-isopropylidene derivative

2.2.2.11.2 Diacetone-*L*-Sorbose Synthesis: Acetone to Sorbose Ratio

The yield of DAS increased with the relative content of acetone, and the protection of the L-sorbose was incomplete when less acetone was used. The effect of the acetone to sorbose ratio on the DAS yield was studied in batch and flow (Tables 7 and 8) under optimum temperature conditions. Raising the acetone to sorbose (A/S, v/w) ratio from 97:1 to 311:1 resulted in complete protection of the *L*-sorbose and increased DAS yield for the flow and the batch synthesis.

Table 7: Effect of Acetone to Sorbose ratio (A/S) on the Diacetone-L-Sorbose yield in the Batch

A/S Ratio	Process Duration, min	Acetonation Temperature, °C	DAS yield, %
97: 1	180	-15, +20	Incomplete protection
194: 1	240	-15, +20	Incomplete protection
233: 1	300	-15, +20	Incomplete protection
311: 1	300	-15, +20	87
311: 1	360	-15, +20	90

Table 8: Effect of acetone to Sorbose ratio (A/S) on the Diacetone-L-Sorbose yield in the Flow

A/S Ratio	Residence time, min	Acetonation temperature, °C	DAS yield, %
97: 1	10	-15, +20	Incomplete protection
194: 1	15	-15, +20	Incomplete protection
233: 1	20	-15, +20	Incomplete protection
233: 1	30	-15, +20	Incomplete protection
311: 1	10	-15, +20	76
311: 1	20	-15, +20	82
311: 1	30	-15, +20	95

2.2.2.12 Comparison of Diacetone-*L*-sorbose Yield in Batch and Flow

Based on a comprehensive analysis of various reaction parameters in the batch during this optimization, including the acetone to sorbose ratio, the acetonation temperature, and reaction duration, trials 6, 8 H, and 8 I yielded the most favourable outcome of DAS yields. These trials employed acetone to a sorbose ratio of 311: 1, a 6-hour reaction time for trials 6 and 8 H, and a 6.5-hour reaction time for 8 I. Drawing from these results, the optimal conditions for this reaction in the batch were proposed and are; Acetone to Sorbose ratio of 311: 1, acetonation temperature of 0 °C to 5 °C and a reaction duration of 6 hours.

These parameters balance the efficient, full *L*-sorbose protection and minimal side product formation, offering a refined protocol for protecting *L*-sorbose using acetone to obtain diacetone-*L*-sorbose. Implementing a flow setup using the optimized parameters yielded remarkable results, achieving improved yield and a significantly reduced reaction or residence time of just 30 minutes in trial 9, in contrast to the 6-hour duration required for the batch process. See Appendices A 53 – A 57.

Table 9: Comparison of Diacetone-L-sorbose yield and the Reaction parameters in Batch versus Flow

L-sorbose protection to Diacetone-*L*-sorbose: Results in Batch versus Flow		
	Batch	Flow
Reaction/ Residence time (mins)	360	30
DAS Yield (mmol)	3.11	3.30
Total Yield (%)	90	95

2.2.3 Protected Sorbose (Diacetone-*L*-Sorbose - DAS) to 2-keto-*L*-gulonic Acid in Batch and Flow

2.2.3.1 Diacetone-*L*-Sorbose (DAS) Oxidation to 2-keto-*L*-gulonic Acid Batch – Trial 1

This step focused on the oxidation of protected sorbose to 2-keto-*L*-gulonic acid. Diacetone-*L*-sorbose (0.91 g, 3.49 mmol) was dissolved in 50 mL of dH_2O. The reaction mixture was placed in an ice bath. NaOH (1.50 g, 37.5 mmol) was added dropwise until universal pH indicator paper indicated the reaction mixture was alkaline. KMnO4 (0.80 g, 5.06 mmol) was dissolved in 50 mL of dH_2O to achieve a 0.1 mol/L concentration. The $KMnO_4$ solution was added dropwise to the diacetone-L-sorbose solution for 15 minutes with constant stirring. The reaction mixture was then heated to 50° C and allowed to react at this temperature. After 2 hours, the reaction was cooled to room temperature and excess KMnO4 was quenched by the slow addition of Sodium bisulphite (2.73 g, 26.23 mmol) until the purple colour of KMnO4 disappeared. The mixture was acidified to pH 2 using concentrated H_2SO_4 (2 mL) and monitored with universal pH indicator paper. The solution was filtered, and the filtrate was concentrated under reduced pressure using a rotary evaporator. The concentrate was extracted with ethyl acetate (10 mL). The organic layer was dried over anhydrous Na_2SO_4 and filtered, and the solvent was evaporated to dryness under reduced pressure using a rotary evaporator. Excess ethyl acetate was removed, leaving 2-keto-*L*-gulonic acid, a white powder (0.58 g, 2.98 mmol, 85%) analyzed by NMR (300 MHz, DMSO-d_6). See Figure 37 and Appendices A 66 to A 68.

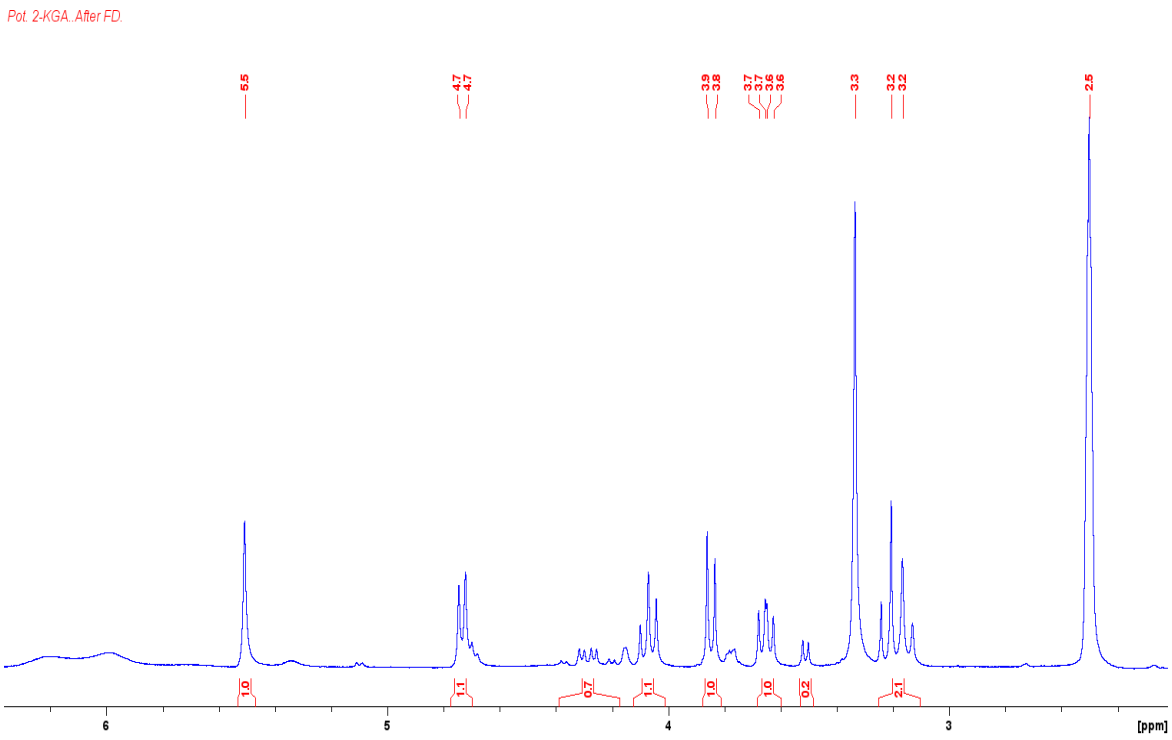

Figure 37: 2-keto-L-gulonic acid ^{1}H-NMR for Batch 1 recorded in DMSO-d_6 (300 MHz).

2.2.3.2 Diacetone-*L*-Sorbose (DAS) Oxidation to 2-keto-*L*-gulonic Acid Batch – Trial 2

For this trial, acetone was used as the solvent to minimize water, especially in the flow. Diacetone-*L*-sorbose (0.34 g, 1.30 mmol) was dissolved in 20 mL of acetone. The reaction mixture was placed in an ice bath. NaOH (0.50 g, 12.5 mmol) was added dropwise until universal pH indicator paper indicated the reaction mixture was alkaline. KMnO4 (0.35 g, 2.21 mmol) dissolved in 20 mL of acetone was added dropwise to the diacetone-L-sorbose solution for 10 minutes with constant stirring. The reaction mixture was then heated to 50° C and allowed to react at this temperature. After 2 hours, the reaction was cooled to room temperature, and excess KMnO4 was quenched by the slow addition of sodium bisulphite (1.20 g, 11.53 mmol) till the disappearance of $KMnO_4$ purple colour. The mixture was acidified to pH 2 using concentrated H_2SO_4 (1 mL) and monitored with universal pH

indicator paper. The solution was filtered, and the filtrate was concentrated under reduced pressure using a rotary evaporator. The concentrate was extracted with ethyl acetate (6 mL). The organic layer was dried over anhydrous Na_2SO_4 and filtered, and the solvent was evaporated to dryness under reduced pressure using a rotary evaporator. Excess ethyl acetate was removed, leaving 2-keto-*L*-gulonic acid, a white powder (0.22 g, 1.13 mmol, 88%) analyzed by NMR (300 MHz, DMSO-d_6). See Figure 38 and Appendices A 69 to A 71.

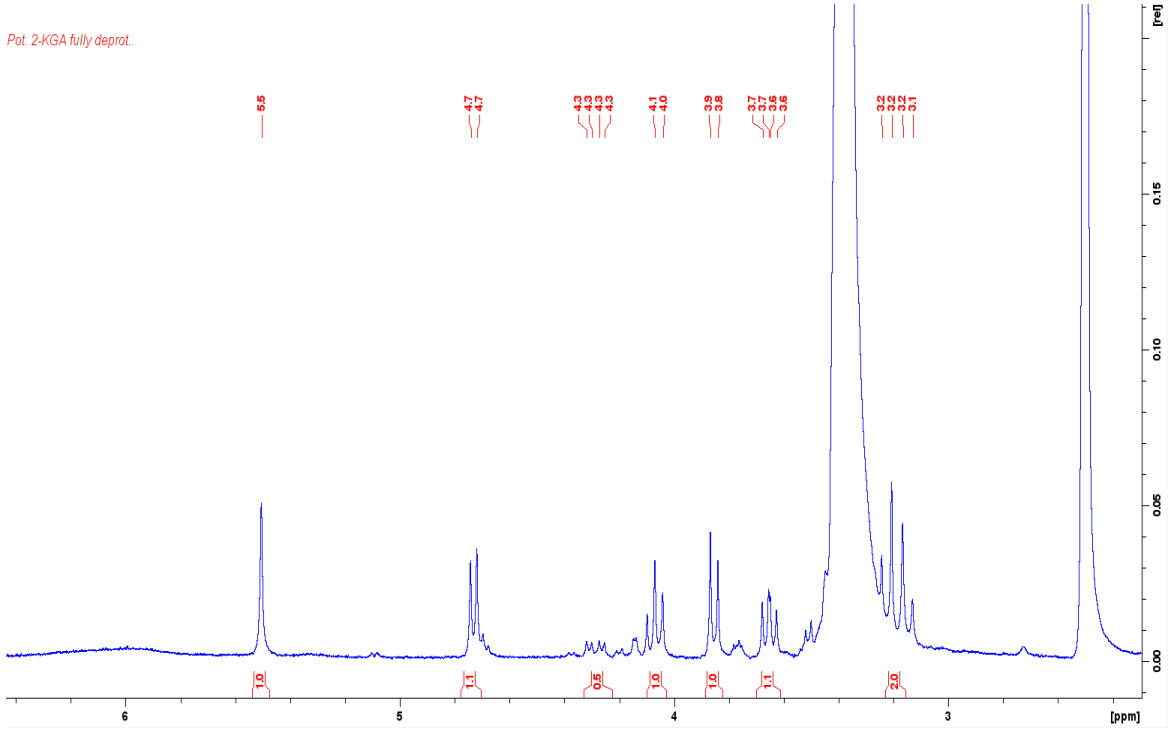

Figure 38 2-keto-L-gulonic acid ^{1}H-NMR for Batch 2 recorded in DMSO-d_6 (300 MHz).

2.2.3.3 Diacetone-*L*-Sorbose (DAS) Oxidation to 2-keto-*L*-gulonic Acid Flow – Trial 3

A flow system was set up using PTFE tubing (0.75 mm inner diameter) and syringe pumps (Scheme 9). Diacetone-*L*-sorbose (0.33 g, 1.26 mmol) was dissolved in 20 mL of acetone. NaOH (0.50 g, 12.5 mmol) was added to this mixture and the solution was added to the flow at a 1 ml/min flow rate from a first pump A. KMnO4 (0.35 g, 2.21 mmol) dissolved in 10 mL

of acetone was added to the flow simultaneously at a 0.5 ml/min flow rate from a second pump B. The reaction mixture introduced into the flow system via a T-mixer (T-mixer 1) was passed through a reactor coil in a hot water bath at an elevated temperature of 50° C. This temperature was consistently maintained throughout the reaction zone to ensure uniform conditions. Sodium bisulphite (1.20 g, 11.53 mmol) dissolved in 5 mL of dH_20 was added to the flow simultaneously at a 0.25 ml/min flow rate from a third pump C. H_2SO_4 (1 mL) diluted in 10 mL of acetone was added to the flow simultaneously at a 0.5 ml/min flow rate from a fourth pump D, and was then allowed to react with the reaction mixture at a second reactor coil for 20 minutes. In the drying unit, 3 A° and 4 A° molecular sieves trapped the aqueous layer. The sieves were pre-dried in the oven at 160° C for 16 hours before use. The product was obtained following a 40-minute residence time in the reactor, and the solvent was evaporated to dryness under reduced pressure using a rotary evaporator. Excess acetone was removed, leaving 2-keto-*L*-gulonic acid, a white powder (0.22 g, 1.13 mmol, 91%) analyzed by NMR (400 MHz, DMSO-d_6) and mass spectrometry. See Figures 39 to 43 and Appendices A 72 to A 77.

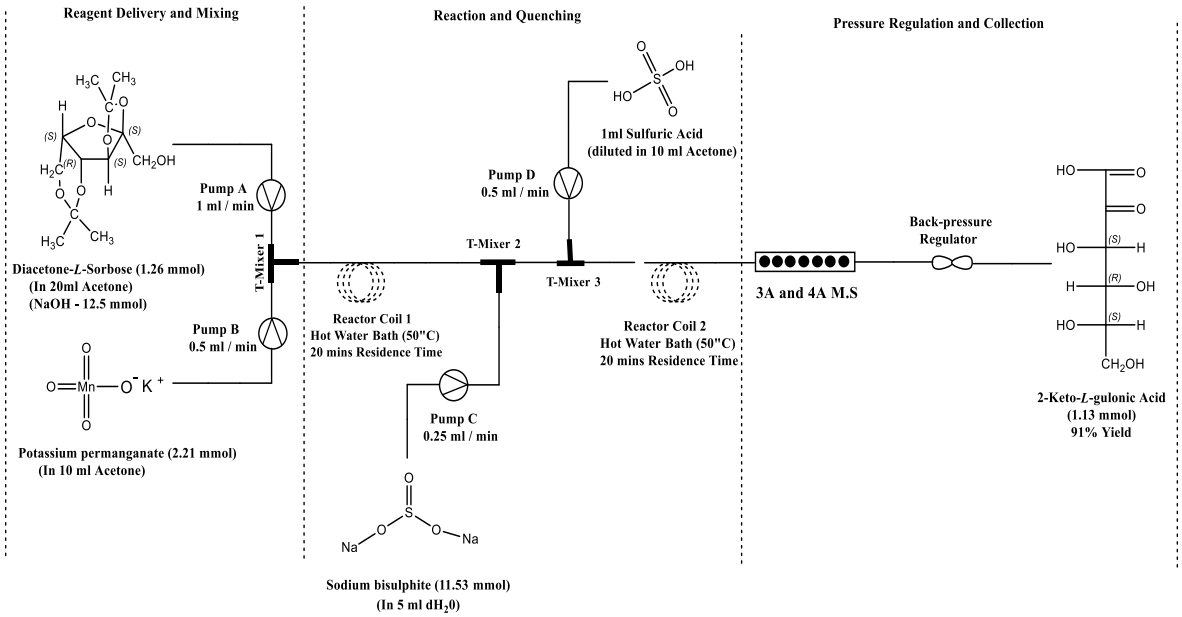

Scheme 9: The Oxidation of Diacetone-L-Sorbose to 2-KGA in the flow, using $KMnO_4$

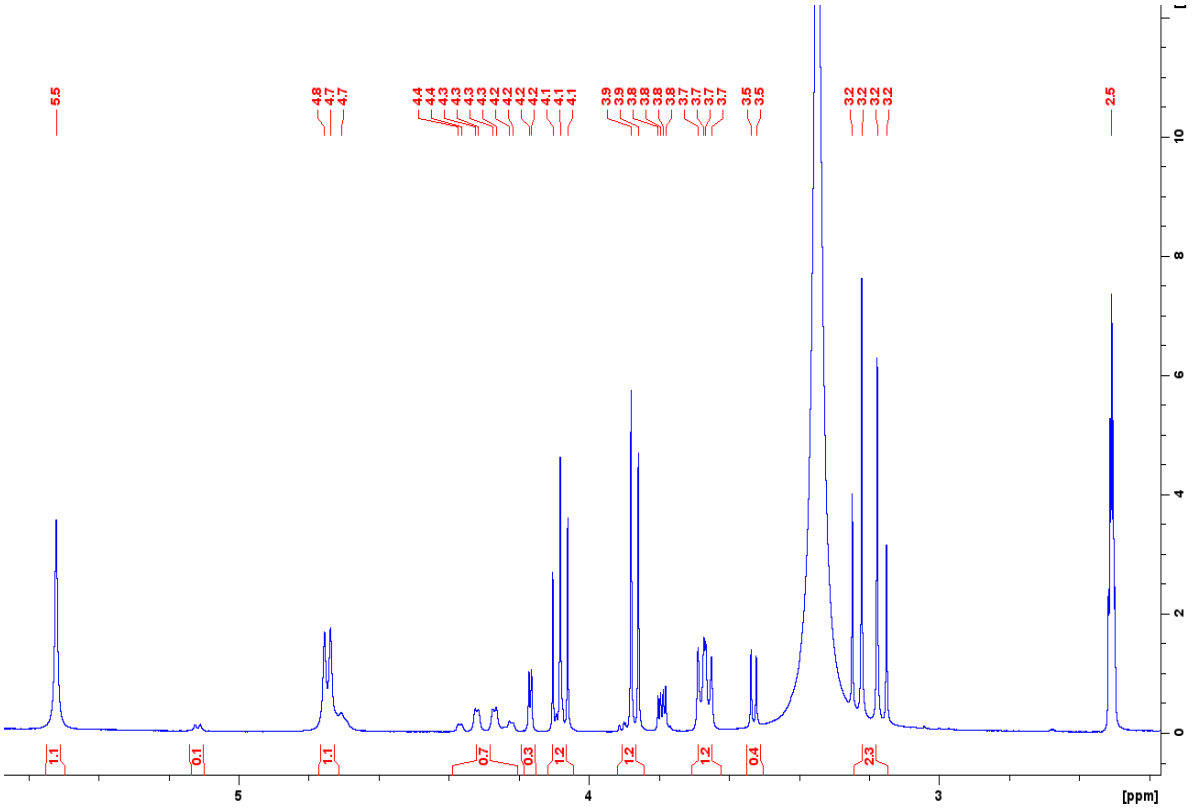

Figure 39: 2-keto-L-gulonic acid ^{1}H-NMR for Flow 3 recorded in DMSO-d_6 (400 MHz).

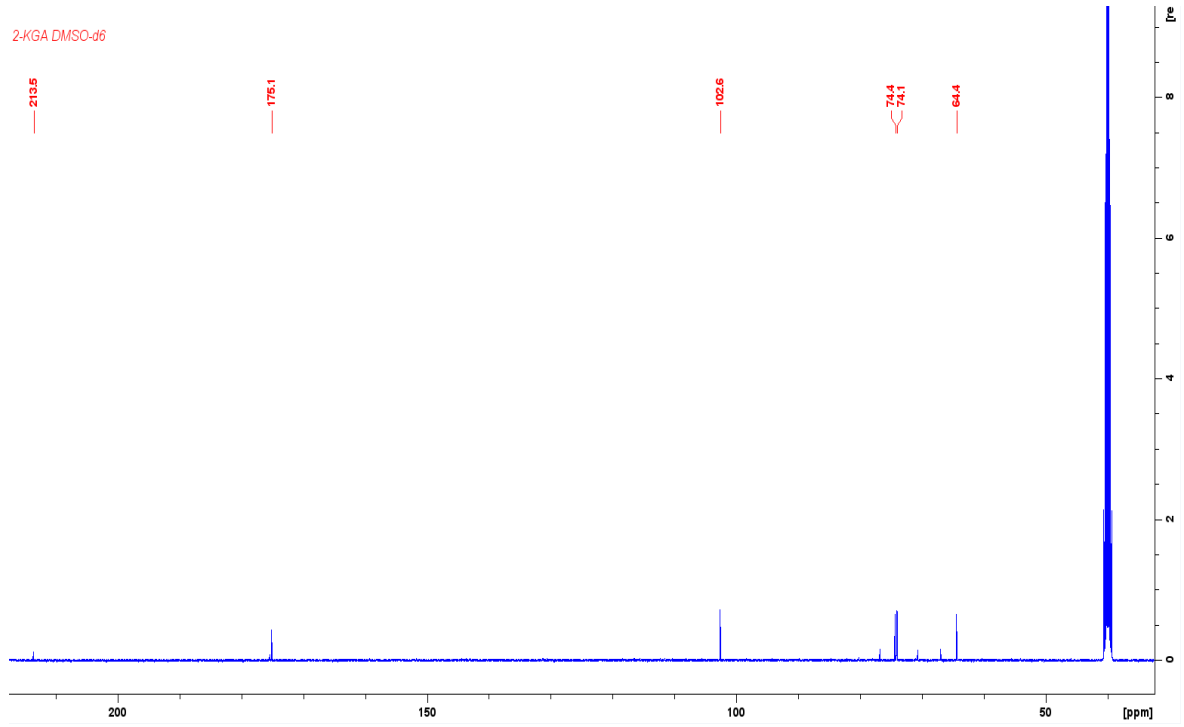

Figure 40: 2-keto-L-gulonic acid ^{13}C-NMR for Flow 3 recorded in DMSO-d$_6$ (400 MHz).

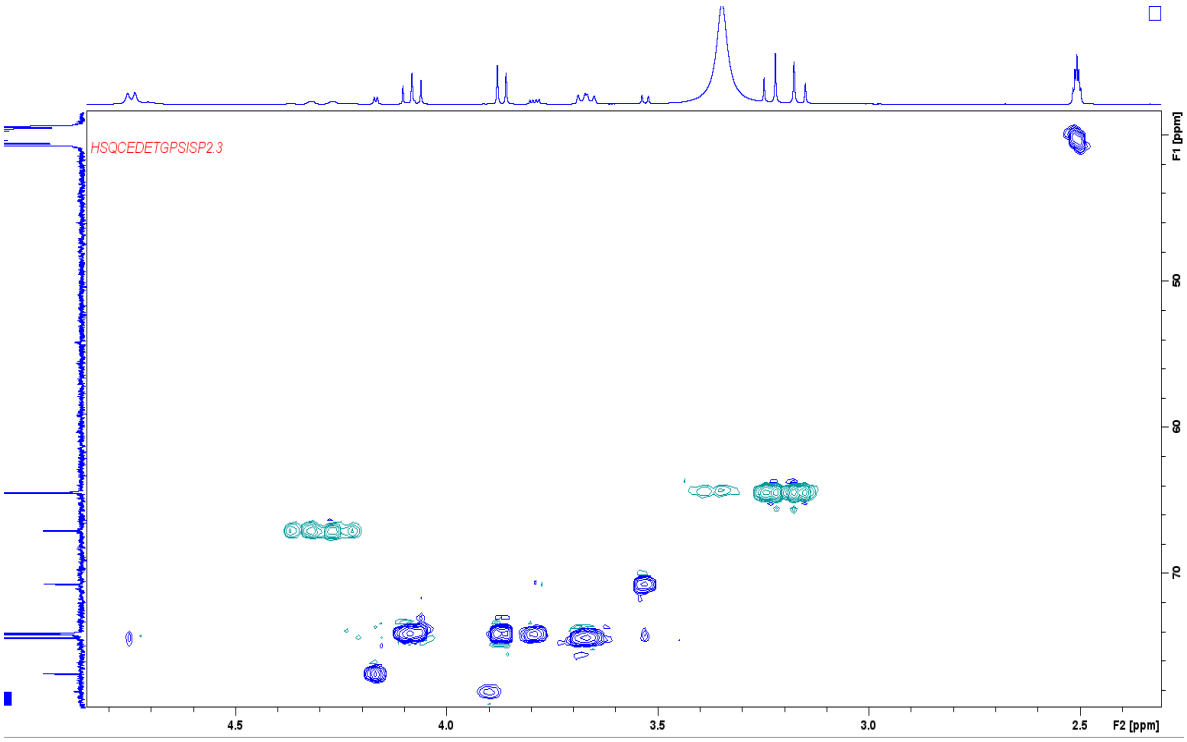

Figure 41: 2-keto-L-gulonic acid HSQC for Flow 3 recorded in DMSO-d$_6$ (400 MHz).

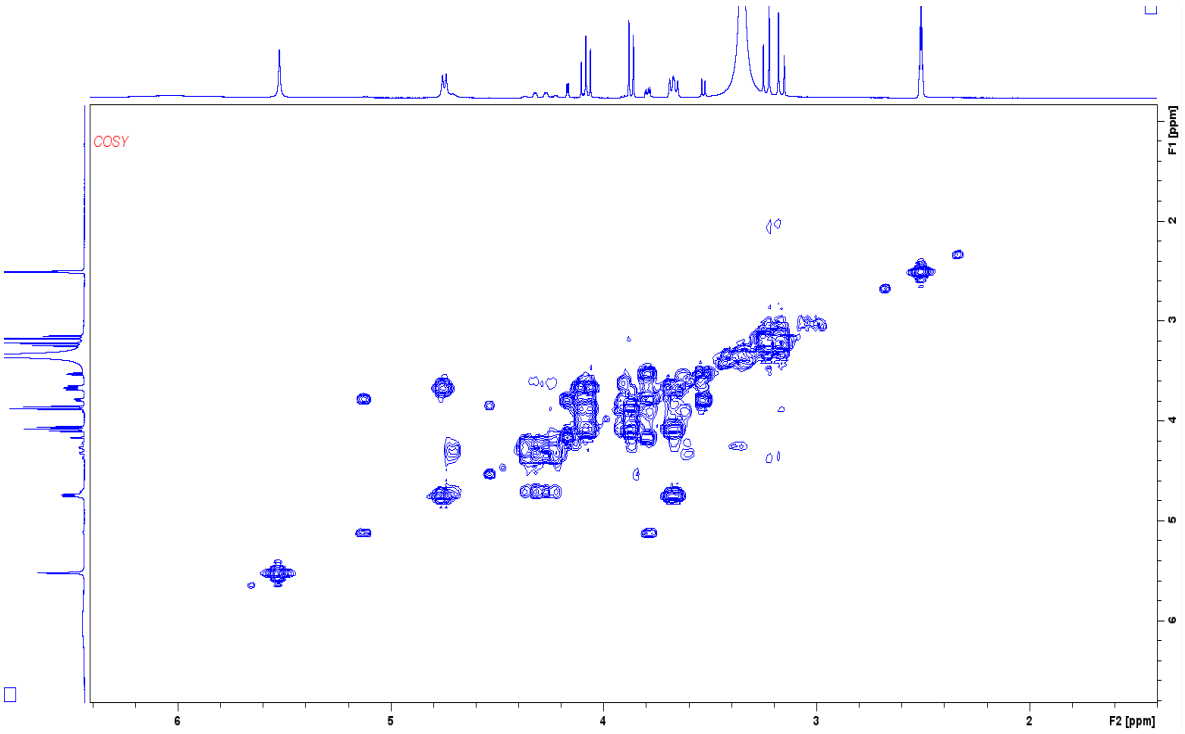

Figure 42: 2-keto-L-gulonic acid COSY for Flow 3 recorded in DMSO-d_6 (400 MHz).

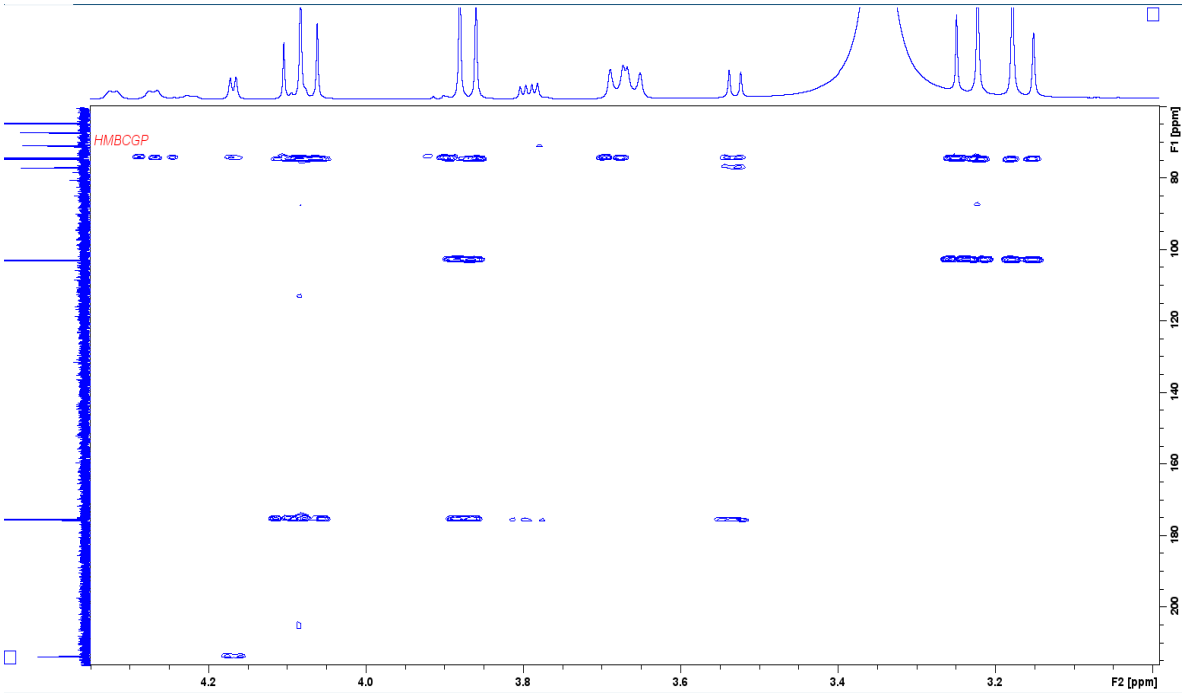

Figure 43: 2-keto-L-gulonic acid HMBC for Flow 3 recorded in DMSO-d_6 (400 MHz).

Table 10: ^{13}C and ^{1}H NMR Data for 2-keto-L-gulonic acid (Flow 3)

Carbon #	^{13}C δ, ppm	^{1}H δ, ppm	COSY	HMBC
1	175.1	-	-	-
2	213.5	-	-	H3
3	76.89	4.168	H4	H4
4	74.4	3.671, 4.751	H3, H5	H3, H5, H5', H6
5	74.1	3.869, 4.077	H4, H6	H3, H4, H6
6	64.4	3.205	H5	H5

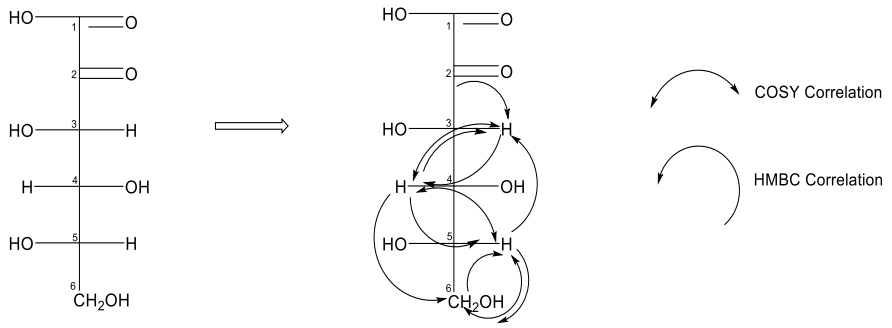

Figure 44: The structure of the 2-keto-L-gulonic acid and the NMR (2-D) correlation.

2.2.3.4 2-keto-*L*-gulonic Acid Yield and Comparison of Batch and Flow

2-keto-*L*-gulonic acid was successfully synthesized from diacetone-*L*-sorbose, and the NMR analysis of the product obtained revealed an intriguing mixture of 2-keto-*L*-gulonic acid (Figures 39 to 43 / Appendices A 72 to A 76). The ^{13}C NMR spectrum (See Figure 40 / Appendix A 73) exhibited a striking array of signals, including a prominent peak at δ 213 ppm, characteristic of the ketone carbon in the open-chain form of 2-keto-*L*-gulonic acid. Simultaneously, a signal at δ 102 ppm was observed, which can be assigned to the anomeric carbon of the cyclic hemiacetal form.[123] The spectrum also displayed additional peaks in the

60-80 ppm range, corresponding to the carbon atoms of both the open-chain and cyclic structures. The proton NMR spectrum (see Figure 39 / Appendix A 72) revealed compelling evidence for the cyclic structure. A sharp doublet is seen at 4.74 ppm, a characteristic of the anomeric proton in the ring form. This signal stood out as a key indicator of cyclization. Further supporting this interpretation, a cluster of overlapping multiplets spanning the 3.5 to 4.4 ppm region was observed. Together, these spectral features clearly show the existence of the cyclic form in the reaction mixture. According to some literature, different solid forms of 2-keto-*L*-gulonic acid have been observed and sometimes, mixtures of two solid forms were obtained, each containing one molecule of water of crystallization.[124] This suggests that different structural arrangements, including cyclic forms, can coexist in a single sample.[124] Additionally, 2-keto-*L*-gulonic acid is known to form a monohydrate when crystallized from water or water-containing organic solvents. The presence of water in the crystal structure could facilitate the equilibrium between open-chain and cyclic forms.[125] Many sugar derivatives are also known to exist in equilibrium between open-chain and cyclic forms in solution.[125]

The formation of cyclic 2-keto-*L*-gulonic acid can be rationalized through intramolecular cyclization following the initial oxidation of diacetone-*L*-sorbose. It can be proposed that this cyclization occurs spontaneously under the reaction conditions, driven by the thermodynamic stability of the cyclic hemiacetal form. The potassium permanganate likely facilitates the initial oxidation step, while the subsequent cyclization is an inherent property of the 2-keto-*L*-gulonic acid structure in solution. This result aligns with previous studies on similar sugar derivatives, where cyclic forms are often observed in solutions due to intramolecular reactions between carbonyl and hydroxyl groups.[125] Aside from NMR, Mass spectrometry

confirmed the product's identity, as seen in Appendix A 77. Implementing a flow setup using the optimized parameters in the batch yielded remarkable results, achieving improved yield and a significantly reduced reaction or residence time for the flow of just 40 minutes in trial 3, in contrast to the 2-hour duration required for the batch process, as shown in Table 11 below.

Table 11: Comparison of 2-keto-L-gulonic acid yields and the Reaction parameters in Batch versus Flow

Diacetone-*L*-sorbose to 2-keto-*L*-gulonic Acid: Batch versus Flow		
	Batch	Flow
Reaction/ Residence time (mins)	120	40
DAS Yield (mmol)	1.13	1.13
Total Yield (%)	88	91

2.2.4 2-keto-*L*-gulonic Acid to Ascorbic Acid in Batch and Flow

2.2.4.1 2-keto-*L*-gulonic Acid to Ascorbic Acid Batch – Trial 1

This step was focused on the lactonization and enolization of 2-keto-*L*-gulonic acid to ascorbic acid. 2-keto-*L*-gulonic acid (0.51 g, 2.62 mmol) was dissolved in 5 mL of methanol and heated at an elevated temperature of 65° C to 100° C under reflux. H_2SO_4 (0.5 mL) was added dropwise to this solution as a catalyst until universal pH indicator paper indicated the reaction mixture was acidified. The solution was allowed to react with constant stirring for 180 minutes. After this, sodium bicarbonate (5 mL) was added dropwise until the universal pH indicator paper indicated that the reaction mixture was moderately acidic. The product

was obtained, and the solvent was evaporated to dryness under reduced pressure using a rotary evaporator. Excess dH_2O was removed, leaving a white powder (0.38 g, 2.15 mmol, 82%) analyzed by NMR (300 MHz, DMSO-d_6). See Figure 45 and Appendices A 78 to A 80.

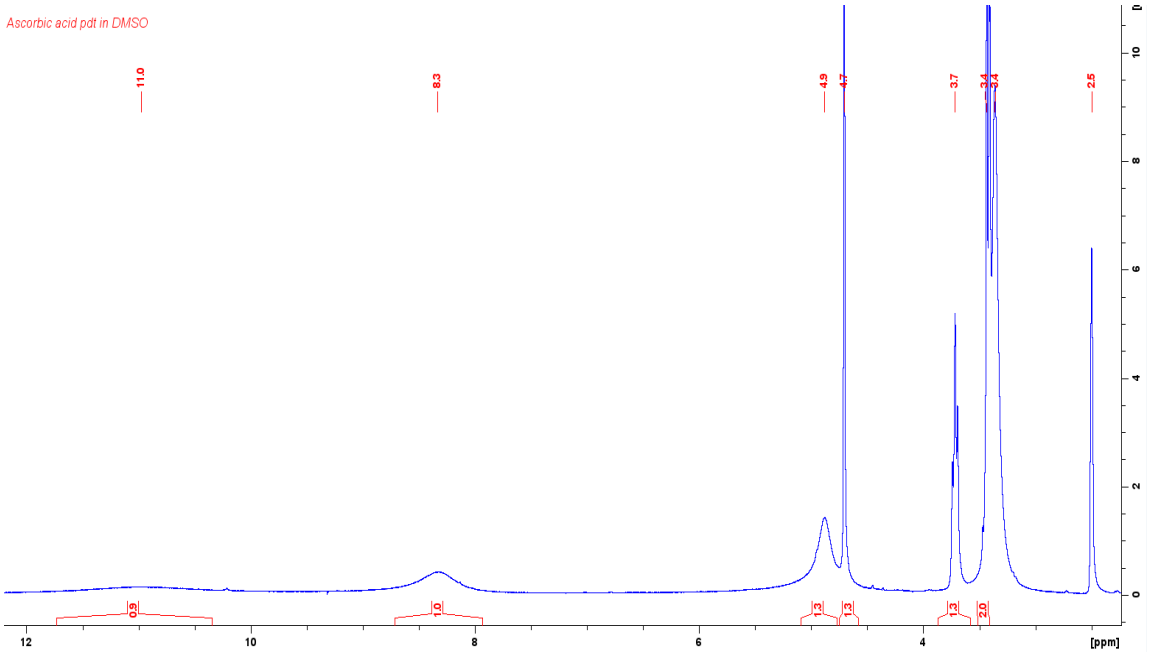

Figure 45: Ascorbic acid ^{1}H-NMR for Batch 1 recorded in DMSO-d_6 (300 MHz).

2.2.4.2 2-keto-*L*-gulonic Acid to Ascorbic Acid Flow – Trial 2

A flow system was set up using PTFE tubing (0.75 mm inner diameter) and syringe pumps. 2-keto-*L*-gulonic acid (0.55 g, 2.83 mmol) was dissolved in 10 mL of methanol and added to the flow at a 0.5 ml/min flow rate from a first Pump A. H_2SO_4 (0.5 mL) diluted in dH_20 (5 mL) was added to the flow simultaneously at a 0.25 ml/min flow rate from a second Pump B. The reaction mixture introduced into the flow system via a T-mixer (T-mixer 1) was passed through a reactor coil in a hot water bath at an elevated temperature of 65° C to 100° C. This temperature was consistently maintained throughout the reaction zone to ensure uniform conditions. Sodium bicarbonate (5 mL) was added to the flow simultaneously at a 0.5 ml/min

flow rate from a third Pump C. The product was obtained following a 20-minute residence time in the reactor, and the solvent was evaporated to dryness under reduced pressure using a rotary evaporator. Excess H_20 was removed, leaving *L*-ascorbic acid, a white powder (0.42 g, 2.38 mmol, 85 %) analyzed by NMR (400 MHz, DMSO-d_6) and Mass spectrometry. See Appendix A 81 and A 82. The crude product (0.21 g, 1.19 mmol) was recrystallized with a mixture of ethanol and water (3:1), and pure ascorbic acid (0.12 g, 0.68 mmol, 57%) was obtained and analyzed by NMR (400 MHz, DMSO-d_6). See Figures 46 to 50 / Appendix A 83 to A 87.

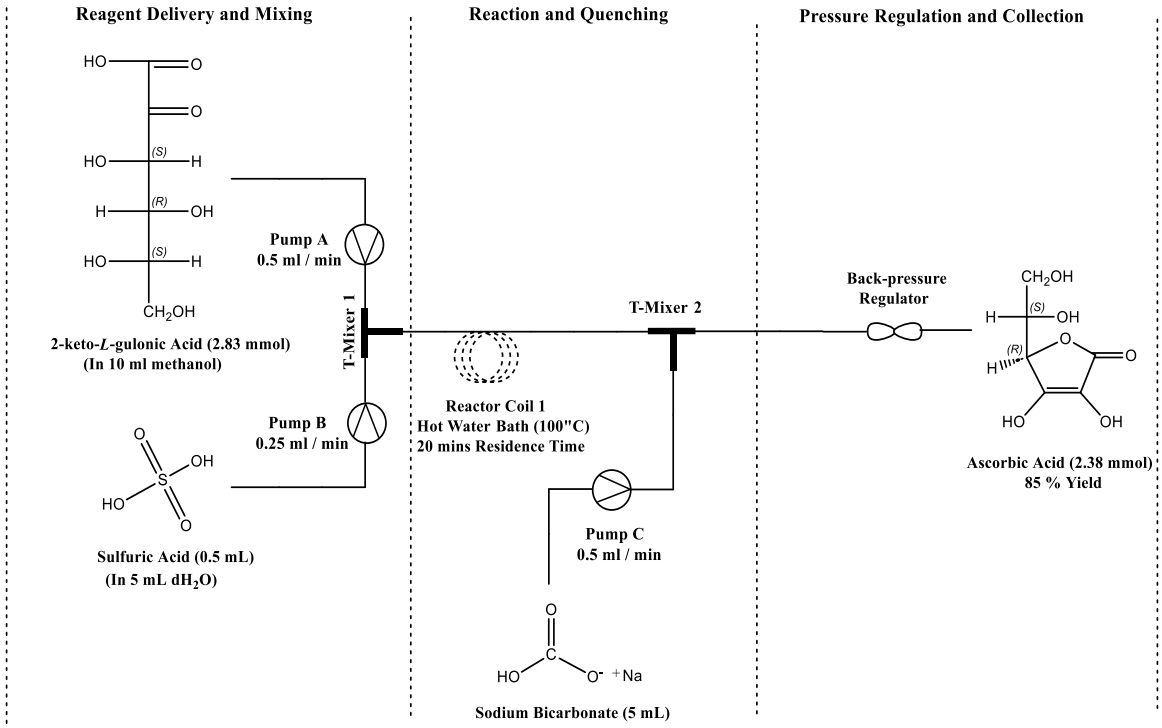

Scheme 10: The lactonization and enolization of 2-KGA to L-ascorbic acid in the flow

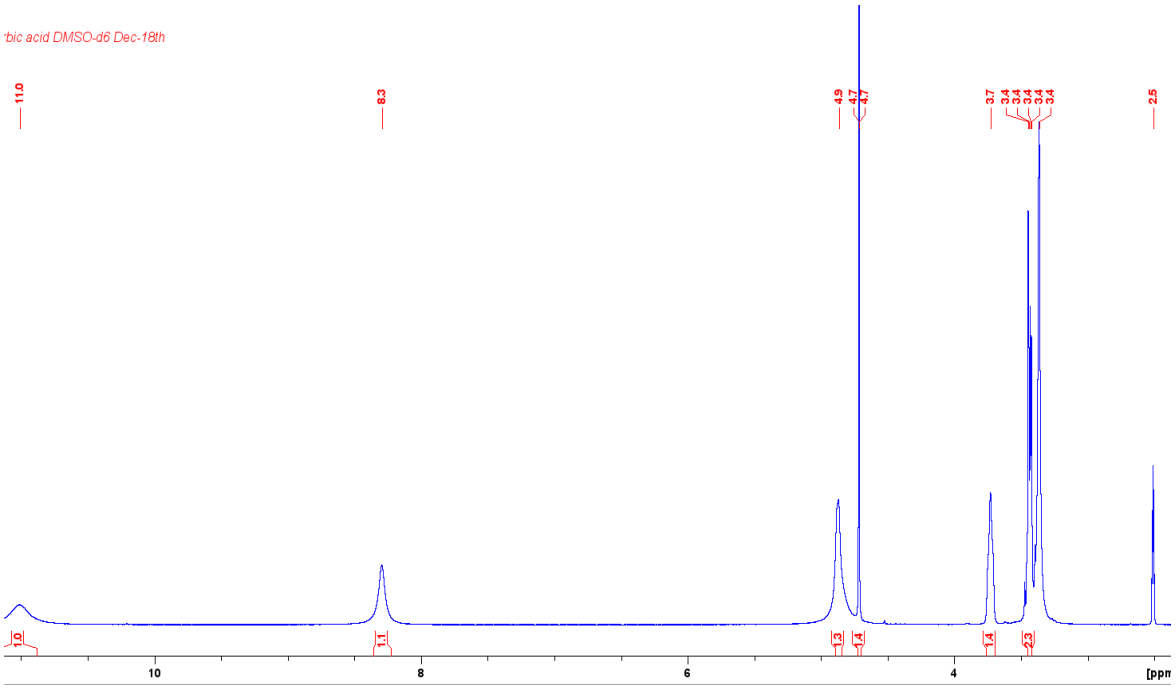

Figure 46: Ascorbic acid ^{1}H-NMR for Flow 2 recorded in DMSO-d$_6$ (400 MHz).

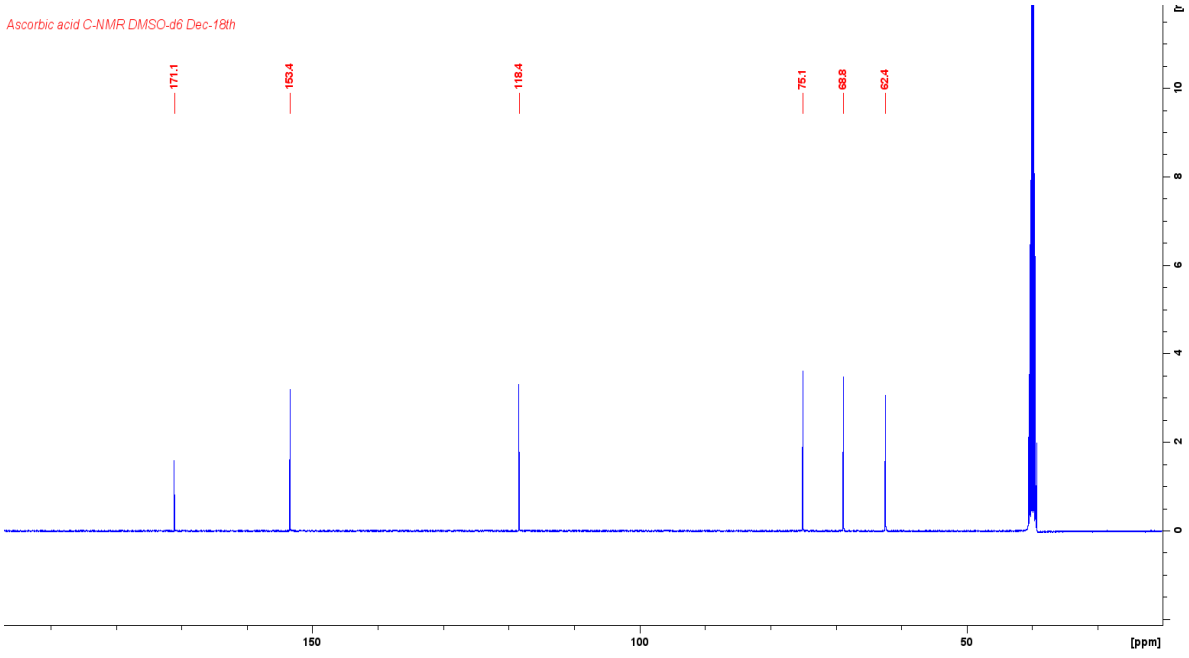

Figure 47: Ascorbic acid ^{13}C-NMR for Flow 2 recorded in DMSO-d$_6$ (400 MHz).

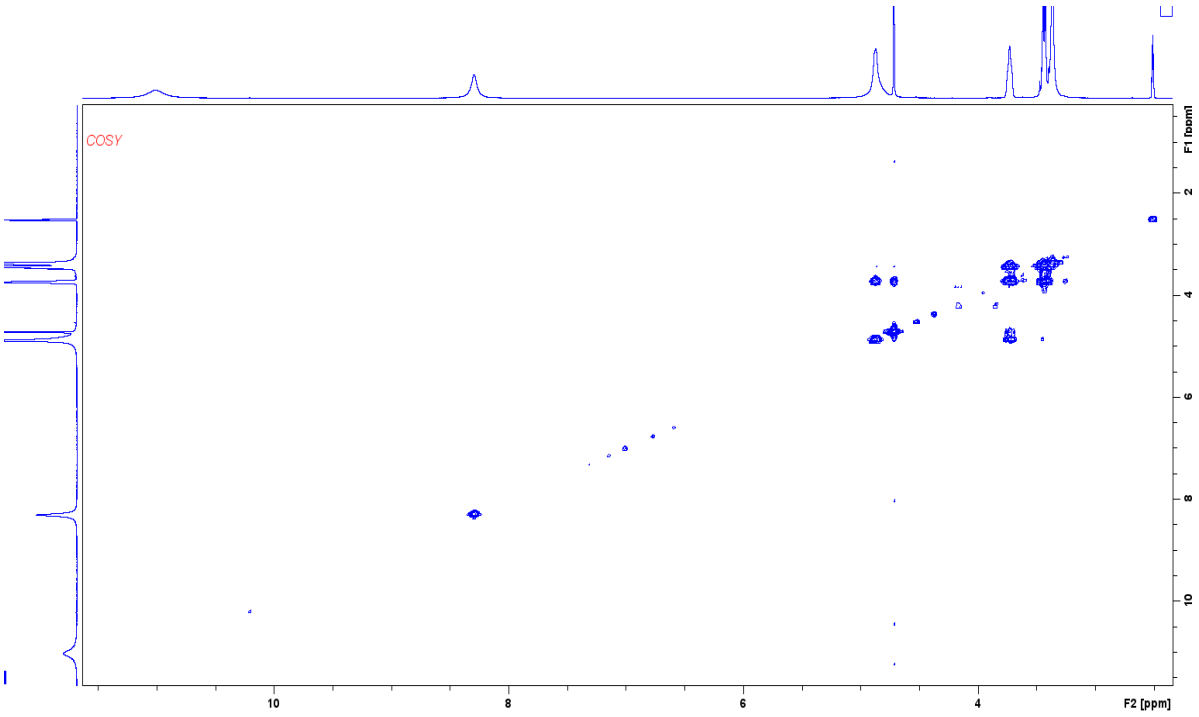

Figure 48: Ascorbic acid COSY for Flow 2 recorded in DMSO-d_6 (400 MHz).

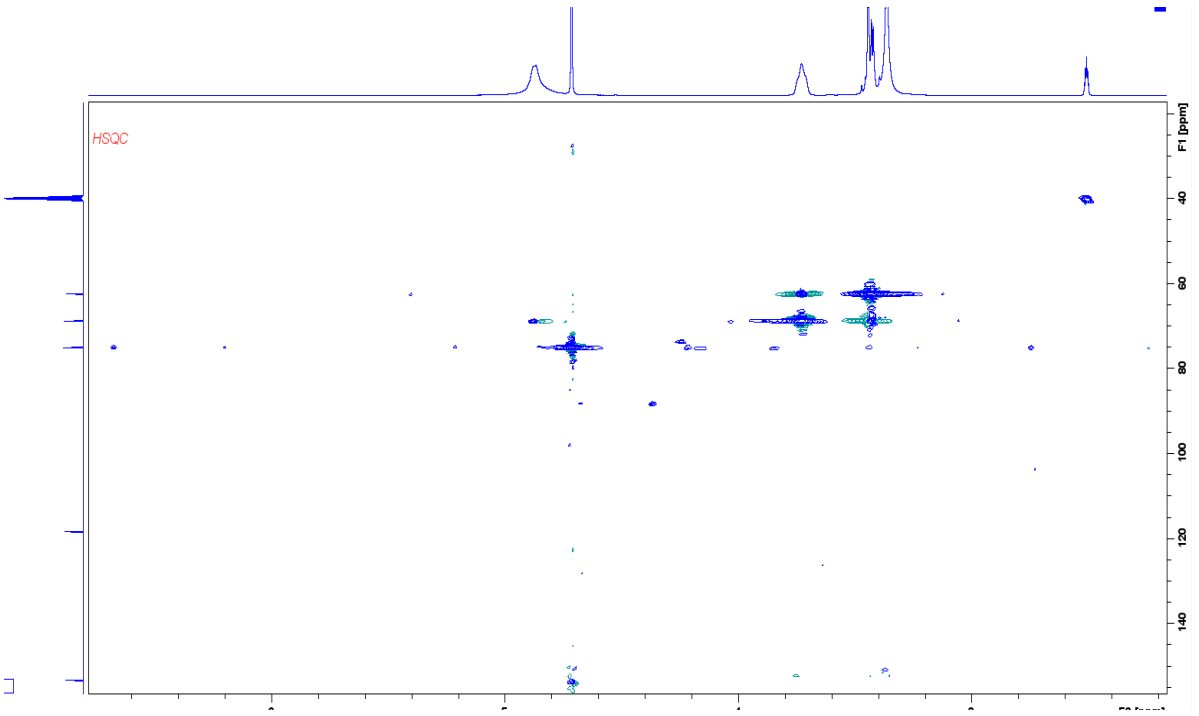

Figure 49: Ascorbic acid HSQC for Flow 2 recorded in DMSO-d_6 (400 MHz).

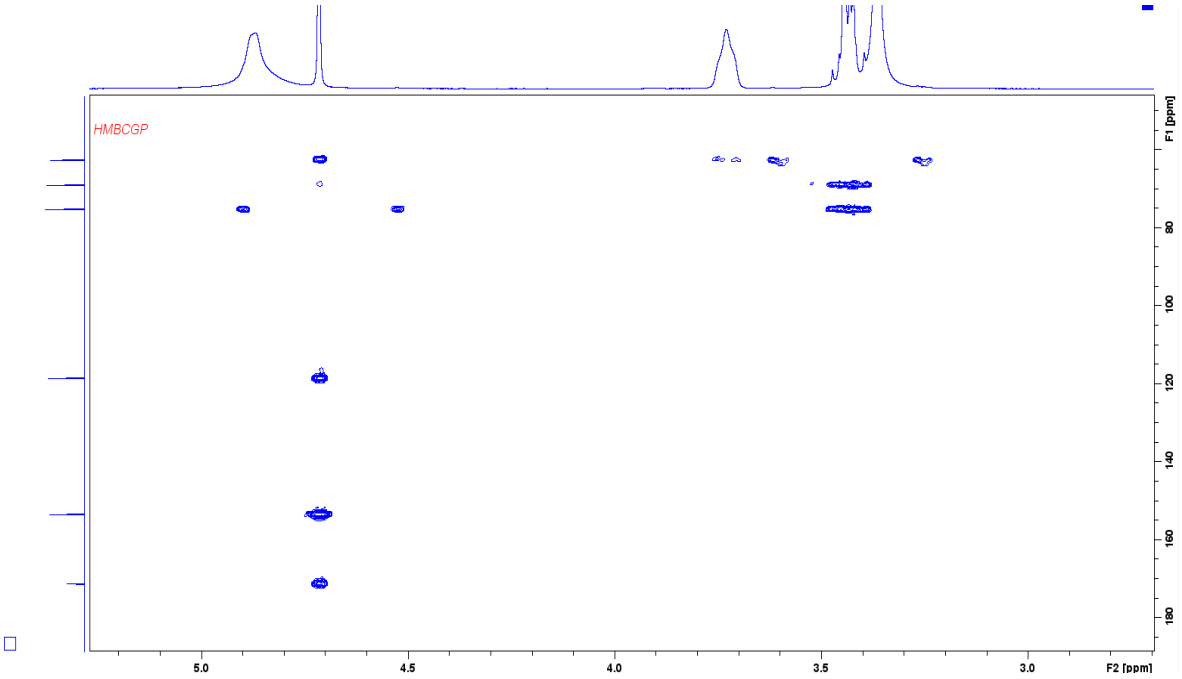

Figure 50: Ascorbic acid HMBC for Flow 2 recorded in DMSO-d_6 (400 MHz).

Table 12: ^{13}C and ^{1}H NMR Data for Ascorbic acid (Flow 2)

Carbon #	^{13}C δ, ppm	^{1}H δ, ppm	COSY	HMBC
1	62.4	3.728, 3.431	H2	H2, H3
2	68.8	4.867, 3.728, 3.431	H1, H3	H1, H3
3	75.0	4.717	H2	H2, H2’
4	118.4	-	-	H3
5	153.3	-	-	H3
6	171.1	-	-	H3

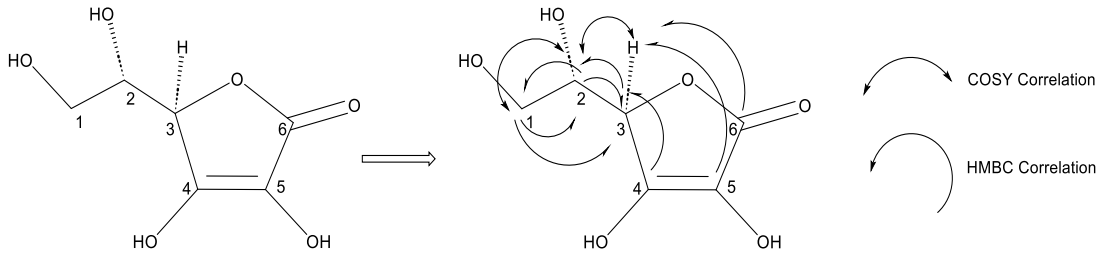

Figure 51: The structure of the Ascorbic acid and the NMR (2-D) correlation.

2.2.4.3 Ascorbic Acid Product Yields and Comparison of Batch and Flow

Ascorbic acid was successfully synthesized from 2-keto-*L*-gulonic acid, as evidenced by the NMR spectroscopic analysis (Figures 46 to 50 / Appendix A 83 to A 87). The NMR spectrum of the product exhibited characteristic signals consistent with the structure of ascorbic acid. Upon careful examination of the ^{1}H-NMR spectrum (See Figure 46 / Appendix A 83), a distinctive doublet emerged at around δ 4.71 ppm. This particular signal indicates the proton attached to the C-4 carbon in the ascorbic acid structure. Two key doublets were spotted hanging out between δ 3.42 and 3.44 ppm. These signals are expected from the protons on C-5 and C-6 in ascorbic acid. The spectral data also revealed the presence of hydroxyl protons, which appeared as broad singlets in the range of δ 8-11 ppm, further corroborating the formation of ascorbic acid. Complementary ^{13}C-NMR data after recrystallization corroborated these findings, showing precisely the 6 carbon signals characteristic of Ascorbic acid (Figure 47 / Appendix A 84). As much as the NMR strongly supports ascorbic acid formation, mass spectrometry confirmed the product's identity, as seen in Appendix A 82. The optimal condition for this step includes using a small amount of water, as too much free water can negatively impact the reaction by increasing reaction time and decreasing yield, partly due to the decomposition of *L*-ascorbic acid in the presence of aqueous acid.[69] A small amount of the base (5 ml) was used since ascorbic acid is more stable in acidic conditions, so full neutralization was avoided to reduce the chances of side reactions and reduction in the yield of ascorbic acid.

Implementing a flow setup using the optimized parameters in the batch yielded remarkable results, achieving improved yield and a significantly reduced reaction or residence time for

the flow of just 20 minutes in trial 2, in contrast to the 3-hour duration required for the batch process.

Table 13: Comparison of Ascorbic acid yields and the Reaction parameters in Batch versus Flow

2-keto-*L*-gulonic Acid to Ascorbic Acid: Batch versus Flow		
	Batch	Flow
Reaction/ Residence time (mins)	180	20
DAS Yield (mmol)	2.15	2.38
Total Yield (%)	82	85

2.3 Conclusion

2.3.1 Comparison of Flow Methods with Batch Processes

Results from our flow system demonstrated significant improvements over traditional batch processes. The reduction of *D*-glucose to *D*-sorbitol was done in 20 minutes, compared to a 60-minute reaction time in the batch. The conversion of *L*-sorbose to diacetone-*L*-sorbose in the flow reached a 95 % yield within a residence time of just 30 minutes, compared to a 90 % yield in 360 minutes for the batch reaction. The subsequent oxidation step showed even more dramatic improvements, with 2-keto-*L*-gulonic acid yields of 91 % achieved in a total residence time of 40 minutes, a substantial reduction from the 2-hour reaction time typically required in batch processes, which gave an 88 % yield. For the 2-keto-*L*-gulonic acid to ascorbic acid conversion, the flow gave a slightly better yield (85 %) in 20 minutes of residence time, while the batch gave an 82 % yield in around 180 minutes of reaction time.

Higher yields and product quality were consistently maintained by adjusting flow rates, reagent-to-solvent ratio, and temperatures. The overall yield of ascorbic acid from *L*-sorbose reached 82-85%, surpassing the typical yields of 70-75% reported for industrial batch processes. Additionally, though the flow approach did not reduce solvent usage significantly compared to batch methods, it contributed to a more environmentally friendly production process via efficient mixing and in-flow of reagents.

2.3.2 Advantages and Limitations of Developed Protocols

The developed flow synthesis protocols for ascorbic acid production demonstrate several advantages over traditional batch processes. Primarily, the flow system achieved remarkable improvements in reaction efficiency and speed. For instance, the conversion of *L*-sorbose to diacetone-*L*-sorbose reached a 95% yield in just 30 minutes, compared to 90% in 360 minutes for batch reactions. Similarly, the oxidation step yielded 91% of 2-keto-*L*-gulonic acid in 40 minutes, drastically reducing the typical 2-hour batch reaction time. While showing a smaller improvement, the final conversion to ascorbic acid still achieved a slightly higher yield (85%) in a fraction of the time required for batch processes. These time reductions could significantly enhance production capacity and reduce energy consumption. The 82-85% yield from *L*-sorbose to ascorbic acid surpasses typical industrial batch yields, indicating the potential for increased production efficiency. Furthermore, while the flow approach did not substantially reduce solvent usage, it contributed to a more environmentally friendly process through efficient mixing and in-flow reagent addition. However, the developed protocols also have limitations. The marginal improvement in solvent usage suggests that further optimization in this area is needed to enhance the environmental benefits. Additionally, the complexity of the flow

system setup and the need for specialized equipment might present challenges in terms of initial investment and operator training. The scalability of the process to industrial levels and its long-term stability under continuous operation would require further investigation. Despite these limitations, the significant improvements in reaction time, yield, and process control make this flow synthesis approach a promising alternative to traditional batch methods for ascorbic acid production.

2.3.3 Potential for Scale-up and Industrial Applications

The discrete flow synthesis steps from *L*-sorbose through to *L*-ascorbic acid have shown that time for reaction completion is improved in flow vs batch synthesis. Furthermore, we demonstrated that the crude products from each synthetic step could be used successfully in the next reaction with minimal purification. Indeed, generally, only solvents were removed to allow structural characterization. Thus, the improved reaction efficiency demonstrates that the flow synthesis approach for ascorbic acid production has potential for scale-up and industrial application. The improved reaction and reduced processing times observed in the laboratory-scale flow system suggest promising outcomes for larger-scale operations.

The next significant step in advancing the synthesis of ascorbic acid from *D*-glucose is transitioning from discrete flow to continuous flow synthesis. This shift presents several challenges that need to be addressed. Firstly, the lack of adequate pumps capable of handling the diverse range of solvents and reagents across all steps must be resolved. Secondly, an inline separator needs to be developed or optimized for efficient aqueous-organic phase separation, particularly crucial in the diacetone-*L*-sorbose to 2-keto-*L*-gulonic acid step. Integrating such a separator is vital for maintaining continuous operation without interrupting manual workup procedures. Though using molecular sieves in the diacetone-*L*-sorbose to 2-keto-*L*-gulonic

acid flow synthesis step is a step towards automation, it still retains elements of manual workup. It may not be optimal for large-scale continuous flow synthesis as translating this into a continuous process would require innovative inline purification techniques. The ongoing research into the *D*-sorbitol to *L*-sorbose conversion presents a critical gap that must be bridged for a truly continuous process. Nevertheless, the potential benefits of product consistency, process safety, and operational efficiency make the flow synthesis of ascorbic acid a promising candidate for industrial-scale implementation, particularly in the pharmaceutical and food industries where high-purity ascorbic acid is in constant demand.

3. Flow synthesis of N5-OH-*L*-Orn towards Chemoenzymatic synthesis of Piperazic acid

3.1 Chapter Overview

The flow synthesis of N5-OH-*L*-Ornithine represents a step towards the chemoenzymatic synthesis of piperazic acid, a valuable building block in natural product synthesis and drug discovery. This approach combines the efficiency of flow chemistry with the selectivity of enzymatic catalysis. N5-OH-*L*-Ornithine acts as a key intermediate in the biosynthesis of piperazic acid, where it is cyclized to form the characteristic nitrogen-nitrogen bond. Recent studies have elucidated the enzymatic pathways involved in this process, with a piperazate synthase playing a central role in converting N5-OH-*L*-Orn to piperazic acid.[126] Thus, to produce piperazic acid via this method, N5-OH-*L*-Orn needs to be made. One strategy is to develop a flow synthesis method to produce N5-OH-*L*-Ornithine, which presents several advantages, including improved reaction control, enhanced heat and mass transfer, and the capacity to integrate without causing disruption. This approach follows the growing movement towards more sustainable and efficient synthetic processes in the pharmaceutical and fine chemical industries, potentially unlocking new opportunities in drug development and natural product synthesis.

3.2. Piperazic Acid: A Versatile Building Block

Piperazic acid, a cyclic nonproteinogenic amino acid[127] containing a rare nitrogen-nitrogen bond,[128,129] has emerged as a valuable component in bioactive natural products and drug discovery. This unusual N-N bond makes piperazic acid the only known example of a natural cyclic hydrazine amino acid.[130] As N-N bonds are found in roughly 10% of pharmaceutical structures,[131] this unique structural feature has garnered significant attention from researchers in recent years,[132] leading to a deeper understanding of its

biosynthesis, synthesis, incorporation into complex molecules, and potential applications. Recent research has shed light on the enzymatic pathways involved in its formation.[126,130] A key enzyme in this process is the piperazate synthase, responsible for cyclizing 5-hydroxylated ornithine to form piperazic acid.[130]

3.2.1 Biological Significance and Applications

Natural products incorporating piperazic acid residues exhibit many potent biological activities, including anti-malarial, anti-apoptotic, and antibacterial properties.[127] These compounds have been found in over 30 families of natural products, representing more than 140 distinct molecules.[127,133] In the pharmaceutical industry, piperazic acid is a valuable building block for creating peptide-based natural product derivatives with antibacterial and antifungal properties.[133–135] Its potential ability to lock amino acids in specific positions within peptides makes it a valuable tool for peptide engineering and developing molecular probes.[134] Finally, as an analogue of proline, it could be worth exploring as an organocatalyst, but currently challenges of accessing this rare amino acid have slowed research in this direction. The unique structural and functional properties of piperazic acid have sparked interest in developing more efficient and cost-effective methods for its production, including green biocatalysis and fermentation techniques, to facilitate its broader application in medicinal chemistry and biotechnology.[134]

3.2.2 Current Synthetic Approaches and Limitations of Piperazic Acid

The current synthetic approaches to piperazic acid involve both traditional chemical synthesis and biotechnological methods. Traditional chemical synthesis of piperazic acid often faces challenges such as low yield, multiple complex steps, and challenges producing

single enantiomers. These limitations have spurred interest in developing more efficient and sustainable methods. Current synthetic approaches focus on innovative methodologies that enhance efficiency and selectivity, yet they face notable limitations. Recent advancements include a selective deprotection strategy that simplifies the synthesis of piperazic acid-containing peptides,[136] improving overall yields, new methods that emphasize C–H functionalization and expand the structural diversity of piperazine derivatives,[137] which is crucial for drug discovery. Various synthetic routes, including transition-metal-catalyzed and rearrangement reactions, have also been explored to enhance the efficiency of piperazine synthesis.[138,139] There are limitations, including the complexity of protection strategies, as the need for multiple protecting groups complicates the synthesis, often leading to increased steps and lower efficiency.[136] Attempts have been made to develop different piperazine synthases into biocatalysts. However, the patents describing this work have been abandoned. [140,141] This attempt sought to couple the enzyme for producing N5-OH-*L*-Ornithine with the piperazate synthase enzyme. Instead, this project seeks to produce N5-OH-*L*-Ornithine via an efficient flow synthesis that could then be coupled to a piperazate synthase immobilized in a packed bed reactor within a flow system. Immobilization has been shown to increase the utility of biocatalysts.[142–145] As such, our approach may hold promise that could not be realized simply through coupling enzymes. Despite these advancements, limitations remain, including the need for specialized equipment and large-scale bioreactors to implement biotechnological processes effectively. Furthermore, while these methods produce high-purity products, the scalability to industrial levels requires further optimization.[134,141] Overall, significant progress has been made, but continued innovation is necessary to fully realize the potential of piperazic

acid as a versatile building block in pharmaceuticals and natural product synthesis.

3.2.3.1 Biosynthesis of Piperazic Acid and the need for N5-OH-*L*-Orn

Piperazic acid biosynthesis has been a subject of significant interest due to its presence in over 30 families of natural products, representing more than 140 compounds with potent biological activities ranging from anti-malarial to anti-bacterial properties.[128] The biosynthesis of piperazic acid involves several key steps, with N5-hydroxy-ornithine (N5-OH-*L*-Orn) playing a crucial role as an intermediate. A piperazate synthase forms the N-N bond, a critical step in producing piperazic acid.[127] The importance of N5-OH-*L*-Orn in this process was elucidated in studies on Kutzneria spp. 744, where it was identified as a key precursor in the biosynthetic pathway.[146] The need for N5-OH-*L*-Orn in piperazic acid biosynthesis stems from its role as a substrate for the piperazate synthase.[128,130,146] The N5-hydroxy ornithine group is necessary for the piperazate synthase enzyme to build the nitrogen-nitrogen bond.[128,130,146].[136]

Biocatalysis and chemoenzymatic approaches in flow systems offer significant advantages for synthesizing complex molecules like piperazic acid. However, coupling multiple enzymes in these systems presents several challenges.[149] While two enzymes could theoretically be used in a flow system to produce piperazic acid, this approach has inherent difficulties. The co-immobilization of multiple enzymes on a single carrier can be particularly challenging, as the carrier properties may affect each enzyme differently, impacting their activity and stability.[149] Furthermore, the need for precise control of reaction conditions, such as pH and cofactor regeneration, becomes more complex in multi-enzyme systems.[150] Flow biocatalysis can also face issues with enzyme stability over time and incompatibility with certain reaction conditions, potentially limiting the efficiency of

cascade reactions.[151] Additionally, using water as the primary solvent may lead to substrate solubility issues and dilute product streams, resulting in lower productivity.[151] To overcome these challenges, a synthetic approach to producing hydroxylated ornithine as a precursor for piperazic acid synthesis may be more advantageous. This strategy could simplify the reaction system, reduce the need for complex enzyme coupling, and allow for better control over reaction conditions.[152] By combining chemical synthesis with a single enzymatic step in the flow, this approach could leverage the benefits of flow chemistry while avoiding the complexities associated with multi-enzyme systems.[151,153]

3.3 Developing the Flow Synthesis Strategy for N5-OH-*L*-Orn

The flow synthesis of N5-OH-*L*-Ornithine encompasses carefully optimized steps, as shown in reaction Scheme 11, designed to enhance efficiency and yield. By transitioning from batch to flow processes, this approach aims to overcome limitations such as extended reaction times, inconsistent product quality, and scalability issues often associated with batch production.

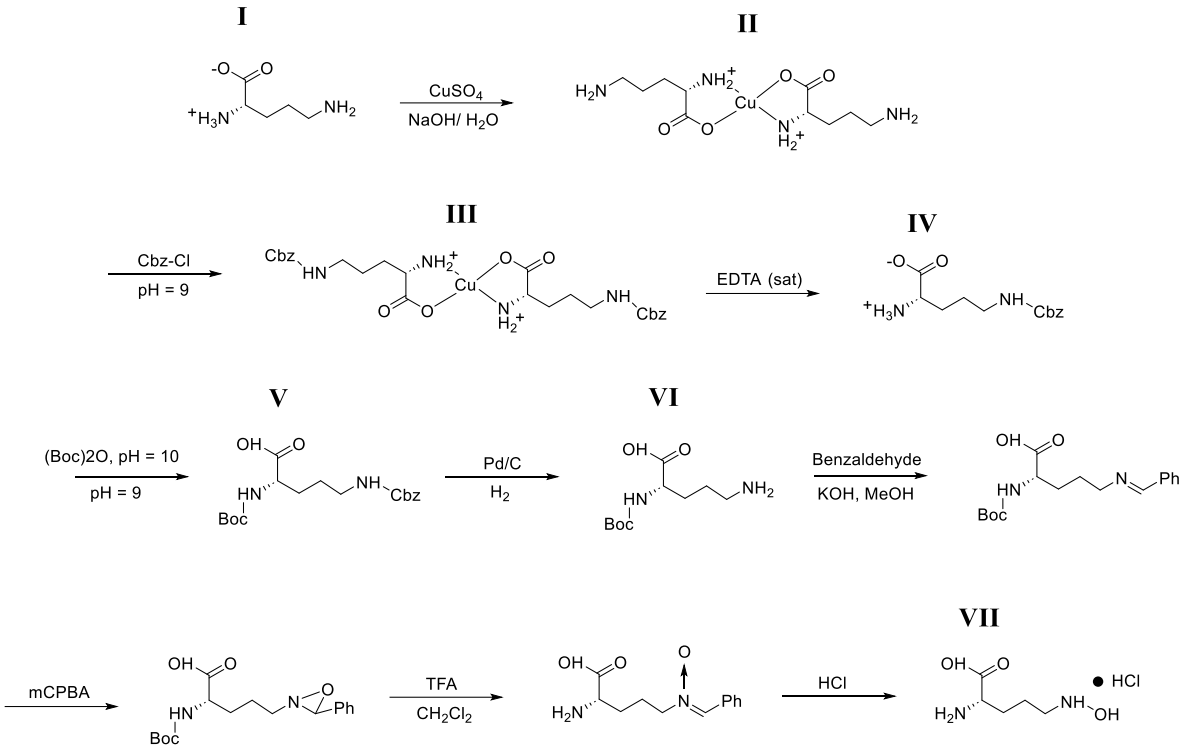

Scheme 11: Reaction Scheme for the Synthesis of N5-OH-Ornithine (Adapted from Neumann et al.).

Scheme 11 outlines the proposed methodology for synthesizing N5-OH-*L*-Ornithine (VII) from *L*-Ornithine (I), drawing inspiration from established batch protocols[154] according to an analogous procedure described for preparing Boc-Lys.[155] This transition to flow synthesis promises improved process control and product consistency and aligns with the increasing need for more sustainable and efficient pharmaceutical manufacturing practices.

This thesis only focused on protecting *L*-Ornithine (I) until the derivative N5-Cbz-Ornithine (IV) is obtained, as shown in scheme 12 below. Benzyl N-succinimidyl carbonate (Cbz-OSu) was preferred (scheme 12) over Benzyl chloroformate (Cbz-Cl) (Scheme 11) for the synthesis of N5-Cbz-Ornithine due to its superior reactivity[156] and selectivity. This reagent allows for faster and more efficient protection of amino groups

under milder reaction conditions,[156] which is particularly beneficial when working with sensitive substrates. Cbz-OSu typically yields higher amounts of the desired protected amino acid[156] while generating fewer side products, simplifying subsequent purification steps. Its enhanced stability and ease of handling compared to the moisture-sensitive Cbz-Cl make it a more practical choice in laboratory settings.[156] Furthermore, Cbz-OSu demonstrates better compatibility with other protecting groups and reaction conditions often encountered in multi-step syntheses.[156] These combined advantages, which are improved reactivity, higher selectivity, better yields, reduced side products, increased stability, and broader compatibility, make Cbz-OSu the reagent of choice for the protection of amino groups in complex amino acid derivatives like N5-OH-Ornithine, especially in scenarios where high yields and product purity are paramount.

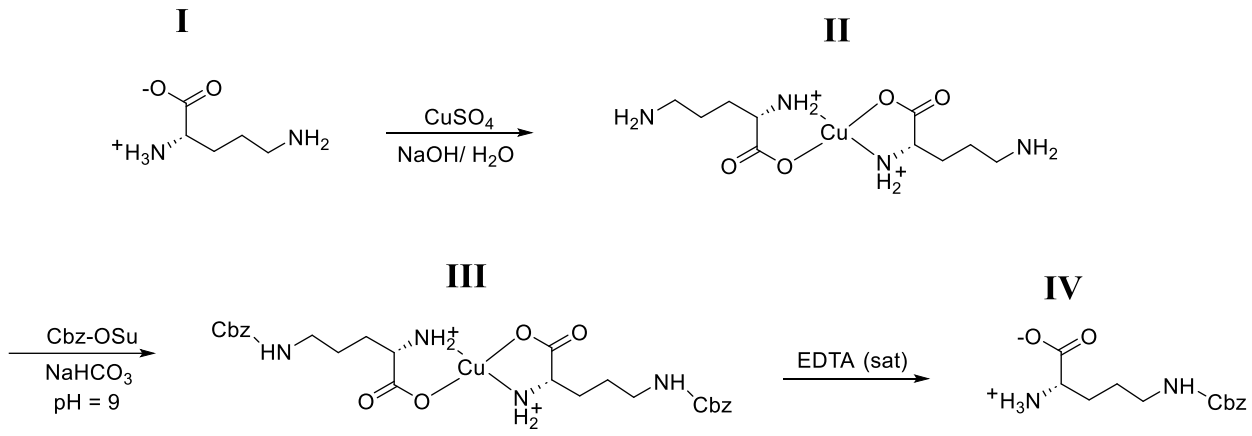

Scheme 12: Proposed Reaction scheme for the synthesis of N5-Cbz-Ornithine (IV) from L-Ornithine (I)

3.3.1 *L*-Ornithine Protection to N5-Cbz-Ornithine in Batch and Flow

3.3.1.1 *L*-Ornithine Protection to N5-Cbz-Ornithine in Batch – Trial 1

Ornithine hydrochloride (350 mg, 2.08 mmol) was dissolved in 0.5M NaOH (4.5 mL). A solution of $CuSO_4$ (200 mg, 1.25 mmol, 0.60 equiv) in dH_2O (18 mL) was added, and the

mixture instantly changed to a deep blue colour. The solution was allowed to react at room temperature with constant stirring for 5 hours. To the resulting ornithine-copper complex (II) after the 5 hours reaction time, $NaHCO_3$ (350 mg, 4.16 mmol, 2 equiv) was added, followed by N-(Benzyloxycarbonyloxy) succinimide (720 mg, 2.89 mmol, 1.39 equiv) in an ice bath. The pH was adjusted to 9 using 4 M NaOH, stirring the solution at room temperature for 3 hours. The reaction mixture became foamy after adding Cbz-OSu, but the colour remained unchanged. The blue precipitate (cupric-ornithine complex III) was filtered after the 3-hour reaction time, washed with a small amount of water, and dried using the freeze dryer and a blue solid product was obtained. The product was then dissolved in 0.5 M EDTA solution (pH 8.0, 35 mL). After stirring the solution for 6 hours at room temperature, the resulting white precipitate was collected by filtration, washed with a small quantity of water, and dried using the freeze dryer to yield the N5-Cbz-Ornithine product (IV) as white solids (180 mg, 0.68 mmol, 51% yield).

3.3.1.2 *L*-Ornithine Protection to N5-Cbz-Ornithine in Flow – Trial 2

3.3.1.2.1 *L*-Ornithine (I) to Ornithine-copper complex (II) solution

A flow system was set up using PTFE tubing (0.75 mm inner diameter) and syringe pumps (Scheme 13). Ornithine hydrochloride (350 mg, 2.08 mmol) was dissolved in 0.5 M NaOH (4.5 mL) and added to the flow at a 0.15 ml/min flow rate from a first Pump A. $CuSO_4$ (200 mg, 1.25 mmol, 0.60 equiv) dissolved in dH_2O (18 mL), was added to the flow simultaneously at a flow rate of 0.6 ml/min from a second Pump B. The reaction mixture introduced into the flow system via a T-mixer (T-mixer 1) was passed through a reactor coil at room temperature. This temperature was consistently maintained throughout the reaction zone to ensure uniform conditions. The reaction mixture turned deep blue when the two

solutions from both pumps met at T-mixer 1, and the product (Ornithine-copper complex (II) solution) was obtained following a 30-minute residence time in the reactor (Scheme 13).

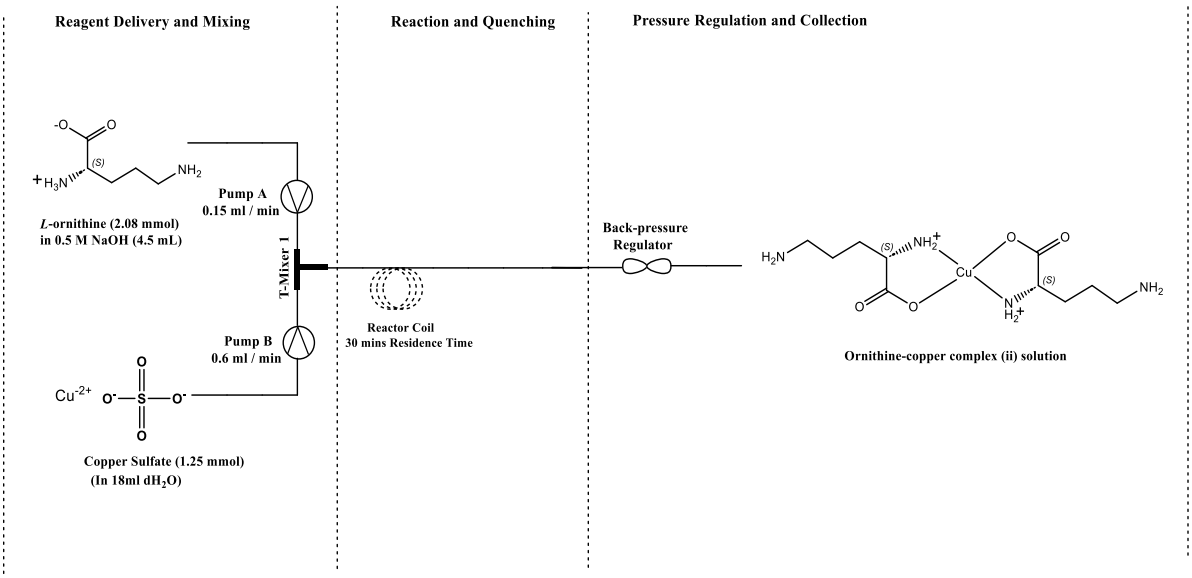

Scheme 13: The protection of L-Ornithine to Ornithine-copper complex (II) solution in the flow

3.3.1.2.2 Ornithine-copper complex (II) solution protection to Cupric-ornithine complex

A flow system was set up using PTFE tubing (0.75 mm inner diameter) and syringe pumps (Scheme 14). Ornithine-copper complex (II) solution (20 mL) was added to the flow at a 2 ml/min flow rate from a first Pump A. $NaHCO_3$ (350 mg, 4.16 mmol) dissolved in dH_2O (10 mL) was added to the flow simultaneously at a 1 ml/min flow rate from a second Pump B. The reaction mixture introduced into the flow system via a T-mixer (T-mixer 1) was passed through a reactor coil in an ice bath (0 - 5 °C). This temperature was consistently maintained throughout the reaction zone to ensure uniform conditions. N-(Benzyloxycarbonyloxy) succinimide (720 mg, 2.89 mmol) dissolved in acetone (10 mL) was added to the flow simultaneously at a 1 ml/min flow rate from a third Pump C. The reaction mixture introduced into the flow system via a T-mixer (T-mixer 2) was passed through a reactor coil in an ice bath (0 - 5 °C). Foaming started immediately after the reaction mixture met at T-mixer 2, and

the reaction did not proceed smoothly since precipitates started to form, which caused clogging in the tubes. The reaction was not completed even when slower flow rates were used, and no product was obtained in this step.

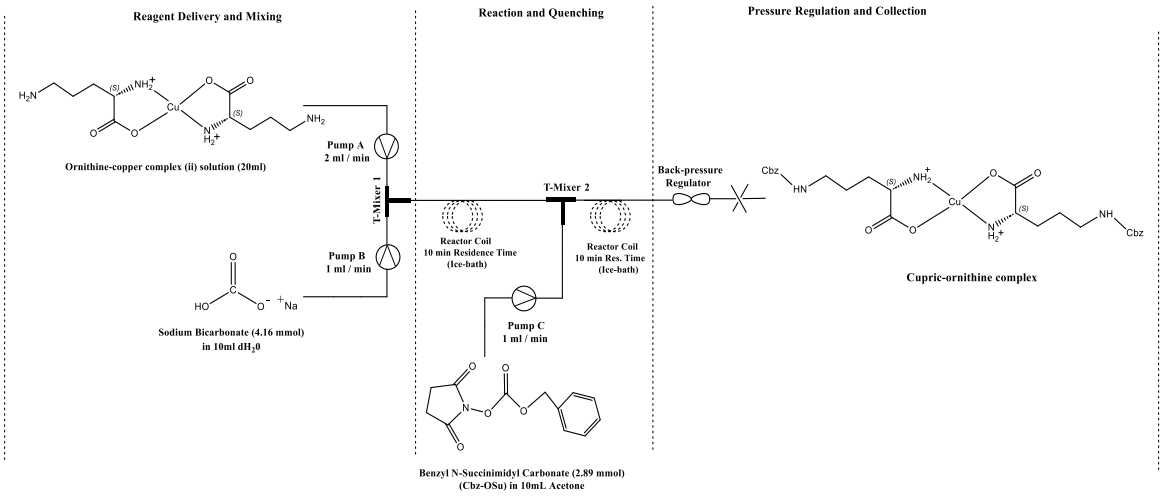

Scheme 14: The protection of Ornithine-copper complex (II) solution to Cupric-ornithine complex in the flow

3.4 Conclusion

3.4.1 Challenges and Limitations of Developed Flow Protocol

The development of a flow synthesis protocol for N5-OH-ornithine, specifically from *L*-ornithine to N5-Cbz-ornithine, encountered significant challenges, particularly during the second step involving the protection of the ornithine-copper complex (II) solution with Cbz-Osu. The primary obstacles were foaming and precipitation, severely impacting the flow process. Foaming, likely caused by the reaction between $NaHCO_3$ and acidic by-products such as N-hydroxysuccinimide (HOSu), which should be the by-product from the reaction, resulted in CO_2 generation and subsequent precipitation within the flow system. The introduction of Cbz-OSu (Benzyl N-Succinimydyl Carbonate) in conjunction with sodium bicarbonate into the system significantly amplified this effect, further compromising the

stability and continuity of the flow process. Nevertheless, given the milder and more sustainable reaction conditions promised by CBz-OSu, the next steps are to attempt the reaction with no added base or a different base than sodium bicarbonate to maintain the appropriate pH of the reaction. Should $NaHCO_3$ prove to be essential for neutralization to prevent acid buildup and maintain reaction equilibrium, a series of other alternatives are contemplated. While potentially crucial for preventing the potential decomposition of reactants or products, it simultaneously contributed to the foaming issue. This delicate balance between maintaining pH and avoiding excessive gas generation highlights the complexity of translating batch processes to flow systems.[157] Precipitation from this reaction led to severe clogging in the flow channels and tubes, persisting even when slower flow rates were employed. The formation of solid precipitates in flow systems is a well-documented challenge in continuous processing, particularly when dealing with inorganic salts or metal complexes.[158] These challenges underscore the need for innovative approaches in flow chemistry when dealing with gas-evolving reactions and precipitation-prone processes.

3.4.2 Proposed Solutions to Overcoming Challenges of Developed Flow Protocol

Several innovative solutions can be implemented to address the challenges encountered in the flow synthesis protocol for N5-Cbz-Ornithine to enhance process efficiency and reliability. Increasing the tubing diameter to 1 mm or more would be a straightforward approach to mitigate clogging risks, as it provides more space for precipitates and reduces the likelihood of blockages.[159] Integrating a gas-liquid separator is crucial for managing CO_2 evolution, allowing for gas-controlled venting while maintaining the liquid phase in the flow system.[160] A particularly promising solution is the incorporation of a Continuous Stirred Tank Reactor (CSTR) into the flow setup. CSTRs offer multiple advantages in addressing the observed

challenges. The efficient mixing provided by an impeller or stirrer ensures homogeneous conditions, reducing foaming and improving reaction uniformity.[27] The stirring action also keeps solids suspended, preventing precipitation-induced clogging that is problematic in simple tubular reactors. Some CSTR designs feature wider outlets or specialized pumps to handle slurries and precipitates effectively.[161] The open or vented design of a CSTR facilitates efficient gas release, which is crucial for managing CO_2 evolution and reducing foam buildup.[162] This feature, combined with the gas-liquid separator, provides a comprehensive solution for gas management in the flow system.

These proposed solutions, when implemented in combination, have the potential to significantly improve the robustness and scalability of the flow synthesis protocol. Integrating a CSTR with enhanced mixing capabilities, strategic gas management, and careful selection of reagents addresses the core issues of foaming, precipitation, and clogging. This approach solves immediate challenges and paves the way for more efficient and scalable continuous flow processes in complex organic syntheses.[23]

4. General Discussions and Conclusion

4.1 Achievement of Objectives and Summary of Key Findings

The primary objectives of this study were to develop a flow synthesis method for ascorbic acid and to protect *L*-Ornithine towards the synthesis of N5-OH-Ornithine using flow chemistry techniques. These objectives were pursued to advance the application of flow chemistry in the synthesis of complex organic compounds, particularly those of pharmaceutical relevance.

For the first objective, significant progress was made in translating the multi-step synthesis of ascorbic acid from batch to flow conditions. The research successfully demonstrated the feasibility of conducting several key steps of ascorbic acid synthesis in a flow process. This study reported the flow synthesis steps of *D*-glucose to *D*-sorbitol, *L*-sorbose to *L*-ascorbic acid and the attempted flow synthesis of the protection of *L*-Ornithine towards N5-OH-Ornithine synthesis.

The flow synthesis method developed for ascorbic acid includes multiple reaction steps, each requiring precise optimization of reaction parameters. These parameters included but were not limited to residence time, reagent concentration, and flow rate. Through systematic investigation and iterative refinement, optimal conditions were established for most synthetic sequences. However, the second step of synthesizing *L*-ascorbic acid, the oxidation of *D*-sorbitol to *L*-sorbose, is still a work in progress by another researcher. Despite this limitation, the successful implementation of the other steps in flow represents a substantial achievement. The work has laid a solid foundation for future optimization efforts and has contributed valuable insights into translating complex, multi-step syntheses from batch to flow processes.

In the ascorbic acid synthesis project, as discussed in Chapter 2 of this thesis, the flow system demonstrated marked improvements over conventional batch methods across multiple reaction steps. The conversion of *L*-sorbose to diacetone-*L*-sorbose in flow conditions achieved a 95% yield within a residence time of just 30 minutes. This gave a better result than the batch reaction, which yielded 90% in 360 minutes. The reduction in reaction time, coupled with an improved yield, shows the potential of flow chemistry in process efficiency. The subsequent oxidation step in the flow to produce 2-keto-*L*-gulonic acid showed improvements. The flow system achieved a yield of 91% within a total residence time of 40 minutes, which gave more yield than the traditional batch process, which required a 3-hour reaction time to achieve an 88% yield. This shows the capacity of flow chemistry to accelerate reaction rates and enhance product yields in complex oxidation processes.

For the final conversion of 2-keto-*L*-gulonic acid to *L*-ascorbic acid, while the yield difference between batch and flow methods was less pronounced, the flow process still offered advantages. The flow system produced a slightly higher yield of 85% in just 20 minutes of residence time compared to the batch process, which yielded 82% in approximately 180 minutes. This result further reinforces the time-efficiency benefits of flow chemistry, even in cases where yield improvements are marginal.

A key advantage of the flow system was the ability to perform real-time optimization of reaction parameters. By adjusting flow rates, reagent-to-solvent ratios, and temperatures, as seen at the *L*-sorbose to diacetone-*L*-sorbose step, consistently higher yields and product quality were maintained throughout the process. The cumulative effect of these improvements resulted in an overall yield of *L*-ascorbic acid from *L*-sorbose reaching 82-85%. This yield surpasses the typical yields of 70-75% reported for industrial batch

processes, demonstrating the potential of flow chemistry to enhance the efficiency of ascorbic acid production at an industrial scale. While our flow approach did not significantly reduce solvent usage compared to batch methods, it contributed to a more environmentally friendly production process through efficient mixing and in-flow addition of reagents, potentially reducing waste and improving overall process sustainability.

Turning to the second objective, the protection of *L*-Ornithine towards synthesizing N5-OH-Ornithine in flow, the research yielded mixed results that nonetheless provide significant contributions to the field. The initial phase of this work involved the successful development of a flow synthesis protocol based on established batch methods.

As discussed in Chapter 3 of this thesis, the flow synthesis of N5-Cbz-Ornithine towards the synthesis of N5-OH-Ornithine, encountered significant challenges that prevented the completion of the full synthesis. However, important findings were still obtained. The first step of the synthesis, the protection of *L*-ornithine, was successfully carried out in flow conditions, achieving the desired transformation in under 30 minutes. This represents a substantial time reduction compared to the batch process, which required 6 hours. This result highlights the potential of flow chemistry to dramatically accelerate certain reaction steps, even in complex amino acid derivatizations. However, the second step of this synthesis presented considerable obstacles in the flow system. Using sodium bicarbonate ($NaHCO_3$) led to significant foaming and precipitation within the flow reactor, disrupting the continuous process, as discussed previously. This challenge underscores critical consideration in flow chemistry: the behaviour of reagents and products under continuous flow conditions can differ markedly from batch processes, particularly when gas evolution or precipitation

occurs. While this issue was not fully resolved within the scope of this research, it provides valuable insights into how this reaction can be modified within flow for the future.

The partial success in the flow synthesis of ascorbic acid demonstrates the potential for applying continuous flow techniques to complex, multi-step syntheses of pharmaceutical intermediates. The work has identified key areas for future optimization and has established a framework upon which subsequent research can build. While the initial objectives of continuous-flow synthesis were not met, the research has substantially contributed towards the effort of producing the important vitamin, ascorbic acid, utilizing flow synthesis. The next steps will build upon these efforts by optimizing reaction conditions, integrating an inline separator, and implementing more advanced pumping systems/ reactor designs to achieve a continuous-flow synthesis.

4.2 Further Studies and Future Recommendations

The study on the flow synthesis of ascorbic acid and the attempted flow synthesis of N5-OH-Ornithine has provided valuable insights and opened up several avenues for further investigation and improvement. This section outlines potential areas for future studies and recommendations to address the challenges encountered and to further optimize the flow chemistry processes developed in this work.

For the ascorbic acid synthesis project, a primary focus for future studies should be implementing more advanced pumping systems. The limitations of the current pumping equipment hindered the continuous-flow synthesis of ascorbic acid. Future work should explore the use of high-performance pumps capable of handling higher pressures and providing more precise flow control. This would help towards achieving a fully continuous-flow synthesis of ascorbic acid. Another focus for future studies would be one of the main

challenges in continuous flow synthesis: the need for inline separation between steps. Traditional batch processes often involve the isolation and purification of intermediates, which is more complex in continuous-flow systems. An inline liquid-liquid extraction using membrane-based separators can be utilized to address this.[163] These can effectively separate aqueous and organic phases continuously. Integrating continuous drying techniques such as membrane pervaporation or molecular sieves[27] should also be studied since drying in the flow is one of the challenges of continuous flow.

In the N5-OH-Ornithine synthesis project, several recommendations can be made to address the challenges of foaming and precipitation. A key area for investigation is the substitution of $NaHCO_3$ with NaOH as the base. This change might reduce or eliminate precipitation issues, as NaOH is generally more soluble than $NaHCO_3$[164]. However, careful consideration must be given to the impact of this substitution on reaction kinetics and product stability. Studies should be conducted to optimize NaOH's concentration and flow rate to maintain the desired pH while minimizing side reactions. To further mitigate issues related to precipitation and gas evolution, the use of larger diameter tubing (1 mm or more) should be explored. Wider tubing could reduce the likelihood of clogging and improve the handling of heterogeneous mixtures. However, this modification may affect residence times and heat transfer, necessitating a comprehensive re-optimization of reaction conditions.[165] Implementing a liquid-gas separator in the flow system presents another promising avenue for improvement. This addition could effectively manage the gas evolution observed in the reaction, preventing disruptions to the flow and improving overall system stability. Various designs of liquid-gas separators should be evaluated for their efficiency and compatibility with the specific reaction conditions of the N5-OH-Ornithine synthesis.[166]

5. Experimental Section

5.1 General Experimental Procedures

All reagents and solvents used were obtained or purchased from Thermo Fischer Scientific and Sigma Aldrich. SGE Syringes, reactor coils (PTFE tubing), T-mixers, Y-mixers, and back pressure regulators were purchased from IDEX Health & Science LLC. Scientific syringe pumps were purchased from New Era Pump Systems Inc.

Synthesized products were isolated using a BÜCHI Rotavapor R-200 Rotary Evaporator and dried in a desiccator or a BÜCHI Lyovapor L-200 Freeze Dryer. Synthesized products were confirmed by analyzing the IR spectrum and ^{1}H, ^{13}C, DEPT-135, ^{1}H-^{13}C HSQC, and ^{1}H-^{13}C HMBC NMR spectra. IR spectra were recorded using a Bruker ALPHA II FT-IR spectrometer. One- and two-dimensional NMR spectra were recorded on a Bruker Fourier 300 MHz NMR spectrometer or 400 MHz Bruker Fourier spectrometer. All samples were run in deuterated chloroform (99.96% isotopic purity) or deuterated DMSO (99.96% isotopic purity), and NMR data was calibrated to the solvent signals of δ_H 7.24 ppm and δ_C 77.0 ppm for deuterated chloroform, and δ_H 2.50 ppm and δ_C 39.52 ppm for deuterated DMSO. All NMR spectra were processed by TopSpin 4.1.1 software for this thesis. Electrospray ionization (ESI) mass spectrometry was run by staff in the Simon Fraser University (SFU) Mass Spectrometry Facility, Department of Chemistry, on a Bruker Esquire ion trap mass spectrometry.

5.2 Synthesis Procedures

5.2.1 Preparation of *D*-sorbitol 2.2.1.10

A flow system was set up using PTFE tubing (0.75 mm inner diameter) and syringe pumps, as shown in Scheme 7. *D*-glucose (1.03 g, 5.71 mmol) was dissolved in 10 mL of dH_2O and added to the flow at a 0.5 ml/min flow rate from a first Pump A. $NaBH_4$ (0.1753 g, 4.63 mmol) dissolved in 10 mL of dH_2O was added to the flow simultaneously at a 0.5 ml/min flow rate from a second Pump B. The reaction mixture introduced into the flow system via a T-mixer (T-mixer 1) was passed through a reactor coil maintained at ambient temperature (20 ± 2°C). This temperature was consistently maintained throughout the reaction zone to ensure uniform conditions. The product was obtained following a 20-minute residence time in the reactor, and the solvent was evaporated to dryness under reduced pressure. Excess H_20 was removed, leaving *D*-sorbitol, a white powder (1.04 g, 5.70 mmol, 100%) analyzed by NMR (300 MHz, DMSO-d_6).

^{1}H NMR (300 MHz, DMSO-*d6*) δ = 7.0-9.0 (impurities), 5.84 (d, J = 6.9 Hz), 4.0-5.0 (multiplet), 2.5-4.0 (multiplet), 1.23 (s, impurity). ^{13}C NMR (300 MHz, DMSO-*d6*) δ = 105.2, 76.2, 75.3, 74.6, 74.2, 73.7, 72.7, 71.9, 69.2, 64.8, 64.3, 63.8, 62.9.

5.2.2 Preparation of partially protected Sorbose 2.2.2.3

L-sorbose (0.625 g, 3.46 mmol) was dissolved in 60 mL of acetone (acetone to sorbose ratio of 233: 1). H_2SO_4 (1.2 mL) was added dropwise to this solution until universal pH indicator paper indicated the reaction mixture was acidified. The solution was allowed to react in an ice-cold water bath with constant stirring for 300 minutes. After this, sodium bicarbonate (20 mL) was added dropwise until universal pH indicator paper indicated the reaction mixture

was neutralized. The solvent was evaporated to dryness under reduced pressure. Excess acetone was removed, leaving a white powder (0.54 g, 2.07 mmol, 60 %) analyzed by NMR (400 MHz, DMSO-d_6).

^{1}H NMR (400 MHz, DMSO-*d6*) δ = 1.20 – 1.40 (6 H, 1.29 (s), 1.39 (s)), 3.40 – 3.64 (5 H, multiplet), 3.75 (1 H, dd, J = 9.2, 6.7 Hz), 4.00 (d, J = 6.9 Hz), 4.1 (1 H, multiplet), 4.30 (s)). ^{13}C NMR (400 MHz, DMSO-*d6*) δ = 27.1, 28.0, 59.4, 62.5, 73.9, 82.3, 85.1, 111.2, 114.7. ESIMS [M+Na] + calculated for $C_9H_{16}O_6Na$ 243.22, found 243.0837.

5.2.3 Preparation of diacetone-*L*-sorbose 2.2.2.9

A flow system was set up using PTFE tubing (0.75 mm inner diameter) and syringe pumps. *L*-sorbose (0.625 g, 3.46 mmol) was dissolved in 80 mL of acetone (acetone to sorbose ratio of 311: 1) and added to the flow at a 4 ml/min flow rate from a first Pump A. H_2SO_4 (1.5 mL) diluted in acetone (20 mL) was added to the flow simultaneously at a 1 ml/min flow rate from a second Pump B. The reaction mixture introduced into the flow system via a T-mixer (T-mixer 1) was passed through a reactor coil in an ice bath (0 - 5 °C). This temperature was consistently maintained throughout the reaction zone to ensure uniform conditions. Sodium bicarbonate (20 mL) was added to the flow simultaneously at a 1 ml/min flow rate from a third Pump C. The product was obtained following a 30-minute residence time in the reactor, and the solvent was evaporated to dryness under reduced pressure. Excess acetone was removed, leaving a white powder (0.86 g, 3.30 mmol, 95 %) analyzed by NMR (400 MHz, $CDCl_3$).

^{1}H NMR (400 MHz, $CDCl_3$) δ = 1.30 – 1.55 (12 H, 1.36 (s, 6 H), 1.43 (s, 3 H), 1.49 (s, 3 H), 2.12 (1 H, dd, J = 7.0, 5.9 Hz), 3.82 (2 H, dd, J = 11.8, 7.0 Hz), 4.05 (2 H, dd, J = 3.3, 5.3

Hz), 4.09 (d, J = 1.7 Hz), 4.31 (d, J = 2.0 Hz), 4.46 (s)). ^{13}C NMR (400 MHz, $CDCl_3$) δ = 18.6, 26.5, 27.3, 29.0, 60.3, 63.7, 72.3, 73.3, 85.0, 97.6, 112.0, 114.5. ESIMS [M+Na] + calculated for $C_{12}H_{20}O_6Na$ 283.290, found 283.1154.

5.2.4 Preparation of 2-keto-*L*-gulonic acid 2.2.3.3

A flow system was set up using PTFE tubing (0.75 mm inner diameter) and syringe pumps (Scheme 9). Diacetone-*L*-sorbose (0.33 g, 1.26 mmol) was dissolved in 20 mL of acetone. NaOH (0.50 g, 12.5 mmol) was added to this mixture and the solution was added to the flow at a 1 ml/min flow rate from a first Pump A. KMnO4 (0.35 g, 2.21 mmol) dissolved in 10 mL of acetone was added to the flow simultaneously at a 0.5 ml/min flow rate from a second Pump B. The reaction mixture introduced into the flow system via a T-mixer (T-mixer 1) was passed through a reactor coil in a hot water bath at an elevated temperature of 50° C. This temperature was consistently maintained throughout the reaction zone to ensure uniform conditions. Sodium bisulphite (1.20 g, 11.53 mmol) dissolved in 5 mL of dH_20 was added to the flow simultaneously at a 0.25 ml/min flow rate from a third Pump C. H_2SO_4 (1 mL) diluted in 10 mL of acetone was added to the flow simultaneously at a 0.5 ml/min flow rate from a fourth Pump D, and was then allowed to react with the reaction mixture at a second reactor coil for 20 minutes. In the drying unit, 3 A° and 4 A° molecular sieves trapped the aqueous layer. The sieves were pre-dried in the oven at 160° C for 16 hours before use. The product was obtained following a 40-minute residence time in the reactor, and the solvent was evaporated to dryness under reduced pressure using a rotary evaporator. Excess acetone was removed, leaving 2-keto-*L*-gulonic acid, a white powder (0.22 g, 1.13 mmol, 91%) analyzed by NMR (400 MHz, DMSO-d_6) and Mass spectrometry.

^{1}H NMR (400 MHz, DMSO-*d6*) δ = 3.10-3.22 (2 H, 3.20 (q, J = 10.6, 17.7, 10.8 Hz), 3.67 (1 H, dd, J = 7.2, 9.0 Hz), 3.85 (1 H, d, J = 9.0 Hz)), 4.05 (1 H, d, J = 9.6 Hz), 4.74 (1 H, d, J = 7.0 Hz).^{13}C NMR (400 MHz, DMSO-*d6*) δ = 64.4, 74.1, 74.4, 76.8, 175.1, 213.5. ESIMS [M+Na] + calculated for $C_6H_{10}O_7Na$ 217.140, found 217.0421 and ESIMS [M+K] + calculated for $C_6H_{10}O_7K$ 233.140, found 233.0172.

5.2.5 Preparation of *L*-ascorbic acid 2.2.4.2

A flow system was set up using PTFE tubing (0.75 mm inner diameter) and syringe pumps. 2-keto-*L*-gulonic acid (0.55 g, 2.83 mmol) was dissolved in 10 mL of methanol and added to the flow at a 0.5 ml/min flow rate from a first Pump A. H_2SO_4 (0.5 mL) diluted in dH_20 (5 mL) was added to the flow simultaneously at a 0.25 ml/min flow rate from a second Pump B. The reaction mixture introduced into the flow system via a T-mixer (T-mixer 1) was passed through a reactor coil in a hot water bath at an elevated temperature of 65° C to 100° C. This temperature was consistently maintained throughout the reaction zone to ensure uniform conditions. Sodium bicarbonate (5 mL) was added to the flow simultaneously at a 0.5 ml/min flow rate from a third Pump C. The product was obtained following a 20-minute residence time in the reactor, and the solvent was evaporated to dryness under reduced pressure using a rotary evaporator. Excess H_20 was removed, leaving *L*-ascorbic acid, a white powder (0.42 g, 2.38 mmol, 85 %). The crude product (0.21 g, 1.19 mmol) was recrystallized with a mixture of ethanol and water (3:1), and pure ascorbic acid (0.12 g, 0.68 mmol, 57%) was obtained and analyzed by NMR (400 MHz, DMSO-d_6).

^{1}H NMR (400 MHz, DMSO-*d6*) δ = 3.40-3.45 (2H, 3.42 (d, J = 6.0 Hz), 3.72 (s), 4.71 (1H, d, J = 3.0 Hz).^{13}C NMR (400 MHz, DMSO-*d6*) δ = 62.4, 68.8, 75.0, 118.4, 153.3, 171.1. ESIMS [M+Na] + calculated for $C_6H_8O_6Na$ 199.12, found 199.0307 and [M+H] + calculated as 177.12, found 177.0482.

References

(1) Ley, S. V.; Fitzpatrick, D. E.; Ingham, Richard. J.; Myers, R. M. Organic Synthesis: March of the Machines. *Angew Chem Int Ed* **2015**, *54* (11), 3449–3464. https://doi.org/10.1002/anie.201410744.

(2) Newman, S. G.; Jensen, K. F. The Role of Flow in Green Chemistry and Engineering. *Green Chem.* **2013**, *15* (6), 1456. https://doi.org/10.1039/c3gc40374b.

(3) Webb, D.; Jamison, T. F. Continuous Flow Multi-Step Organic Synthesis. *Chem. Sci.* **2010**, *1* (6), 675. https://doi.org/10.1039/c0sc00381f.

(4) Britton, J.; Raston, C. L. Multi-Step Continuous-Flow Synthesis. *Chem. Soc. Rev.* **2017**, *46* (5), 1250–1271. https://doi.org/10.1039/C6CS00830E.

(5) Gutmann, B.; Cantillo, D.; Kappe, C. O. Continuous-Flow Technology—A Tool for the Safe Manufacturing of Active Pharmaceutical Ingredients. *Angew Chem Int Ed* **2015**, *54* (23), 6688–6728. https://doi.org/10.1002/anie.201409318.

(6) Hartman, R. L.; McMullen, J. P.; Jensen, K. F. Deciding Whether To Go with the Flow: Evaluating the Merits of Flow Reactors for Synthesis. *Angew Chem Int Ed* **2011**, *50* (33), 7502–7519. https://doi.org/10.1002/anie.201004637.

(7) Movsisyan, M.; Delbeke, E. I. P.; Berton, J. K. E. T.; Battilocchio, C.; Ley, S. V.; Stevens, C. V. Taming Hazardous Chemistry by Continuous Flow Technology. *Chem. Soc. Rev.* **2016**, *45* (18), 4892–4928. https://doi.org/10.1039/C5CS00902B.

(8) Wiles, C.; Watts, P. Continuous Flow Reactors: A Perspective. *Green Chem.* **2012**, *14* (1), 38–54. https://doi.org/10.1039/C1GC16022B.

(9) Wiles, C.; Watts, P. Continuous Process Technology: A Tool for Sustainable Production. *Green Chem.* **2014**, *16* (1), 55–62. https://doi.org/10.1039/C3GC41797B.

(10) Bennett, J. J.; Murphy, P. V. Flow Chemistry Based Catalytic Hydrogenation for Improving the Synthesis of 1-Deoxynojirimycin (DNJ) from an l-Sorbose Derived Precursor. *Carbohydrate Research* **2023**, *529*, 108845. https://doi.org/10.1016/j.carres.2023.108845.

(11) Burange, A. S.; Osman, S. M.; Luque, R. Understanding Flow Chemistry for the Production of Active Pharmaceutical Ingredients. *iScience* **2022**, *25* (3), 103892. https://doi.org/10.1016/j.isci.2022.103892.

(12) Porta, R.; Benaglia, M.; Puglisi, A. Flow Chemistry: Recent Developments in the Synthesis of Pharmaceutical Products. *Org. Process Res. Dev.* **2016**, *20* (1), 2–25. https://doi.org/10.1021/acs.oprd.5b00325.

(13) How Batch Processing Differs from Continuous Flow Processing. https://www.generalkinematics.com/blog/batch-processing-vs-continuous-flow/.

(14) *Flow Chemistry vs. Batch Chemistry*. https://kilolabs.com/resources/flow-chemistry-vs-batch-chemistry/.

(15) Bukhtiyarova, M. V.; Nuzhdin, A. L.; Bukhtiyarova, G. A. Comparative Study of Batch and Continuous Flow Reactors in Selective Hydrogenation of Functional Groups in Organic Compounds: What Is More Effective? *IJMS* **2023**, *24* (18), 14136. https://doi.org/10.3390/ijms241814136.

(16) Holtze, C.; Boehling, R. Batch or Flow Chemistry? – A Current Industrial Opinion on Process Selection. *Current Opinion in Chemical Engineering* **2022**, *36*, 100798. https://doi.org/10.1016/j.coche.2022.100798.

(17) Peña, L. F.; González-Andrés, P.; Parte, L. G.; Escribano, R.; Guerra, J.; Barbero, A.; López, E. Continuous Flow Chemistry: A Novel Technology for the Synthesis of Marine Drugs. *Marine Drugs* **2023**, *21* (7), 402. https://doi.org/10.3390/md21070402.
(18) *Batch Versus Flow in Pharma: The upsides of continuous chemistry*. https://helgroup.com/blog/batch-versus-flow-in-pharma-the-upsides-of-continuous-chemistry/.
(19) Bennett, J. A.; Campbell, Z. S.; Abolhasani, M. Role of Continuous Flow Processes in Green Manufacturing of Pharmaceuticals and Specialty Chemicals. *Current Opinion in Chemical Engineering* **2019**, *26*, 9–19. https://doi.org/10.1016/j.coche.2019.07.007.
(20) *Flow-Chemistry*. https://www.mt.com/us/en/home/applications/L1_AutoChem_Applications/continuous.html.
(21) Akwi, F. M.; Watts, P. Continuous Flow Chemistry: Where Are We Now? Recent Applications, Challenges and Limitations. *Chem. Commun.* **2018**, *54* (99), 13894–13928. https://doi.org/10.1039/C8CC07427E.
(22) Alfano, A. I.; Pelliccia, S.; Rossino, G.; Chianese, O.; Summa, V.; Collina, S.; Brindisi, M. Continuous-Flow Technology for Chemical Rearrangements: A Powerful Tool to Generate Pharmaceutically Relevant Compounds. *ACS Med. Chem. Lett.* **2023**, *14* (3), 326–337. https://doi.org/10.1021/acsmedchemlett.3c00010.
(23) Baumann, M.; Moody, T. S.; Smyth, M.; Wharry, S. Overcoming the Hurdles and Challenges Associated with Developing Continuous Industrial Processes. *Eur J Org Chem* **2020**, *2020* (48), 7398–7406. https://doi.org/10.1002/ejoc.202001278.
(24) Adebar, N.; Nastke, A.; Löwe, J.; Gröger, H. Segmented Flow Processes to Overcome Hurdles of Whole-Cell Biocatalysis in the Presence of Organic Solvents. *Angew Chem Int Ed* **2021**, *60* (29), 15863–15869. https://doi.org/10.1002/anie.202015887.
(25) *Advantages of continuous flow production*. https://www.vapourtec.com/flow-chemistry/advantages-of-continuous-flow-production/.
(26) Britton, J.; Raston, C. L. Multi-Step Continuous-Flow Synthesis. *Chem. Soc. Rev.* **2017**, *46* (5), 1250–1271. https://doi.org/10.1039/C6CS00830E.
(27) Britton, J.; Jamison, T. F. The Assembly and Use of Continuous Flow Systems for Chemical Synthesis. *Nat Protoc* **2017**, *12* (11), 2423–2446. https://doi.org/10.1038/nprot.2017.102.
(28) Jiao, J.; Nie, W.; Yu, T.; Yang, F.; Zhang, Q.; Aihemaiti, F.; Yang, T.; Liu, X.; Wang, J.; Li, P. Multi-Step Continuous-Flow Organic Synthesis: Opportunities and Challenges. *Chemistry A European J* **2021**, *27* (15), 4817–4838. https://doi.org/10.1002/chem.202004477.
(29) *Smoothflow Pumps for Continuous Flow Chemistry*. https://www.tacminausa.com/smoothflow-pumps-for-continuous-flow-chemistry/.
(30) *Continuous infusion - Dual pump system*. https://www.syringepump.com/continuous.php.
(31) *Continuous flow mixer*. https://www.spxflow.com/lightnin/products/line-blender-continuous-flow-mixer/.
(32) *Y mixing machine*. https://foodtechprocess.com/en/mixers/206-y-mixing-machine-.html.
(33) Rahimi, M.; Azimi, N.; Parsamogadam, M. A.; Rahimi, A.; Masahy, M. M. Mixing Performance of T, Y, and Oriented Y-Micromixers with Spatially Arranged Outlet

Channel: Evaluation with Villermaux/Dushman Test Reaction. *Microsyst Technol* **2017**, *23* (8), 3117–3130. https://doi.org/10.1007/s00542-016-3118-6.
(34) Camarri, S.; Mariotti, A.; Galletti, C.; Brunazzi, E.; Mauri, R.; Salvetti, M. V. An Overview of Flow Features and Mixing in Micro T and Arrow Mixers. *Ind. Eng. Chem. Res.* **2020**, *59* (9), 3669–3686. https://doi.org/10.1021/acs.iecr.9b04922.
(35) *When to use Back Pressure Regulators*. https://www.processindustryforum.com/article/use-back-pressure-regulators.
(36) *How the Equilibar Back Pressure Regulator Works*. https://www.equilibar.com/back-pressure-regulators/how-it-works/.
(37) *Back Pressure Regulators*. https://www.jordanvalve.com/products/back-pressure-regulators/.
(38) *Pressure Regulator vs. Backpressure Regulator*. https://plastomatic.com/technical-article/pressure-regulator-vs-backpressure-regulator/.
(39) *Definition of Back Pressure Regulator*. https://www.equilibar.com/back-pressure-regulators/how-it-works/bpr-definition/.
(40) García-Lacuna, J.; Baumann, M. Inline Purification in Continuous Flow Synthesis – Opportunities and Challenges. *Beilstein J. Org. Chem.* **2022**, *18*, 1720–1740. https://doi.org/10.3762/bjoc.18.182.
(41) *Inline Magnetic Separator Working Principle*. https://www.greatmagtech.com/info/inline-magnetic-separator-working-principle-87053700.html.
(42) Lei, Z.; Ang, H. T.; Wu, J. Advanced In-Line Purification Technologies in Multistep Continuous Flow Pharmaceutical Synthesis. *Org. Process Res. Dev.* **2024**, *28* (5), 1355–1368. https://doi.org/10.1021/acs.oprd.2c00374.
(43) Karadaghi, L. R.; Pan, B.; Baddour, F. G.; Malmstadt, N.; Brutchey, R. L. A Techno-Economic Approach to Guide the Selection of Flow Recyclable Ionic Liquids for Nanoparticle Synthesis. *RSC Sustain.* **2023**, *1* (7), 1861–1873. https://doi.org/10.1039/D3SU00182B.
(44) Williams, D. B. G.; Lawton, M. Drying of Organic Solvents: Quantitative Evaluation of the Efficiency of Several Desiccants. *J. Org. Chem.* **2010**, *75* (24), 8351–8354. https://doi.org/10.1021/jo101589h.
(45) Cybulski, M.; Przybylek, P. Application of Molecular Sieves for Drying Transformers Insulated with Mineral Oil, Natural Ester, or Synthetic Ester. *Energies* **2021**, *14* (6), 1719. https://doi.org/10.3390/en14061719.
(46) *Molecular Sieve Desiccant All You Need To Know*. https://www.jalonzeolite.com/molecular-sieve-desiccant-application-all-you-need-to-know/.
(47) *Adsorbents for Heat Reactivated Compressed Air Dryers*. https://www.airbestpractices.com/system-assessments/air-treatmentn2/adsorbents-heat-reactivated-compressed-air-dryers.
(48) Liu, Y.; Lucas, É.; Sullivan, I.; Li, X.; Xiang, C. Challenges and Opportunities in Continuous Flow Processes for Electrochemically Mediated Carbon Capture. *iScience* **2022**, *25* (10), 105153. https://doi.org/10.1016/j.isci.2022.105153.
(49) Liu, Y.; Lucas, É.; Sullivan, I.; Li, X.; Xiang, C. Challenges and Opportunities in Continuous Flow Processes for Electrochemically Mediated Carbon Capture. *iScience* **2022**, *25* (10), 105153. https://doi.org/10.1016/j.isci.2022.105153.

(50) Mishra, B. B.; Tiwari, V. K. Natural Products: An Evolving Role in Future Drug Discovery. *European Journal of Medicinal Chemistry* **2011**, *46* (10), 4769–4807. https://doi.org/10.1016/j.ejmech.2011.07.057.
(51) Haefner, B. Drugs from the Deep: Marine Natural Products as Drug Candidates. *Drug Discovery Today* **2003**, *8* (12), 536–544. https://doi.org/10.1016/S1359-6446(03)02713-2.
(52) Rey-Ladino, J.; Ross, A. G.; Cripps, A. W.; McManus, D. P.; Quinn, R. Natural Products and the Search for Novel Vaccine Adjuvants. *Vaccine* **2011**, *29* (38), 6464–6471. https://doi.org/10.1016/j.vaccine.2011.07.041.
(53) Cragg, G. M.; Newman, D. J. Natural Products: A Continuing Source of Novel Drug Leads. *Biochimica et Biophysica Acta (BBA) - General Subjects* **2013**, *1830* (6), 3670–3695. https://doi.org/10.1016/j.bbagen.2013.02.008.
(54) Butler, M. S. The Role of Natural Product Chemistry in Drug Discovery. *J. Nat. Prod.* **2004**, *67* (12), 2141–2153. https://doi.org/10.1021/np040106y.
(55) Aware, C. B.; Patil, D. N.; Suryawanshi, S. S.; Mali, P. R.; Rane, M. R.; Gurav, R. G.; Jadhav, J. P. Natural Bioactive Products as Promising Therapeutics: A Review of Natural Product-Based Drug Development. *South African Journal of Botany* **2022**, *151*, 512–528. https://doi.org/10.1016/j.sajb.2022.05.028.
(56) Mahdi, J. G. Medicinal Potential of Willow: A Chemical Perspective of Aspirin Discovery. *Journal of Saudi Chemical Society* **2010**, *14* (3), 317–322. https://doi.org/10.1016/j.jscs.2010.04.010.
(57) Gaynes, R. The Discovery of Penicillin—New Insights After More Than 75 Years of Clinical Use. *Emerg. Infect. Dis.* **2017**, *23* (5), 849–853. https://doi.org/10.3201/eid2305.161556.
(58) Lopes, N. P.; Roberto Da Silva, R. From Structural Determination of Natural Products in Complex Mixtures to Single Cell Resolution: Perspectives on Advances and Challenges for Mass Spectrometry. *Front. Nat. Prod.* **2023**, *2*, 1109557. https://doi.org/10.3389/fntpr.2023.1109557.
(59) Nahar, L.; Sarker, S. D. Medicinal Natural Products—An Introduction. In *Annual Reports in Medicinal Chemistry*; Elsevier, 2020; Vol. 55, pp 1–44. https://doi.org/10.1016/bs.armc.2020.02.008.
(60) Dias, D.; Urban, S. A Historical Overview of Natural Products in Drug Discovery. **2012**, *2* (2), 303–336.
(61) Atanasov, A. G.; Waltenberger, B.; Pferschy-Wenzig, E.-M.; Linder, T.; Wawrosch, C.; Uhrin, P.; Temml, V.; Wang, L.; Schwaiger, S.; Heiss, E. H.; Rollinger, J. M.; Schuster, D.; Breuss, J. M.; Bochkov, V.; Mihovilovic, M. D.; Kopp, B.; Bauer, R.; Dirsch, V. M.; Stuppner, H. Discovery and Resupply of Pharmacologically Active Plant-Derived Natural Products: A Review. *Biotechnology Advances* **2015**, *33* (8), 1582–1614. https://doi.org/10.1016/j.biotechadv.2015.08.001.
(62) Krishnamurti, C.; Rao, Sscc. The Isolation of Morphine by Serturner. *Indian J Anaesth* **2016**, *60* (11), 861. https://doi.org/10.4103/0019-5049.193696.
(63) Gachelin, G.; Garner, P.; Ferroni, E.; Tröhler, U.; Chalmers, I. Evaluating *Cinchona* Bark and Quinine for Treating and Preventing Malaria. *J R Soc Med* **2017**, *110* (2), 73–82. https://doi.org/10.1177/0141076816688411.
(64) Pal, R. S.; Pal, Y.; Lalitha Chaitanya, M. V. N.; Mazumder, A.; Khurana, N.; Tharu, P. K. Discerning the Multi-Dimensional Role of Salicin: Bioactive GlycosideBeyond

Analgesic: Different Perspectives. *CDTH* **2024**, *19* (7), 757–764. https://doi.org/10.2174/0115748855272391231114042540.
(65) Wang, M.-L. The Modern Pharmaceutical Industry: History, Current Position and Challenges. In *Global Health Partnerships*; Palgrave Macmillan UK: London, 2009; pp 33–80. https://doi.org/10.1057/9780230582873_2.
(66) Newman, D. J.; Cragg, G. M. Natural Products as Sources of New Drugs from 1981 to 2014. *J. Nat. Prod.* **2016**, *79* (3), 629–661. https://doi.org/10.1021/acs.jnatprod.5b01055.
(67) Mahdi, J. G.; Mahdi, A. J.; Mahdi, A. J.; Bowen, I. D. The Historical Analysis of Aspirin Discovery, Its Relation to the Willow Tree and Antiproliferative and Anticancer Potential. *Cell Proliferation* **2006**, *39* (2), 147–155. https://doi.org/10.1111/j.1365-2184.2006.00377.x.
(68) Arrigoni, O.; De Tullio, M. C. Ascorbic Acid: Much More than Just an Antioxidant. *Biochimica et Biophysica Acta (BBA) - General Subjects* **2002**, *1569* (1–3), 1–9. https://doi.org/10.1016/S0304-4165(01)00235-5.
(69) Crawford, T. C.; Crawford, S. A. Synthesis of L-Ascorbic Acid. In *Advances in Carbohydrate Chemistry and Biochemistry*; Elsevier, 1980; Vol. 37, pp 79–155. https://doi.org/10.1016/S0065-2318(08)60020-7.
(70) Patel, R. N. TOUR DE PACLITAXEL: Biocatalysis for Semisynthesis. *Annu. Rev. Microbiol.* **1998**, *52* (1), 361–395. https://doi.org/10.1146/annurev.micro.52.1.361.
(71) *Presidential Green Chemistry Challenge: 2004 Greener Synthetic Pathways Award*. United States Environmental Protection Agency. https://www.epa.gov/greenchemistry/presidential-green-chemistry-challenge-2004-greener-synthetic-pathways-award (accessed 2024-12-01).
(72) Corsello, M. A.; Garg, N. K. Synthetic Chemistry Fuels Interdisciplinary Approaches to the Production of Artemisinin. *Nat. Prod. Rep.* **2015**, *32* (3), 359–366. https://doi.org/10.1039/C4NP00113C.
(73) Turconi, J.; Griolet, F.; Guevel, R.; Oddon, G.; Villa, R.; Geatti, A.; Hvala, M.; Rossen, K.; Göller, R.; Burgard, A. Semisynthetic Artemisinin, the Chemical Path to Industrial Production. *Org. Process Res. Dev.* **2014**, *18* (3), 417–422. https://doi.org/10.1021/op4003196.
(74) You, Z.-Y.; Liu, Z.-Q.; Zheng, Y.-G. Chemical and Enzymatic Approaches to the Synthesis of Optically Pure Ethyl (R)-4-Cyano-3-Hydroxybutanoate. *Appl Microbiol Biotechnol* **2014**, *98* (1), 11–21. https://doi.org/10.1007/s00253-013-5357-0.
(75) Cicero, A. F. G.; Fogacci, F.; Banach, M. Red Yeast Rice for Hypercholesterolemia. *Methodist DeBakey Cardiovascular Journal* **2019**, *15* (3), 192. https://doi.org/10.14797/mdcj-15-3-192.
(76) Dujovne, C. A. Red Yeast Rice Preparations: Are They Suitable Substitutions for Statins? *The American Journal of Medicine* **2017**, *130* (10), 1148–1150. https://doi.org/10.1016/j.amjmed.2017.05.013.
(77) *Red Yeast Rice: What You Need To Know*. National Center for Complementary and Integrative Health. https://www.nccih.nih.gov/health/red-yeast-rice (accessed 2024-12-01).
(78) *Red Yeast Rice: Uses, Side Effects, Interactions, Dosage, and Warning*. WebMD. https://www.webmd.com/vitamins/ai/ingredientmono-925/red-yeast-rice (accessed 2024-12-01).

(79) Berenstein, N. Making a Global Sensation: Vanilla Flavor, Synthetic Chemistry, and the Meanings of Purity. *Hist Sci* **2016**, *54* (4), 399–424. https://doi.org/10.1177/0073275316681802.
(80) Lahlou, M. The Success of Natural Products in Drug Discovery. *PP* **2013**, *04* (03), 17–31. https://doi.org/10.4236/pp.2013.43A003.
(81) Wang, Y.; Liu, L.; Jin, Z.; Zhang, D. Microbial Cell Factories for Green Production of Vitamins. *Front. Bioeng. Biotechnol.* **2021**, *9*, 661562. https://doi.org/10.3389/fbioe.2021.661562.
(82) Shackleton, S.; Campbell, B.; Lotz-Sisitka, H.; Shackleton, C. Links between the Local Trade in Natural Products, Livelihoods and Poverty Alleviation in a Semi-Arid Region of South Africa. *World Development* **2008**, *36* (3), 505–526. https://doi.org/10.1016/j.worlddev.2007.03.003.
(83) Westman, J. O.; Ylitervo, P.; Franzén, C. J.; Taherzadeh, M. J. Effects of Encapsulation of Microorganisms on Product Formation during Microbial Fermentations. *Appl Microbiol Biotechnol* **2012**, *96* (6), 1441–1454. https://doi.org/10.1007/s00253-012-4517-y.
(84) Kissin, I. The Development of New Analgesics Over the Past 50 Years: A Lack of Real Breakthrough Drugs. *Anesthesia & Analgesia* **2010**, *110* (3), 780–789. https://doi.org/10.1213/ANE.0b013e3181cde882.
(85) Waiganjo, N.; Ochanda, H.; Yole, D. Phytochemical Analysis of the Selected Five Plant Extracts. **2012**, *3* (9).
(86) *Vitamin | Definition, Types, & Facts | Britannica*. https://www.britannica.com/science/vitamin (accessed 2024-12-24).
(87) *Vitamins: MedlinePlus Medical Encyclopedia*. https://medlineplus.gov/ency/article/002399.htm (accessed 2024-12-24).
(88) *Vitamin C (Ascorbic acid) Information | Mount Sinai - New York*. Mount Sinai Health System. https://www.mountsinai.org/health-library/supplement/vitamin-c-ascorbic-acid (accessed 2024-12-24).
(89) Yang, W.; Xu, H. Industrial Fermentation of Vitamin C. In *Industrial Biotechnology of Vitamins, Biopigments, and Antioxidants*; Vandamme, E. J., Revuelta, J. L., Eds.; Wiley, 2016; pp 161–192. https://doi.org/10.1002/9783527681754.ch7.
(90) Dresen, E.; Lee, Z.; Hill, A.; Notz, Q.; Patel, J. J.; Stoppe, C. History of Scurvy and Use of Vitamin C in Critical Illness: A Narrative Review. *Nut in Clin Prac* **2023**, *38* (1), 46–54. https://doi.org/10.1002/ncp.10914.
(91) Magiorkinis, E.; Beloukas, A.; Diamantis, A. Scurvy: Past, Present and Future. *European Journal of Internal Medicine* **2011**, *22* (2), 147–152. https://doi.org/10.1016/j.ejim.2010.10.006.
(92) *Scurvy: Symptoms, Risk Factors, Treatment, Recovery, and More*. Healthline. https://www.healthline.com/health/scurvy (accessed 2024-12-24).
(93) Traber, M. G.; Stevens, J. F. Vitamins C and E: Beneficial Effects from a Mechanistic Perspective. *Free Radical Biology and Medicine* **2011**, *51* (5), 1000–1013. https://doi.org/10.1016/j.freeradbiomed.2011.05.017.
(94) Grzybowski, A.; Pietrzak, K. Albert Szent-Györgyi (1893-1986): The Scientist Who Discovered Vitamin C. *Clinics in Dermatology* **2013**, *31* (3), 327–331. https://doi.org/10.1016/j.clindermatol.2012.08.001.

(95) Pappenberger, G.; Hohmann, H.-P. Industrial Production of L-Ascorbic Acid (Vitamin C) and d-Isoascorbic Acid. In *Biotechnology of Food and Feed Additives*; Zorn, H., Czermak, P., Eds.; Advances in Biochemical Engineering/Biotechnology; Springer Berlin Heidelberg: Berlin, Heidelberg, 2013; Vol. 143, pp 143–188. https://doi.org/10.1007/10_2013_243.
(96) Davies, M. B.; Austin, J.; Partridge, D. A. *Vitamin C: Its Chemistry and Biochemistry*; RSC Paperbacks; Royal Society of Chemistry: Cambridge, 1991. https://doi.org/10.1039/9781847552303.
(97) Telang, P. Vitamin C in Dermatology. *Indian Dermatol Online J* **2013**, *4* (2), 143. https://doi.org/10.4103/2229-5178.110593.
(98) Nishikawa, Y.; Kurata, T. Interconversion between Dehydro-L-Ascorbic Acid and L-Ascorbic Acid. *Biosci Biotechnol Biochem* **2000**, *64* (3), 476–483. https://doi.org/10.1271/bbb.64.476.
(99) Yin, X.; Chen, K.; Cheng, H.; Chen, X.; Feng, S.; Song, Y.; Liang, L. Chemical Stability of Ascorbic Acid Integrated into Commercial Products: A Review on Bioactivity and Delivery Technology. *Antioxidants (Basel)* **2022**, *11* (1), 153. https://doi.org/10.3390/antiox11010153.
(100) Nishikawa, Y.; Kurata, T. Interconversion between Dehydro-L-Ascorbic Acid and L-Ascorbic Acid. *Bioscience, Biotechnology, and Biochemistry* **2000**, *64* (3), 476–483. https://doi.org/10.1271/bbb.64.476.
(101) Linster, C. L.; Van Schaftingen, E. Vitamin C: Biosynthesis, Recycling and Degradation in Mammals. *The FEBS Journal* **2007**, *274* (1), 1–22. https://doi.org/10.1111/j.1742-4658.2006.05607.x.
(102) Market.us. *Global Ascorbic Acid Market Report 2024 - 2033*; 2023. https://market.us/report/ascorbic-acid-market/ (accessed 2024-11-13).
(103) *Vitamin C and its derivatives, unmixed exports by country |2019*. https://wits.worldbank.org/trade/comtrade/en/country/ALL/year/2019/tradeflow/Exports/partner/WLD/product/293627 (accessed 2025-01-10).
(104) Zhou, J.; Du, G.; Chen, J. Metabolic Engineering of Microorganisms for Vitamin C Production. In *Reprogramming Microbial Metabolic Pathways*; Wang, X., Chen, J., Quinn, P., Eds.; Subcellular Biochemistry; Springer Netherlands: Dordrecht, 2012; Vol. 64, pp 241–259. https://doi.org/10.1007/978-94-007-5055-5_12.
(105) García, B.; Orozco-Saumell, A.; López Granados, M.; Moreno, J.; Iglesias, J. Catalytic Transfer Hydrogenation of Glucose to Sorbitol with Raney Ni Catalysts Using Biomass-Derived Diols as Hydrogen Donors. *ACS Sustainable Chem. Eng.* **2021**, *9* (44), 14857–14867. https://doi.org/10.1021/acssuschemeng.1c04957.
(106) García, B.; Moreno, J.; Morales, G.; Melero, J. A.; Iglesias, J. Production of Sorbitol via Catalytic Transfer Hydrogenation of Glucose. *Applied Sciences* **2020**, *10* (5), 1843. https://doi.org/10.3390/app10051843.
(107) Li, Z.; Liu, Y.; Wu, S. Efficient Conversion of D-Glucose into D-Sorbitol over Carbonized Cassava Dregs-Supported Ruthenium Nanoparticles Catalyst. *BioResources* **2018**, *13* (1), 1278–1288. https://doi.org/10.15376/biores.13.1.1278-1288.
(108) Guo, X.; Wang, X.; Guan, J.; Chen, X.; Qin, Z.; Mu, X.; Xian, M. Selective Hydrogenation of D-Glucose to D-Sorbitol over Ru/ZSM-5 Catalysts. *Chinese Journal of Catalysis* **2014**, *35* (5), 733–740. https://doi.org/10.1016/S1872-2067(14)60077-2.

(109) Macauley-Patrick, S.; McNeil, B.; Harvey, L. M. By-Product Formation in the d-Sorbitol to l-Sorbose Biotransformation by Gluconobacter Suboxydans ATCC 621 in Batch and Continuous Cultures. *Process Biochemistry* **2005**, *40* (6), 2113–2122. https://doi.org/10.1016/j.procbio.2004.07.014.
(110) Zebiri, I.; Balieu, S.; Guilleret, A.; Reynaud, R.; Haudrechy, A. The Chemistry of L -Sorbose. *Eur J Org Chem* **2011**, *2011* (16), 2905–2910. https://doi.org/10.1002/ejoc.201001578.
(111) Lim, S. M.; Lau, M. S. L.; Tiong, E. I. J.; Goon, M. M.; Lau, R. J. C.; Yeo, W. S.; Lau, S. Y.; Mubarak, N. M. Process Design and Economic Studies of Two-Step Fermentation for Production of Ascorbic Acid. *SN Appl. Sci.* **2020**, *2* (5), 816. https://doi.org/10.1007/s42452-020-2604-8.
(112) Jung Kim, H.; Hyun Kim, J.; Soo Shin, C. Conversion of D-Sorbitol to l-Sorbose by Gluconobacter Suboxydans Cells Co-Immobilized with Oxygen-Carriers in Alginate Beads. *Process Biochemistry* **1999**, *35* (3–4), 243–248. https://doi.org/10.1016/S0032-9592(99)00056-4.
(113) Xu, S.; Wang, X.; Du, G.; Zhou, J.; Chen, J. Enhanced Production of L-Sorbose from D-Sorbitol by Improving the mRNA Abundance of Sorbitol Dehydrogenase in Gluconobacter oxydansWSH-003. *Microb Cell Fact* **2014**, *13* (1), 146. https://doi.org/10.1186/s12934-014-0146-8.
(114) Tian, Y.-S.; Deng, Y.-D.; Zhang, W.-H.; Yu-Wang; Xu, J.; Gao, J.-J.; Bo-Wang; Fu, X.-Y.; Han, H.-J.; Li, Z.-J.; Wang, L.-J.; Peng, R.-H.; Yao, Q.-H. Metabolic Engineering of Escherichia Coli for Direct Production of Vitamin C from D-Glucose. *Biotechnol Biofuels* **2022**, *15* (1), 86. https://doi.org/10.1186/s13068-022-02184-0.
(115) Tucaliuc, A.; Cîșlaru, A.; Kloetzer, L.; Blaga, A. C. Strain Development, Substrate Utilization, and Downstream Purification of Vitamin C. *Processes* **2022**, *10* (8), 1595. https://doi.org/10.3390/pr10081595.
(116) Hancock, R. D.; Viola, R. Biotechnological Approaches for L-Ascorbic Acid Production. *Trends in Biotechnology* **2002**, *20* (7), 299–305. https://doi.org/10.1016/S0167-7799(02)01991-1.
(117) *Health Canada's Proposed Changes to the Core Nutrients Declared in the Canadian Nutrition Facts Table*. https://www.canada.ca/en/health-canada/services/food-nutrition/public-involvement-partnerships/technical-consultation-proposed-changes-core-nutrients-declared-canadian-nutrition-facts-table/consultation.html.
(118) Plouffe, P.; Macchi, A.; Roberge, D. M. From Batch to Continuous Chemical Synthesis—A Toolbox Approach. *Org. Process Res. Dev.* **2014**, *18* (11), 1286–1294. https://doi.org/10.1021/op5001918.
(119) Tas, O.; Ertugrul, U.; Grunin, L.; Oztop, M. H. Investigation of the Hydration Behavior of Different Sugars by Time Domain-NMR. *Foods* **2022**, *11* (8), 1148. https://doi.org/10.3390/foods11081148.
(120) Chen, C.; Li, W. Z.; Song, Y. C.; Weng, L. D.; Zhang, N. Formation of Water and Glucose Clusters by Hydrogen Bonds in Glucose Aqueous Solutions. *Computational and Theoretical Chemistry* **2012**, *984*, 85–92. https://doi.org/10.1016/j.comptc.2012.01.013.
(121) Bornaghi, L. F.; Poulsen, S.-A. Microwave-Accelerated Fischer Glycosylation. *Tetrahedron Letters* **2005**, *46* (20), 3485–3488. https://doi.org/10.1016/j.tetlet.2005.03.126.

(122) Biela-Banaś, A.; Gallienne, E.; Martin, O. R. A Reinvestigation of the Synthesis and Revision of Spectral Data of 1,2-O-Isopropylidene-α-l-Sorbofuranose, 1,2:4,6-Di-O-Isopropylidene-α-l-Sorbofuranose and Derivatives. *Carbohydrate Research* **2013**, *380*, 23–28. https://doi.org/10.1016/j.carres.2013.05.019.
(123) *^{13}C NMR spectra: a commercial 2-keto-d-gluconic acid and b...* ResearchGate. https://www.researchgate.net/figure/C-NMR-spectra-a-commercial-2-keto-d-gluconic-acid-and-b-2-keto-d-gluconic-acid_fig3_339776760 (accessed 2025-01-02).
(124) Gaspar, N. J.; Los, J. M. ON THE CONSTITUTION OF 2-KETO- L -GULONIC ACID. *Can. J. Chem.* **1959**, *37* (2), 495–497. https://doi.org/10.1139/v59-064.
(125) Böttcher, A.; Burst, W. Preparation of 2-Keto-L-Gulonic Esters. US6573400B1, June 3, 2003. https://patents.google.com/patent/US6573400B1/en (accessed 2025-01-02).
(126) Robinson, R.; Qureshi, I. A.; Klancher, C. A.; Rodriguez, P. J.; Tanner, J. J.; Sobrado, P. Contribution to Catalysis of Ornithine Binding Residues in Ornithine N5-Monooxygenase. *Archives of Biochemistry and Biophysics* **2015**, *585*, 25–31. https://doi.org/10.1016/j.abb.2015.09.008.
(127) Morgan, K. D.; Andersen, R. J.; Ryan, K. S. Piperazic Acid-Containing Natural Products: Structures and Biosynthesis. *Nat. Prod. Rep.* **2019**, *36* (12), 1628–1653. https://doi.org/10.1039/C8NP00076J.
(128) Wei, Z.-W.; Niikura, H.; Morgan, K. D.; Vacariu, C. M.; Andersen, R. J.; Ryan, K. S. Free Piperazic Acid as a Precursor to Nonribosomal Peptides. *J. Am. Chem. Soc.* **2022**, *144* (30), 13556–13564. https://doi.org/10.1021/jacs.2c03660.
(129) García-Gutiérrez, C.; Pérez-Victoria, I.; Montero, I.; Fernández-De La Hoz, J.; Malmierca, M. G.; Martín, J.; Salas, J. A.; Olano, C.; Reyes, F.; Méndez, C. Unearthing a Cryptic Biosynthetic Gene Cluster for the Piperazic Acid-Bearing Depsipeptide Diperamycin in the Ant-Dweller Streptomyces Sp. CS113. *IJMS* **2024**, *25* (4), 2347. https://doi.org/10.3390/ijms25042347.
(130) Higgins, M. A.; Shi, X.; Soler, J.; Harland, J. B.; Parkkila, T.; Lehnert, N.; Garcia-Borràs, M.; Du, Y.-L.; Ryan, K. S. Structural and Mechanistic Views of Enzymatic, Heme-Dependent Nitrogen-Nitrogen Bond Formation. December 15, 2023. https://doi.org/10.1101/2023.12.15.571702.
(131) He, H.-Y.; Niikura, H.; Du, Y.-L.; Ryan, K. S. Synthetic and Biosynthetic Routes to Nitrogen–Nitrogen Bonds. *Chem. Soc. Rev.* **2022**, *51* (8), 2991–3046. https://doi.org/10.1039/C7CS00458C.
(132) Le Goff, G.; Ouazzani, J. Natural Hydrazine-Containing Compounds: Biosynthesis, Isolation, Biological Activities and Synthesis. *Bioorganic & Medicinal Chemistry* **2014**, *22* (23), 6529–6544. https://doi.org/10.1016/j.bmc.2014.10.011.
(133) Chen, H.; Kong, C.-C.; Wei, X.; Chi, Z.; Liu, G.-L.; Chi, Z.-M. Overproduction of L-Piperazic Acid by Overexpression of ArgB Gene in Aureobasidium Melanogenum DFAK1. *Process Biochemistry* **2023**, *126*, 157–162. https://doi.org/10.1016/j.procbio.2022.12.035.
(134) Hu, Y.; Van Dyke-Blodgett, J.; Richards, J. Biological and Biochemical Production of Enantiopure L-Piperazic Acid. https://tech.wustl.edu/tech-summary/biological-and-biochemical-production-of-enantiopure-l-piperazic-acid/ (accessed 2024-11-25).
(135) Handy, E. L.; Totaro, K. A.; Lin, C. P.; Sello, J. K. Efficient and Regiospecific Syntheses of Peptides with Piperazic and Dehydropiperazic Acids via a

Multicomponent Reaction. *Org. Lett.* **2014**, *16* (13), 3488–3491. https://doi.org/10.1021/ol501425b.
(136) Sun, Y.; Tang, W.; Wang, M.; Ni, H.; Long, Y. Synthesis of Piperazic Acid-Containing Cyclodepsipeptide Core of Verucopeptin. *Chin. J. Chem.* **2023**, *41* (17), 2077–2081. https://doi.org/10.1002/cjoc.202300106.
(137) Durand, C.; Szostak, M. Recent Advances in the Synthesis of Piperazines: Focus on C–H Functionalization. *Organics* **2021**, *2* (4), 337–347. https://doi.org/10.3390/org2040018.
(138) Sharma, U.; Kumar, R.; Mazumder, A.; Salahuddin; Kukreti, N.; Tyagi, P. K.; Khurana, N. Recent Advances in Synthetic Strategies of Piperazine & Its Analogs Via Rearrangement Reactions: A Review. *LOC* **2025**, *22* (2), 116–127. https://doi.org/10.2174/0115701786307643240625074530.
(139) Gangwar, M.; Kumar, R.; Yadav, R. K.; Mazumder, A.; Salahuddin; Kukreti, N.; Tyagi, P. K.; Kapoor, B. Recently Adopted Synthetic Protocols for Piperazines: A Review. *LOC* **2025**, *22* (2), 92–101. https://doi.org/10.2174/0115701786315719240712070219.
(140) Van Dyke-Blodgett, J.; Hu, Y. Transgenic Microorganisms and Synthesis of Piperazic Acid, Piperazic Acid Containing Products, and Derivatives Thereof.
(141) Hu, Y.; Qi, Y.; Stumpf, S. D.; D'Alessandro, J. M.; Blodgett, J. A. V. Bioinformatic and Functional Evaluation of Actinobacterial Piperazate Metabolism. *ACS Chem. Biol.* **2019**, *14* (4), 696–703. https://doi.org/10.1021/acschembio.8b01086.
(142) Hölting, K.; Aßmann, M.; Bubenheim, P.; Liese, A.; Kuballa, J. Modelling Approach for the Continuous Biocatalytic Synthesis of N-Acetylneuraminic Acid in Packed Bed Reactors. *Processes* **2024**, *12* (10), 2191. https://doi.org/10.3390/pr12102191.
(143) Shivaprasad, P.; Carolina Emanuelsson, E. A. Process Intensification of Immobilized Enzyme Reactors. In *Intensification of Biobased Processes*; Górak, A., Stankiewicz, A., Eds.; The Royal Society of Chemistry, 2018; pp 249–267. https://doi.org/10.1039/9781788010320-00249.
(144) Simões, A.; Ramos, L.; Freitas, L.; Santos, J. C.; Zanin, G. M.; De Castro, H. F. Performance of an Enzymatic Packed Bed Reactor Running on Babassu Oil to Yield Fatty Ethyl Esters (FAEE) in a Solvent-Free System. *Biofuel Res. J.* **2015**, *2* (2), 242–247. https://doi.org/10.18331/BRJ2015.2.2.6.
(145) Britton, J.; Majumdar, S.; Weiss, G. A. Continuous Flow Biocatalysis. *Chem Soc Rev* **2018**, *47* (15), 5891–5918. https://doi.org/10.1039/c7cs00906b.
(146) Stephan, P.; Langley, C.; Winkler, D.; Basquin, J.; Caputi, L.; O'Connor, S. E.; Kries, H. Directed Evolution of Piperazic Acid Incorporation by a Nonribosomal Peptide Synthetase. April 3, 2023. https://doi.org/10.1101/2023.04.03.535426.
(147) Schröder, S.; Maier, A.; Schmidt, S.; Mügge, C.; Tischler, D. Enhancing Biocatalytical N N Bond Formation with the Actinobacterial Piperazate Synthase KtzT. *Molecular Catalysis* **2024**, *553*, 113733. https://doi.org/10.1016/j.mcat.2023.113733.
(148) Shin, D.; Byun, W. S.; Kang, S.; Kang, I.; Bae, E. S.; An, J. S.; Im, J. H.; Park, J.; Kim, E.; Ko, K.; Hwang, S.; Lee, H.; Kwon, Y.; Ko, Y.-J.; Hong, S.; Nam, S.-J.; Kim, S. B.; Fenical, W.; Yoon, Y. J.; Cho, J.-C.; Lee, S. K.; Oh, D.-C. Targeted and Logical Discovery of Piperazic Acid-Bearing Natural Products Based on Genomic and Spectroscopic Signatures. *J. Am. Chem. Soc.* **2023**, *145* (36), 19676–19690. https://doi.org/10.1021/jacs.3c04699.

(149) Fernandes, P.; De Carvalho, C. C. C. R. Multi-Enzyme Systems in Flow Chemistry. *Processes* **2021**, *9* (2), 225. https://doi.org/10.3390/pr9020225.
(150) Crotti, M.; Robescu, M. S.; Bolivar, J. M.; Ubiali, D.; Wilson, L.; Contente, M. L. What's New in Flow Biocatalysis? A Snapshot of 2020–2022. *Front. Catal.* **2023**, *3*, 1154452. https://doi.org/10.3389/fctls.2023.1154452.
(151) Santi, M.; Sancineto, L.; Nascimento, V.; Braun Azeredo, J.; Orozco, E. V. M.; Andrade, L. H.; Gröger, H.; Santi, C. Flow Biocatalysis: A Challenging Alternative for the Synthesis of APIs and Natural Compounds. *Int J Mol Sci* **2021**, *22* (3), 990. https://doi.org/10.3390/ijms22030990.
(152) *Flow Biocatalysis: A Challenging Alternative for the Synthesis of APIs and Natural Compounds*. https://www.mdpi.com/1422-0067/22/3/990 (accessed 2025-01-27).
(153) Gruber, P.; Marques, M. P. C.; O'Sullivan, B.; Baganz, F.; Wohlgemuth, R.; Szita, N. Conscious Coupling: The Challenges and Opportunities of Cascading Enzymatic Microreactors. *Biotechnology Journal* **2017**, *12* (7), 1700030. https://doi.org/10.1002/biot.201700030.
(154) Neumann, C. S.; Jiang, W.; Heemstra, J. R.; Gontang, E. A.; Kolter, R.; Walsh, C. T. Biosynthesis of Piperazic Acid via N^5-Hydroxy-Ornithine in *Kutzneria* Spp. 744. *ChemBioChem* **2012**, *13* (7), 972–976. https://doi.org/10.1002/cbic.201200054.
(155) Zeidler, J.; Sayer, B. G.; Spenser, I. D. Biosynthesis of Vitamin B_1 in Yeast. Derivation of the Pyrimidine Unit from Pyridoxine and Histidine. Intermediacy of Urocanic Acid. *J. Am. Chem. Soc.* **2003**, *125* (43), 13094–13105. https://doi.org/10.1021/ja030261j.
(156) 葛胜祥; 袁伟芳; 徐红岩. A Kind of Synthetic Method of Double Different Protected Amino Acids. CN109824547A, May 31, 2019. https://patents.google.com/patent/CN109824547A/en (accessed 2024-12-12).
(157) Huijgen, W. J. J.; Witkamp, G.-J.; Comans, R. N. J. Mineral CO_2 Sequestration by Steel Slag Carbonation. *Environ. Sci. Technol.* **2005**, *39* (24), 9676–9682. https://doi.org/10.1021/es050795f.
(158) Sassenburg, M.; Kelly, M.; Subramanian, S.; Smith, W. A.; Burdyny, T. Zero-Gap Electrochemical CO_2 Reduction Cells: Challenges and Operational Strategies for Prevention of Salt Precipitation. *ACS Energy Lett.* **2023**, *8* (1), 321–331. https://doi.org/10.1021/acsenergylett.2c01885.
(159) Pieber, B.; Gilmore, K.; Seeberger, P. H. Integrated Flow Processing — Challenges in Continuous Multistep Synthesis. *J Flow Chem* **2017**, *7* (3–4), 129–136. https://doi.org/10.1556/1846.2017.00016.
(160) Xie, K.; Ozden, A.; Miao, R. K.; Li, Y.; Sinton, D.; Sargent, E. H. Eliminating the Need for Anodic Gas Separation in CO2 Electroreduction Systems via Liquid-to-Liquid Anodic Upgrading. *Nat Commun* **2022**, *13* (1), 3070. https://doi.org/10.1038/s41467-022-30677-x.
(161) Misyura, S.; Strizhak, P.; Meleshkin, A.; Morozov, V.; Gaidukova, O.; Shlegel, N.; Shkola, M. A Review of Gas Capture and Liquid Separation Technologies by CO2 Gas Hydrate. *Energies* **2023**, *16* (8), 3318. https://doi.org/10.3390/en16083318.
(162) Senthil Raja, D.; Tsai, D.-H. Recent Advances in Continuous Flow Synthesis of Metal–Organic Frameworks and Their Composites. *Chem. Commun.* **2024**, *60* (65), 8497–8515. https://doi.org/10.1039/D4CC02088J.

(163) *In-Line Liquid-Liquid Separation – Prof Steven V. Ley CBE FMedSci FRS*. http://www.leygroup.ch.cam.ac.uk/research/medicinal-chemistry/in-line-liquid-liquid-separation (accessed 2025-01-27).
(164) Shim, J.-G.; Lee, D. W.; Lee, J. H.; Kwak, N.-S. Experimental Study on Capture of Carbon Dioxide and Production of Sodium Bicarbonate from Sodium Hydroxide. *Environmental Engineering Research* **2016**, *21* (3), 297–303. https://doi.org/10.4491/eer.2016.042.
(165) Gnädinger, U.; Poier, D.; Trombini, C.; Dabros, M.; Marti, R. Development of Lab-Scale Continuous Stirred-Tank Reactor as Flow Process Tool for Oxidation Reactions Using Molecular Oxygen. *Org. Process Res. Dev.* **2024**, *28* (5), 1860–1868. https://doi.org/10.1021/acs.oprd.3c00424.
(166) *Continuous Stirred Tank Reactor (CSTR)*. Vapourtec. https://www.vapourtec.com/flow-chemistry/continuous-stirred-tank-reactor-cstr/ (accessed 2024-12-19).
(167) *CSTR Continuous Stirred Tank Reactor*. AM Technology. https://www.amt.uk/continuous-stirred-tank-reactor (accessed 2024-12-19).

Appendix A: Spectroscopic Data

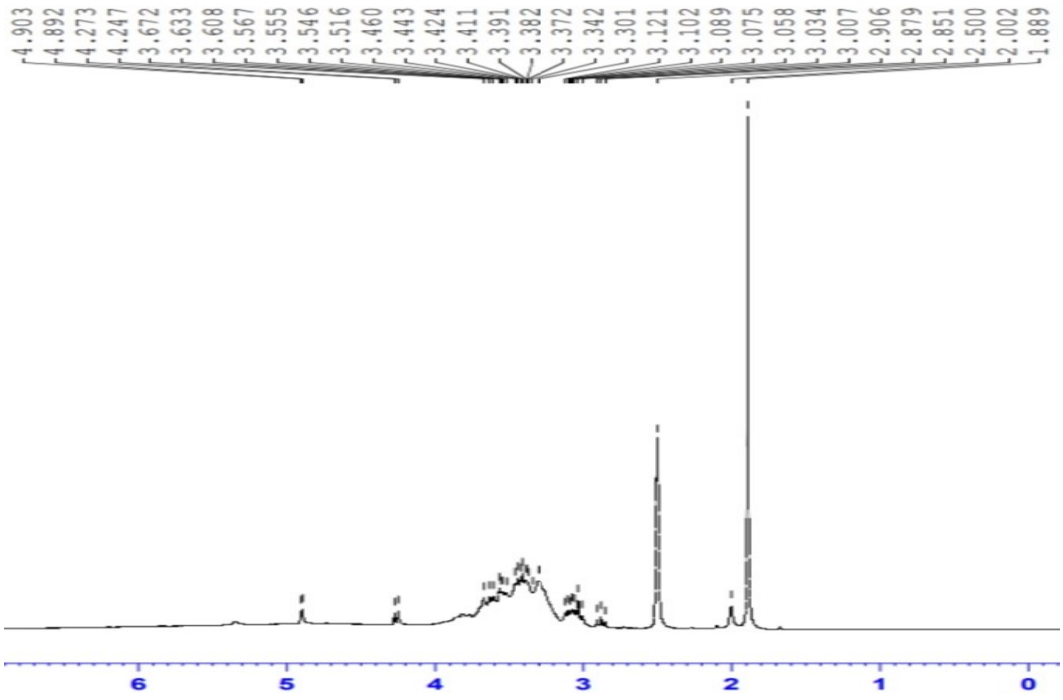

Fig. A 1 - Sorbitol ^{1}H-NMR for Batch 1 recorded in DMSO-d_6 (300 MHz).

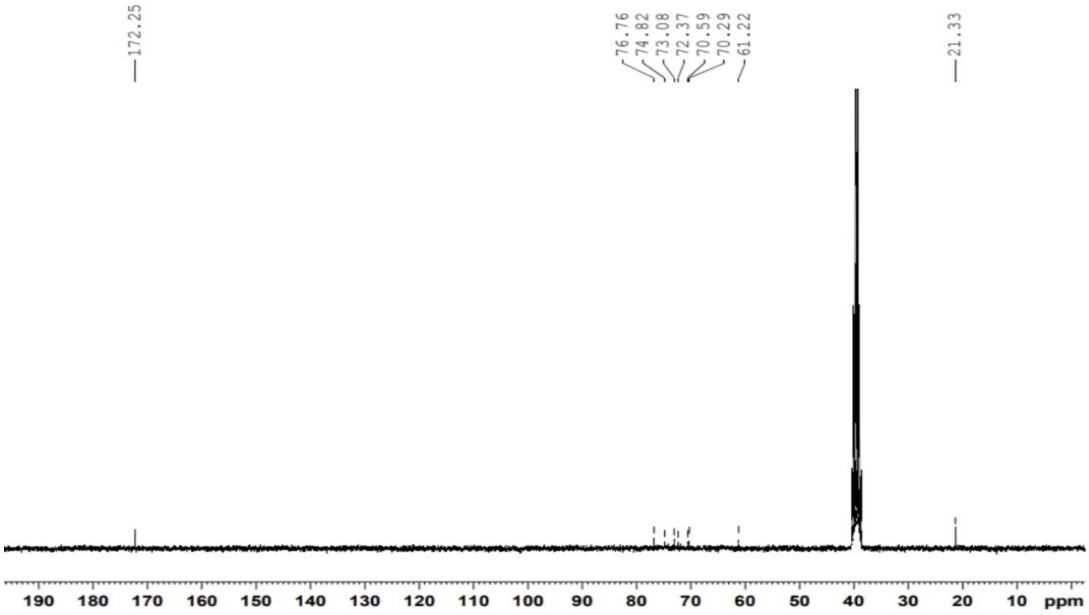

Fig. A 2 - Sorbitol ^{13}C-NMR for Batch 1 recorded in DMSO-d_6 (300 MHz).

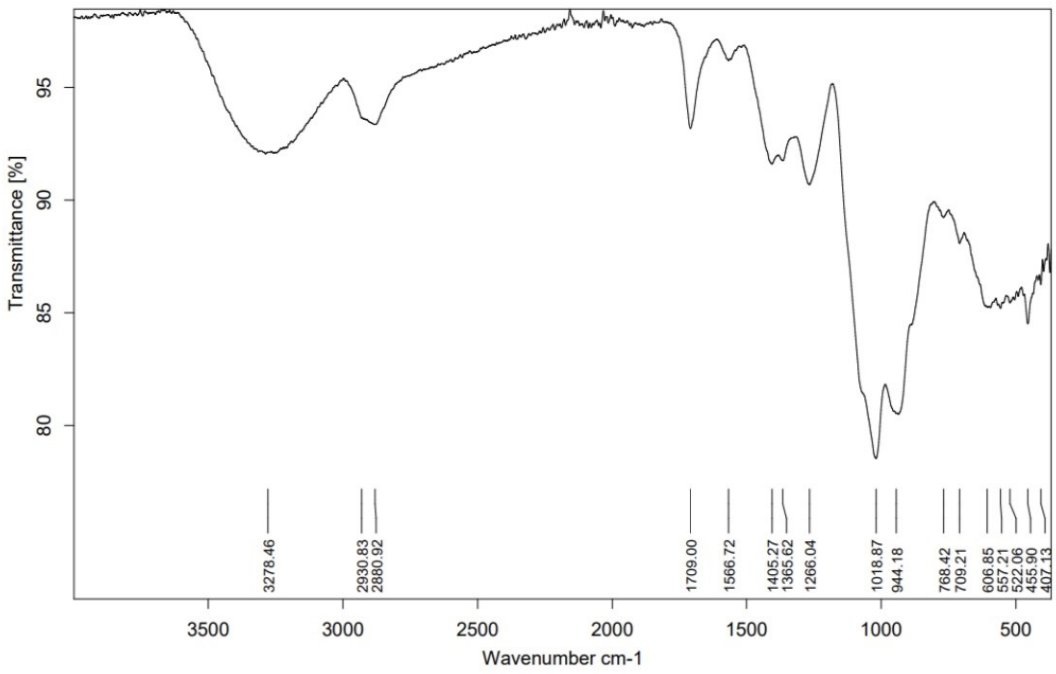

Fig. A 3 - Sorbitol IR spectrum for Batch 1

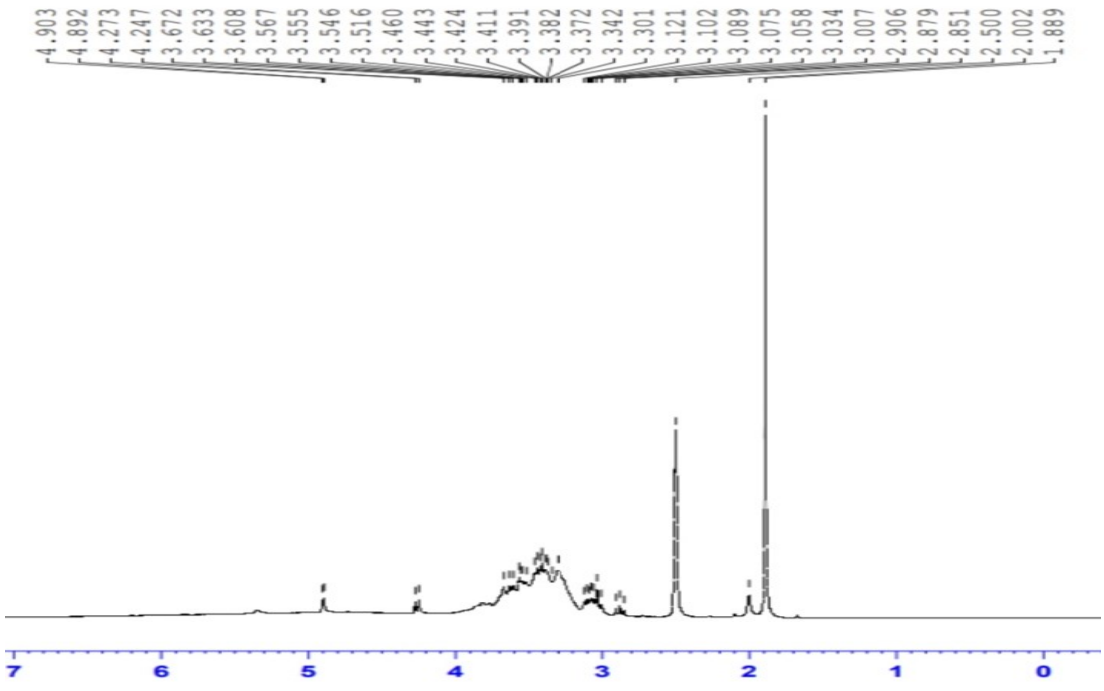

Fig. A 4 - Sorbitol ^{1}H-NMR for Flow 2 recorded in DMSO-d_6 (300 MHz).

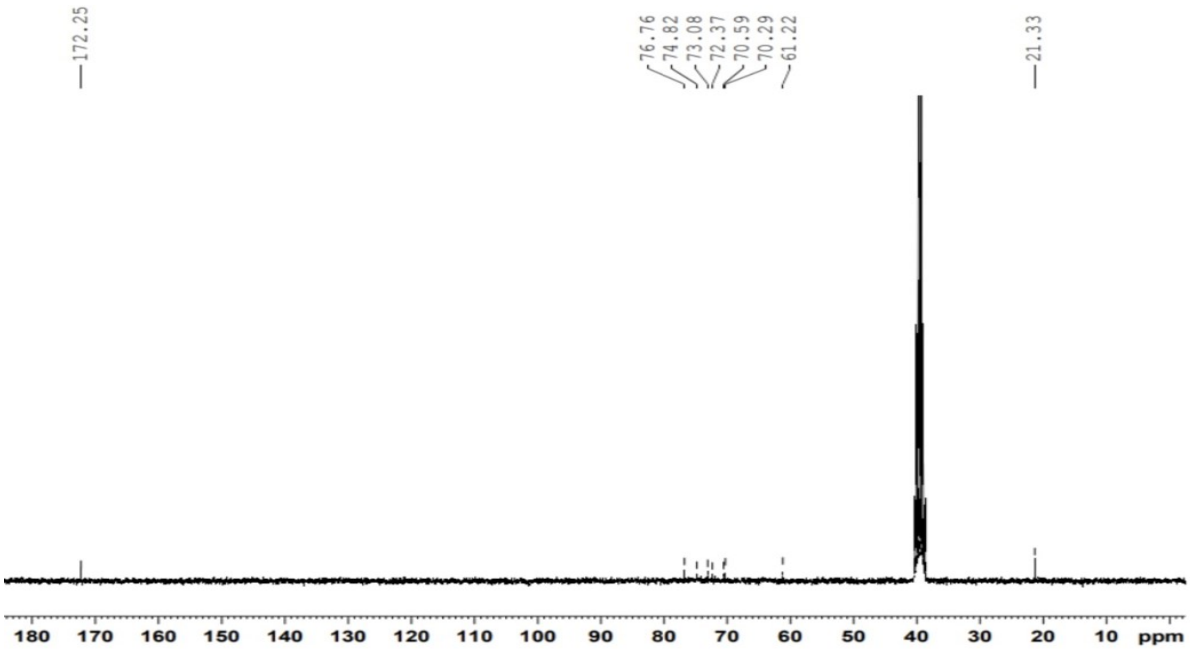

Fig. A 5 - Sorbitol 13C-NMR for Flow 2 recorded in DMSO-d_6 (300 MHz).

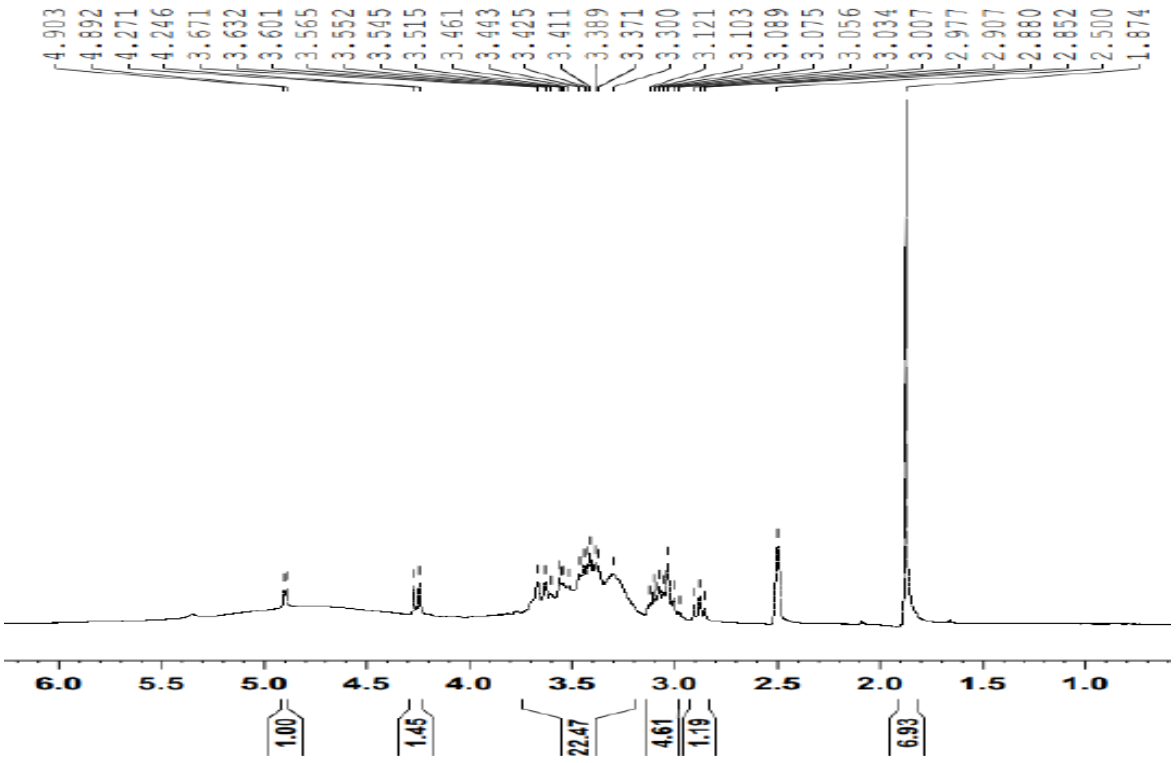

Fig. A 6 - Sorbitol ^{1}H-NMR for Batch 3 recorded in DMSO-d_6 (300 MHz).

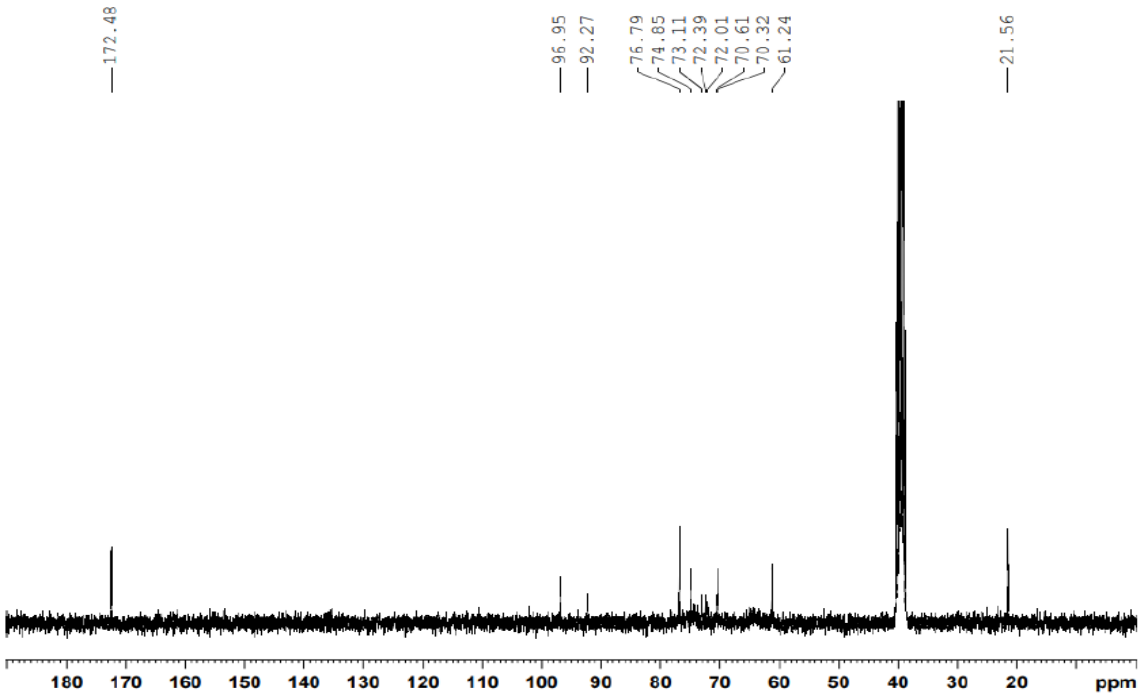

Fig. A 7 - Sorbitol ^{13}C-NMR for Batch 3 recorded in DMSO-d_6 (300 MHz).

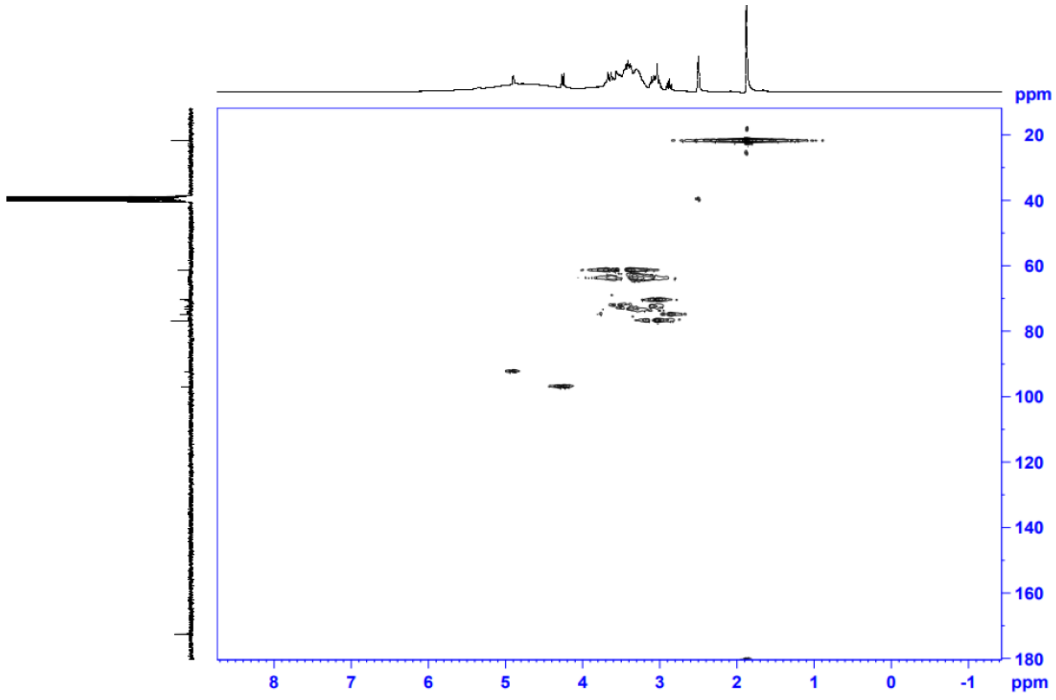

Fig. A 8 - Sorbitol HSQC for Batch 3 recorded in DMSO-d_6 (300 MHz).

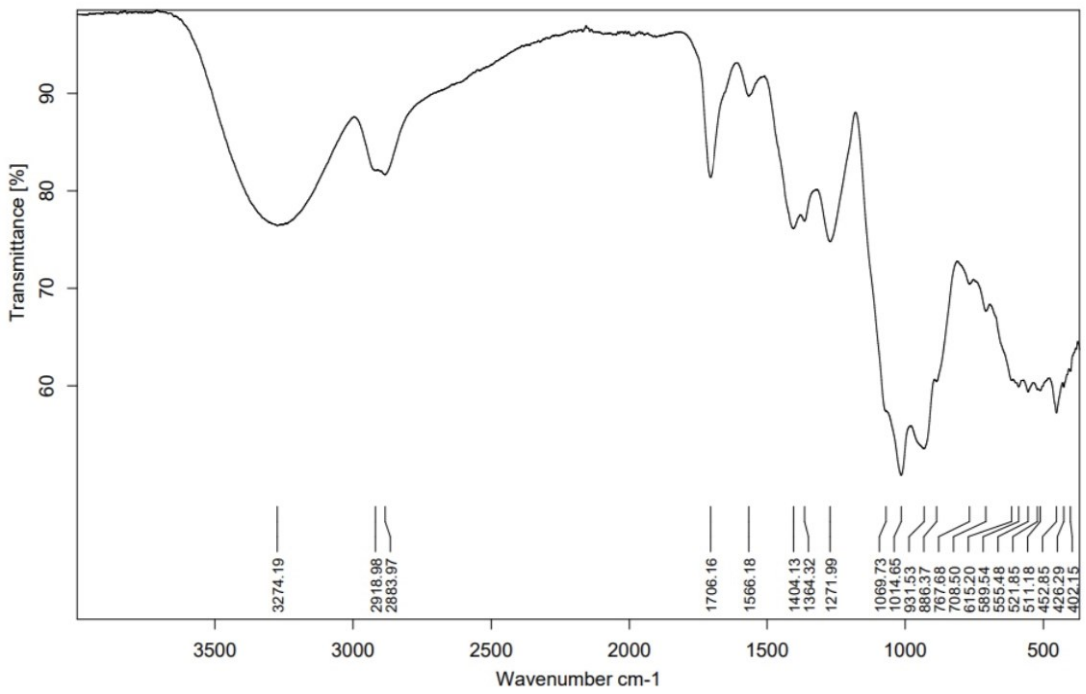

Fig. A 9 - Sorbitol IR spectrum for Batch 3

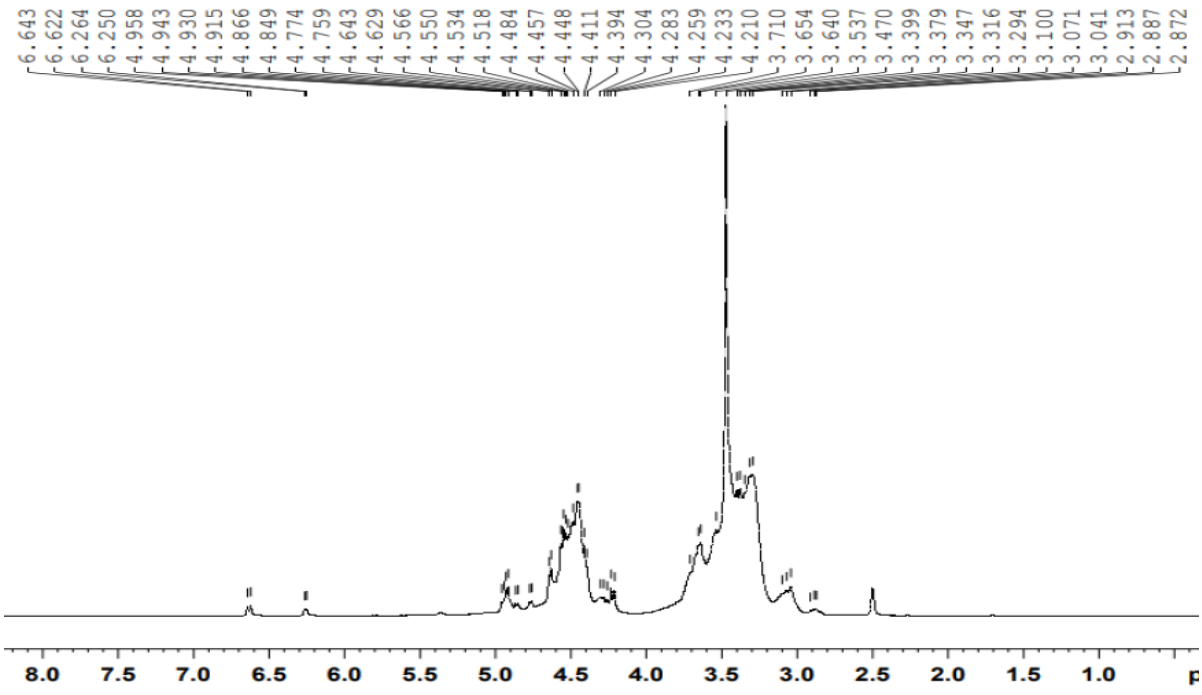

Fig. A 10 - Sorbitol ^{1}H-NMR for Batch 4 recorded in DMSO-d_6 (300 MHz).

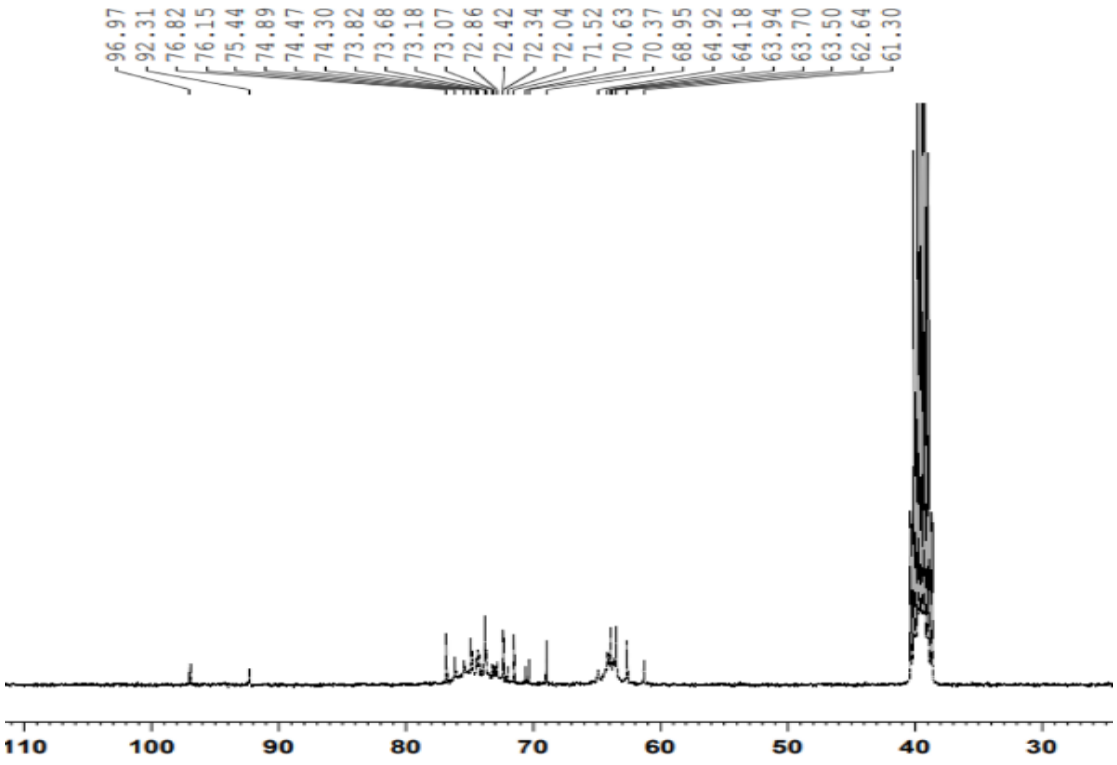

Fig. A 11- Sorbitol ^{13}C-NMR for Batch 4 recorded in DMSO-d$_6$ (300 MHz).

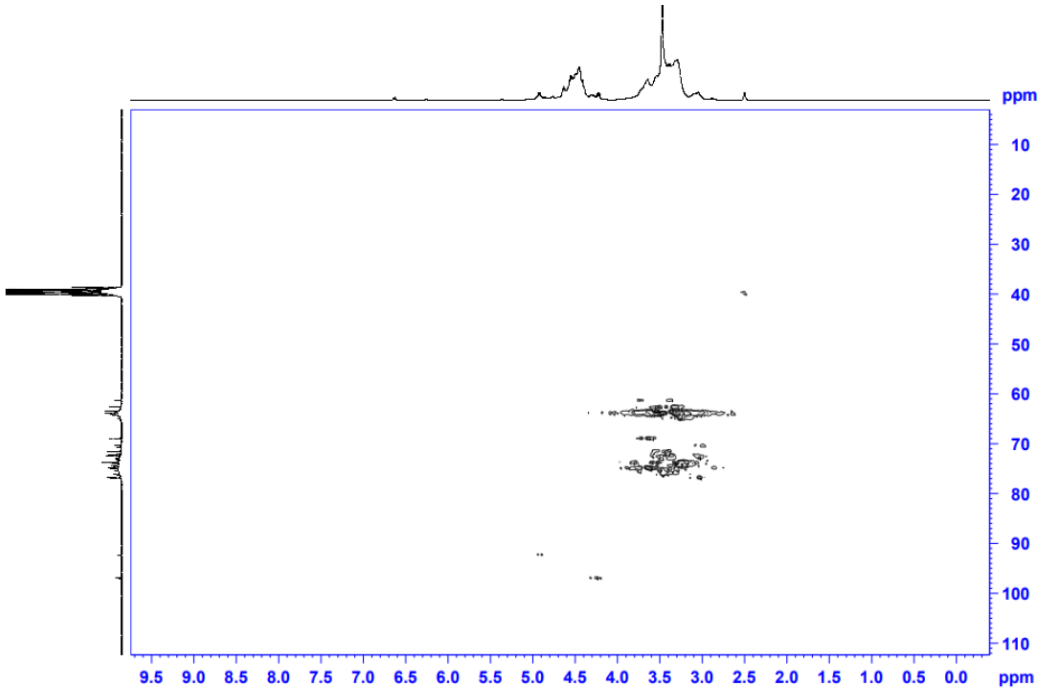

Fig. A 12 - Sorbitol HSQC for Batch 4 recorded in DMSO-d$_6$ (300 MHz).

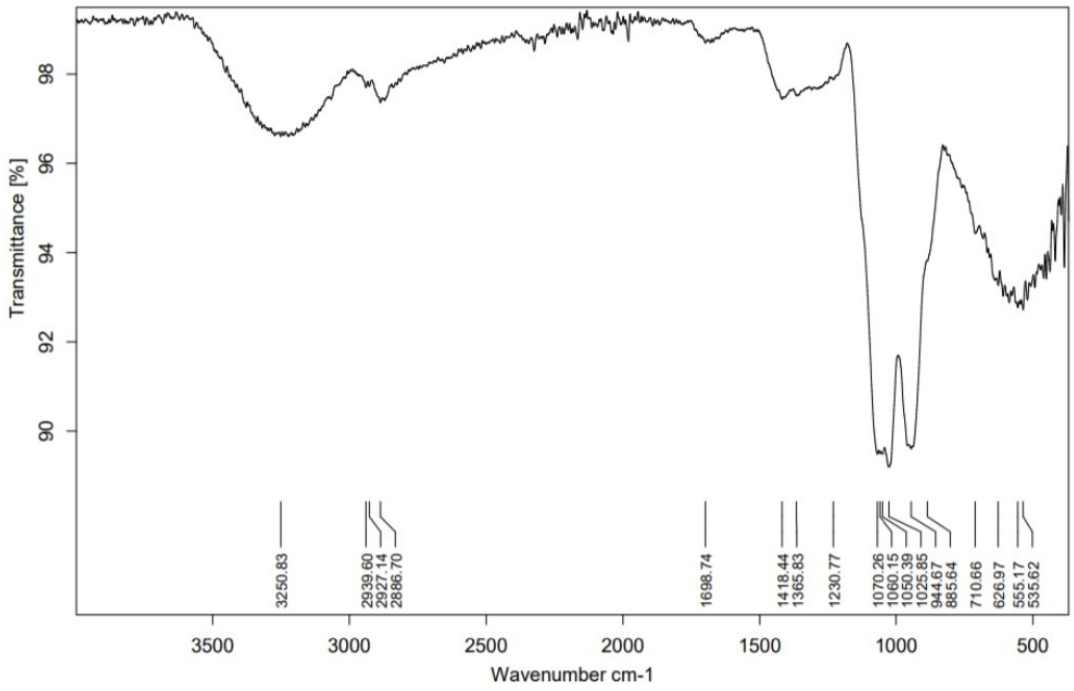

Fig. A 13 - Sorbitol IR spectrum for Batch 4

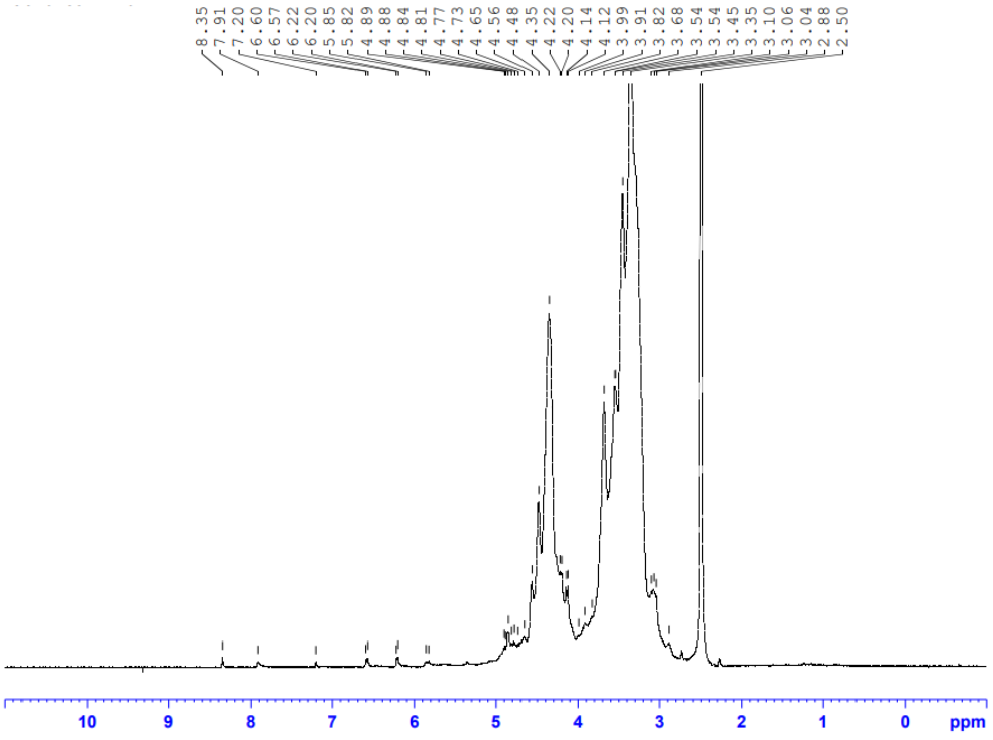

Fig. A 14- Sorbitol ^{1}H-NMR for Batch 5 recorded in DMSO-d_6 (300 MHz).

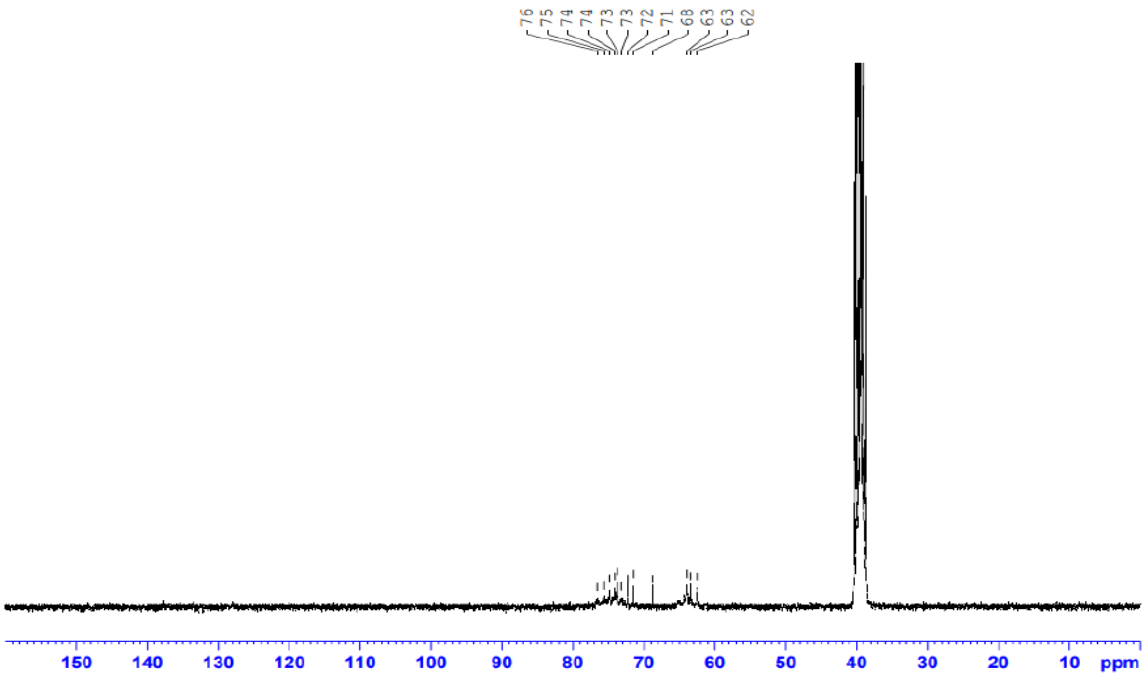

Fig. A 15 - Sorbitol ^{13}C-NMR for Batch 5 recorded in DMSO-d$_6$ (300 MHz).

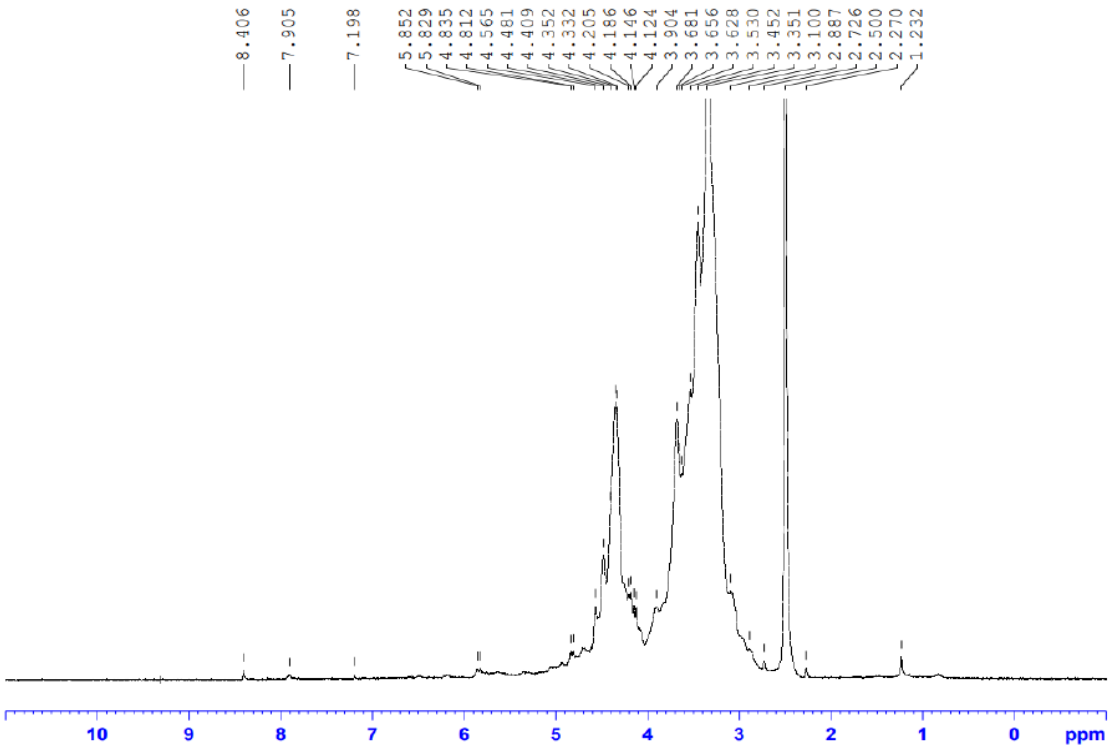

Fig. A 16 - Sorbitol ^{1}H-NMR for Batch 6 recorded in DMSO-d$_6$ (300 MHz).

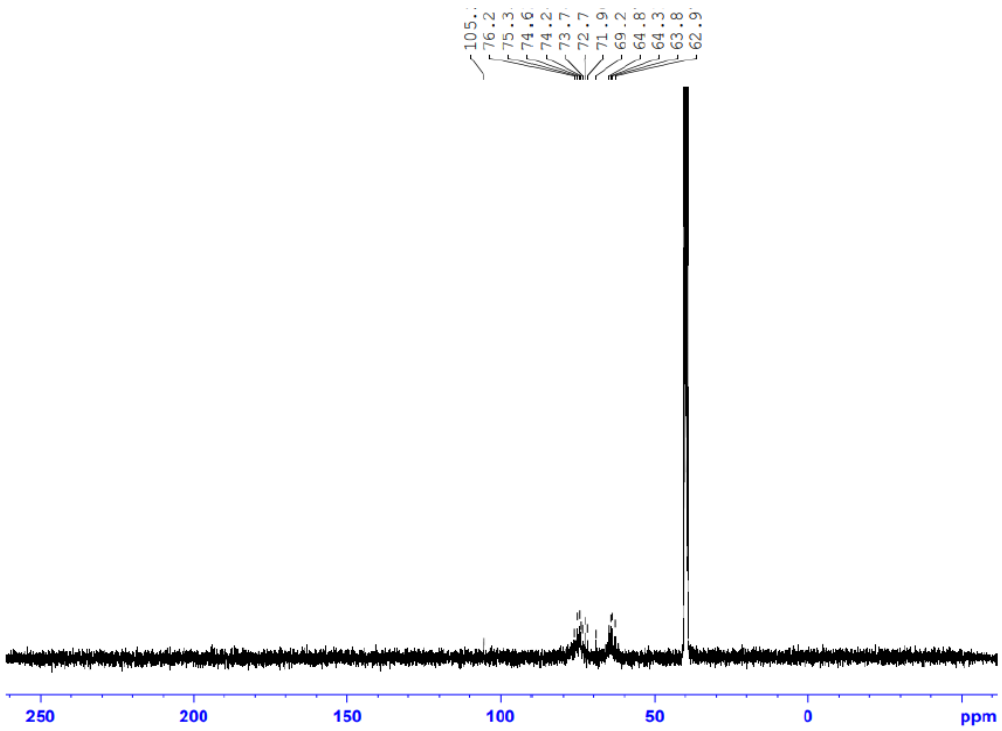

Fig. A 17 - Sorbitol ^{13}C-NMR for Batch 6 recorded in DMSO-d_6 (300 MHz).

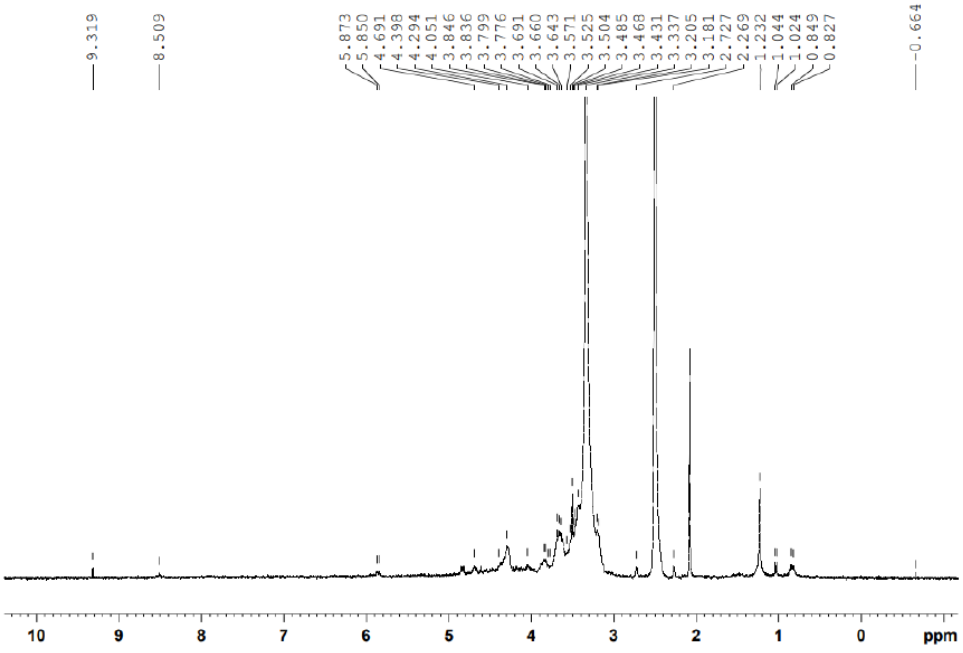

Fig. A 18 - Sorbitol ^{1}H-NMR for Batch 7 recorded in DMSO-d_6 (300 MHz).

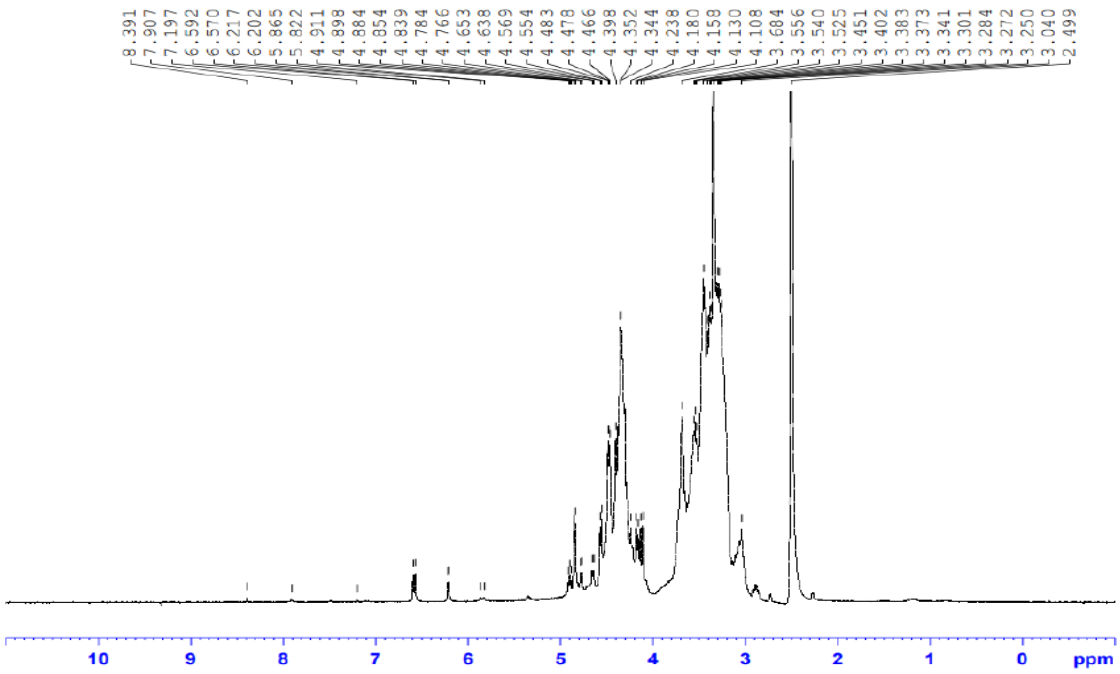

Fig. A 19 - Sorbitol ^{1}H-NMR for Batch 8-A recorded in DMSO-d_6 (300 MHz).

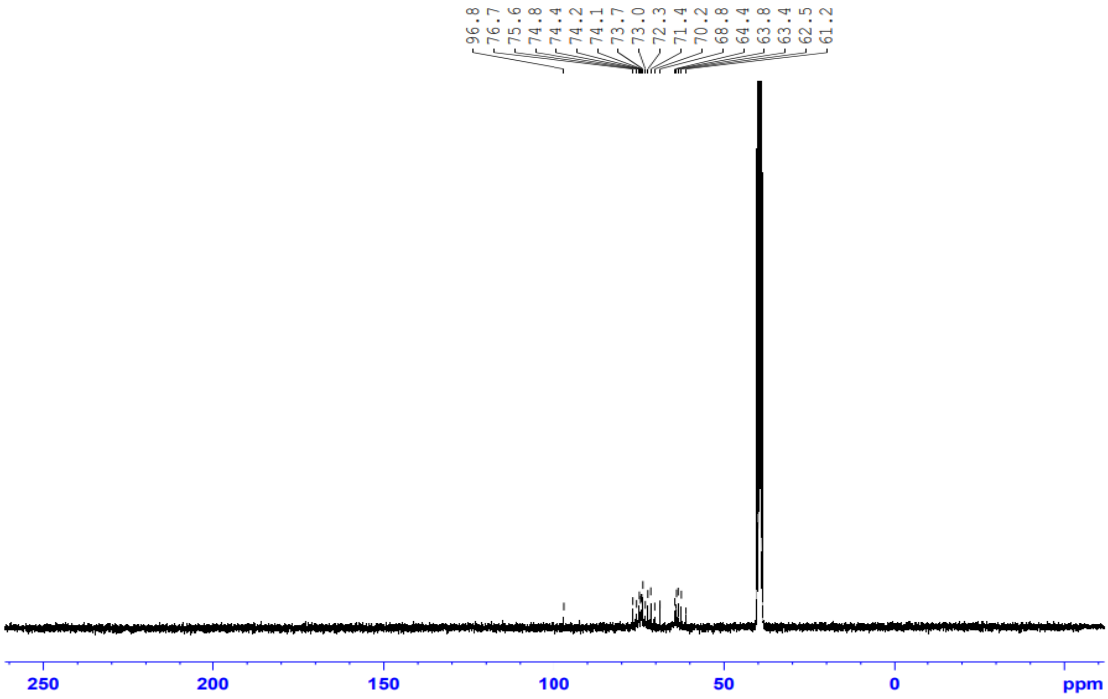

Fig. A 20 - Sorbitol ^{13}C-NMR for Batch 8-A recorded in DMSO-d_6 (300 MHz).

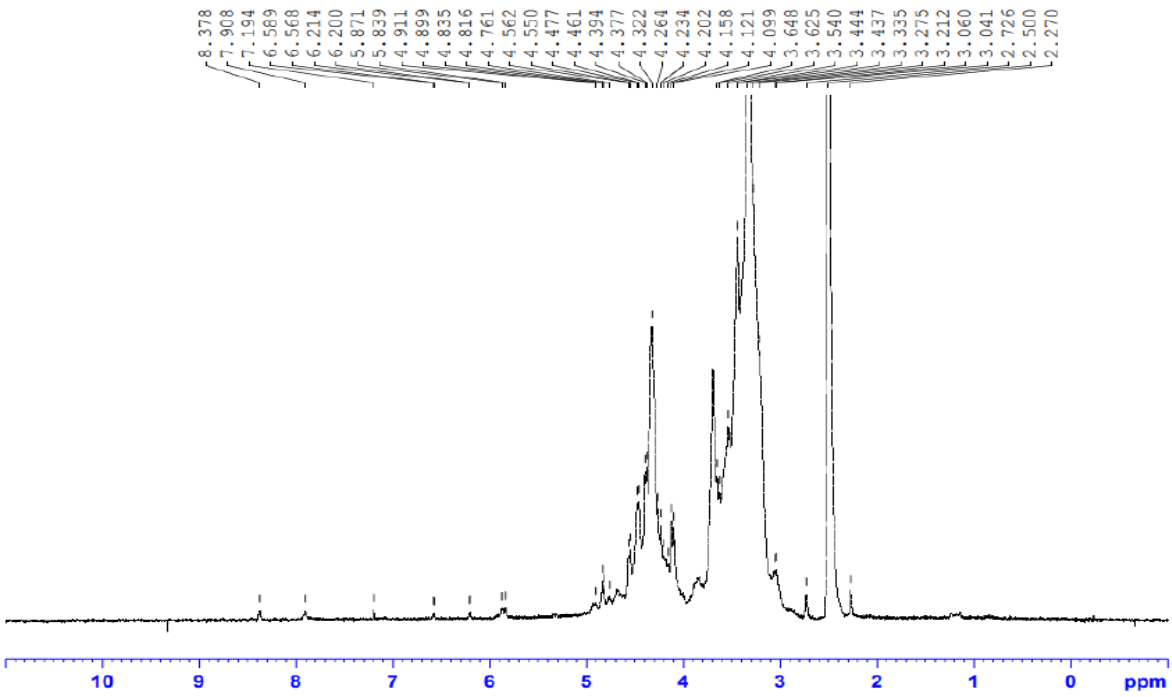

Fig. A 21 - Sorbitol ^{1}H-NMR for Batch 8-B recorded in DMSO-d$_6$ (300 MHz).

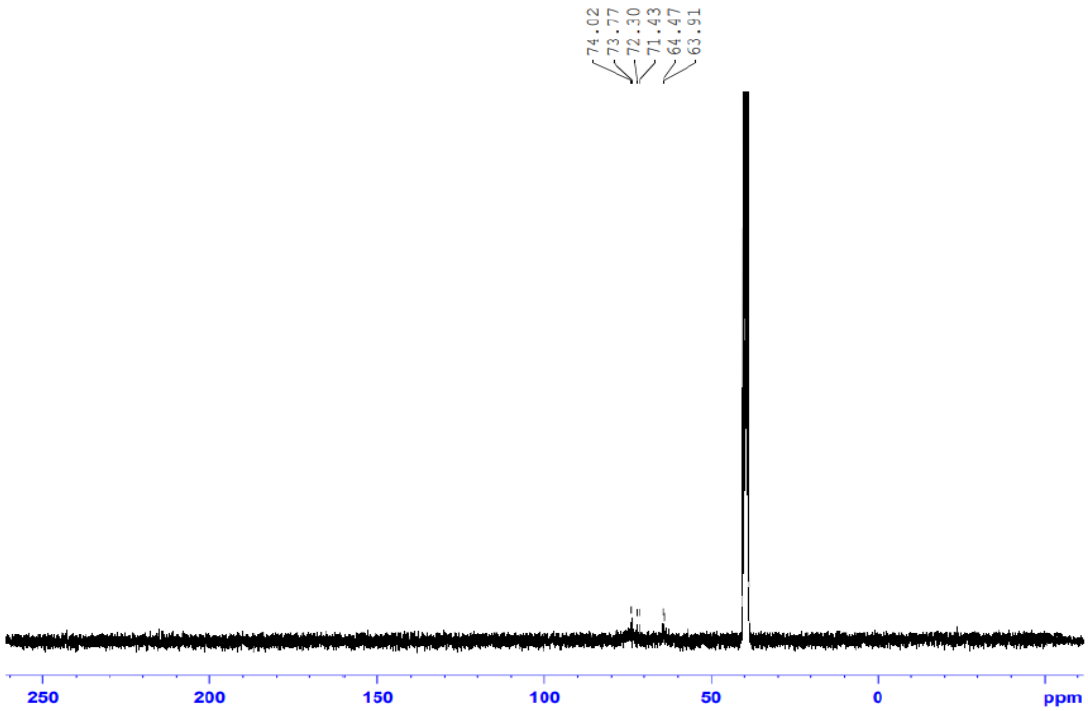

Fig. A 22 - Sorbitol ^{13}C-NMR for Batch 8-B recorded in DMSO-d$_6$ (300 MHz).

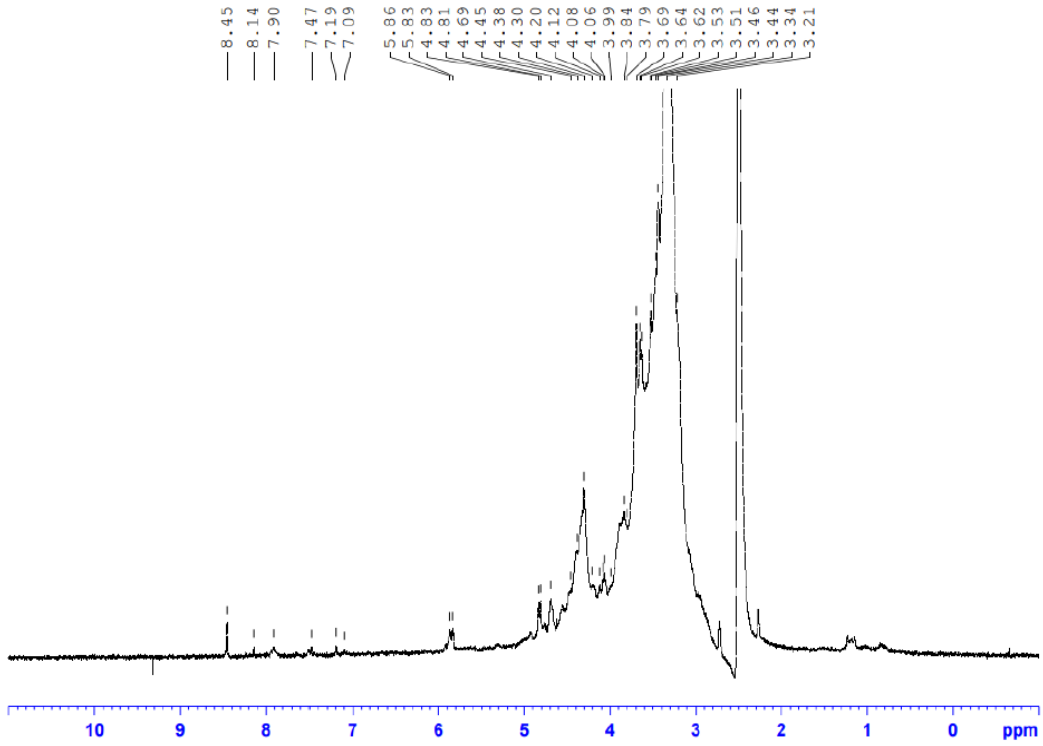

Fig. A 23 - Sorbitol ^{1}H-NMR for Batch 8-C recorded in DMSO-d_6 (300 MHz).

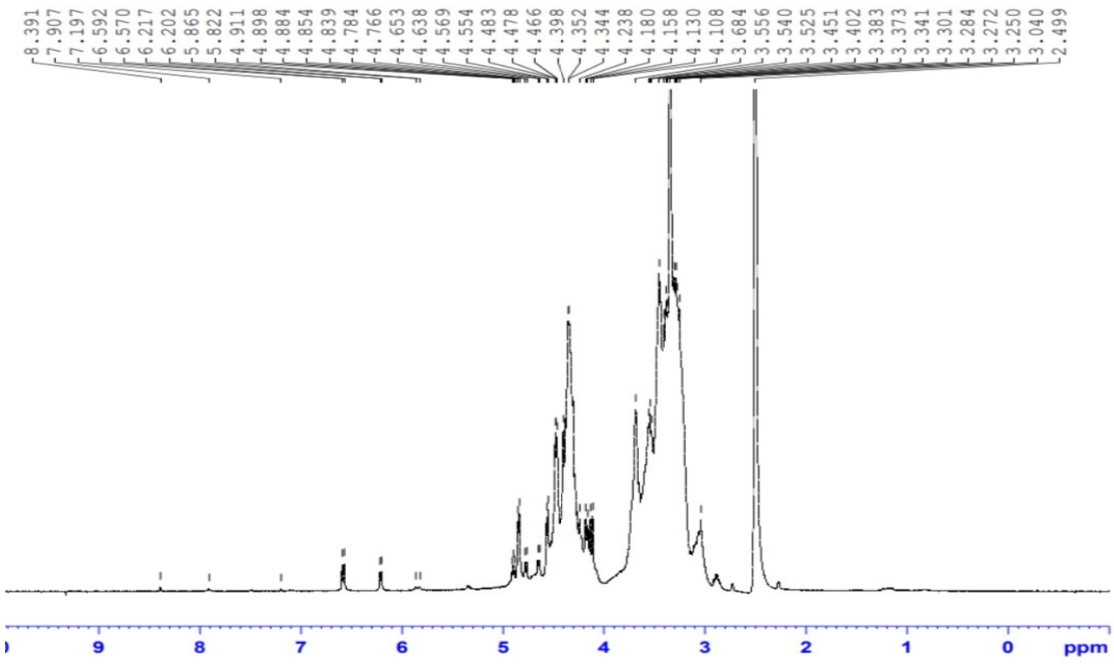

Fig. A 24 - Sorbitol ^{1}H-NMR for Flow 9 recorded in DMSO-d_6 (300 MHz).

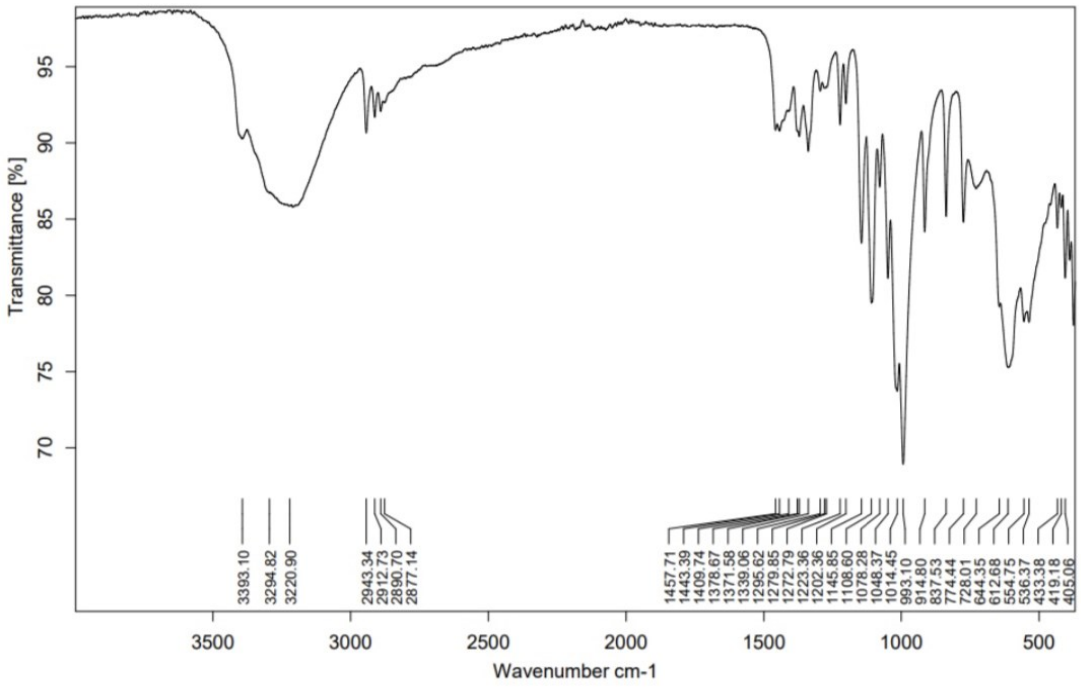

Fig. A 25 - Glucose Sample IR spectrum.

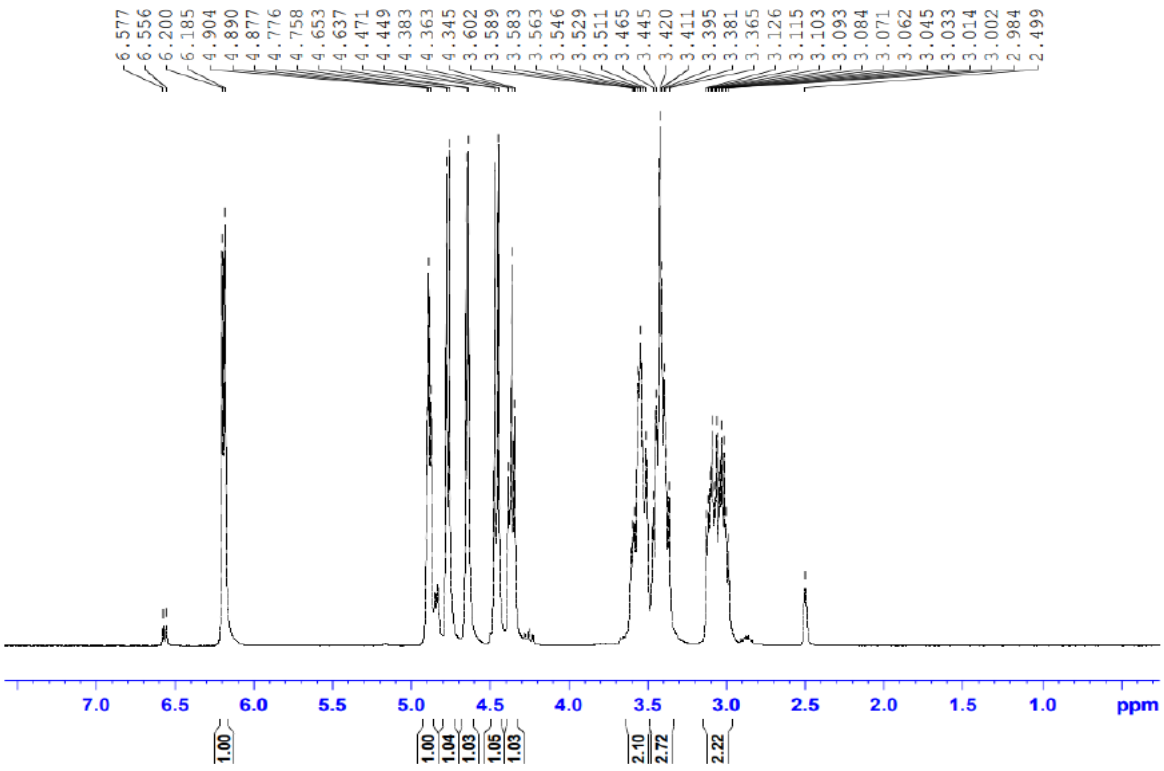

Fig. A 26 - Glucose Sample ^{1}H-NMR recorded in DMSO-d_6 (300 MHz).

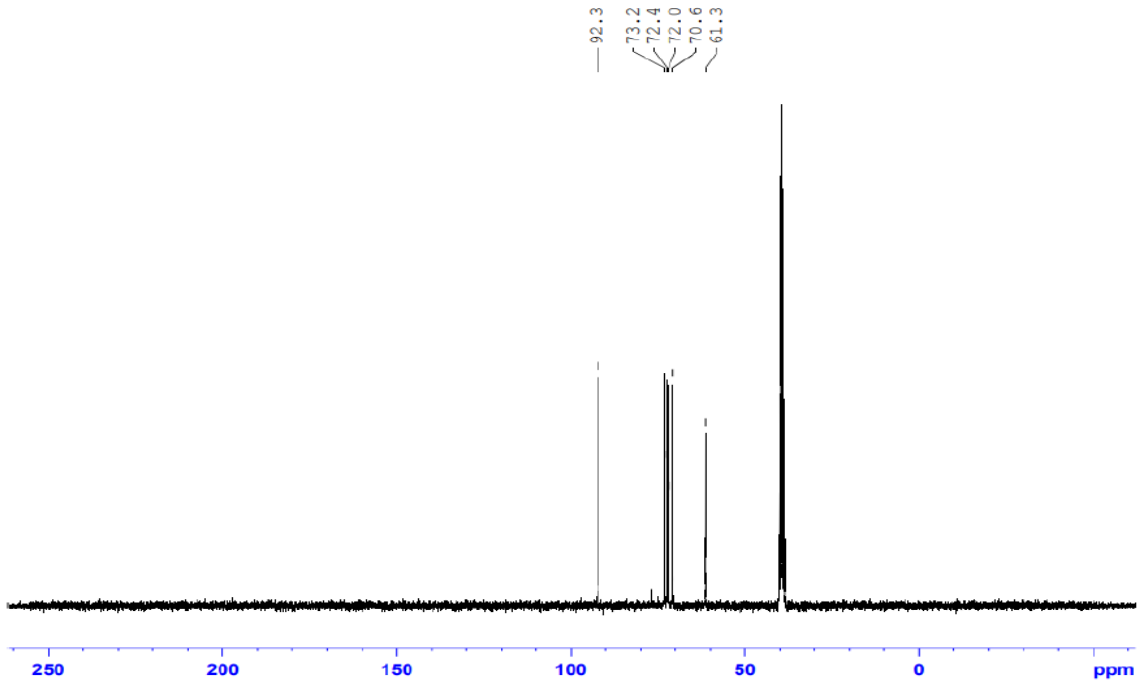

Fig. A 27 - Glucose Sample ^{13}C-NMR recorded in DMSO-d$_6$ (300 MHz).

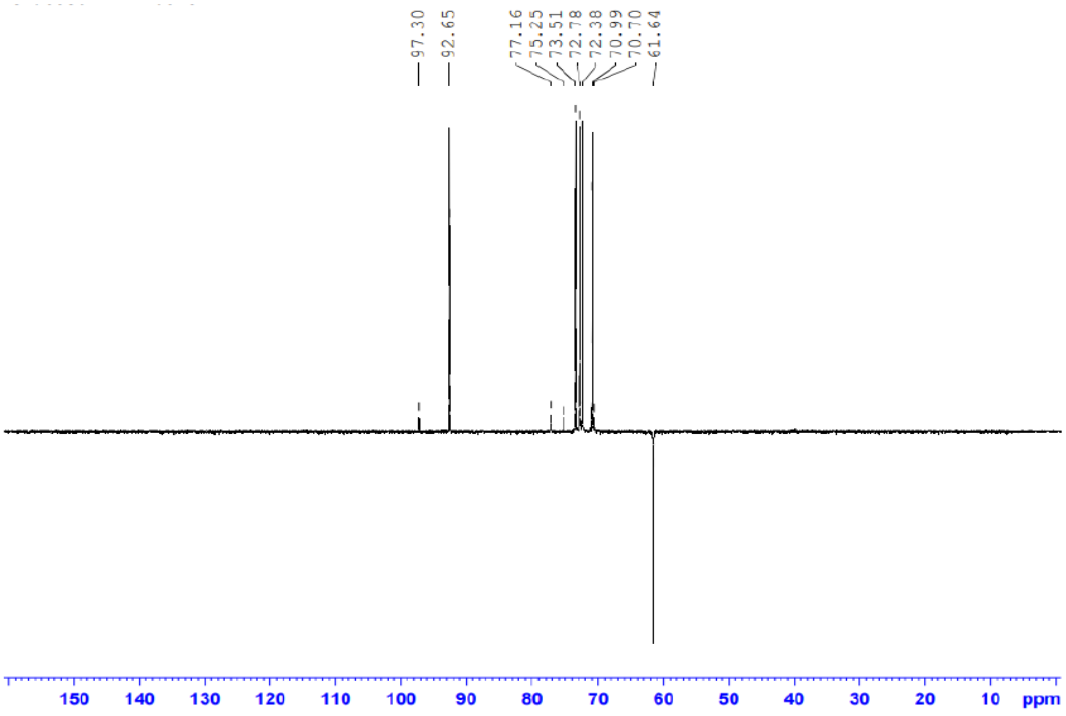

Fig. A 28 - Glucose Sample DEPT-135 recorded in DMSO-d$_6$ (300 MHz).

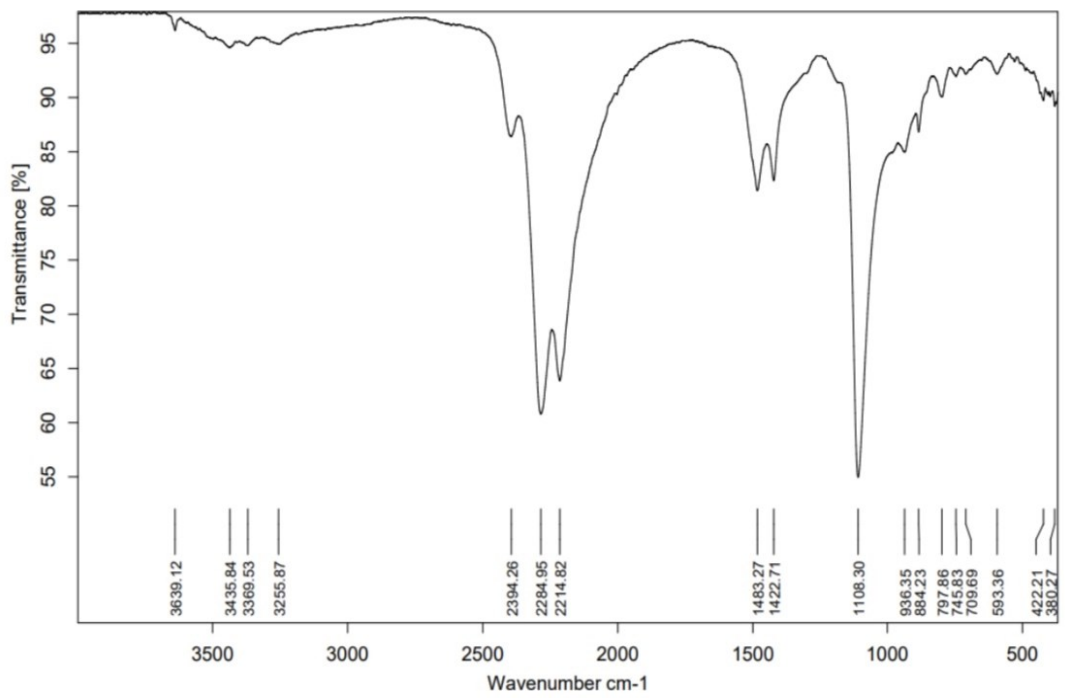

Fig. A 29 - Sodium borohydride Sample IR spectrum

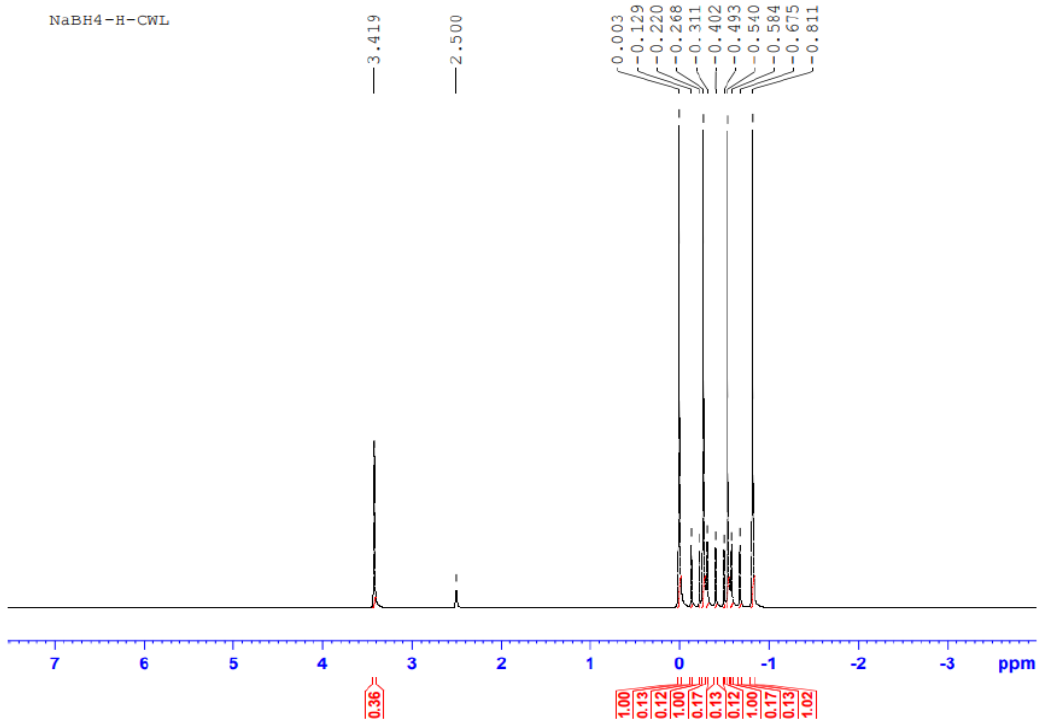

Fig. A 30 - Sodium borohydride Sample ^{1}H-NMR recorded in DMSO-d_6 (300 MHz).

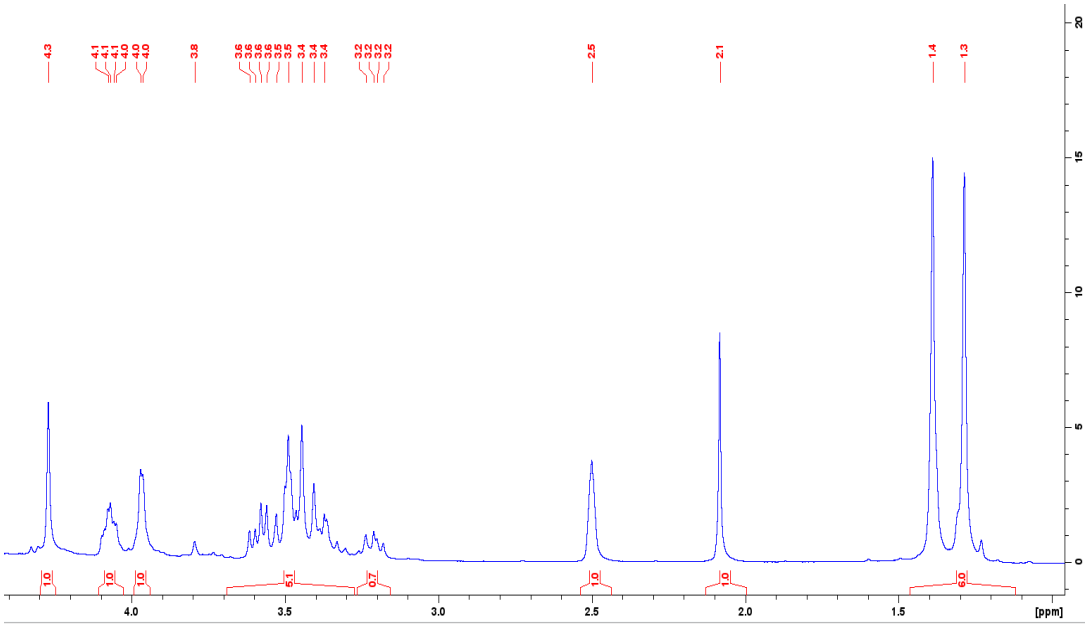

Fig. A 31 - DAS Product ^{1}H-NMR for Batch 1 recorded in DMSO-d_6 (300 MHz).

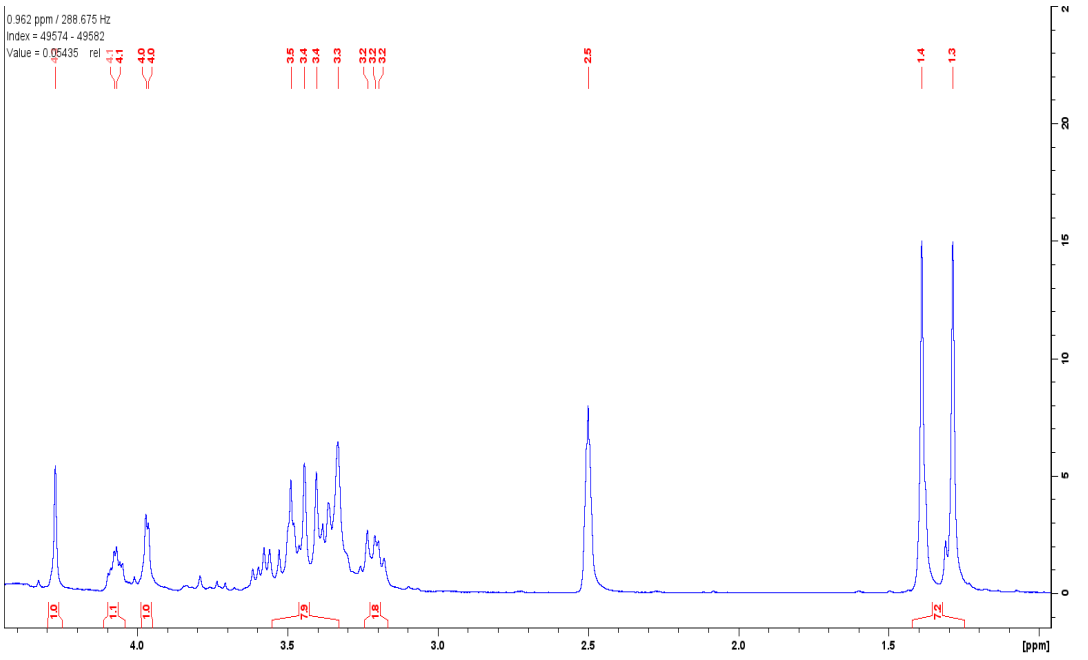

Fig. A 32 - DAS Product ^{1}H-NMR for Batch 2 recorded in DMSO-d_6 (300 MHz).

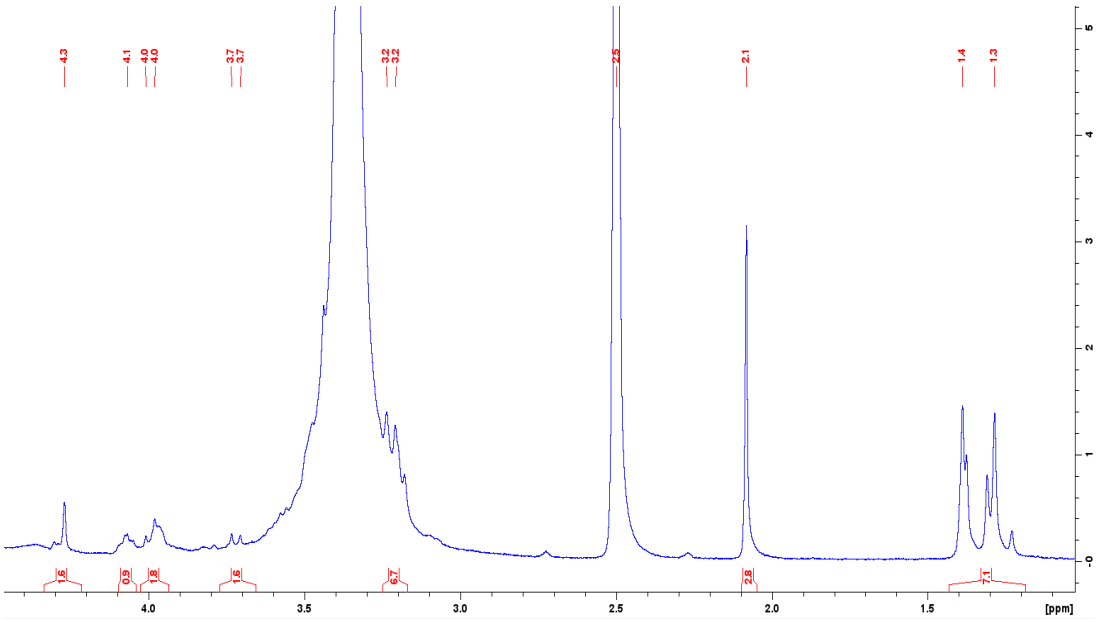

Fig. A 33 - DAS Product ^{1}H-NMR for Batch 3 recorded in DMSO-d_6 (300 MHz).

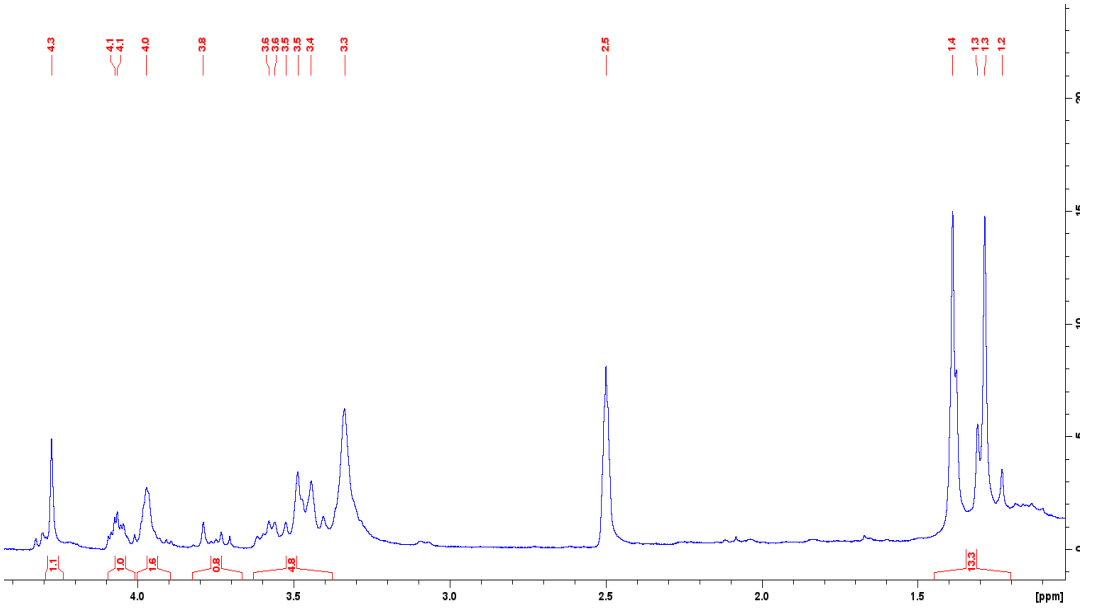

Fig. A 34 - DAS Product ^{1}H-NMR for Batch 4 recorded in DMSO-d_6 (300 MHz).

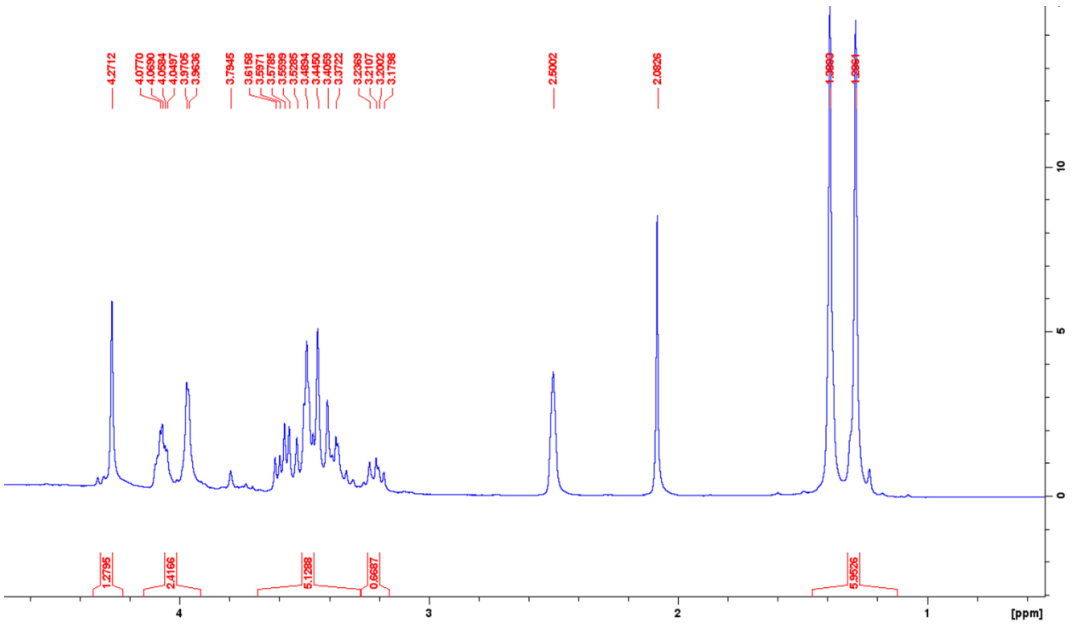

Fig. A 35 - DAS Product ^{1}H-NMR for Flow 5 recorded in DMSO-d_6 (300 MHz).

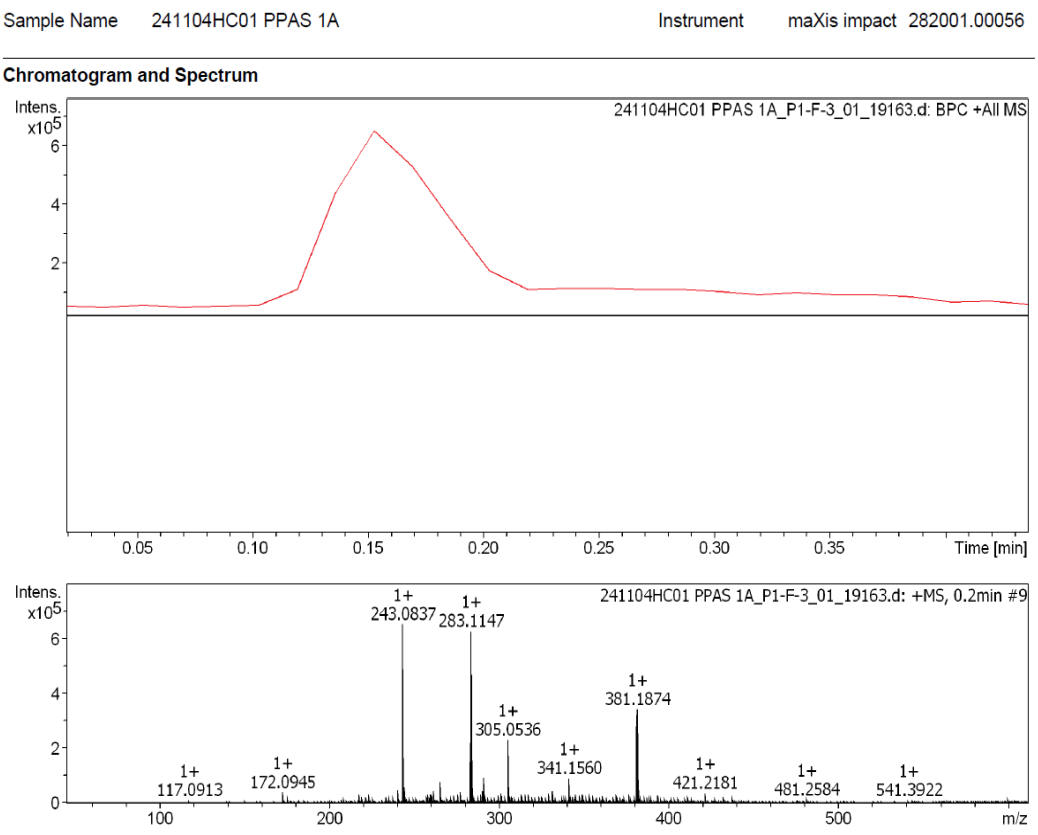

Fig. A 36 - DAS Product Mass Spectrum for Flow 5

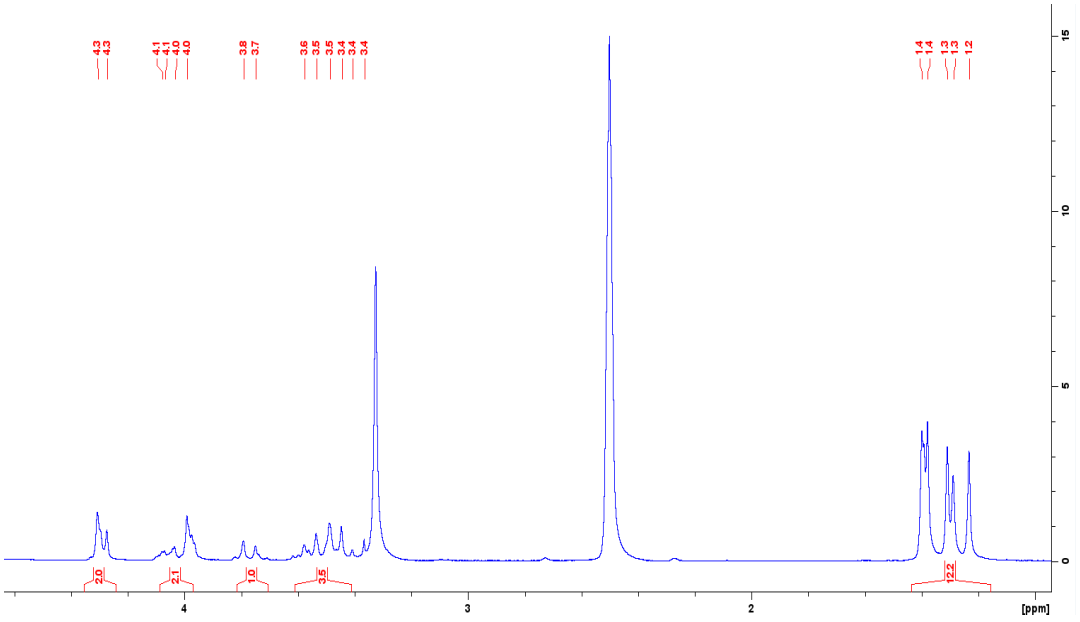

Fig. A 37 - DAS Product ^{1}H-NMR for Batch 6 recorded in DMSO-d_6 (300 MHz).

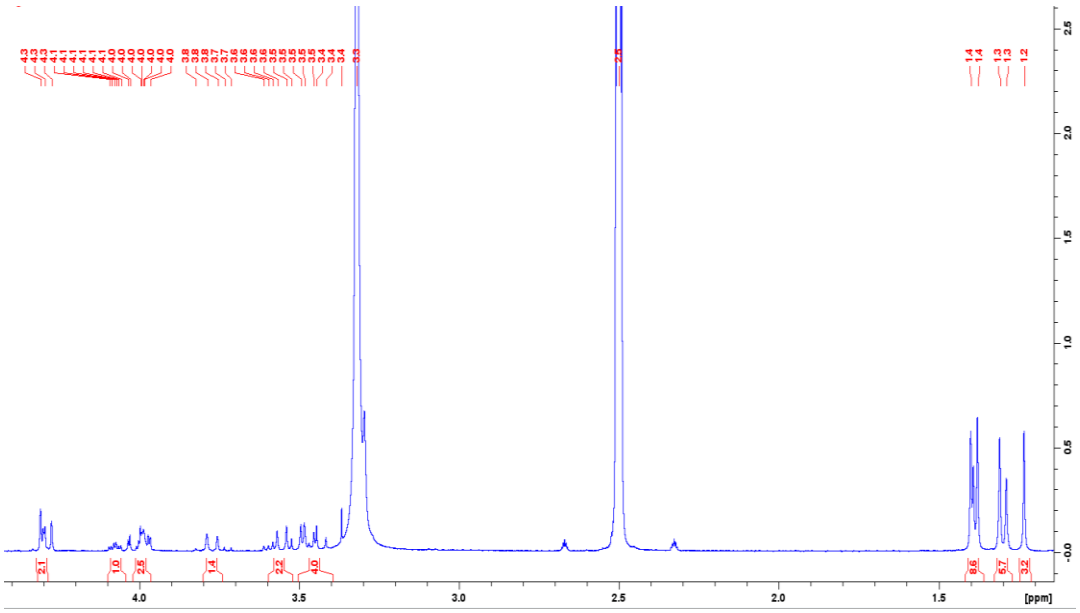

Fig. A 38 - DAS Product ^{1}H-NMR for Flow 7 recorded in DMSO-d_6 (400 MHz).

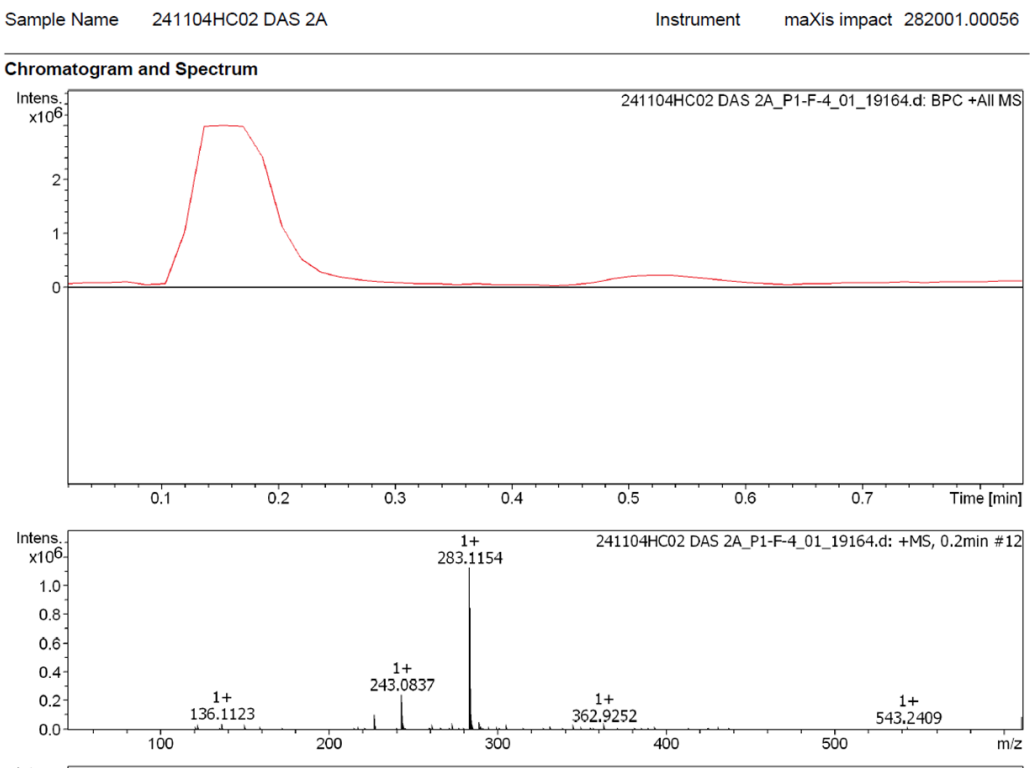

Fig. A 39 - DAS Product Mass Spectrum for Flow 7

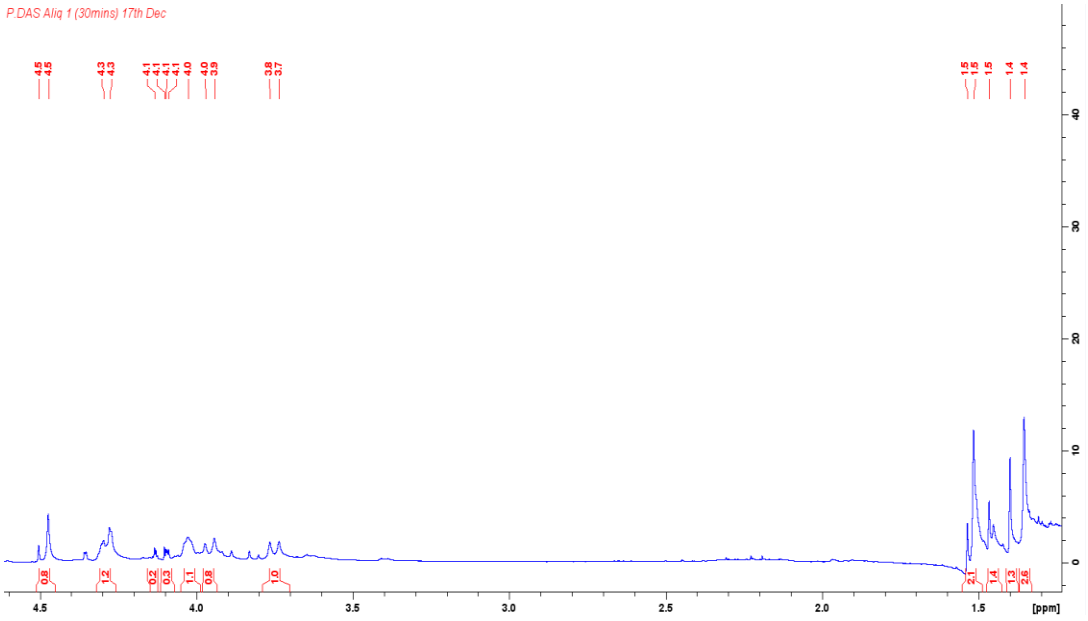

Fig. A 40 - DAS product ^{1}H-NMR for Batch 8-A recorded in $CDCl_3$ (400 MHz).

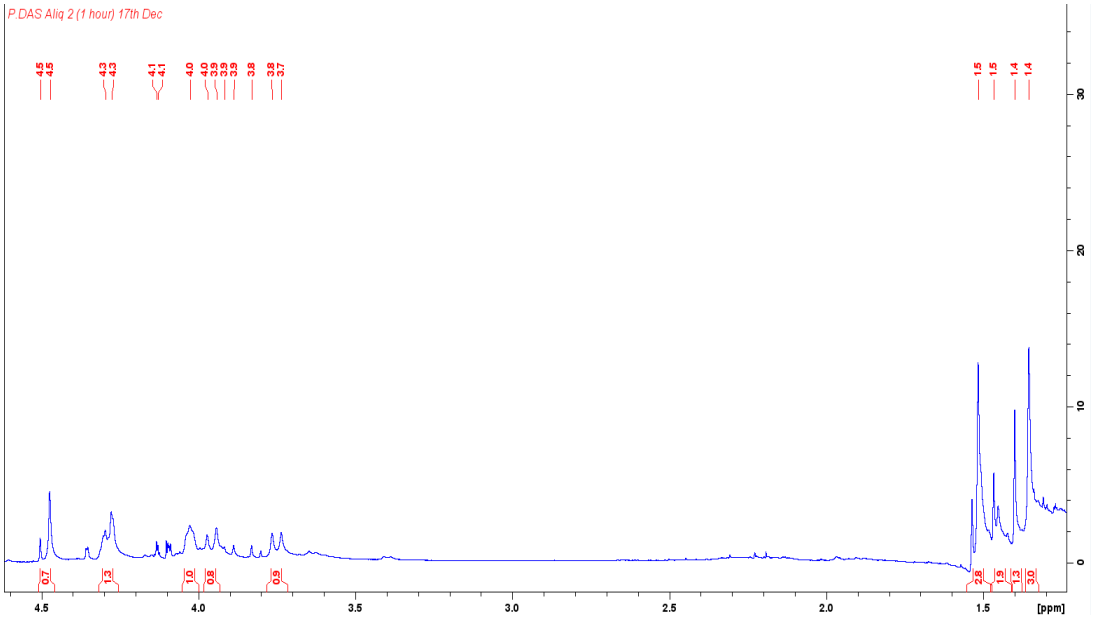

Fig. A 41 - DAS product ^{1}H-NMR for Batch 8-B recorded in $CDCl_3$ (400 MHz).

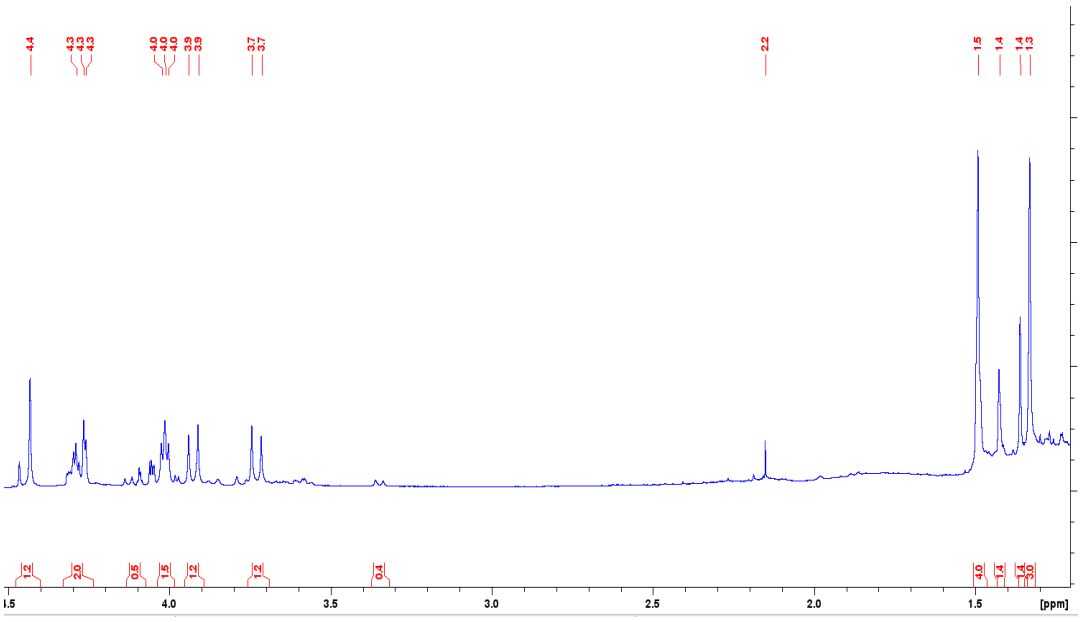

Fig. A 42 -DAS product ^{1}H-NMR for Batch 8-C recorded in $CDCl_3$ (400 MHz).

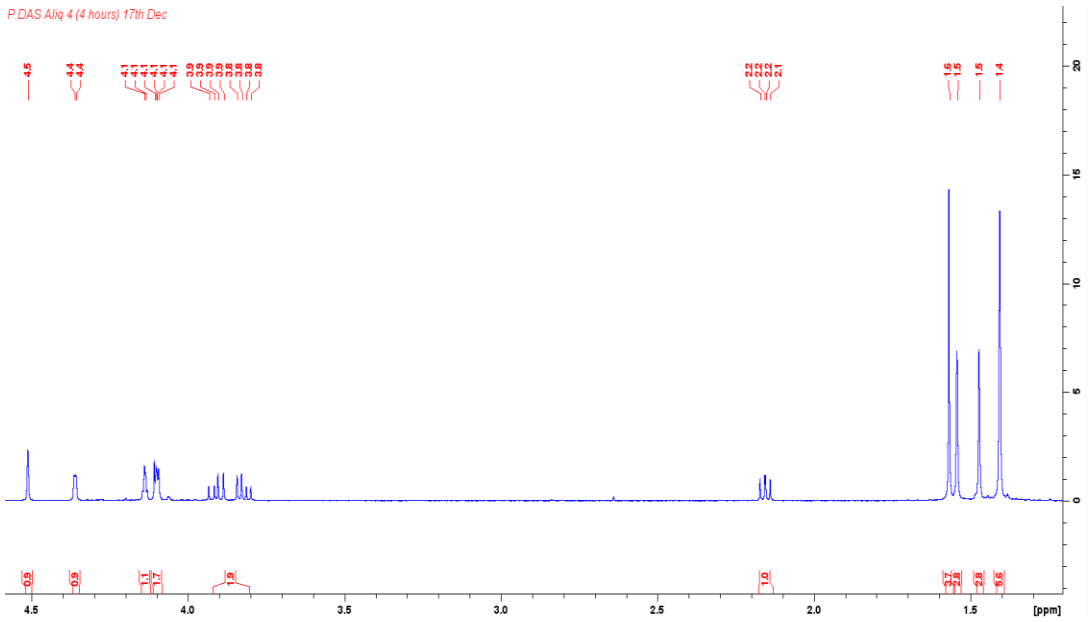

Fig. A 43 - DAS product ^{1}H-NMR for Batch 8-D recorded in $CDCl_3$ (400 MHz).

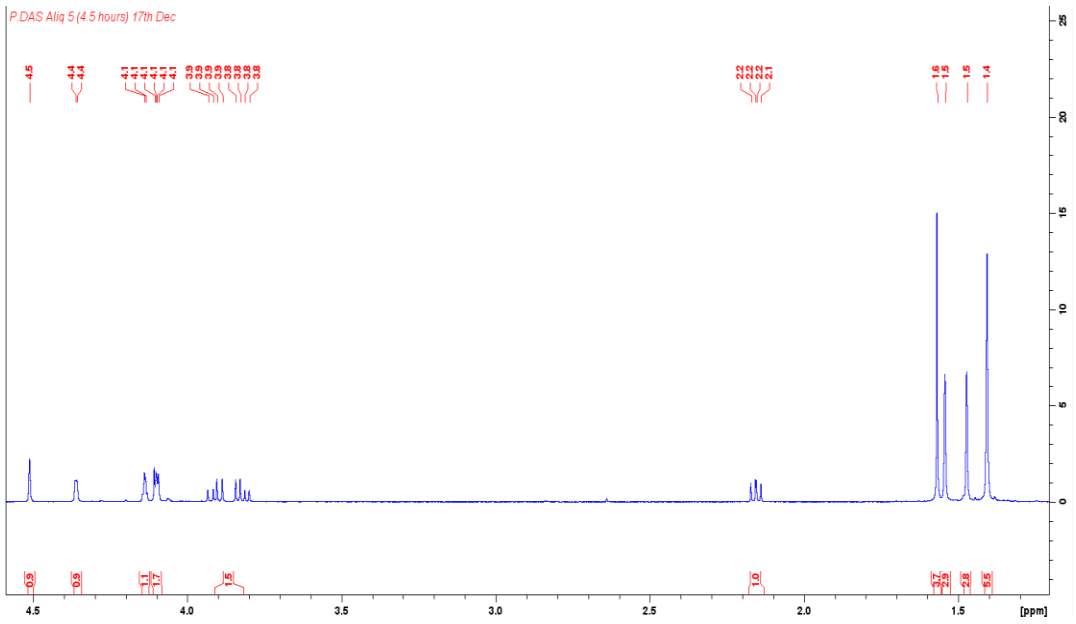

Fig. A 44 - DAS product ^{1}H-NMR for Batch 8-E recorded in $CDCl_3$ (400 MHz).

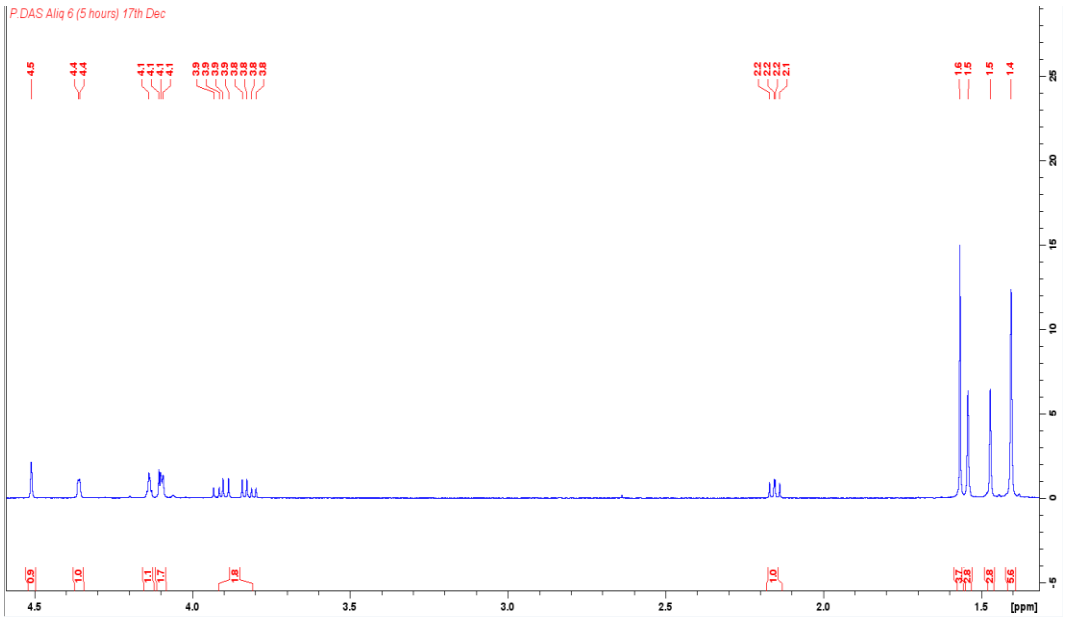

Fig. A 45 - DAS product ^{1}H-NMR for Batch 8-F recorded in $CDCl_3$ (400 MHz).

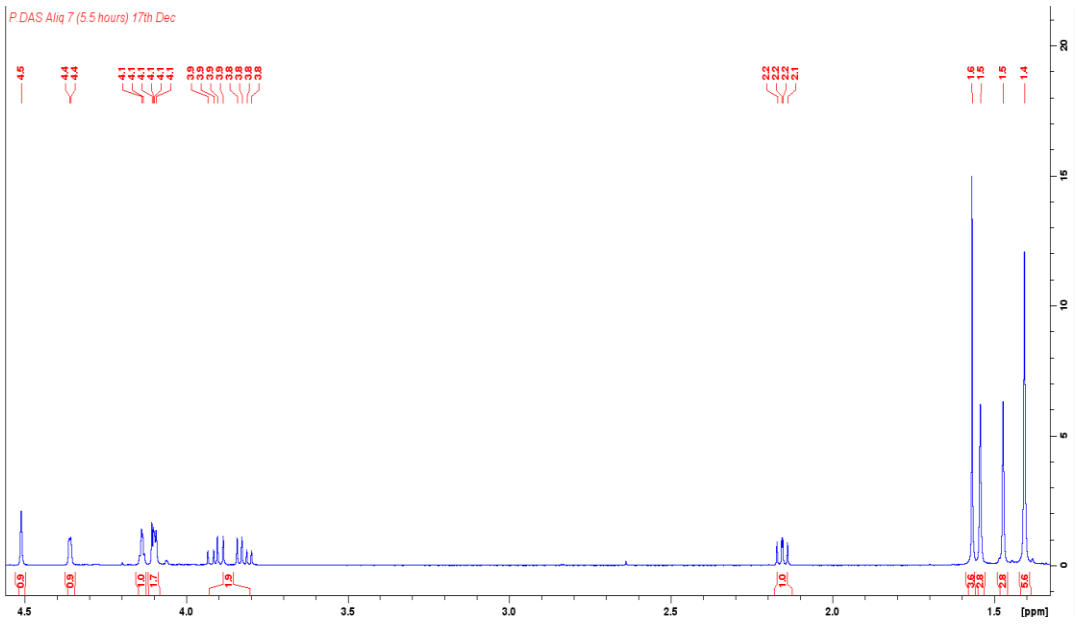

Fig. A 46 - DAS product ^{1}H-NMR for Batch 8-G recorded in $CDCl_3$ (400 MHz).

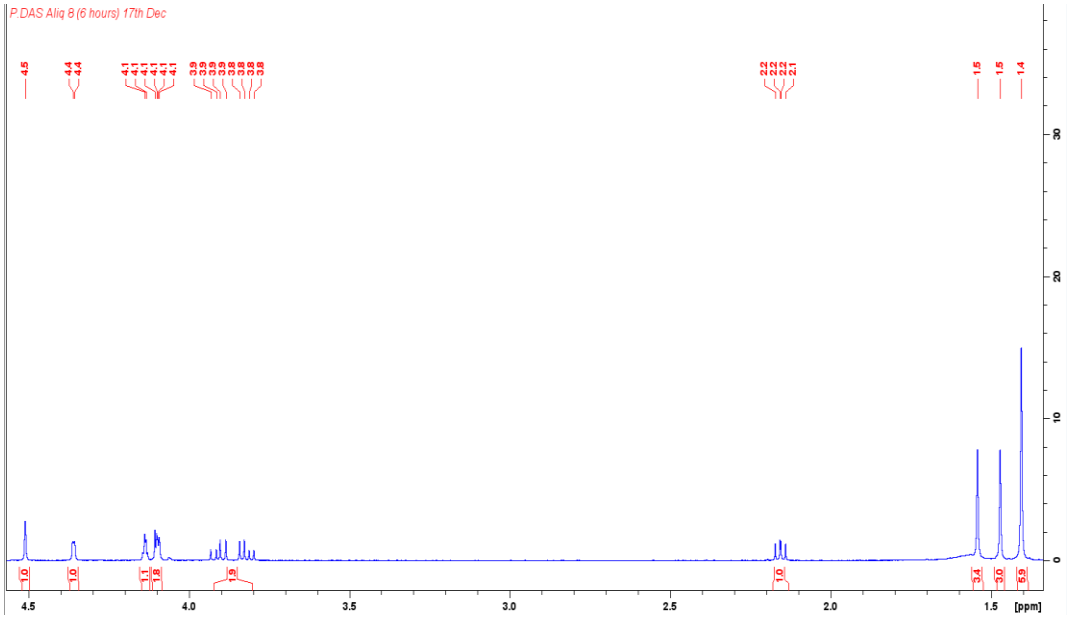

Fig. A 47 - DAS product ^{1}H-NMR for Batch 8-H recorded in $CDCl_3$ (400 MHz).

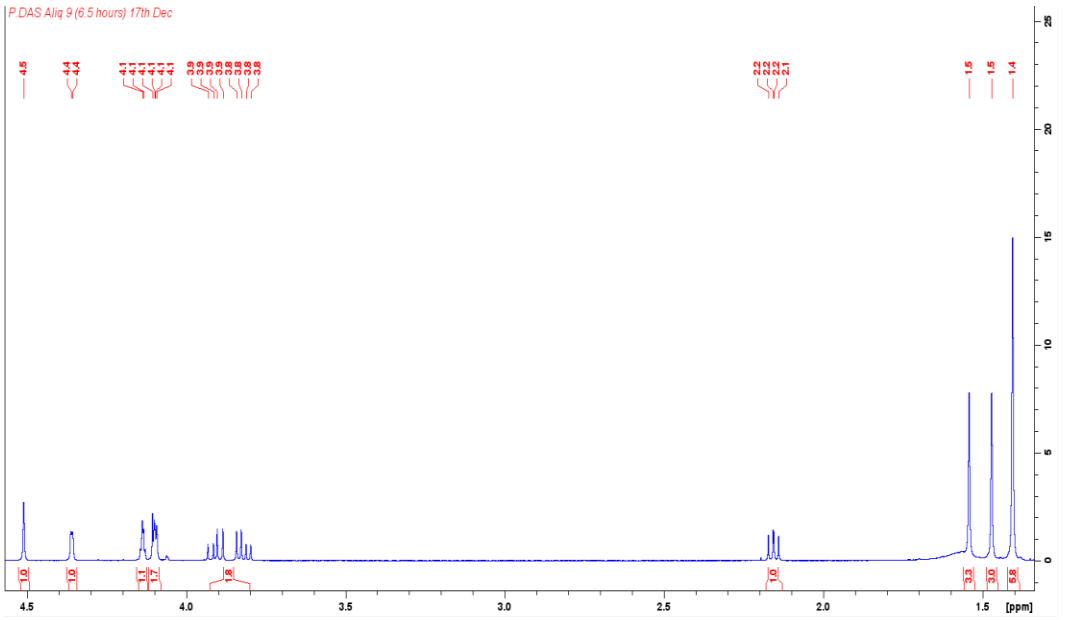

Fig. A 48 - DAS product ^{1}H-NMR for Batch 8-I recorded in $CDCl_3$ (400 MHz).

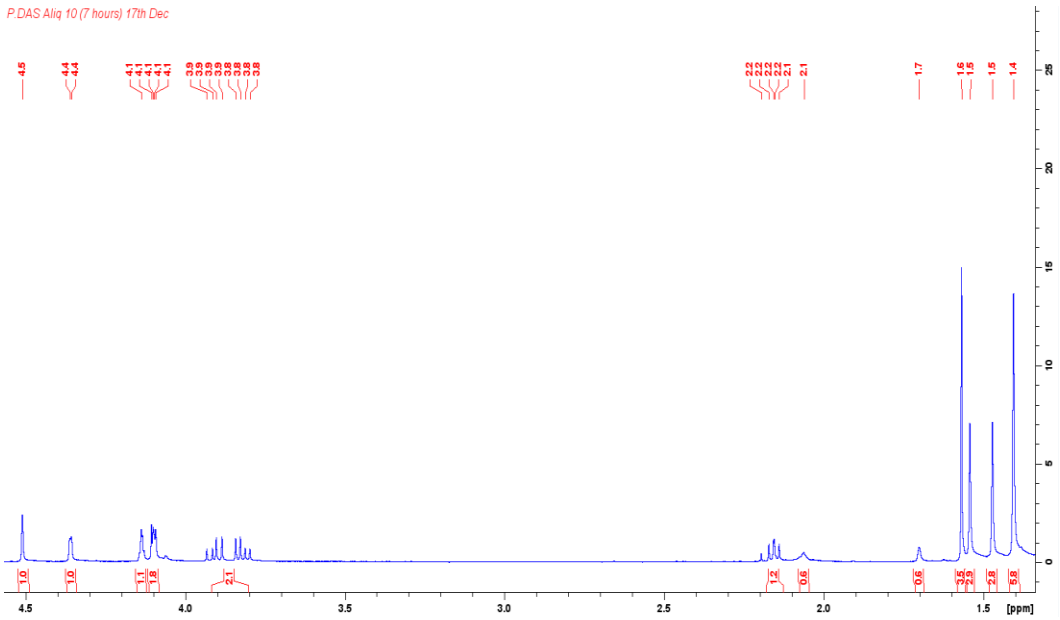

Fig. A 49 - DAS product ^{1}H-NMR for Batch 8-J recorded in $CDCl_3$ (400 MHz).

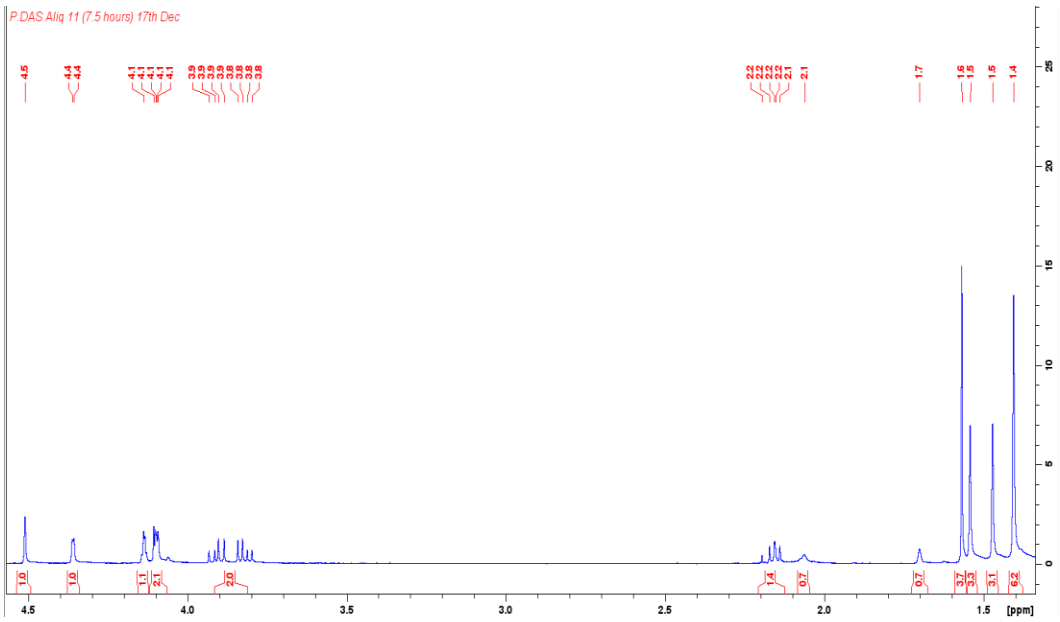

Fig. A 50 - DAS product ^{1}H-NMR for Batch 8-K recorded in $CDCl_3$ (400 MHz).

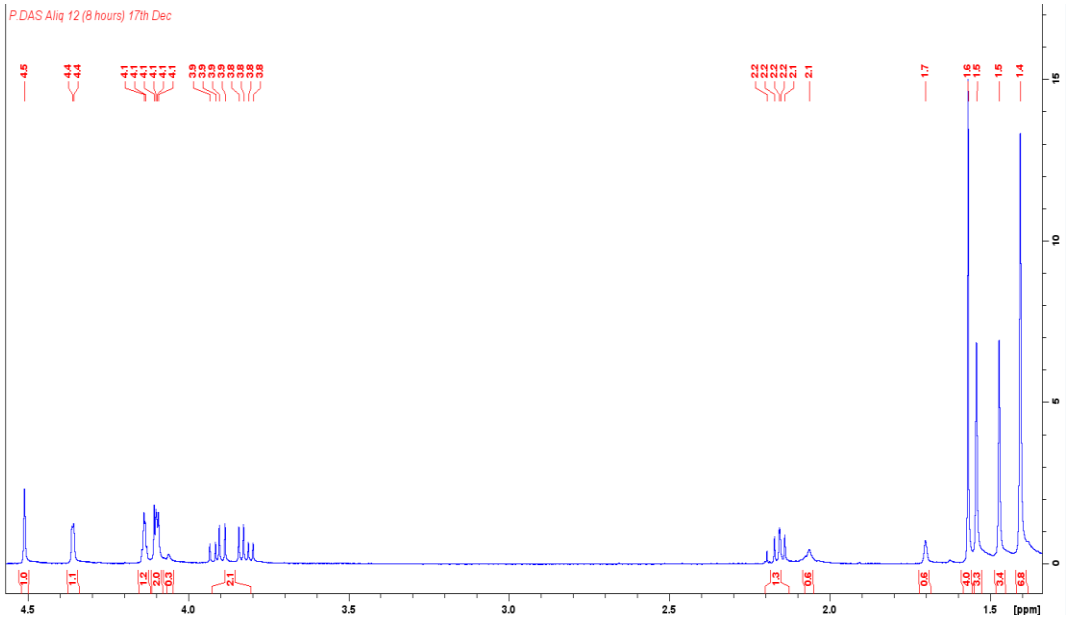

Fig. A 51 - DAS product ^{1}H-NMR for Batch 8-L recorded in $CDCl_3$ (400 MHz).

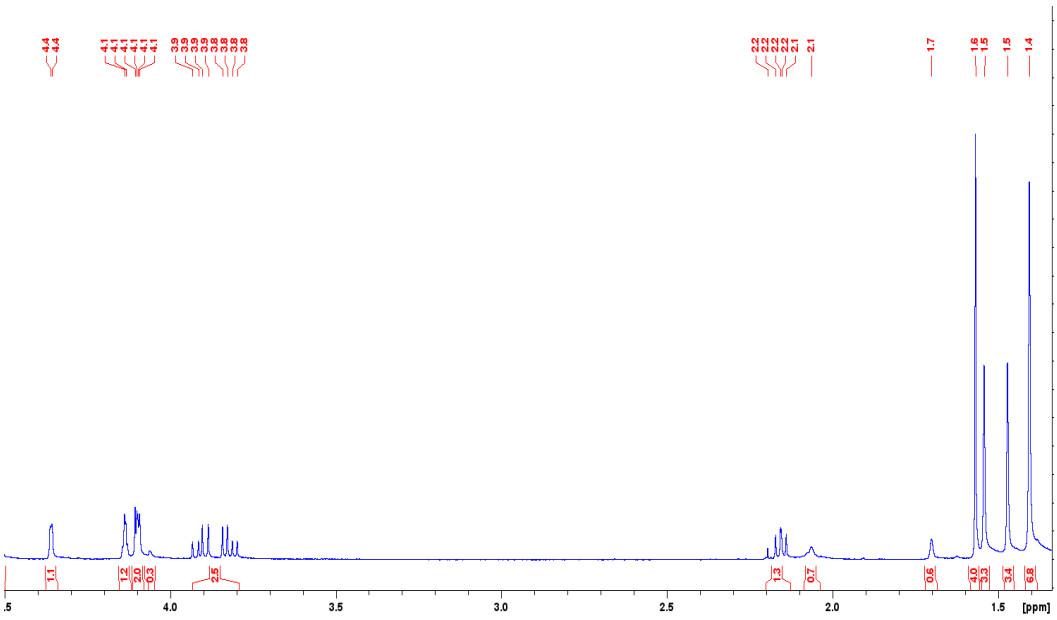

Fig. A 52 - DAS product ^{1}H-NMR for Batch 8-M recorded in $CDCl_3$ (400 MHz).

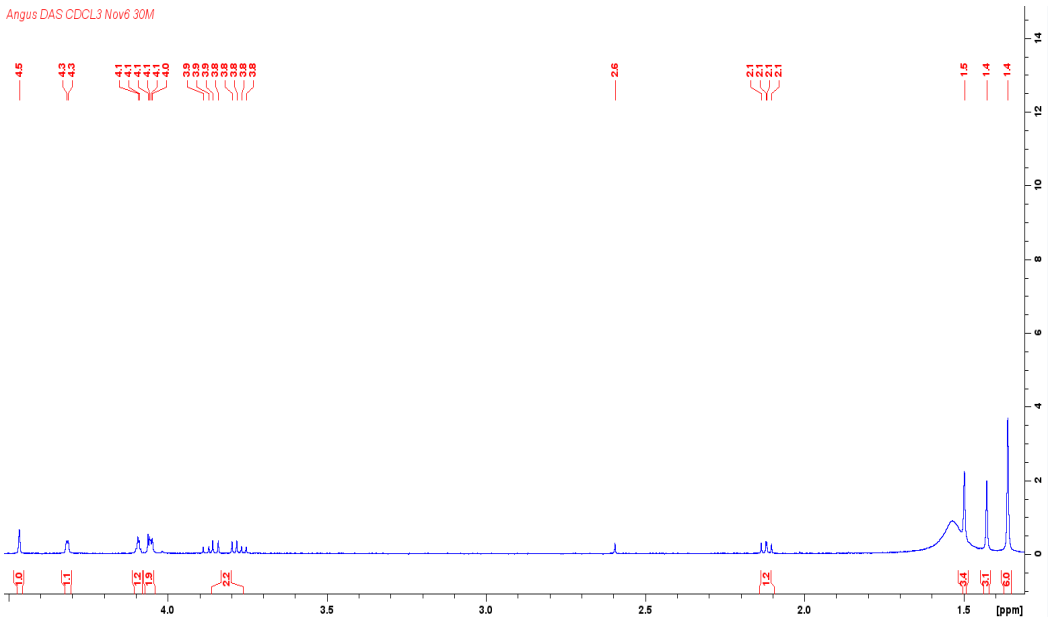

Fig. A 53 – Diacetone-L-sorbose ^{1}H-NMR for Flow 9 recorded in $CDCl_3$ (400 MHz).

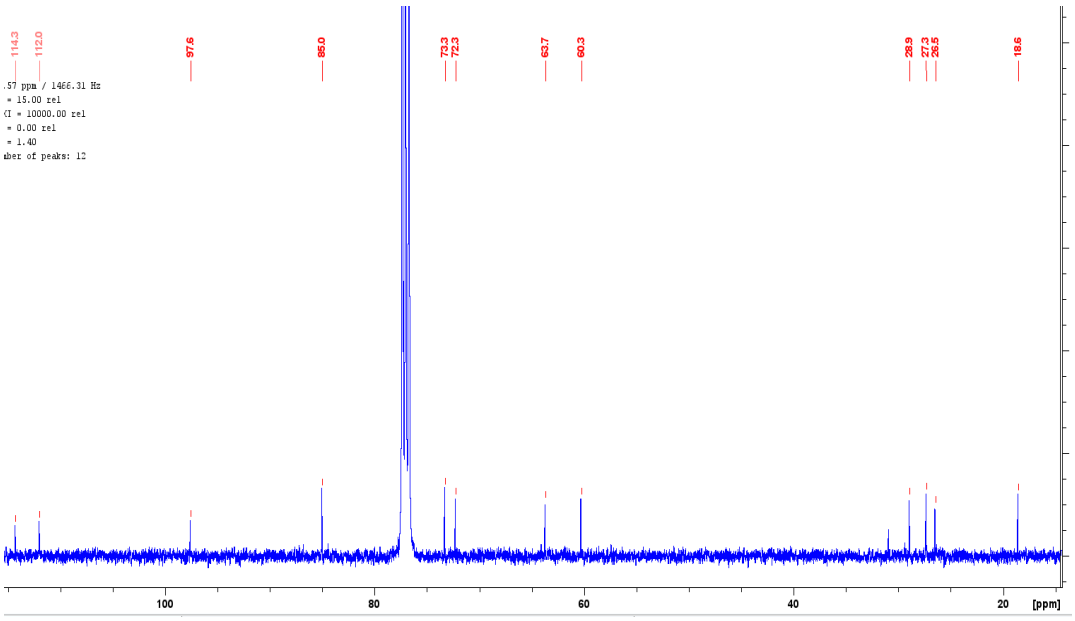

Fig. A 54 - Diacetone-L-sorbose ^{13}C-NMR for Flow 9 recorded in $CDCl_3$ (400 MHz).

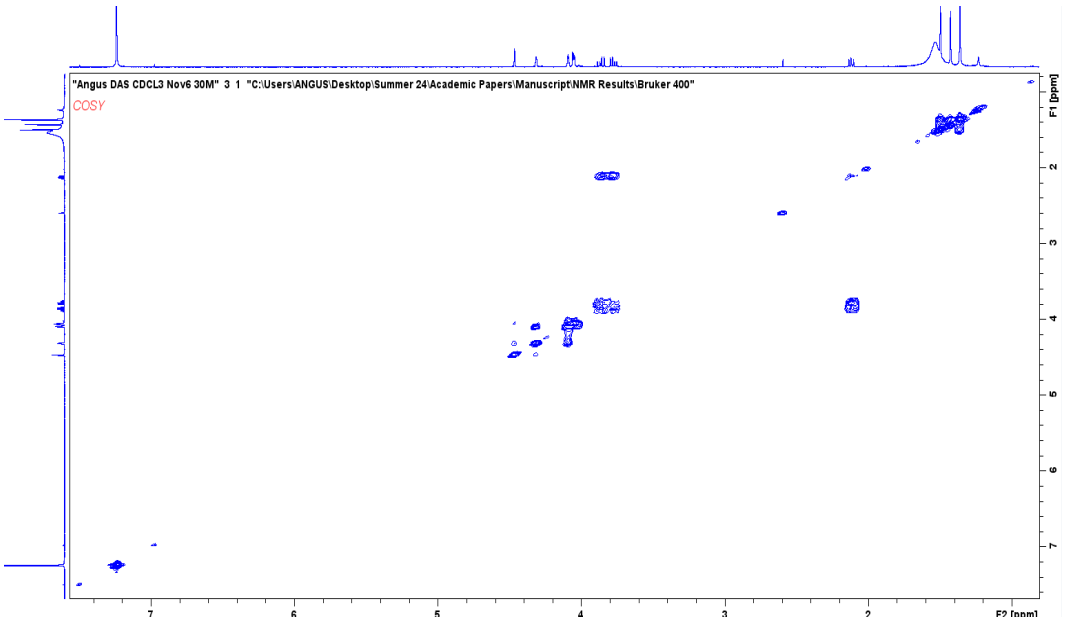

Fig. A 55 - Diacetone-L-sorbose COSY for Flow 9 recorded in $CDCl_3$ (400 MHz).

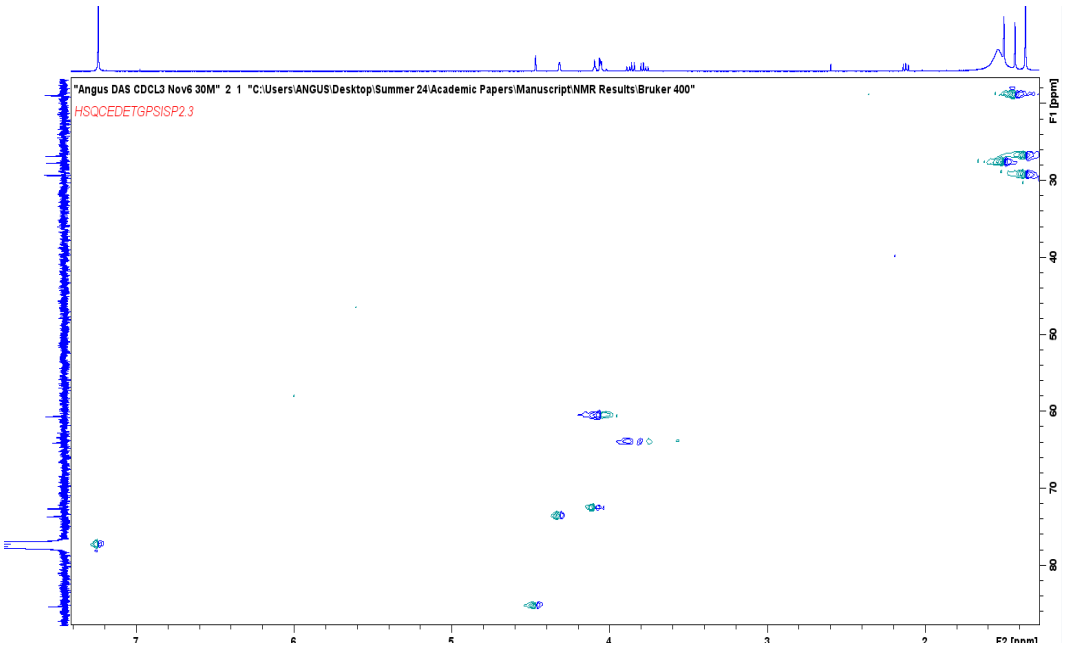

Fig. A 56 - Diacetone-L-sorbose HSQC for Flow 9 recorded in $CDCl_3$ (400 MHz).

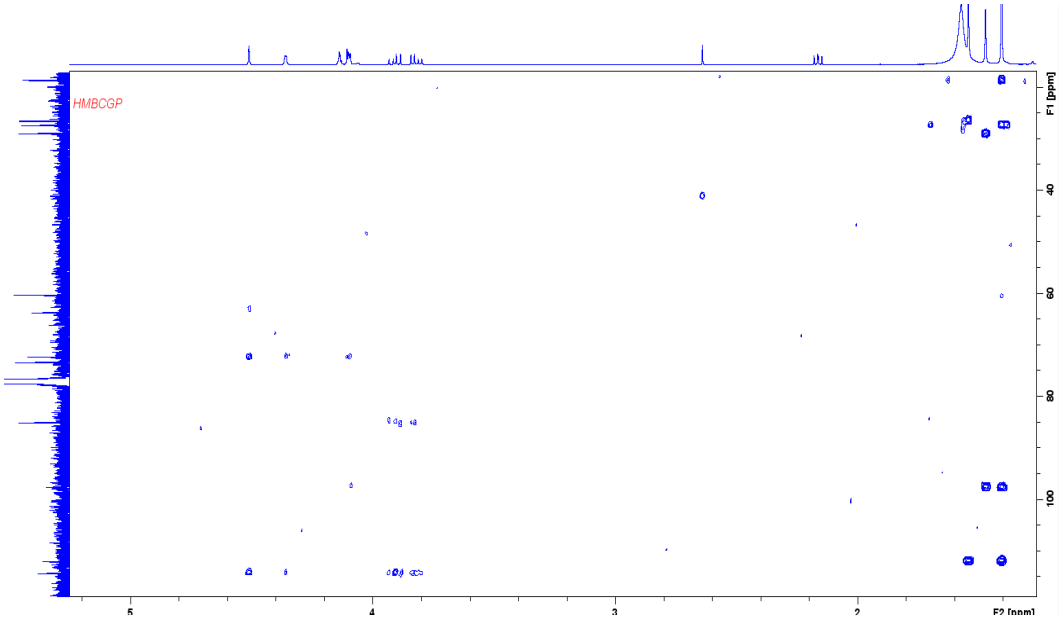

Fig. A 57 - Diacetone-L-sorbose HMBC for Flow 9 recorded in $CDCl_3$ (400 MHz).

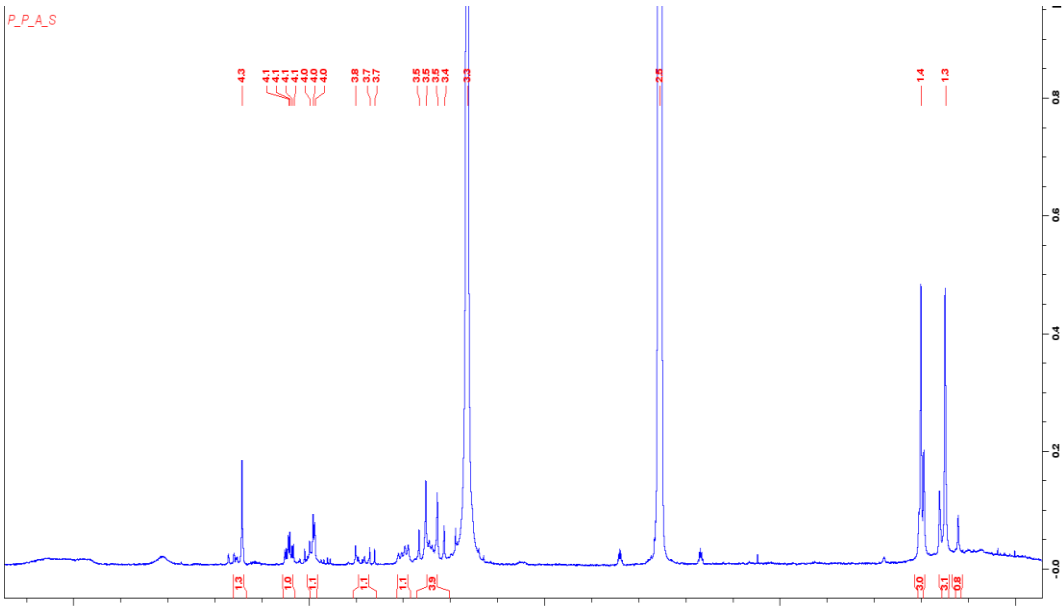

Fig. A 58 - DAS product ^{1}H-NMR for Batch 3 recorded in DMSO-d_6 (400 MHz).

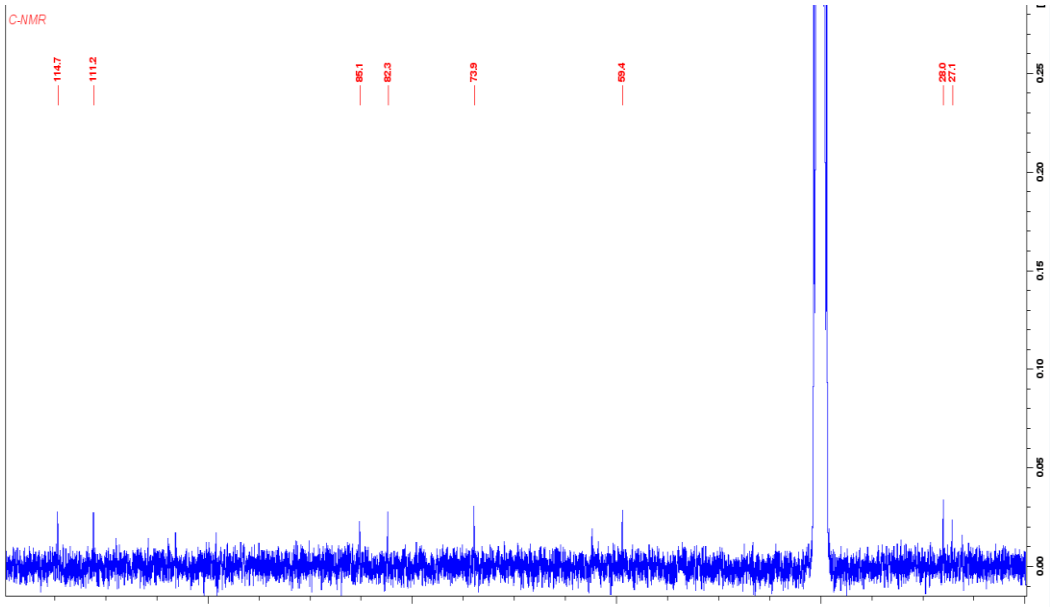

Fig. A 59 - DAS product ^{13}C-NMR for Batch 3 recorded in DMSO-d$_6$ (400 MHz).

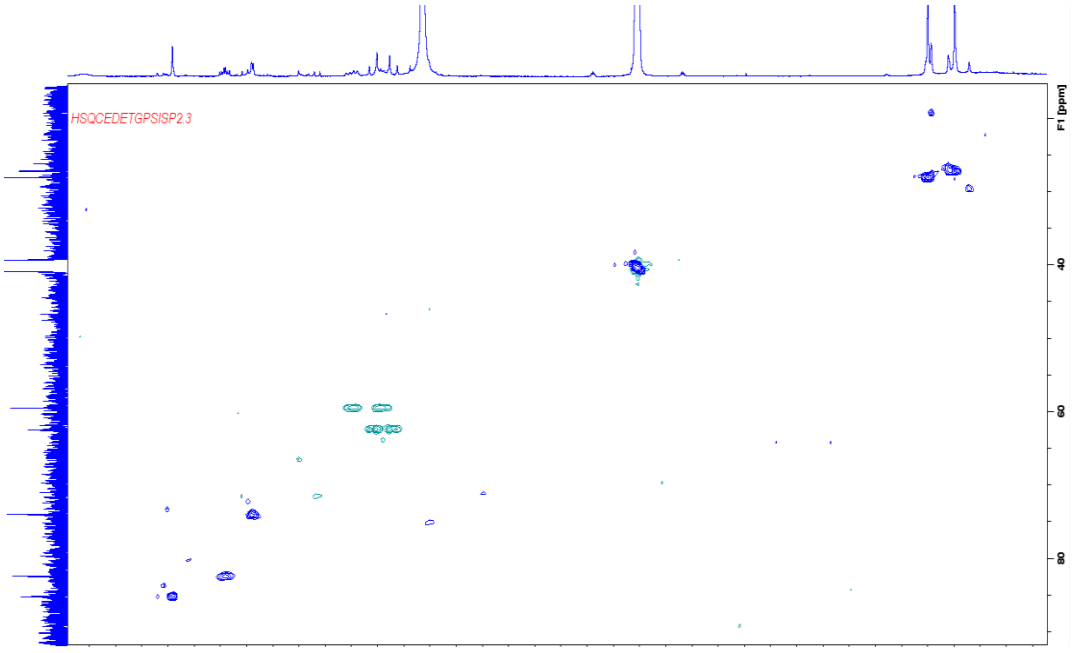

Fig. A 60 - DAS product HSQC for Batch 3 recorded in DMSO-d$_6$ (400 MHz).

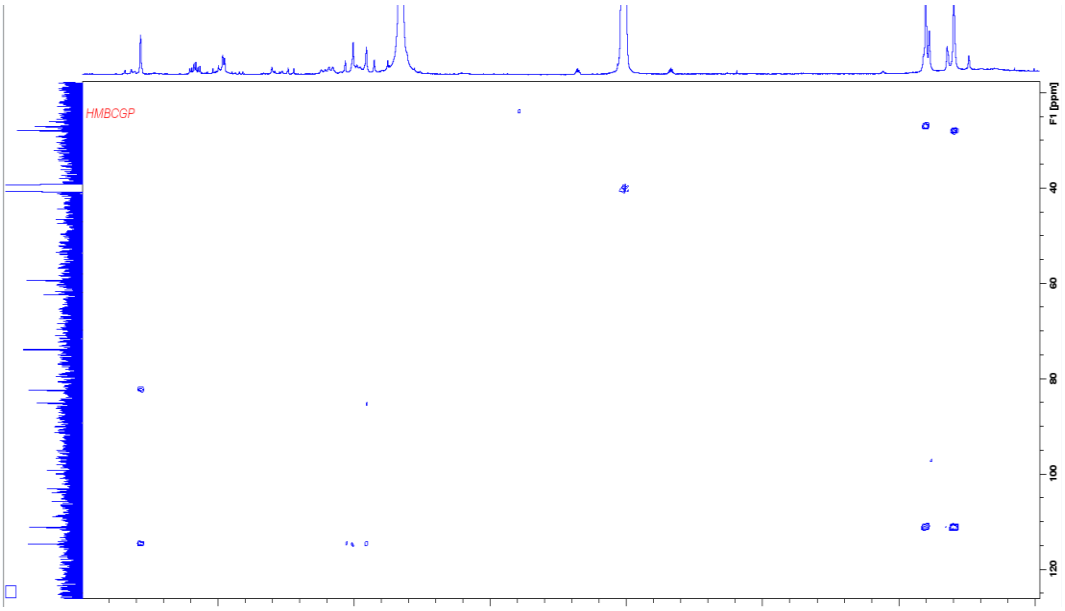

Fig. A 61 - DAS product HMBC for Batch 3 recorded in DMSO-d_6 (400 MHz).

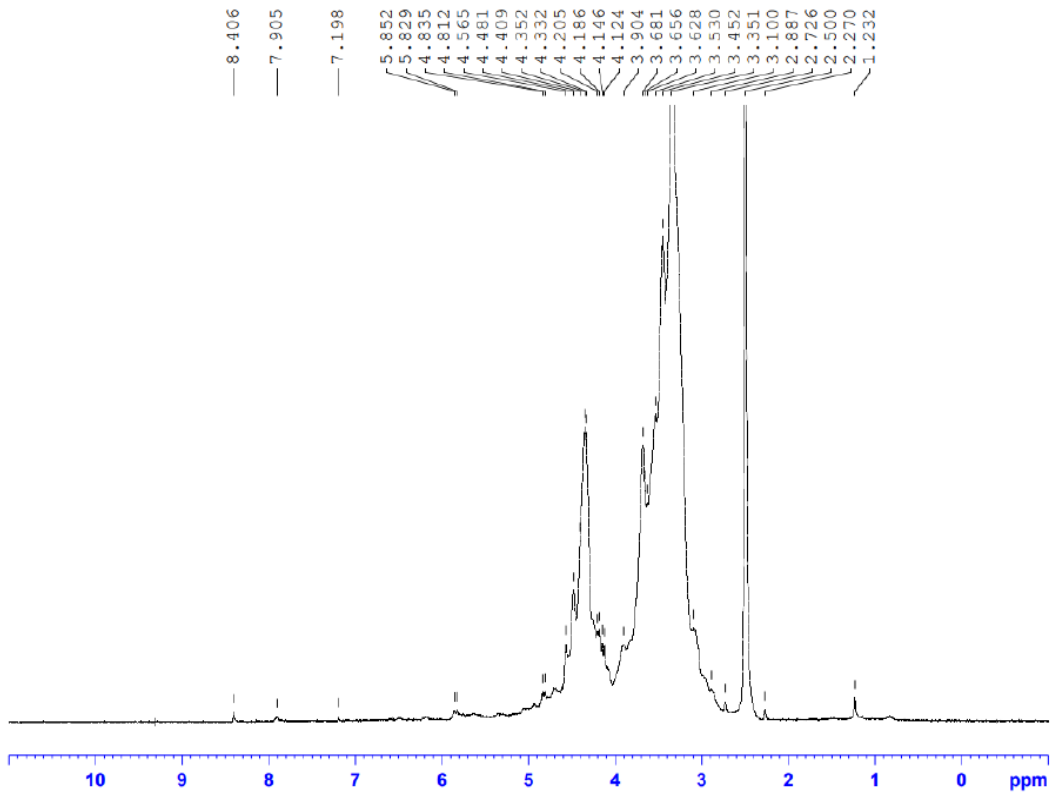

Fig. A 62 - Sorbitol ^{1}H-NMR for Flow 10 recorded in DMSO-d_6 (300 MHz).

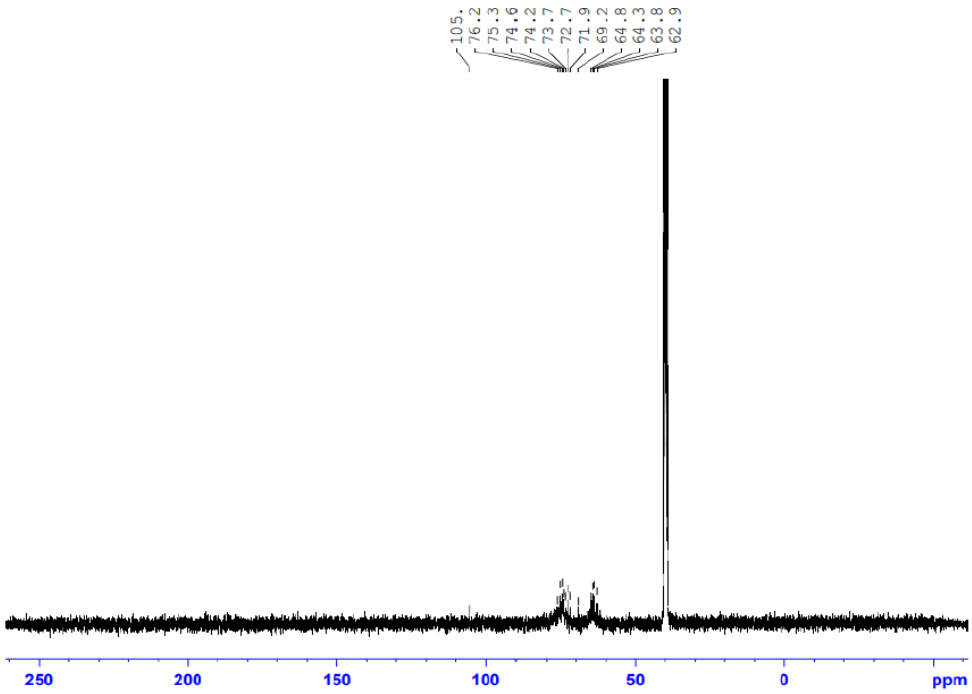

Fig. A 63 - Sorbitol ^{13}C-NMR for Flow 10 recorded in DMSO-d$_6$ (300 MHz).

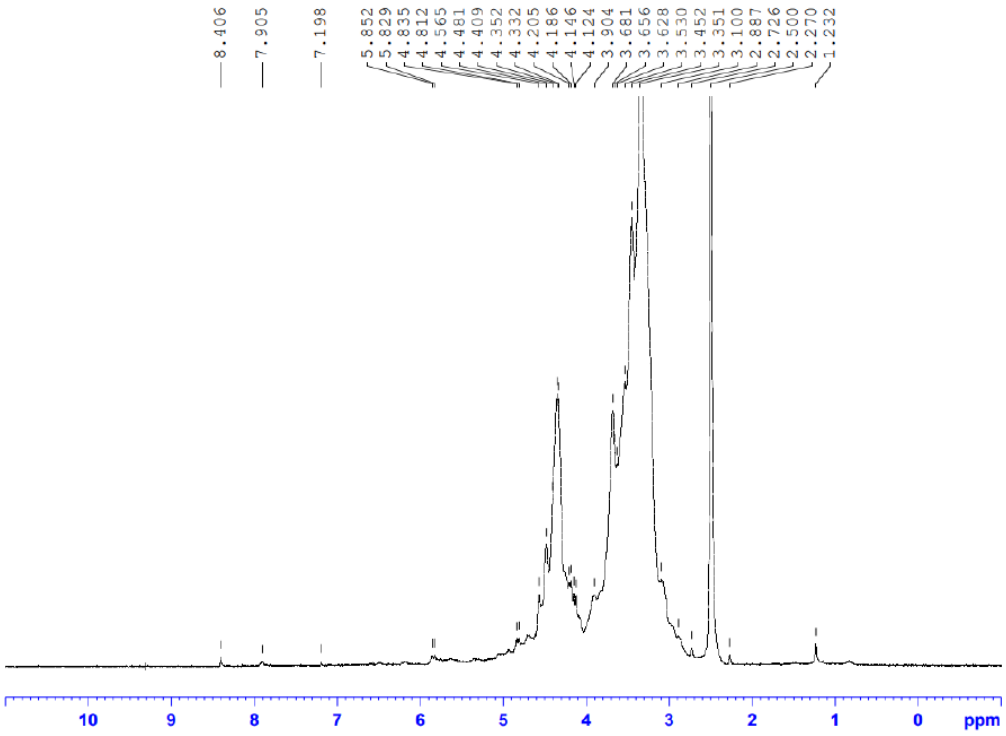

Fig. A 64 - Sorbitol ^{1}H-NMR for Flow 10 recorded in DMSO-d$_6$ (300 MHz).

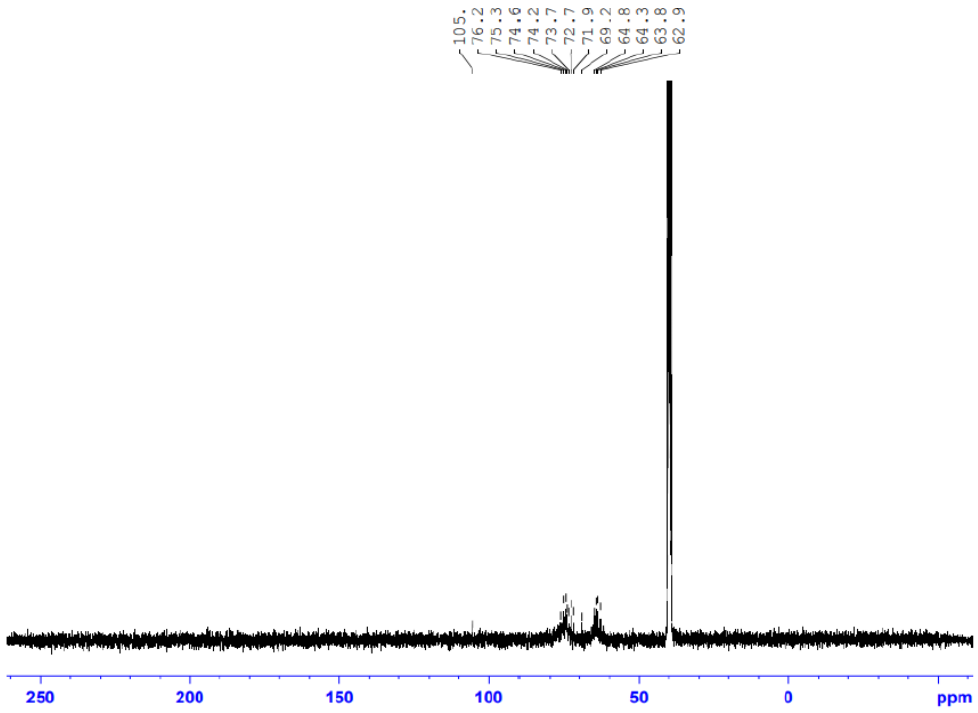

Fig. A 65 - Sorbitol ^{13}C-NMR for Flow 10 recorded in DMSO-d$_6$ (300 MHz).

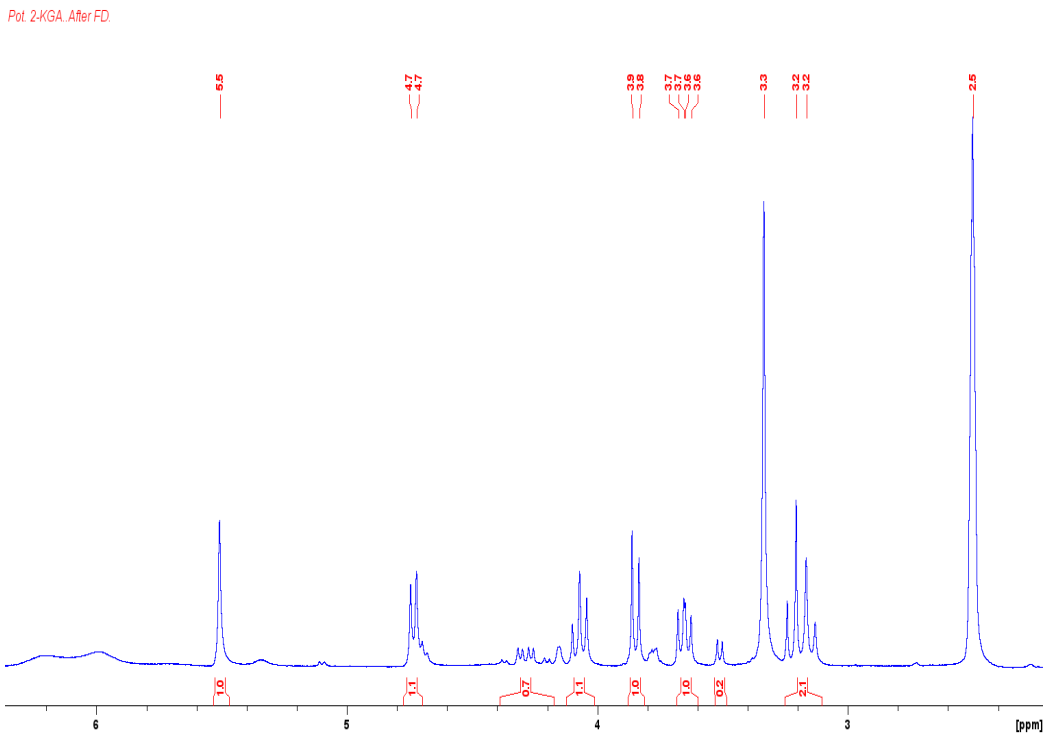

Fig. A 66 – 2-keto-L-gulonic acid ^{1}H-NMR for Batch 1 recorded in DMSO-d$_6$ (300 MHz).

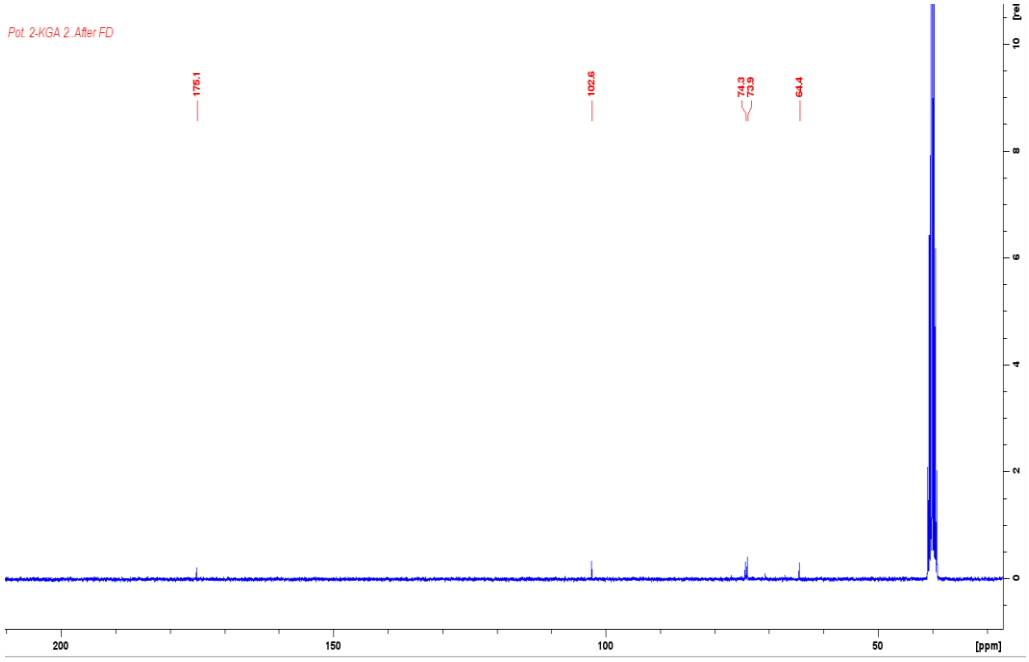

Fig. A 67 - 2-keto-L-gulonic acid ^{13}C-NMR for Batch 1 recorded in DMSO-d$_6$ (300 MHz).

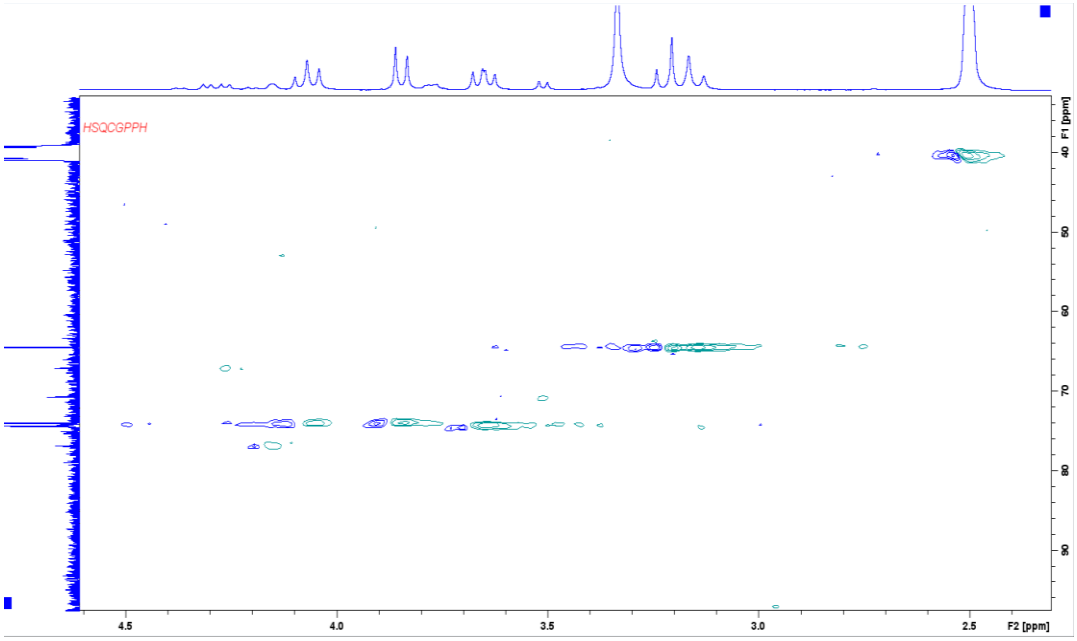

Fig. A 68 - 2-keto-L-gulonic acid HSQC for Batch 1 recorded in DMSO-d$_6$ (300 MHz).

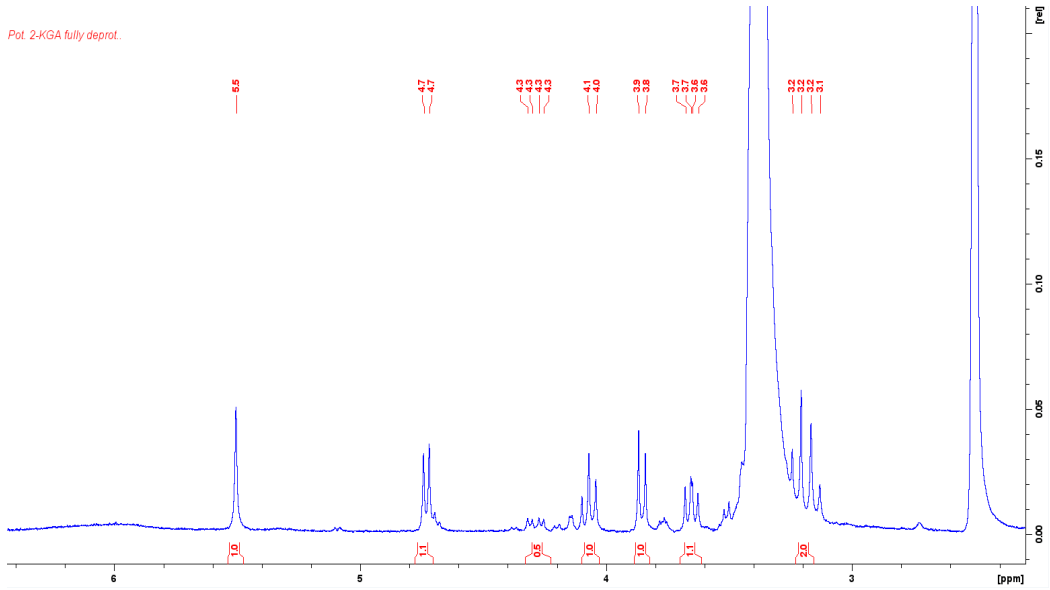

Fig. A 69 – 2-keto-L-gulonic acid ^{1}H-NMR for Batch 2 recorded in DMSO-d$_6$ (300 MHz).

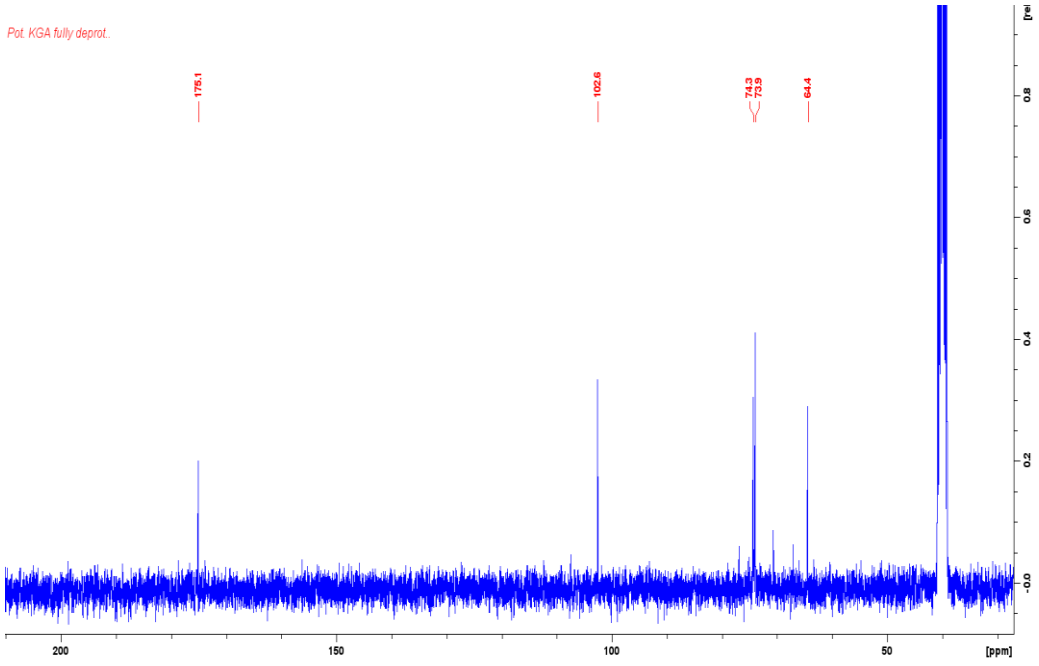

Fig. A 70 - 2-keto-L-gulonic acid ^{13}C-NMR for Batch 2 recorded in DMSO-d$_6$ (300 MHz).

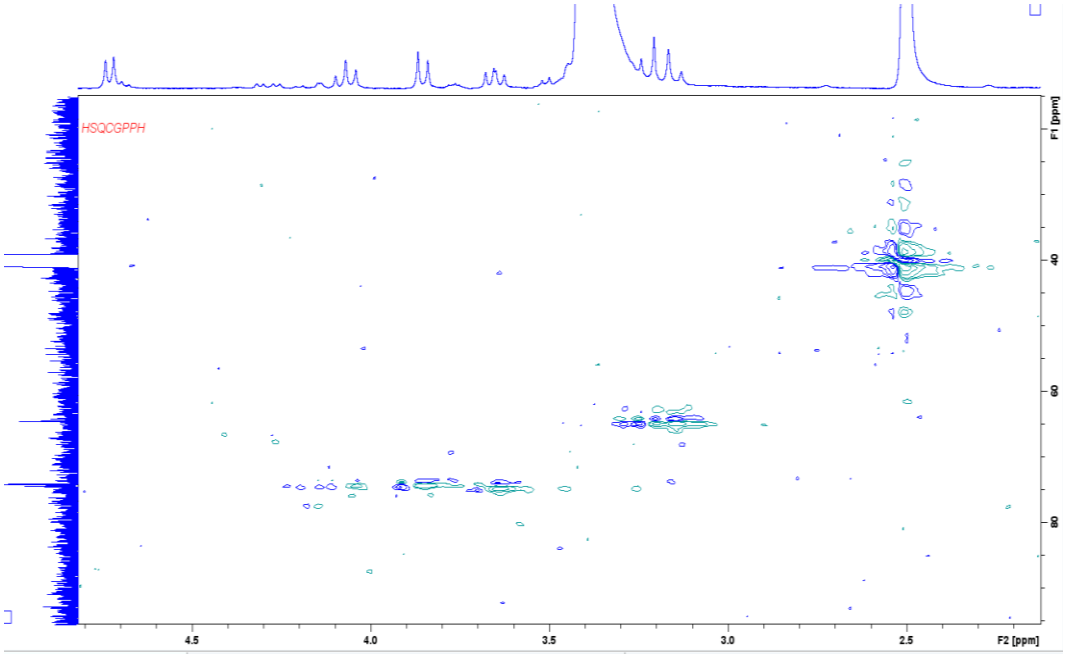

Fig. A 71 - 2-keto-L-gulonic acid HSQC for Batch 2 recorded in DMSO-d$_6$ (300 MHz).

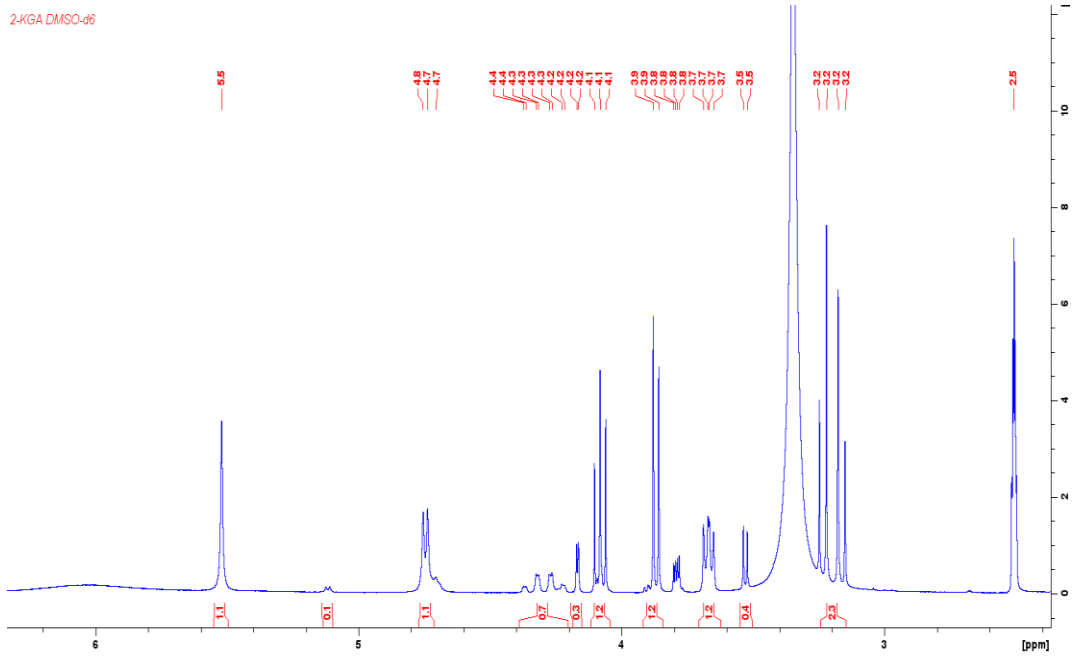

Fig. A 72 – 2-keto-L-gulonic acid ^{1}H-NMR for Flow 3 recorded in DMSO-d$_6$ (400 MHz).

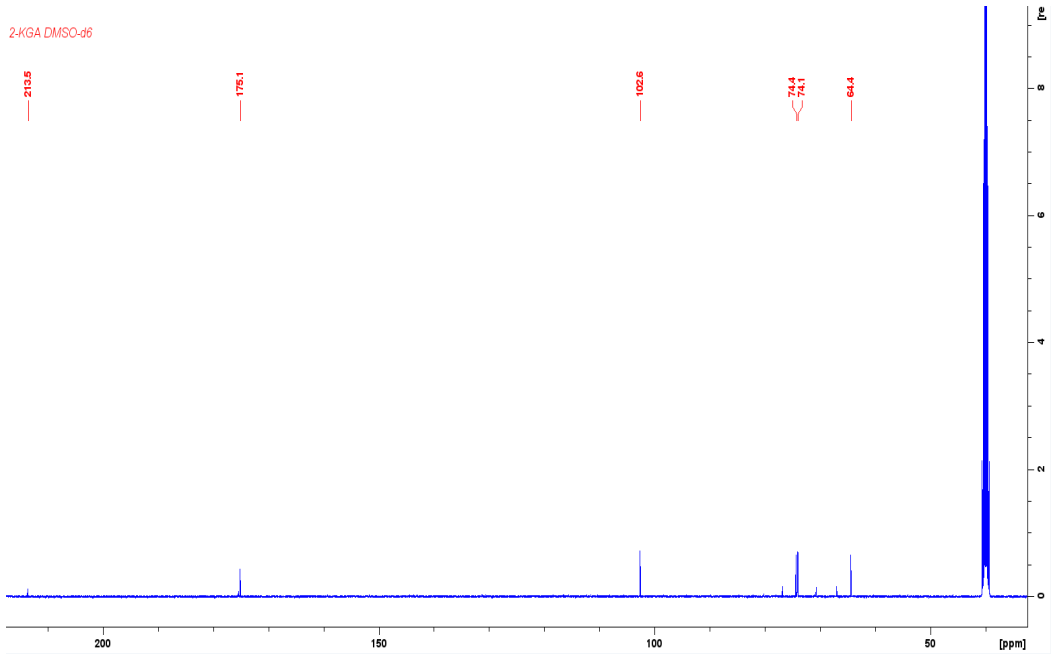

Fig. A 73 - 2-keto-L-gulonic acid ^{13}C-NMR for Flow 3 recorded in DMSO-d$_6$ (400 MHz).

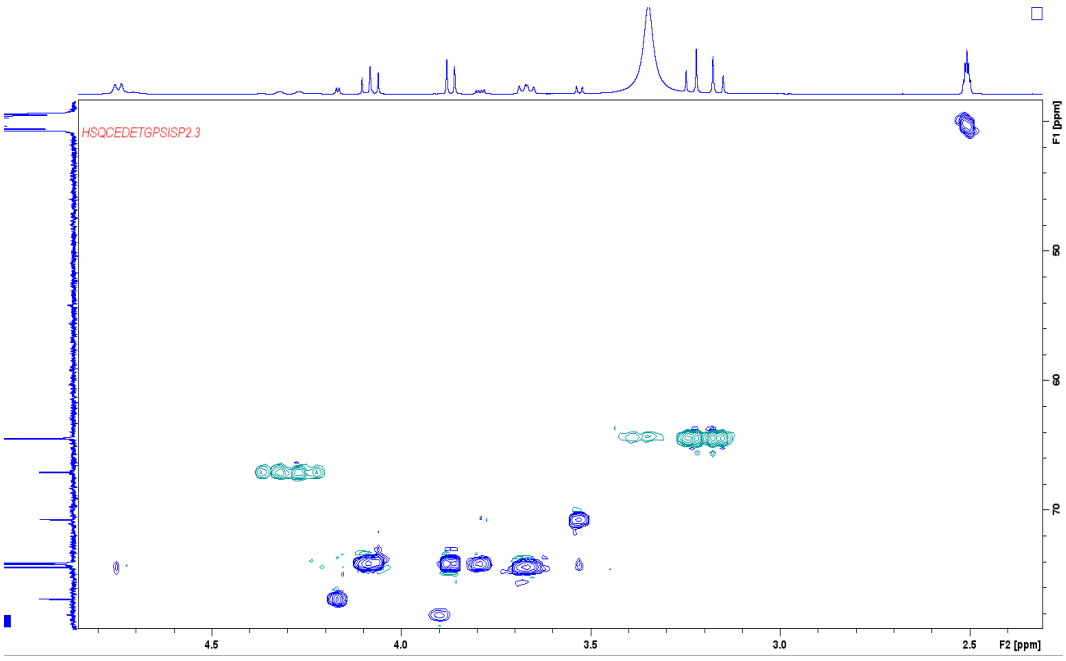

Fig. A 74 - 2-keto-L-gulonic acid HSQC for Flow 3 recorded in DMSO-d$_6$ (400 MHz).

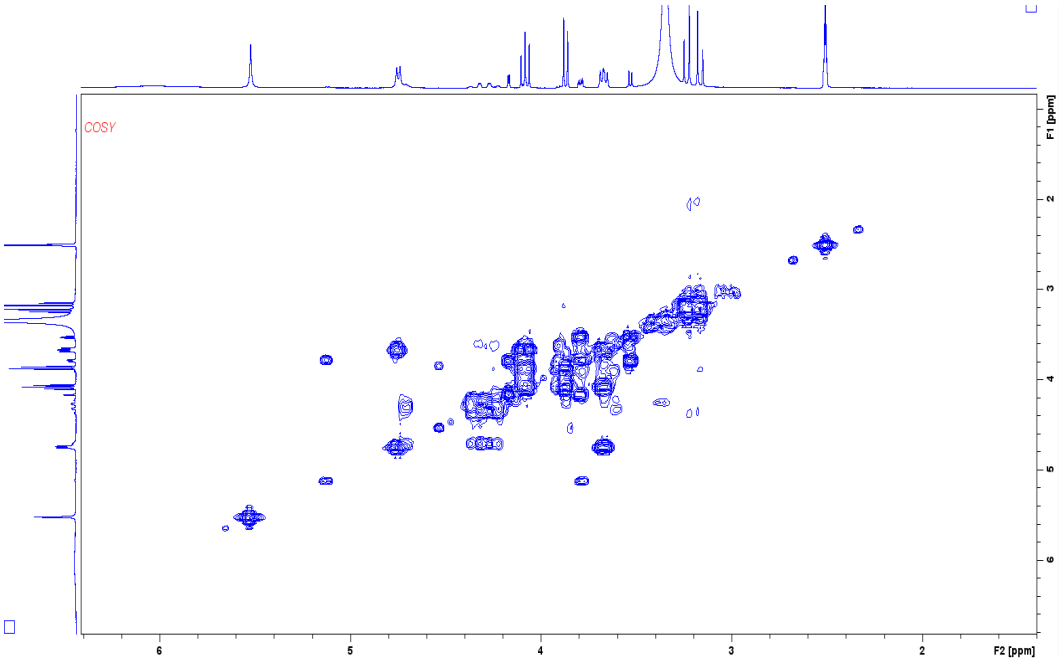

Fig. A 75 - 2-keto-L-gulonic acid COSY for Flow 3 recorded in DMSO-d_6 (400 MHz).

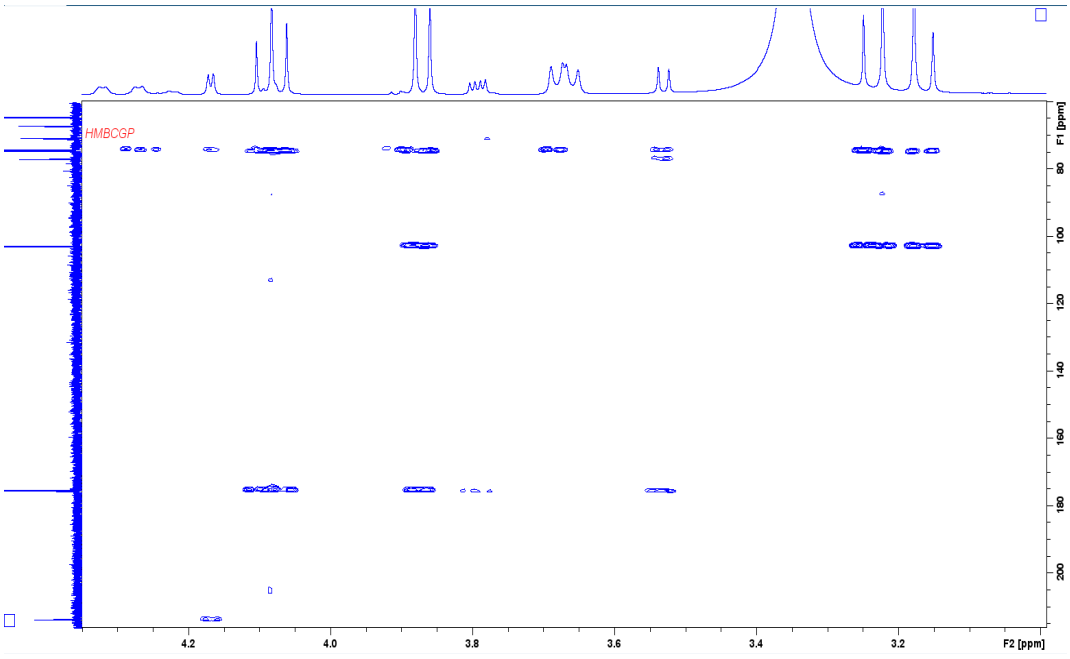

Fig. A 76 - 2-keto-L-gulonic acid HMBC for Flow 3 recorded in DMSO-d_6 (400 MHz).

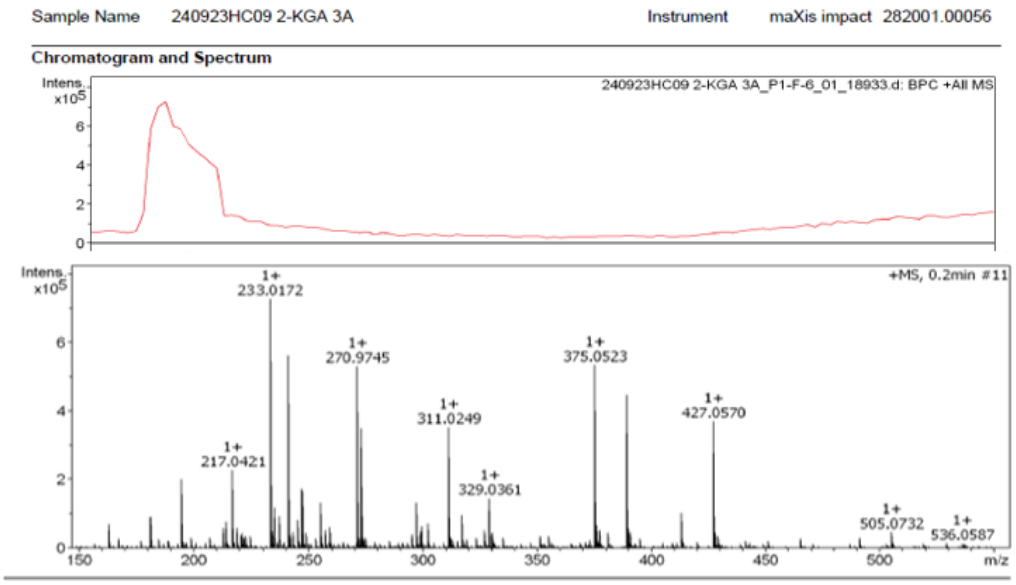

Fig. A 77 - 2-keto-L-gulonic acid Mass spectrum for Flow 3

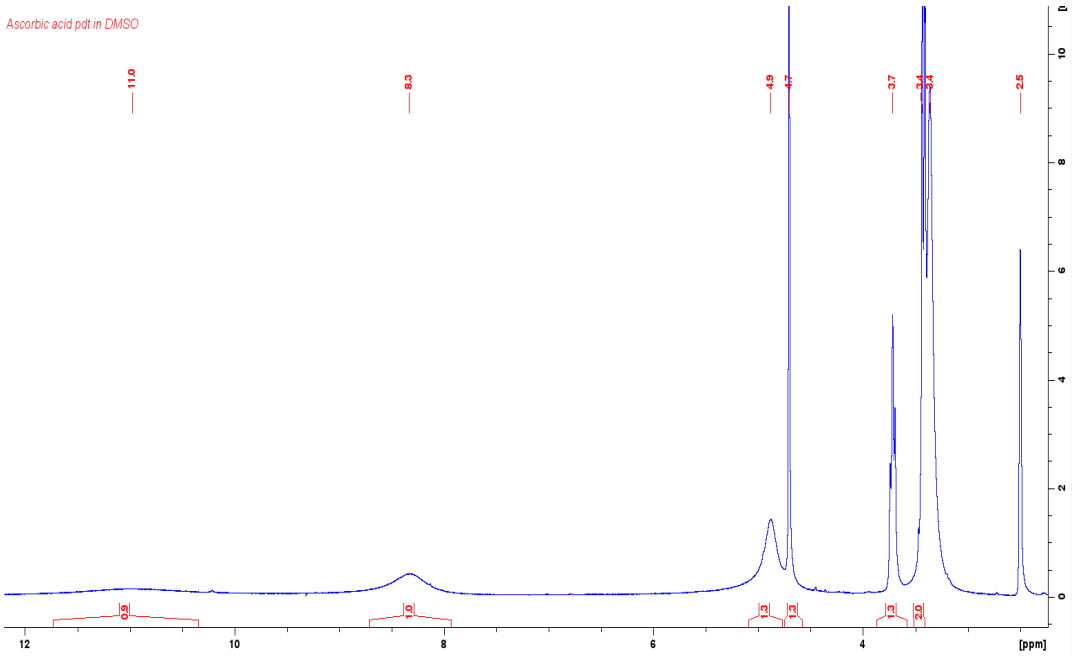

Fig. A 78 – Ascorbic acid ^{1}H-NMR for Batch 1 recorded in DMSO-d_6 (300 MHz).

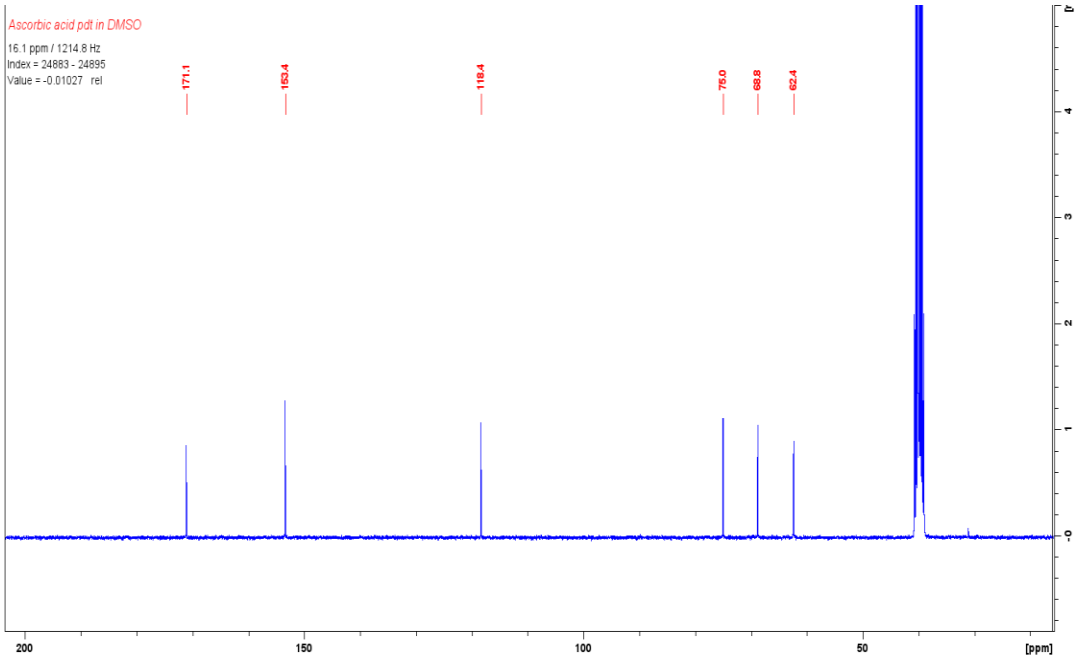

Fig. A 79 – Ascorbic acid ^{13}C-NMR for Batch 1 recorded in DMSO-d_6 (300 MHz).

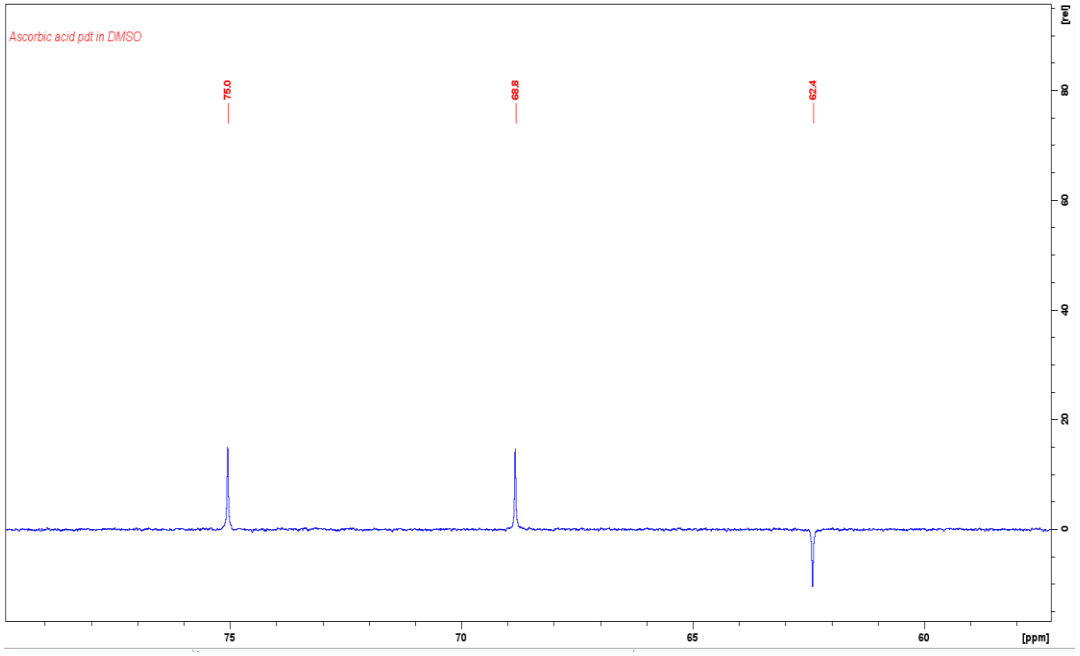

Fig. A 80 - Ascorbic acid DEPT-135 for Batch 1 recorded in DMSO-d_6 (300 MHz).

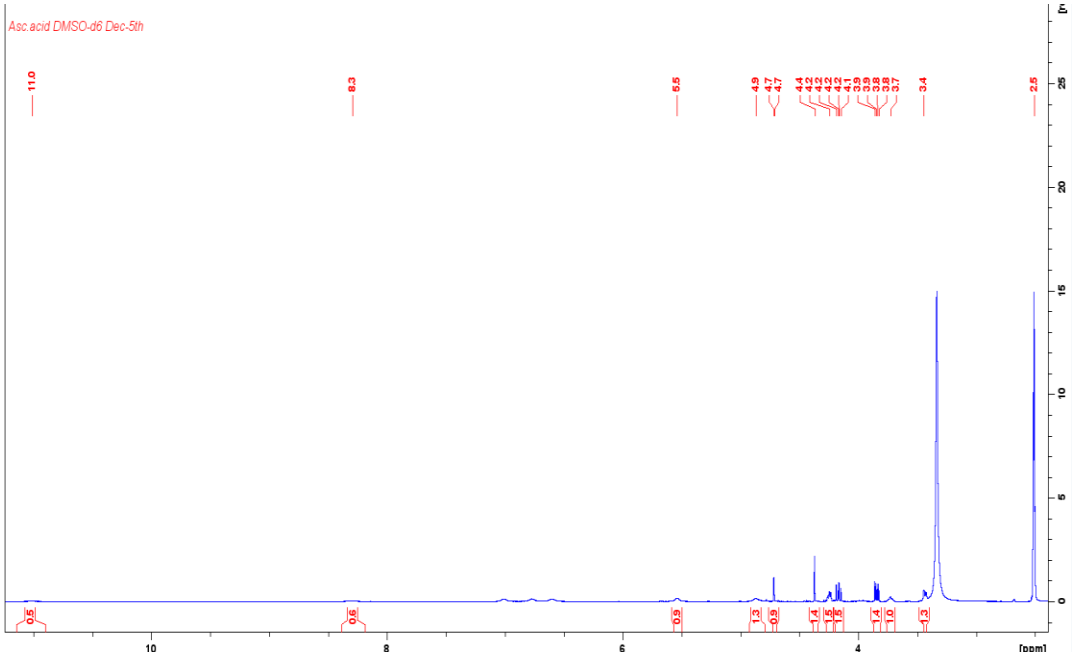

Fig. A 81 – Ascorbic acid crude product ^{1}H-NMR for Flow 2 recorded in DMSO-d_6 (400 MHz).

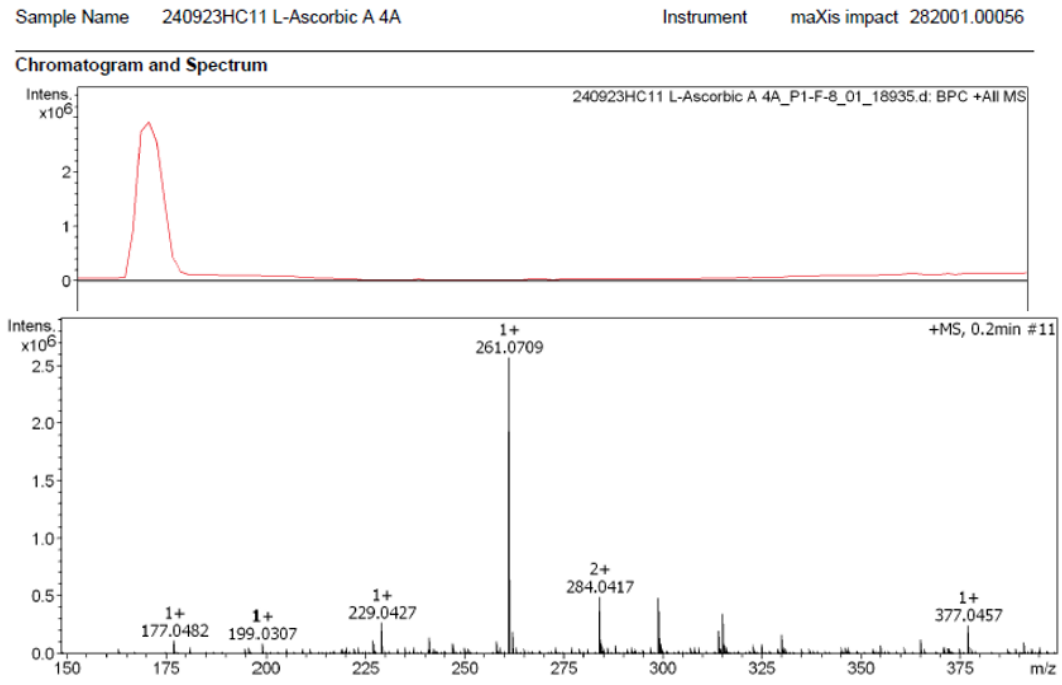

Fig. A 82 – Ascorbic acid Mass Spectrum for Flow 2

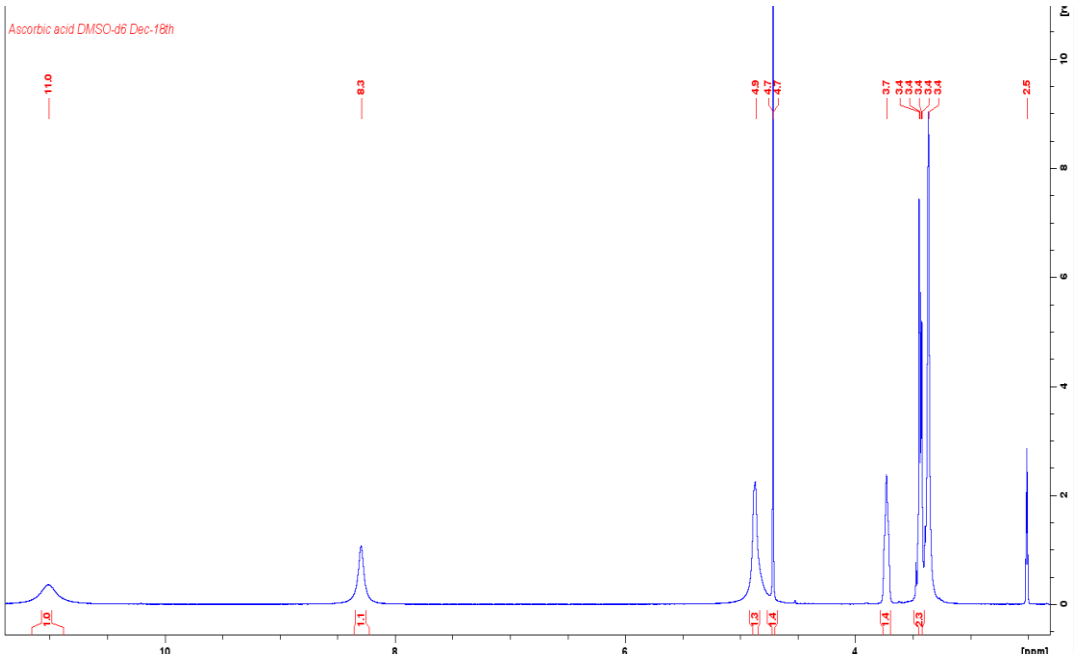

Fig. A 83 – Ascorbic acid ^{1}H-NMR for Flow 2 recorded in DMSO-d_6 (400 MHz).

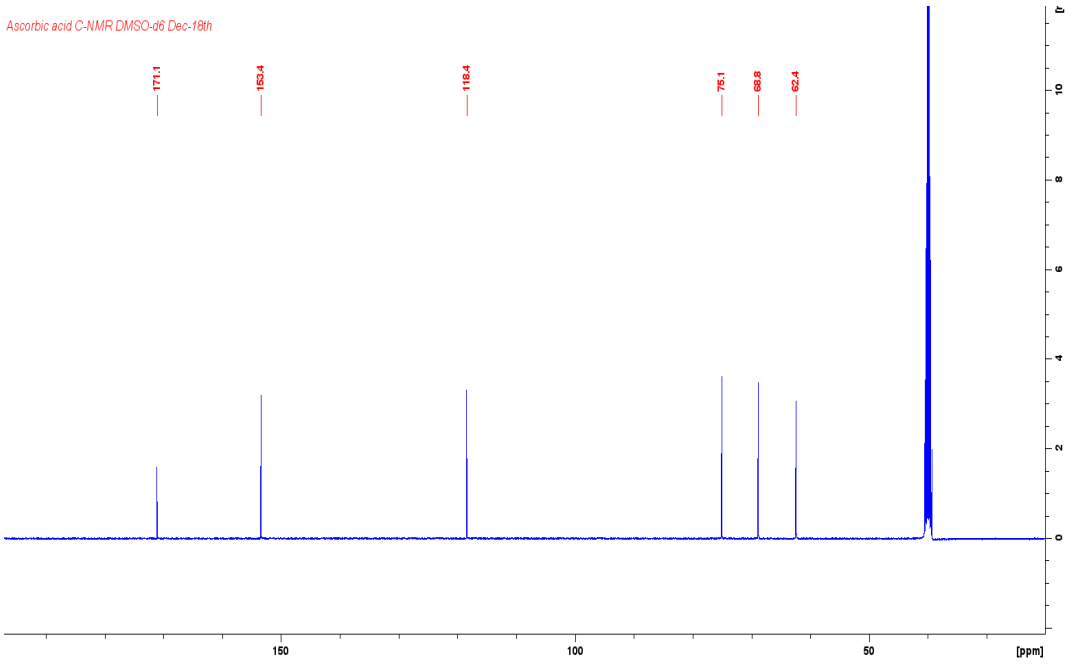

Fig. A 84 – Ascorbic acid ^{13}C-NMR for Flow 2 recorded in DMSO-d_6 (400 MHz).

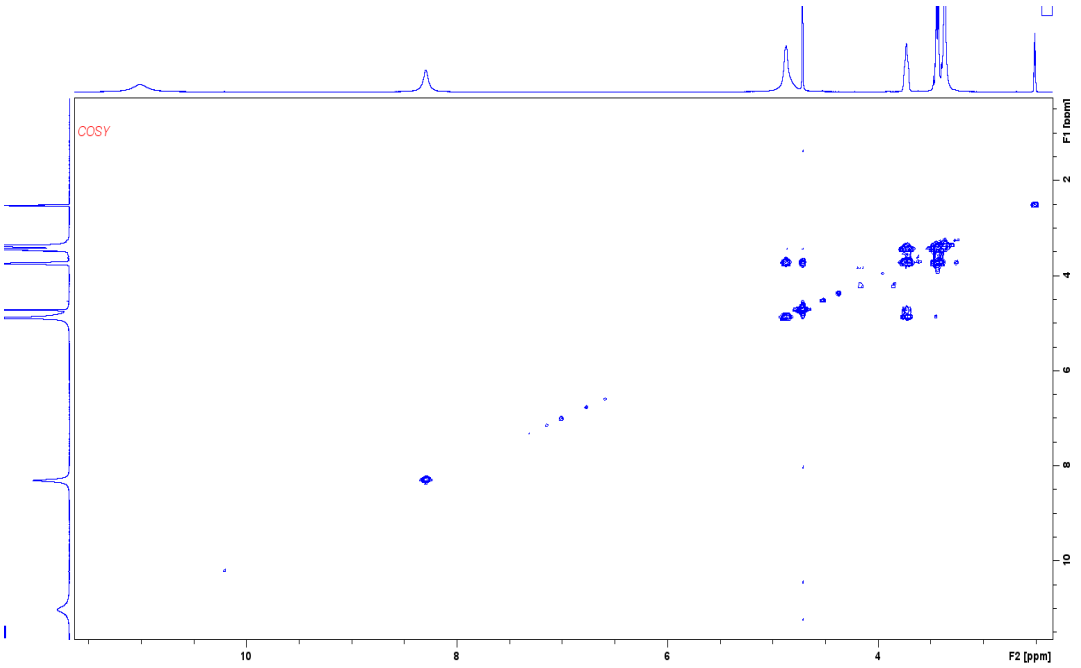

Fig. A 85 - Ascorbic acid COSY for Flow 2 recorded in DMSO-d_6 (400 MHz).

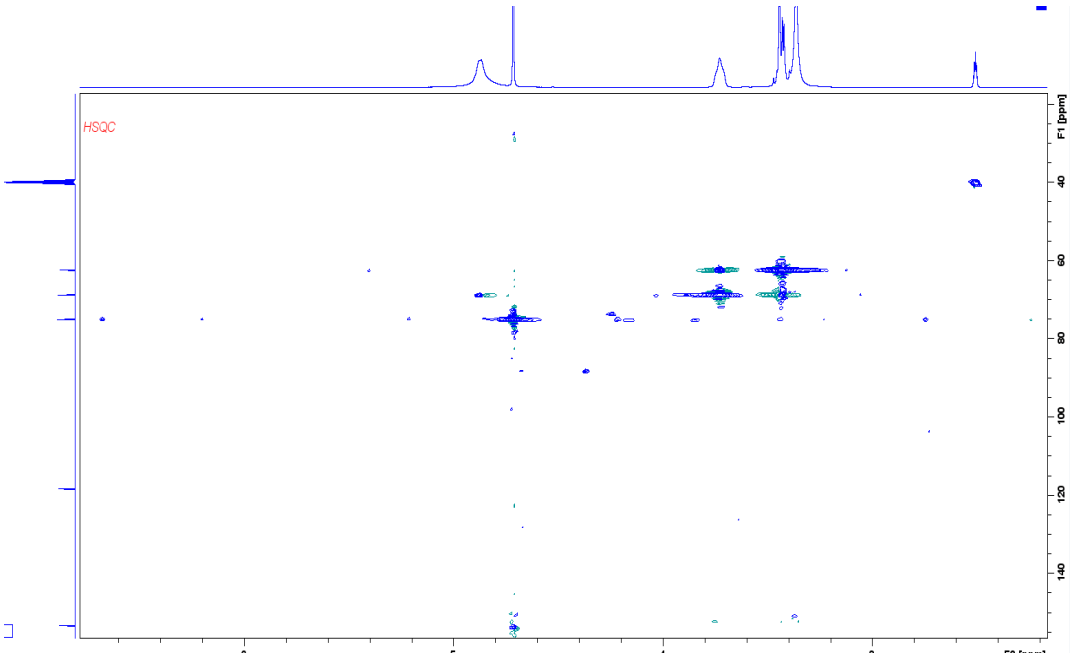

Fig. A 86 – Ascorbic acid HSQC for Flow 2 recorded in DMSO-d_6 (400 MHz).

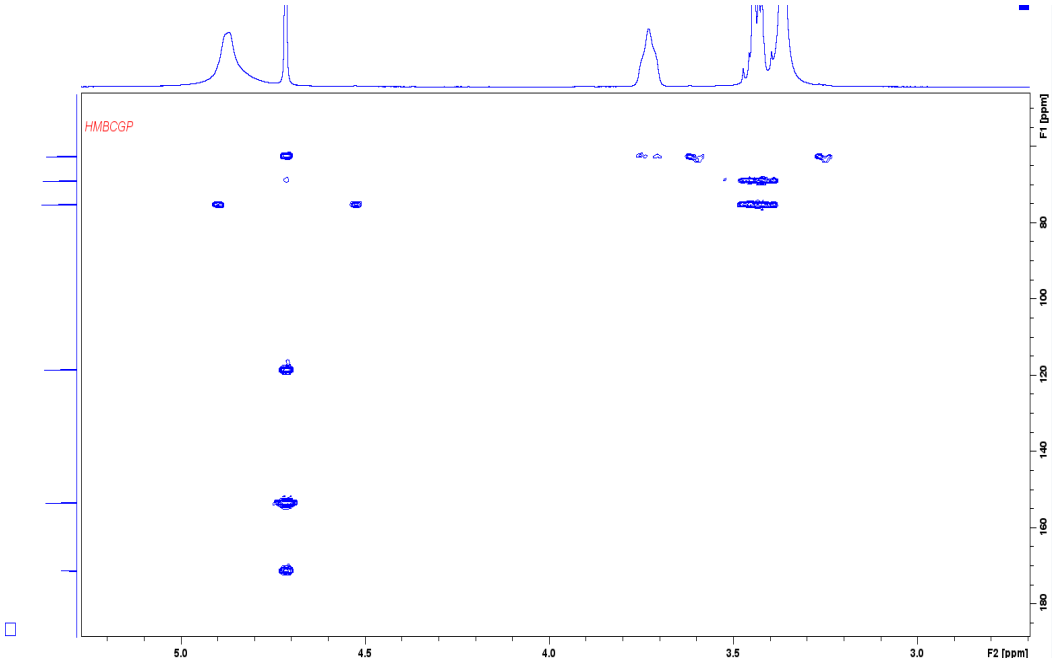

Fig. A 87 – Ascorbic acid HMBC for Flow 2 recorded in DMSO-d_6 (400 MHz).